Dysregulated activation of immune-inflammatory responses contributes to vascular damage in atherosclerosis and hypertension

Muhammad Oneeb Rehman Mian
Division of Experimental Medicine
McGill University

Final thesis submission in July 2015

(A thesis submitted to McGill University in partial fulfillment of the requirements of the degree of PhD Experimental Medicine – Thesis)

Abstract

Atherosclerosis and hypertension (HTN) are major contributors to the development and progression of cardiovascular disease (CVD). The underlying pathophysiology of atherosclerosis and HTN is similar in that both affect the structural and functional properties of the vasculature as a result of enhanced immune-inflammatory processes in the vascular wall. Vasoactive peptides such as angiotensin (Ang) II and endothelin (ET)-1 can contribute to vascular inflammatory responses and damage, and have been implicated in the progression of both atherosclerosis and HTN. We hypothesize that dysregulated activation of immune-inflammatory mechanisms by vasoactive peptides contributes to the progression of vascular damage in atherosclerosis and HTN.

The objectives of this thesis were 1) to determine the role of ET-1-mediated vascular immune-inflammatory mechanisms in progression of hyperlipidemia-induced atherosclerosis and formation of abdominal aortic aneurysms (AAA), 2) to investigate the contribution of pro-inflammatory ET-1 signaling to small artery dysfunction in hyperlipidemia-induced atherosclerosis, and 3) to study the role of anti-inflammatory T regulatory lymphocytes on vascular immune-inflammatory responses in Ang II-induced HTN.

The first study shows that endothelium-specific ET-1 overexpression in atherosclerotic apolipoprotein E knockout (*Apoe*$^{-/-}$) mice fed a high fat diet exaggerates development of aortic atherosclerotic plaques and triggers formation of AAA. This is accompanied by increase in aortic immune-inflammatory responses, spleen pro-inflammatory monocytes, and expression of matrix metalloproteinase-2 in atherosclerotic plaques. This study also suggests that the suppressive capacity of T regulatory lymphocytes may be reduced during atherosclerosis progression.

The second study shows that ET-1 overexpression in high fat diet-fed atherosclerotic *Apoe*$^{-/-}$ mice results in remodeling of endothelial signaling pathways and potassium channels mediating endothelium-dependent relaxation. Although this remodeling manifests as compensatory preservation of endothelial

function, it may in fact represent loss of regulation of endothelium-dependent relaxation in resistance arteries.

The third study demonstrates that absence of T regulatory lymphocytes exaggerates microvascular damage in Ang II-induced HTN. The findings of this study show that T regulatory lymphocytes exert vascular protection in part by controlling innate and adaptive immune responses.

To conclude, chronic low-grade vascular inflammation in atherosclerosis and HTN involves vasoactive peptide-mediated dysregulation of pro-inflammatory and anti-inflammatory mechanisms in favor of the former. Targeting immune-inflammatory mechanisms may allow us to limit the progression of atherosclerosis and HTN, and therefore the development of CVD.

Resume

L'athérosclérose et l'hypertension (HTN) sont les causes majeures du développement ainsi que l'aggravation des maladies cardio-vasculaires. Les causes de ses maladies sont similaires dans les deux cas, une altération de la structure et de la fonction des vaisseaux induites par une inflammation dans la paroi de ceux-ci. Les peptides vaso-actifs tels que l'angiotensine (Ang) II et l'endotheline (ET)-1 participent aux réponses inflammatoires et aux dommages que subissent les vaisseaux, et sont impliqués dans la progression de l'athérosclérose et de l'hypertension. Nous supposons que cette dysfonction inflammatoire par les peptides vaso-actifs contribue aux dommages vasculaires liés à l'athérosclérose et à l'hypertension.

Les objectifs de cette thèse sont 1) de déterminer le rôle inflammatoire d'ET-1 dans les mécanismes de progression de l'hyperlipidémie induisant l'athérosclérose et dans la formation des anévrismes de l'aorte abdominale (AAA), 2) d'étudier la contribution pro-inflammatoire d'ET-1 dans la dysfonction endothéliale des artères de résistances dans l'athérosclérose induite par l'hyperlipidémie 3) d'évaluer le rôle des lymphocytes T régulateurs anti-inflammatoires sur les réponses immunitaires vasculaires T dépendantes dans HTN induite par l'Ang II.

La première étude montre, dans un modèle murin de surexpression d'ET-1 endothélium-spécifique, sur des souris n'exprimant pas l'apolipoprotéine E (ApoE -/-) et nourris avec un régime riche en graisses, une exagération des plaques d'athérome aortique favorisant la formation des AAA. Ceci s'accompagne d'une augmentation de la réponse inflammatoire dans l'aorte, et d'une augmentation des monocytes pro-inflammatoires dans la rate. L'ensemble de ces mécanismes sont liés à la métalloprotéinase 2 dans les plaques d'athérome. Cette étude suggère également que la capacité suppressive des lymphocytes T régulateurs peut être réduite au cours de l'athérosclérose.

La deuxième étude montre, dans le même modèle, une altération des voies de signalisation des canaux potassiques favorisant la relaxation

endothélium. Cependant, elle se manifeste par un remodelage compensatoire afin de préserver la fonction endothéliale dans les artères de résistance.

La troisième étude démontre que l'absence de lymphocytes T régulateurs exagère les lésions microvasculaires dans HTN induite par l'AngII. Les résultats de cette étude montrent que les lymphocytes T régulateurs exercent une protection vasculaire en contrôlant les réponses immunitaires innées et adaptatives.

Pour conclure, l'inflammation vasculaire chronique à bas bruit, dans l'athérosclérose et HTN, le dérèglement est médié par les peptides vaso-actifs et leurs composantes pro-inflammatoires ce qui altère les mécanismes anti-inflammatoires protecteurs dans ces pathologies. Cibler les mécanismes immunitaires inflammatoires peut nous permettre de limiter la progression de l'athérosclérose et HTN, et donc le développement des maladies cardio-vasculaires.

Table of Contents

Abbreviations

AAA	Abdominal aortic aneurysms
ACE	Angiotensin converting enzyme
ADMA	Asymmetric dimethylarginine
AML1	Acute myeloid leukemia 1
Ang	Angiotensin
AP-1	Activator protein-1
APCs	Antigen presenting cells
Apoe	Apolipoprotein E
Arg-1	Arginase-1
AT_1R	angiotensin type 1 receptor
AT_2R	angiotensin type 2 receptor
ATP	Adenosine triphosphate
BH_4	Tetrahydrobiopterin
BK_{Ca}	Big conductance calcium-activated potassium channels
Ca^{2+}	Calcium ions
cAMP	Cyclic adenosine monophosphate
CCL	Chemokine ligand
CCR	Chemokine receptor
CD	Cluster of differentiation
cGMP	Cyclic guanosine monophosphate
COX	Cyclooxygenases
CTLA-4	Cytotoxic T-lymphocyte-associated antigen 4
CVD	Cardiovascular disease
CXCR1	CX-chemokine receptor 1
ECE	Endothelin converting enzyme
EDHF	Endothelium-derived hyperpolarizing factor
EDR	Endothelium-dependent relaxation
EETs	Epoxy-eicosatrienoic acids
eNOS	endothelial nitric oxide synthase

eET-1	Endothelium-specific endothelin-1 overexpression
ET-1	Endothelin-1
ET_aR	Endothelin type A receptor
ET_bR	Endothelin type B receptor
ERK	Extracellular signal regulated kinase
Fe^{3+}	Iron ions
FOXP3	Forkhead box P3
GITR	Glucocorticoid-induced tumor necrosis factor receptor
GPCRs	G-protein coupled receptors
H_2O_2	Hydrogen peroxide
HDL	High density lipoprotein
HFD	High fat diet
HIF-1	Hypoxia-inducible factor-1
HOCl	Hypochlorus acid
HTN	Hypertension
ICAM-1	Intracellular adhesion molecule-1
IDL	Intermediate density lipoprotein
IFN-γ	Interferon-γ
IκB	natural inhibitor of kappa B
IK_{Ca}	Intermediate conductance calcium-activated potassium Channels
IKK	inhibitor of kappa B kinase
IL	Interleukin
iNOS	inducible nitric oxide synthase
IPEX	Immunodysregulation polyendocrinopathy enteropathy X-linked
JAM	Junctional adhesion molecules
JNK	c-jun N-terminal protein kinase
K^+	Potassium ions
K_{IR}	Inward rectifying potassium channels
LDL	Low density lipoprotein

LDL-R	LDL receptor
LFA-1	Lymphocyte function-associated antigen-1
M1	Classically-activated macrophages
M2	Alternate-activated macrophages
MAPK	Mitogen-activated protein kinase
MCP-1	Monocyte chemoattractant protein-1
M-CSF	Macrophage-colony stimulating factor
MHC	Major Histocompatibility Complex
MLC	Myosin light chain
MMPs	Matrix metalloproteases
MR	Mineralocorticoid receptor
NADPH oxidase	Nicotinamide adenine dinucleotide phosphate oxidase
NEP	Neutral endopeptidase
NFAT	Nuclear factor activated in T cells
NFκB	Nuclear factor kappa B
NK cells	Natural killer cells
nNOS	neuronal nitric oxide synthase
NO	Nitric oxide
$\bullet O_2^-$	Superoxide anion
•OH	Hydroxyl radical
$ONOO^-$	Peroxynitrite
PECAM-1	Platelet-endothelial adhesion molecule-1
PI3K	Phosphoinositide 3-kinase
PKB	Protein kinase B/Akt
PPAR	Peroxisome proliferator-activated receptor
PVAT	Perivascular adipose tissue
RAAS	Renin-angiotensin-aldosterone system
Rag1	Recombination activating gene-1
ROS	Reactive oxygen species
RUPP	Reduced-uterine perfusion pressure
RXR	9-cis retinoic acid receptor

SAPK	Stress-activated protein kinase
sGC	Soluble guanylate cyclase
SHRs	Spontaneously hypertensive rats
SK_{Ca}	Small conductance calcium-activated potassium channels
SOD	Superoxide dismutase
TGF-β	Transforming growth factor-β
Th	T helper lymphocytes
TIMPs	Tissue inhibitors of metalloproteases
TNF-α	Tumor necrosis factor-α
Treg	T regulatory lymphocytes
VCAM-1	Vascular cell adhesion molecule-1
VE-cadherins	vascular endothelial (VE)-cadherin
VEGF-C	Vascular endothelial growth factor C
VLA-4	Very late antigen-4
VLDL	Very low density lipoprotein
VSMCs	Vascular smooth muscle cells
XDH	Xanthine dehydrogenase
XO	Xanthine oxidase
XOR	Xanthine oxidoreductase

List of tables

CHAPTER II

CHAPTER III

CHAPTER IV

List of figures

CHAPTER I

CHAPTER II

CHAPTER III

CHAPTER IV

Contribution of authors

First study - Endothelin-1 overexpression exacerbates atherosclerosis and induces aortic aneurysms in apolipoprotein e knockout mice

Melissa W. Li*:

- Design of experiments
- Collection of samples
- Technical setup for most of the experiments
- Blood pressure measurement
- Immunofluorescence and immunohistochemistry
- Statistical analysis
- Draft of the manuscript

Muhammad Oneeb Rehman Mian*:

- Design of experiments
- Collection of samples
- Technical setup for most of the experiments
- Immunofluorescence and immunohistochemistry
- Plasma cytokine analysis
- Statistical analysis
- Draft and revision of the manuscript

Tlili Barhoumi:

- Flow cytometery

Asia Rehman:

- Cryosectioning for immunuflourescence

Koren Mann:

- Technical expertise for flow cytometry

Pierre Paradis:

- Design of experiments
- Supervision of work and evaluation of raw data
- Correction of manuscript

Ernesto L. Schiffrin:

- Originated the study as PI of a CIHR grant
- Design of experiments
- Supervision of work and evaluation of raw data
- Correction of manuscript
- Funding of studies

**These authors contributed equally*

Second study - Preservation of endothelium-dependent relaxation in atherosclerotic mice with endothelium-restricted endothelin-1overexpression.

Muhammad Oneeb Rehman Mian*:

- Design of experiments
- Collection of samples
- Technical setup of the experiments
- Myography
- Statistical analysis
- Draft and revision of the manuscript

Nourredine Idris-Khodja*:

- Design of experiments
- Collection of samples
- Technical setup of the experiments
- Myography

Melissa W. Li:

- Collection of samples (Partial)
- Myography (Partial)

Avshalom Leibowitz:

- Collection of samples (Partial)
- Myography (Partial)

Pierre Paradis:

- Design of experiments

- Supervision of work and evaluation of raw data
- Correction and submission of manuscript

Yohann Rautureau:

- Supervision

Ernesto L. Schiffrin:

- Originated the study as PI of a CIHR grant
- Design of experiments
- Supervision and evaluation of raw data
- Correction of manuscript
- Funding of study

**These authors contributed equally*

Third study - FOXP3$^+$ T regulatory cells blunt angiotensin II-induced microvascular injury by controlling innate and adaptive immune responses

Muhammad Oneeb Rehman Mian

- Design of experiments
- Collection of samples
- Technical setup of the experiments
- Blood pressure
- Myography
- Immunofluorescence
- Plasma cytokine analysis
- Statistical analysis
- Draft of the manuscript

Tlili Barhoumi

- Isolation of cells and adoptive transfer
- Flow cytometry

Marie Briet

- Myography (partial)

Pierre Paradis

- Design of experiments
- Supervision of work and evaluation of raw data
- Correction and submission of manuscript

Ernesto L. Schiffrin

- Originated the study as PI of a CIHR grant
- Design of experiments
- Supervision and evaluation of raw data
- Correction of manuscript
- Funding of study

Acknowledgements

I would like to express my sincerest thanks to several people, who were there every step of the way to help and support me through my PhD.

To my family, especially my mother, who have always been very supportive of my academic pursuits and following my dream.

To Dr. Ernesto L. Schiffrin for his excellent mentorship, supportive supervision and invaluable guidance throughout my graduate studies.

To Dr. Pierre Paradis for pitching in with his important scientific expertise and advice.

To all my colleagues in Dr. Schiffrin's lab for their help, friendship, and support along the way.

To Marie-Eve Deschenes, Adriana Cristina Ene, Veronique Michaud, and Christian Young for their excellent technical support.

To the members of my thesis committees (Dr. Mark Blostein, Dr. Lorraine Chalifour, Dr. Kostas Pantopoulos, and Dr. Denis deBlois) for their helpful comments.

To the Faculty of Medicine-McGill University, Lady Davis Institute for Medical Research-SMBD Jewish General Hospital, and Canadian Vascular Network for their financial support.

To the Division of Experimental Medicine, including Ms. Dominique Besso and Ms. Marylin Linhares, for their help.

CHAPTER I: Introduction

Review of Literature and Objectives

1. Introduction

The cardiovascular system is an organ system composed of the heart and the network of blood vessels (arteries, capillaries and veins) that allows for the transport of oxygen, nutrients, messenger molecules and cells between peripheral tissues via the blood. Alterations in this system result in impaired exchange of essential nutrients and gases within the body, and is the basis for cardiovascular disease (CVD). CVD continues to be the leading cause of morbidity and mortality in the world [1].

Atherosclerosis and hypertension (HTN) are two pathological processes that affect the arterial system, and thereby are major underlying contributors to the development and progression of CVD. As multifactorial chronic conditions, atherosclerosis and HTN have an impact on several organ systems in the human body, and can independently or cooperatively cause CVD and associated conditions such as cerebrovascular and coronary artery disease, peripheral vascular disease, chronic kidney disease, congestive heart failure, renal failure, stroke and atrial fibrillation.

Atherosclerosis and HTN are clinically distinct yet inter-related conditions. The underlying pathophysiology of atherosclerosis and essential HTN is similar in that both affect the structural and functional properties of the vasculature as a result of enhanced pro-inflammatory and pro-oxidative stress processes in the vascular wall [2]. In both conditions, signaling of vasoconstrictor peptides such as angiotensin II (Ang II) and endothelin-1 (ET-1) are known to participate in the enhancement of vascular inflammation and, consequently, vascular damage [3, 4]. This thesis demonstrates how the dysregulated activation of immune-inflammatory responses enhances vascular damage in ET-1 exaggerated high fat diet (HFD)-induced atherosclerosis or in Ang II-induced HTN, respectively.

In this chapter, a brief introduction about the structural, functional and mechanical features of arteries and relevant vasoactive factors, and the physiology and pathophysiology behind atherosclerosis and hypertension will be given. Next, the various elements of vascular inflammation in context of CVD will

be described in detail. Finally the experimental animal models of atherosclerosis and HTN relevant to research presented in this thesis will be briefly mentioned. The review of literature will be followed by three recent studies conducted that suggest a cooperative role of signaling of vasoactive peptides and aberrant activation of immune-inflammatory responses in exaggerating structural and functional vascular changes in atherosclerosis and HTN (chapters II, III, and IV). Finally, in chapter V, a general discussion about vascular immune-inflammatory responses in the development and progression of atherosclerotic and hypertensive vascular injury will be provided, linking to but also going beyond context of the research presented in this thesis, and some novel concepts will be addressed.

2. The arterial wall

The arterial system is the network of blood vessels that carry blood away from the heart. Arteries of the systemic circulation carry oxygenated blood to the organs and tissues in the body. Alterations in the systemic arterial system negatively impacts delivery of oxygen and essential nutrients to vital organs, which is the basis of CVD.

Systemic arteries can be broadly subdivided into large and small arteries. Among the former, two types are found, elastic and muscular, depending on the relative composition of elastic and muscular tissue in the vascular wall. Larger arteries, for example the aorta, carotids, mesenteric, renal, iliac and femoral or epicardic coronary arteries are generally elastic whereas smaller vessels issuing from these vessels have a relatively thicker muscular media. Under pathological conditions, such as in atherosclerosis, elastic arteries are affected, whereas in HTN, both large and small arteries are develop lesions. An appreciation of the pathological changes in large and small arteries in CVD requires a basic understanding of the anatomy and physiology of normal arteries.

2.1 Structural features of the normal artery wall

The arterial wall is a well-organized connective tissue structure consisting of three layers (or tunicae), the intima, the media, and the adventitia, with various components of extracellular matrix in between, and the perivascular adipose tissue (PVAT) surrounding it (Figure I-1) [5].

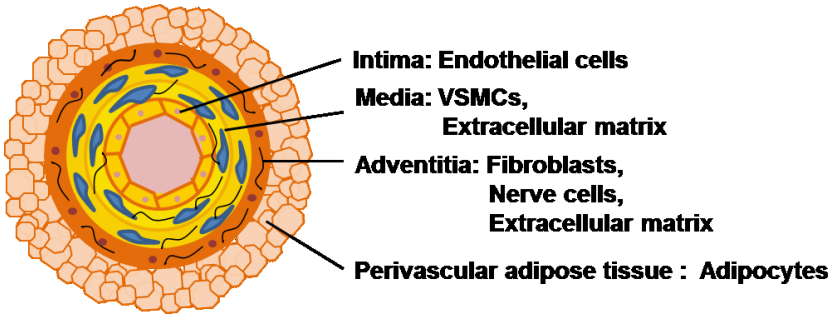

Figure I-1: Structure of a normal artery

2.1.1 Intima

The intima is the innermost layer of the arterial wall, and acts as a physical barrier between blood components and extravascular tissues. The intimal layer consists of a continuous monolayer of flat cells, the endothelium, then the sub-endothelial area, and finally the internal elastic lamina made of elastic fibers. The endothelium layer is present on all surfaces that are in contact with the blood, and is therefore a consistent feature throughout the circulation. A healthy endothelium is important for the normal functionality of the arteries. Endothelial cells (ECs) play a major role in controlling vascular tone by sensing mechanical forces caused by flowing blood and extrinsic vasoactive factors circulating in the blood, and produce and release vasoactive mediators that act on neighboring smooth muscle cells [6] as well as at a distance. The integrity of endothelial cytoskeletal structures and inter-endothelial junctions controls vascular permeability to nutrients and cells [7]. During inflammation, for example, changes in endothelial cell morphology can occur, which results in changes in cellular

junctions and endothelial cytoskeletal structures and consequently vascular permeability to macromolecules [8]. ECs also control leukocyte trafficking to underlying tissues; a complex process that will be discussed in section 7.

2.1.2 Media

The medial layer of arteries consists predominantly of vascular smooth muscle cells (VSMCs) surrounded by extracellular matrix components, which include collagen, elastin fibers and fibronectin. The extracellular matrix deposited by VSMCs in the media account for the majority of the passive mechanical properties of arteries. Large elastic arteries consist of more layers of VSMCs and higher elastin content, and thus possess recoil properties, than small muscular arteries [9]. The main function of VSMCs is to control vascular diameter via vasoconstriction and vasodilatory processes. Signaling by vasoactive factors from the circulation and those produced by ECs alter the polarization state of VSMCs that determines the contractility of the artery. Ion channels in VSMCs play an important role in this regulation of vascular tone [10]. VSMCs also control vessel diameter by detecting and reacting to mechanical forces on the vascular wall, perhaps via their close association with extracellular matrix structures, a process known as cellular mechanotransduction [11].

2.1.3 Adventitia

The adventitia consists predominantly of a collagen-rich extracellular matrix produced by myofibroblast cells [12]. Vascular rupture at extremely high pressures is prevented by the high collagen content in the adventitia [13]. This region may also contain a network of small blood vessels, the vasa vasorum, as well as non-myelinated nerve endings. The vasa vasorum provides nutrients to the adventitia and media, especially in large arteries, and the nerve endings regulate the function of medial VSMCs [5, 9]. Traditionally considered as a structural support for vessels, the adventitial layer has more recently been

recognized as an important source of vascular inflammation. Adventitial fibroblasts are known to produce reactive oxygen species (ROS), cellular growth factors, and vasoactive compounds all of which influence VSMC proliferation and vascular tone [14, 15].

2.1.4 The extracellular matrix

An important component of the vessel wall is the extracellular matrix, primarily synthesized and organized by the VSMCs, which not only defines the mechanical properties of the artery but also plays a role in the regulation of immune cell activation and modulation of the effects of growth factors and other stimuli [16]. Under physiological conditions, the extracellular matrix is highly regulated by a careful balance between synthesis and degradation. Changes in the extracellular matrix of arteries contribute to the pathogenesis of cardiovascular conditions, including atherosclerosis and HTN [17].

The composition of the extracellular matrix varies with the size, the nature and position of the vessel in the arterial tree [18, 19]. The extracellular matrix consists predominantly of elastin fibers and collagen of various types, attached to vascular cells via glycoproteins such as fibronectin. Elastin is found most abundantly in the wall of the large arteries, and to a much lesser extent in small muscular arteries [20]. Crosslinking between elastin fibers confers its principal function, i.e. elasticity, which is essential in large arteries to cope with the large pulsatile pressure generated by the contraction of the heart [21, 22]. In contrast to elastin, collagen in the media provides rigidity/tensile strength to the vascular wall. As the pressure in the artery increases, collagen fibers become aligned circumferentially to support tension on the wall and restrict distention [23, 24]. Type I and IIII collagens are the most abundant collagen fibers found in the vasculature [25]. The glycoprotein fibronectin is another extracellular matrix component that also contributes to the rigidity of the arterial wall by enabling interactions between other extracellular matrix components and vascular cells [26, 27].

2.1.4.1 Remodeling of the extracellular matrix: role of matrix metalloproteases

Matrix metalloproteases (MMPs), released by VSMCs and also by immune cells, are a family of zinc-dependent endopeptidases that play a key role in remodeling of extracellular matrix [28]. Activated MMPs can degrade collagen, elastin, and other extracellular molecules [29]. The activity of MMPs is regulated by tissue inhibitors of metalloproteases (TIMPs). MMPs play an active role in arterial remodeling. MMPs can degrade collagen to induce proliferation of VSMCs leading to intima-media thickening [30], upregulate signaling of the fibrotic transforming growth factor (TGF)-β to promote arterial fibrosis [28, 31], and adventitial expansion [32], and also induce alkaline phosphatase activity to cause vascular calcification [33], amongst other functions. MMP-2 and -9 have been particularly implicated in the physiological and pathophysiological remodeling of arteries [17].

The cells within the three layers and the various extracellular matrix components of the vascular wall are interconnected in multiple fashions, and interact dynamically to define the functional and mechanical properties of arteries.

2.2 Vascular function

Arterial function is determined by the balance of vasoconstrictor and vasodilatory signaling mediated by various factors that act on the endothelium and VSMCs. The net result of signaling by vasoactive agents determines whether the vessel contracts or relaxes. Vascular tone refers to the contractile activity of VSMCs. Signaling by various vasoactive agents directly or indirectly affects the intracellular calcium (Ca^{2+}) concentrations in VSMCs, which in turn determines its contractility. Increased intracellular Ca^{2+} concentrations in VSMCs

causes calmodulin-dependent activation of myosin light chain kinase that phosphorylates myosin light chain (MLC). Phosphorylation of MLC enhances myosin-actin interactions resulting in VSMC contraction [34]. The endothelium is intricately involved in the regulation of the vascular tone.

2.2.1 Factors released by ECs

The endothelium releases several factors that influence the vascular tone, and hence control blood flow through the arteries. These factors include nitric oxide (NO), eicosanoids (e.g. prostacyclin), endothelium-derived hyperpolarizing factor (EDHF), and ET-1. The later will be discussed in detail in section 3. The major endothelium-derived factors mediating VSMC relation are illustrated in Figure I-2.

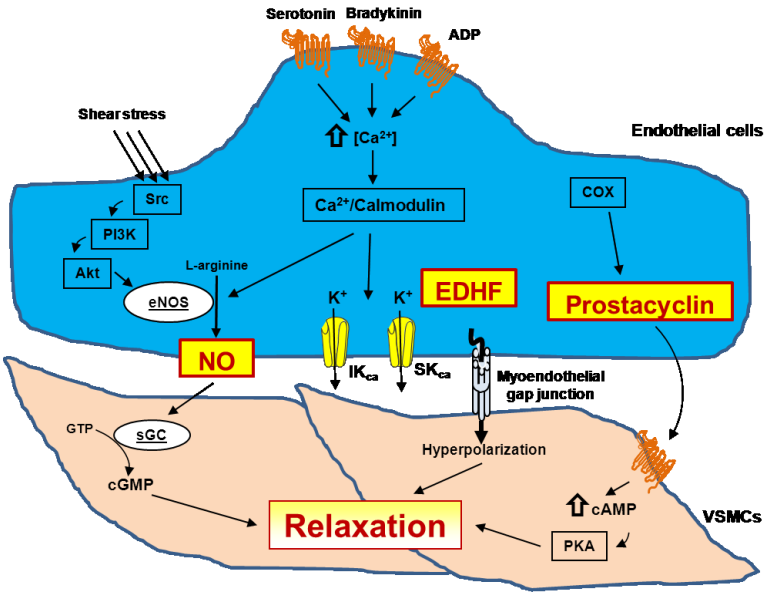

Figure I-2: Endothelium-derived factors that mediate VSMC relaxation.

2.2.1.1 Nitric oxide

NO is the main vasodilator produced by ECs. In the endothelium, NO is produced when the enzyme endothelial NO synthase (eNOS) catalyzes the conversion of L-arginine to L-citrulline in a Ca^{2+}-dependent manner [35]. NO can also be produced by the two other isoforms of NOS: inducible NOS (iNOS) and neuronal NOS (nNOS). During inflammatory processes, iNOS activity is induced in ECs and macrophages, which are cells of the innate immunity, to produce large amounts of NO [36].

The activity of eNOS is regulated by several different stimuli. Agonists such as acetylcholine [37] and physical stimuli such as shear stress [38] upregulate eNOS activity in ECs. On the other hand, certain inflammatory cytokines such as tumor necrosis factor (TNF)-α can limit eNOS activity [39].

Once produced, NO passively diffuses into the underlying VSMCs where it activates soluble guanylate cyclase (sGC), which leads to increased cyclic guanosine monophosphate (cGMP) formation [40]. The resultant prevention of Ca^{2+} entry into the VSMCs produces vasorelaxation [41].

2.2.1.2 Eicosanoids

Eicosanoids are vasoactive factors formed from polyunsaturated 20-carbon fatty acids, the most predominant precursor being arachidonic acid. Eicosanoids include prostaglandins, thromboxanes, leukotrienes, and hydroxyl-eicosatetraenoic acids. Arachidonic acid released from cell membrane phospholipids is a substrate for cyclooxygenases (COX)-1 and -2, lipoxygenases, or cytochrome P450 enzymes [42]. COX-1 and-2 convert arachidonic acid into prostaglandin H2, a vasoconstrictor that undergoes further enzymatic conversion into prostaglandins such as prostacyclin and thromboxane. Whereas COX-1 is constitutively expressed in most tissues, the expression of COX-2 is increased with cell activation, for example during inflammation [42].

The main prostaglandin produced in ECs is prostacyclin that causes relaxation of VSMCs by activating adenylyl cyclase, which results in increase in intracellular levels of cyclic adenosine monophosphate (cAMP) and subsequently a decrease in Ca^{2+} concentration [43]. ECs can also produce thromboxane, which mediates vasoconstriction [42].

2.2.1.2 Endothelium-derived hyperpolarizing factor

Earlier evidence in the 1980s indicated that even after pharmacological or genetic manipulations to inhibit the vasodilatory effects of NO and prostacyclin, there was residual endothelium-dependent relaxation in response to chemical or mechanical stimulations. This phenomenon was particularly observed in small arteries. The unknown vasodilatory factor responsible for this effect became to be known as “endothelium-derived hyperpolarizing factor” since it led to the hyperpolarization of VSMCs and ECs [44]. EDHF is thought to hyperpolarize and relax VSMCs by directly or indirectly opening the various potassium (K^+) channels on VMSCs or by hyperpolarizing ECs, which facilitates the electrical coupling between ECs and VSMCs [45].

Although the identity of EDHF remains unknown, several factors have been proposed. Epoxy-eicosatrienoic acids (EET), metabolites of arachidonic acid in the cytochrome P450 pathway, synthesized by ECs show EDHF activity in certain vascular beds by enhancing the opening of big conductance calcium-activated potassium channels (BK_{Ca}) and hyperpolarizing VSMCs [46]. Cannabinoid anandamide, another product of arachidonic acid metabolism, may also act as an EDHF by acting through its receptors on ECs and VSMCs to hyperpolarize the latter [47]. K^+ (potassium ions) has also been proposed to be the EDHF. Stimulation of endothelial cell receptors increase the probability of opening of small and intermediate conductance calcium-activated potassium channels (SK_{Ca} and IK_{Ca}) in ECs, leading to K^+ efflux and increase in extracellular K^+ concentration. Increase in endothelial K^+ can activate the inward

rectifying pottasium channels (K_{IR}) and the Na^+-K^+-ATPase found in the gap junctions between EC and VSMCs, which results in hyperpolarization and relaxation of VSMCs [45, 48]. Inhibitors of K^+ channels can be used to identify their role in mediating vascular relaxation in physiological and pathophysiological conditions.

2.3 Vascular mechanics

Flowing blood and blood pressure impart forces on the artery wall. Stress is the force applied per unit area. Artery walls sustain shear stress due to flowing blood and circumferential stress due to blood pressure [5]. Forces that cause stress also deform the vessel wall. Strain refers to the dimensions of the deformed vessel relative to the un-deformed vessel [49]. Arterial distensibility is the measure of the ability of the artery to expand or contract to increasing or decreasing intra-luminal pressures [50]. As previously described, this mechanical property of arteries is predominantly dependent on the composition of the extracellular matrix components deposited by the VSMCs in the media, and is therefore different for large and small arteries. The stress-strain relationship at different intra-luminal pressures is used to characterize the distensibility or the "stiffness" of arteries in different vascular beds. A decrease in distensibility, or an increase in arterial stiffness, has been associated with a number of CVDs including atherosclerosis and HTN [51].

The vasoconstrictor peptides Ang II and ET-1 perform important physiological and pathophysiological roles by having direct and indirect effects on the arterial wall.

3. Angiotensin II and endothelin-1

Ang II and ET-1 are two vasoconstrictors that act on the arteries to play important homeostatic roles, including the physiological control of blood

pressure. Alterations in these two peptide systems and their signaling have been implicated in the development and progression of CVD. In this section, a brief description of these two vasoconstrictors and their actions will be given.

3.1 Angiotensin II

Ang II is one of the main bioactive compounds of the renin-angiotensin-aldosterone system (RAAS), which is critical for the maintenance of blood pressure control and fluid-electrolyte balance [52]. Proteolytic cleavage of angiotensinogen by renin, which is released by the juxtaglomerular cells in the kidney, produces the peptide Ang I. Ang I undergoes further cleavage by the enzyme angiotensin converting enzyme (ACE) to form Ang II. Renin release in the kidney is the rate-limiting step in Ang II synthesis [53]. Ang I and Ang II can undergo further modifications to give rise to the other peptides of the RAAS, including Ang (1-7), Ang III, and Ang IV, the varying cardiovascular effects of which are not relevant to this thesis and will not be described. In addition to the circulating RAAS, local RAAS components have been identified in the brain, heart, kidneys, vasculature, adipose tissue and the immune system [54-56]. Local RAAS is important for Ang II to mediate its localized physiological and pathological effects in these compartments.

Ang II mediates its effects via G-protein coupled receptors (GPCRs) [52]. In humans, there are two types of Ang II receptors: angiotensin type 1 and 2 receptors (AT_1R and AT_2R) [57]. In rodents, two separate genes encode for two isoforms of the AT_1R, namely $AT_{1a}R$ and $AT_{1b}R$ [58], which exhibit differential distribution and regulation [59]. Mice knockout for both isoforms of AT_1R exhibit lower blood pressures and vascular alterations compared to wild-type mice [60], suggesting that these receptors play a role in normal vascular function. The vasoconstrictor and electrolyte balancing actions of Ang II are mediated via AT_1R [61], although in rodents the contribution of each isoform may be different. Mice knockout for $AT_{1a}R$, but not $AT_{1b}R$, have been shown to have lower blood pressure at baseline compared to wild-type mice [60, 62], and impaired response

to Ang II infusion [63]. This suggests that $AT_{1a}R$ is the main receptor for regulation of vasoconstriction and blood pressure in rodents and is responsible for blood pressure elevation in experimental HTN caused by Ang II infusion. In addition to its vasoconstrictor effects, Ang II acts via the AT_1R to contribute to the growth and hypertrophy of cardiomyocytes [64], VSMCs [65], and renal cells [66], which is implicated in cardiovascular pathology. Ang II is also a potent inducer of oxidative stress and inflammatory processes associated with its signaling via the AT_1R [67].

Although less well characterized, studies indicate that AT_2R-mediated Ang II signaling counteracts AT_1R signaling. The action of Ang II via the AT_2R limits vasoconstriction and cell growth and proliferation that occurs due to AT_1R activation [52, 68]. Knockout of AT_2R in mice that are prone atherosclerosis development resulted in exaggerated atherosclerotic lesions as a result of enhanced vascular inflammation, indicating that this receptor also limits AT_1R-dependent pro-inflammatory responses of Ang II [69].

Beyond its direct effects, Ang II can also indirectly influence the vasculature by stimulating the production and release of other vasoactive mediators, including ET-1 [70, 71].

3.2 Endothelin-1

ET-1 belongs to a group of peptides that includes ET-2 and ET-3, each containing 21 amino acids. ET-1 is the main isoform expressed and secreted in the vasculature predominantly by ECs [72], but can also be produced by man other tissues. ET-1 is the most potent vasoconstrictor currently known [73]. ET-1 expression is enhanced by many stimuli, including vasoactive peptides such as Ang II [71], growth factors [74], shear stress [75], lipoproteins [76, 77], and inflammation [78]. NO [79], natriuretic peptides [80], and prostaglandins [81] are amongst the negative regulators of ET-1 production.

Stimulation of ECs results in the production of pre-proendothelin-1, which is converted first to proendothelin-1 and then to the biologically inactive big ET-1

[82, 83]. Big ET-1 is cleaved by endothelin converting enzyme (ECE) to form mature ET-1 [82]. Neutral endopeptidase (NEP) degrades mature ET-1. Big ET-1 can also be cleaved by the enzyme chymase to give rise to ET-1 (1-31), which has weaker vasoconstrictor effects [84] and can induce vascular inflammatory responses [85], or by MMP2 to yield the potent vasoconstrictor ET-1 (1-32) [86]. Mature ET-1 is secreted more towards the adjacent VSMCs than into the lumen [87]. Therefore, ET-1 acts more in an autocrine and paracrine than in an endocrine fashion.

ET-1 acts via its two G-protein coupled receptors: ET_aR and ET_bR. In the vasculature, ET_aR is expressed on the VSMCs, whereas ET_bR is expressed on both VSMCs and ECs [88, 89]. Binding of ET-1 to ET_aR and ET_bR on VSMCs stimulates vasoconstriction. ET_bR on VSMCs are also involved in the clearance of circulating ET-1 [90]. Endothelial cell ET_bR activation results in vasodilation via the production of endothelium-derived vasodilators, NO and prostacyclin [91]. The overall action of ET-1 is therefore dependent on the relative balance of ET_aR and ET_bR in the vascular. ET-1 receptors are also found on cells outside the vasculature, including on immune cells, cardiomyocytes, and fibroblasts [92, 93].

Like Ang II, ET-1 has effects on the vasculature and other tissues beyond its classical vasoconstrictor function. ET-1 has potent mitogenic effects on VSMCs [94], cardiomyocytes [95], and glomerular mesangial cells in the kidney [96]. ET-1 signaling can induce local vascular inflammatory responses independently of increase in blood pressure or systemic inflammation [97]. ET-1 signaling via the ET_aR can also interact and cooperate with the RAAS to enhance the effects on the vasculature and other tissues [98]. In various immune cells, ET-1 signaling potentiates migration and production of pro-inflammatory mediators [99-101].

Both Ang II and ET-1 signaling have been implicated in the pathophysiology of atherosclerosis and hypertension.

4. Pathophysiology of atherosclerosis

Atherosclerosis refers to the thickening and hardening of the arterial wall caused as a result of pathological lipid deposition in the intima along with infiltration of inflammatory and immune cells [102]. This phenomenon occurs mainly in large and medium sized elastic arteries, although smaller elastic arteries are also sometimes affected. Affected arteries develop atherosclerotic plaques, the composition and pathobiology of which is very complex and evolves over time. Sub-clinically, atherosclerotic lesions start to develop in childhood and adolescence as fatty streaks [103]. However, these lesions remains asymptomatic for decades since they do not affect blood flow. Symptomatic atherosclerosis occurs later in life, and can lead to arterial stenosis or thrombosis. Depending on the artery affected, atherosclerosis can result in potentially dangerous clinical conditions such as myocardial infarction and stroke.

Atherosclerotic plaques generally contain dead and living immune cells, lipids, VSMCs and extracellular matrix. Lipids that are pathologically deposited in arteries to become part of the atherosclerotic plaques arise from the circulation where they are transported in particles called lipoproteins.

4.1 Lipoproteins and lipid transport

Cholesterol and other lipids are insoluble in water, and are therefore transported in the blood between tissues in complex particles called lipoproteins. Lipoproteins are broadly classified into five types according to size from smallest to largest as HDL, LDL, IDL, VLDL (high, low, intermediate, and very low density lipoproteins), and chylomicrons. Lipoproteins also differ from each other in terms of their protein components, which are known as apolipoproteins [104]. Alteration in the lipid transport system results in abnormal lipid or lipoprotein levels in the circulation, and is a critical part of the atherosclerotic process but beyond the scope of this thesis. In context of CVD, higher levels of HDL are associated with lower levels of heart disease, therefore higher levels of HDL are considered to be

protective [105]. For this reason, HDL cholesterols has been termed as the ‘good cholesterol’. In contrast, it is now well accepted that other lipoproteins in the circulation, including VLDL, IDL, LDL, and the remnant particles, and the lipids they carry are highly atherogenic. High plasma cholesterol (hypercholesterolemia) is a major risk factor for atherosclerosis [106]. Mice with a genetic deletion of the LDL receptor (*Ldlr*$^{-/-}$) or of apolipoprotein E (*Apoe*$^{-/-}$) are prone to atherosclerosis due to dysfunctional handling of lipids, and are the most widely used models to understand the pathophysiology of atherosclerosis.

4.2 Vascular pathology in atherosclerosis

The process of atherosclerosis begins with early fatty streak development (Figure I-3) [107, 108]. An initial insult to the endothelium sets off an inflammatory cascade in the vascular wall. The most well documented insult to the endothelium is the accumulation of LDL in the intima of the arterial wall where they become modified and oxidized to potent pro-inflammatory particles. Oxidized LDL particles promote activation of ECs, which then express adhesion molecules, and provoke the VSMCs to secrete chemokines and chemoattractants; molecules that draw immune cells, including monocytes of the innate immune system and lymphocytes of the adaptive immune system, into the arterial wall. Infiltrating monocytes mature into macrophages and take up lipids to become foam cells. Throughout this process, VSMCs also secrete extracellular matrix components, including collagen and elastin. Early fatty streaks usually start at branch points of arteries, where hemodynamic stresses already favor remodeling and thickening of the arterial wall.

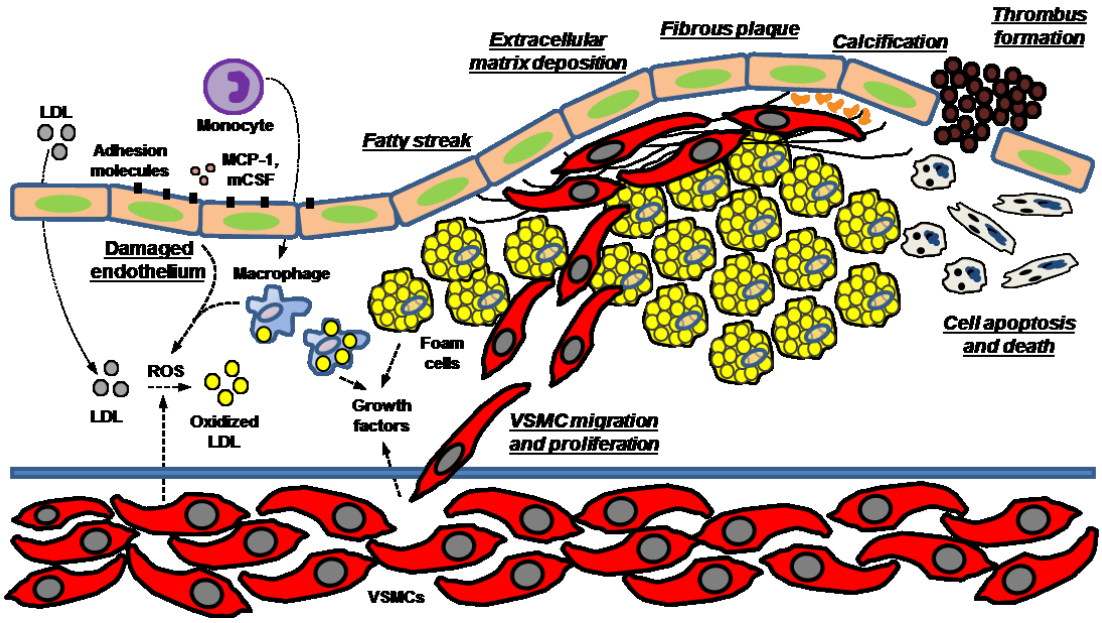

Figure I-3: Progression of atherosclerosis. Adapted from Madamanchi *et al.* [109].

With the constant infiltration of macrophages and other activated inflammatory cells, fatty streaks evolve into early fibroatheroma [110, 111]. Secretion of extracellular proteoglycans by VSMCs increases lipid retention within the arterial wall. Secreted factors promote the necrosis of macrophages and VSMCs, which contributes further to uncontrolled inflammation. A fibrous tissue cap forms just under the endothelium to cover the necrotic core, the basis of the fibrous plaque lesion that develops into more advanced lesions.

As the fibrous plaque lesion evolves into advancing atheroma, proteolytic enzymes act on the fibrous cap to make it thin and weakened [112, 113], resulting in the formation of thin-cap fibroatheroma. This thin-cap lesion is known as the vulnerable plaque because of the high risk of rupture and subsequent thrombus formation. Ruptures of thin-cap fibroatheroma can be clinically silent if they heal by forming fibrous tissue consisting of cells, collagen and extracellular space [111, 114]. Repeated cycles of rupture and healing results in the development of complex lesion. Vascular calcification occurs increasingly

throughout the natural history of plaque development [115]. Increasing mass of plaques by itself may cause stenosis of the artery.

Another vascular pathology that is frequently observed in association with atherosclerosis progression is the development of aneurysms in the abdominal aorta.

4.2.1 Abdominal aortic aneurysms

Aneurysm refers to the progressive dilation of the aorta due to the weakening of the aortic wall. Aneurysms that occur in the abdominal aorta are referred to as abdominal aortic aneurysms (AAAs). AAAs usually develop around the region where renal arteries branch off from the abdominal aorta. Although various definitions have been used to consider aortic dilation as an AAA [116, 117], in general it is classified as such when there is at least 50% increase in abdominal aortic diameter above normal. The pathophysiology of AAAs is still poorly understood. Mechanisms contributing to the initiation and progression of AAAs have been identified from cross-sectional studies in humans and from animal models. Inflammation, extracellular matrix degradation, stenosis, thrombosis, and hemodynamic forces have all been implicated in the formation of AAA [118-120]. Extracellular matrix degradation involves elastin breaks and fragmentation. Together, these mechanisms progressively contribute directly or indirectly to weakening the aortic wall, and the lumen of the aorta expands to normalize shear stresses. If left untreated, this may lead to rupture at the site of aneurysm [121].

AAAs frequently develop in association with atherosclerosis. Several studies have linked coronary heart disease and peripheral atherosclerosis with AAAs [121]. However, it is widely debated whether this link is causal or is due to common risk factors that contribute to the development of both atherosclerosis and AAAs. Evidence for the later theory is provided by the fact that the incidence of AAA is not associated with severity of atherosclerosis [122]. Furthermore, the effectiveness of drugs used for atherosclerosis, for example statins, in inhibiting

AAA progression have yielded conflicting reports [123, 124]. It is possible that the development of atherosclerosis and AAAs occurs in parallel and involves multiple mechanisms that are interrelated as well as exclusive to each condition [125]. ET-1 signaling is one mechanism that has been implicated in pathophysiology of both atherosclerosis and AAAs.

4.2.2 Endothelin-1, atherosclerosis, and abdominal aortic aneurysms

Evidence from human subjects and experimental animal models have suggested a role for ET-1 signaling in the progression of atherosclerosis and AAAs. ET-1 levels in the plasma and coronary arteries are increased in early and advanced atherosclerosis in humans, and there is a correlation between the immune-reactivity of plasma ET-1 and severity of atherosclerosis [126, 127]. Plasma ET-1 levels are also increased in patients with AAAs, and are correlated with the size of the aneurysms [128-130]. Western-type diet-fed *Ldlr*$^{-/-}$ and *Apoe*$^{-/-}$ mice exhibited increased aortic ET-1 levels [131, 132], and the development of atherosclerosis was shown to be blunted by mixed $ET_{A/B}$ and selective ET_A receptor antagonists in Western-type diet-fed *Ldlr*$^{-/-}$ mice [131], *Apoe*$^{-/-}$ mice [132, 133], and hamsters [134]. Transgenic mice overexpressing ET-1 selectively in the endothelium (eET-1 mice) exhibited increase in gene expression associated with lipid biosynthesis in the vascular wall, and overexpression of ET-1 in the endothelium of *Apoe*$^{-/-}$ mice exacerbated HFD-induced atherosclerotic lesions in the descending thoracic aorta [135]. Despite all this evidence, it remains unclear how increased ET-1 signaling in the vasculature contributes to the progression of atherosclerosis and AAA formation. Vascular inflammatory responses induced by ET-1 signaling could play a role in the progression of atherosclerosis and development of AAAs under hyperlipidemic conditions. However, this has not been demonstrated experimentally before, and was one of the objectives of this thesis.

Although the pathobiology of atherosclerosis is complex, several risk factors have been associated with the progression of the disease.

4.3 Risk factors for atherosclerosis

Hyperlipidemia, HTN, diabetes, and smoking are all known to contribute major risk towards the progression of atherosclerosis. Only hyperlipidemia and HTN will be briefly described here as they are the most relevant to this thesis.

4.3.1 Hyperlipidemia

Alterations in lipoprotein metabolism can result in abnormal levels of lipid and lipoproteins in the blood, a condition known as dyslipidemia. The most common form of dyslipidemia is hyperlipidemia, which involves abnormally elevated levels of lipids and lipoproteins in the blood. Hyperlipidemia can be primary, which are predominantly due to genetic causes, or secondary, which are due to underlying causes such as diabetes [136, 137]. The association between hyperlipidemia and atherosclerosis has been appreciated for many years [138]. Primary and secondary hyperlipidemias increase the risk for atherosclerosis usually by increasing levels of one or more of the atherogenic lipoproteins (LDL, VLDL, chylomicrons), with a concomitant increase in plasma lipids (either cholesterol, or triglycerides or both) [137, 139]. Some hyperlipidemias may also cause a decrease in the good HDL cholesterol. It has been known for a long time that increase in LDL cholesterol, which constitutes the major fraction of cholesterol being transported in the circulation, is an independent risk factor for the development of coronary artery disease [140-142]. More recently, however, elevated triglyceride levels have also been considered as an important risk factor [143, 144], while HDL cholesterol levels have been shown to have a strong inverse correlation with the incidence of coronary artery disease [145]. Whether ET-1 signaling affects circulating levels of lipids and lipoproteins is unknown.

4.2.2 Hypertension

Clinical and experimental data show that high blood pressure, or HTN, increases the risk for atherosclerosis. In clinical trials, HTN has been shown to contribute significantly towards the risk for atherosclerosis, even after taking into account the added risks of cholesterol and smoking [146, 147]. Induction of HTN in Watanabe heritable hyperlipidemic rabbit resulted in a dramatic enhancement of atherosclerotic lesion formation [148]. However, it is still unclear how HTN plays a role in the progression of atherosclerosis. It is possible that vascular inflammatory mechanisms that mediate vascular injury in HTN are common to that in atherosclerosis, and, in the presence of hyperlipidemia, are responsible for the enhanced development of atherosclerotic lesions [2].

5. Pathophysiology of hypertension

HTN is a chronic condition characterized by elevated blood pressure in the arteries. HTN is defined as systolic blood pressure above 140 mmHg and/or diastolic blood pressure above 90 mmHg [149], or blood pressures over 130/80 mmHg in individuals suffering from diabetes mellitus. HTN is in most cases essential or primary and the cause for it is unknown. In rare cases, HTN occurs secondary to an identifiable cause such as renal disorder, adrenal tumors or pregnancy. Although the etiology of essential HTN is unknown, genetics, the environment, diet, sympathetic hyperactivity and renal defects are all thought to be involved [150]. The pathophysiology of essential HTN is therefore complex and involves multiple interrelated mechanisms. Chronic HTN is characterized by the inability of kidneys to excrete sodium and water, sympathetic hyperactivity from the central nervous system, and importantly increased peripheral vascular resistance [151]. Like in atherosclerosis, HTN is associated with altered structure of large and small arteries [152]. Along with the contribution of kidneys and the central nervous system, structural and functional vascular changes are key processes for the development and maintenance of essential HTN.

5.1 Blood pressure and peripheral vascular resistance

Blood pressure refers to the force exerted by the circulating blood on the walls of the arteries. Maintenance of blood pressure is required for adequate perfusion of organs and tissues. If the blood pressure falls too low, as it occurs in patients with septic shock [153], perfusion to vital organs is affected and can result in a life-threatening condition. Blood pressure is affected by the hemodynamic effects of cardiac output and the peripheral vascular resistance to blood flow. Although elevation of peripheral resistance is the hallmark of essential hypertension, in some forms of hypertension increases in cardiac output may also contribute to blood pressure elevation in HTN.

Peripheral vascular resistance refers to the total resistance opposing the blood flow in the systemic circulation. The resistance to the blood flow across an organ determines what fraction of cardiac output perfuses the organ [154]. Moreover, the distribution of resistances across various organs determines the distribution of cardiac output to these organs. Therefore, a change to the resistance to blood flow alters the distribution of blood volume by the cardiovascular system to different tissues.

Although in isolated systolic hypertension and in the elderly, large artery stiffness may be the main contributor to resistance to flow and blood pressure elevation, classically, small resistance arteries are the main determinants of vascular resistance. An increase in flow resistance is generated with the narrowing of the lumen of resistance arteries [19]. Resistance arteries that have a lumen diameter of <300 um when relaxed are the major site of vascular resistance [149]. The total vascular resistance across a vessel can be determined by the Hagen–Poiseuille equation, which is expressed as:

$$R = \frac{8}{\pi} \times \frac{v \times L}{r_i^4}$$

where R is vascular resistance, v is viscosity, L is vessel length and r_i is the vessel radius. Since resistance is inversely proportional to the fourth power of the

blood vessel radius, a small decrease in lumen diameter can cause a marked increase in vascular resistance. Structural and functional changes in the resistance arteries can result in decreased lumen size and, consequently, increased resistance. Vascular tone in the walls of small arteries is the major determinant of the resistance to blood flow through the circulation [10]. In HTN, increased peripheral vascular resistance occurs due to vascular remodeling as a result of structural and functional changes in the arterial wall [154].

5.2 Vascular pathology in hypertension

Structural and functional changes alter the vascular tone and stiffness of arteries, all of which is collectively described as vascular remodeling. In HTN, vascular remodeling is frequently characterized in terms of changes in the ratio between media thickness and lumen diameter (media-to-lumen ratio), and the cross-sectional area of the media. Both large and small arteries exhibit vascular remodeling in HTN, but the type of remodeling is distinct (Figure I-4).

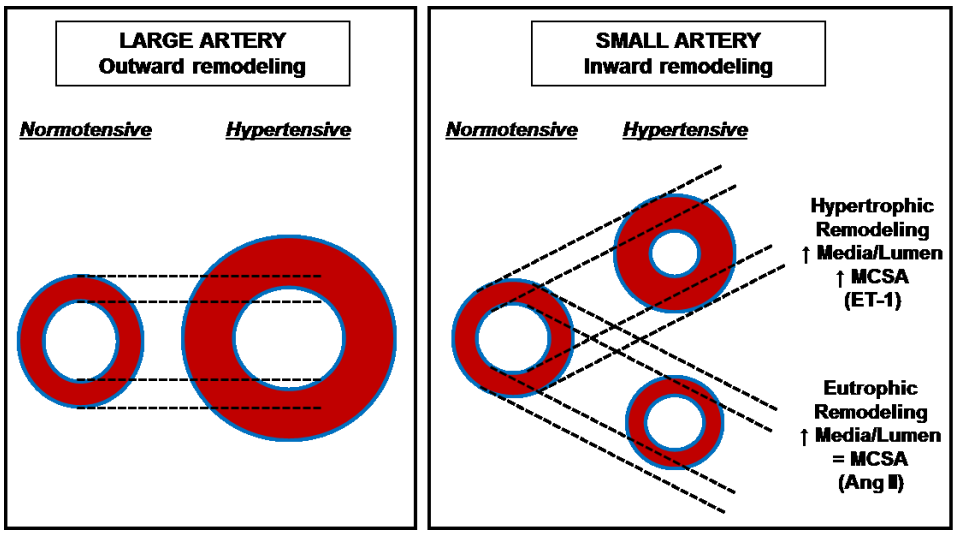

Figure I-4: Large and small artery remodeling during HTN. Adapted from Schiffrin [155].

Large arteries, such as the aorta, undergo outward hypertrophic remodeling and increased stiffness with age, and this seems to be accelerated in HTN [156, 157]. Outward hypertrophic remodeling is characterized by an increase in media cross-sectional area along with an increase in lumen diameter. In large arteries, VSMC hypertrophy (increase in size) occurs, as opposed to VSMC hyperplasia (increase in number) in smaller arteries [158, 159]. Apoptosis of VSMCs may occur to compensate or modify growth of the media in large arteries [160, 161]. This is further accompanied by alterations in the extracellular matrix, including elastic fiber duplication and fragmentation [162], and increased deposition of collagen and fibronectin [162, 163], all of which contribute to increased arterial stiffness. In HTN, large arteries also present with a dysfunctional endothelium as a result of structural and molecular alterations in ECs [164, 165]. Over time, increased pressure on the stiff but dysfunctional, degenerative arterial wall causes lumen expansion, resulting in outward hypertrophic remodeling [156, 157, 166]. Stiffening is associated with less buffering of systolic volume and consequently systolic blood pressure elevation. As well, changes in characteristic impedance along the vascular tree result in wave reflection. As pulse wave velocity is increased in the stiffened vessels, the reflected waves arrive earlier, in systole rather than in diastole as in arteries that have not stiffened, and elevate systolic blood pressure centrally in the aorta [167].

In HTN, small arteries exhibit inward remodeling whereby there is reduction in lumen diameter. This type of remodeling can be eutrophic in which media-to-lumen ratio is increased but media cross-sectional area is unaltered, or hypertrophic in which both parameters are increased [168, 169]. Eutrophic remodeling occurs in small arteries isolated from experimental rodent models of HTN associated with an activated RAAS [170] and from individuals with essential HTN [171]. Inward eutrophic remodeling may be a consequence of a balance between apoptosis of outer peripheral cells and inward growth, resulting in decreased lumen diameter without altering the media cross-sectional area [19]. Hypertrophic remodeling, on the other hand, is observed in patients with

secondary HTN [172] and in animal models of salt-sensitive hypertension [173, 174], where the ET-1 system is activated. Extracellular matrix deposition, or vascular fibrosis, also occurs as part of remodeling of small arteries in HTN. Clinical and experimental data show that there is accumulation of collagen [175-177] and fibronectin [178-180], as well as increase in cell-matrix attachment sites (integrins) [177] in resistance arteries, which collectively contribute to stiffening of the arteries over time. Altered expression of MMPs/TIMPs by VSMCs and immune cells may be involved in the pathological remodeling of the extracellular matrix in the small arteries during HTN [181]. Inflammation, characterized by infiltration of immune cells and increased oxidative stress, plays a key role in vascular remodeling by promoting a pro-inflammatory, pro-fibrotic milieu that contributes to vascular growth, dysfunction and fibrosis [163, 182].

5.2.1 Angiotensin II and vascular remodeling in HTN

Large and small artery remodeling is reversed in part by Ang II receptor blockade in both rodents and humans [163], indicating that Ang II signaling is intricately involved in arterial remodeling during HTN.

In addition to its growth effects on VSMCs, Ang II can trigger apoptosis, predominantly by signaling via its AT_2R. Normotensive rats infused with Ang II exhibit increased apoptosis in the thoracic aorta via activation of AT_1R and AT_2R [160]. In another study, treatment with an AT_1R blocker in spontaneously hypertensive rats (SHRs), a model of genetic hypertension, has been shown to enhance apoptosis of aortic VSMCs, an effect blunted by AT_2R antagonism [183].

Ang II also contributes to vascular fibrosis by stimulating the production of collagen I in VSMCs. Ang II signaling increases the secretion of TGF-β in an AT_1R-dependent manner, which in turn triggers collagen synthesis [184, 185]. In resistance arteries of SHRs, ACE inhibition or AT_1R blockade normalizes the relative content of collagen [177], most likely independently of the blood pressure lowering effect of these treatments [186]. AT_1R receptor antagonism also

reduces collagen I, III, and IV mRNA in large and small vessels in other rat models of hypertension [187, 188]. Ang II also stimulates the production of fibronectin via AT_1R-dependent signaling [170].

Importantly, the actions of Ang II that most influence arterial remodeling during HTN are through stimulation of pro-oxidant and pro-inflammatory responses in the vasculature. Specifically, Ang II signaling upregulates production of ROS and activates redox-sensitive genes, such as nuclear factor kappa B (NFκB) in vascular cells [189]. Endothelial injury and activation, or endothelial dysfunction, as a consequence of Ang II signaling leads to increased expression of chemokines and adhesion molecules that promote infiltration of immune cells [190]. It is now widely accepted that infiltrating immune cells are key contributors to the pro-inflammatory milieu in the vasculature that causes structural and functional changes in large and small arteries. This will be addressed in detail in section 7.

Endothelial dysfunction is a key process that is observed early on in the pathogenesis of both atherosclerosis and HTN. It is a pathological change that contributes to the initiation of vascular inflammation, which is involved in the remodeling of the vascular wall.

6. Endothelial dysfunction

Endothelial dysfunction is characterized by pathological change in the actions of the endothelium towards an impaired vasodilatory, and increased pro-inflammatory and pro-thrombotic state [190]. A dysfunctional endothelium initiates processes including vasoconstriction, vascular remodeling, and inflammation that have been implicated in the development of atherosclerosis and HTN. Reduced NO bioavailability and enhanced oxidative stress are the key molecular changes that define the pathological properties of a dysfunctional endothelium.

In both atherosclerosis and HTN, ROS production is increased in the vascular wall [2]. ROS are powerful inhibitors of endothelium-dependent vasodilatory pathways mediated by NO and prostacyclin. Impaired vasodilatory responses have been reported in several vascular beds in both atherosclerosis and hypertension [190, 191]. As described previously, NO is the main vasodilator produced by eNOS in ECs. It acts on the neighboring VSMCs to induce vasodilation by inhibiting influx of Ca^{2+} ions into the VSMCs. NO interacts with superoxide anion ($\bullet O_2^-$), a form of ROS, to form peroxynitrite ($ONOO^-$). $ONOO^-$ is highly reactive, and can induce the tyrosine nitration of prostacyclin synthase to inhibit the formation of another potent vasodilator prostacyclin [192]. $ONOO^-$ also activates thomboxane A_2 synthase and COX, which can then potentiate vasoconstriction [193]. Moreover, $ONOO^-$ can uncouple eNOS by oxidizing its key cofactor tetrahydrobiopterin (BH_4) into the $\bullet BH_3$ radical [192]. Uncoupled eNOS produces $\bullet O_2^-$ instead of NO thereby further reducing NO bioavailability and enhancing oxidative stress production.

Elevated levels of asymmetric dimethylarginine (ADMA), an endogenous competitive inhibitor of eNOS, have been associated with endothelial dysfunction and atherosclerosis [194]. In context of HTN, blood pressure can be modulated by eNOS expression and eNOS activity [195]. Together, this evidence provide support for a role of endothelial dysfunction in atherosclerosis and HTN.

In addition to its vasodilatory effects, NO has potent anti-inflammatory and anti-growth properties. NO can inhibit platelet aggregation [195], expression of adhesion molecules [196], and oxidative modification of LDL [195]. Moreover, NO signaling also inhibits growth of VSMCs [197]. Therefore, reduced NO bioavailability as a consequence of enhanced oxidative stress not only perturbs vasodilation but also promotes the initiation of vascular inflammatory and remodeling responses. Enhanced oxidative stress is linked to a pro-inflammatory state of the vessel wall. ROS upregulate the expression of adhesion and chemotactic molecules [198], thereby facilitating the infiltration of immune cells into the vasculature. Ample evidence shows that both Ang II and ET-1 contribute to endothelial dysfunction, associated with reduced NO and increased ROS

production [199, 200]. However, the role of ET-1 in atherosclerosis-induced vascular dysfunction is unknown.

Under normal circumstances, inflammation is part of a complex healing process involving interaction between circulating cells and vascular cells to regulate hemodynamic changes that affect the homeostasis of the vascular wall [201]. However, inflammation is harmful when it becomes chronic, as in the case of atherosclerosis and HTN.

7. Vascular inflammation

Vascular inflammation is an essential component of the vascular pathology in atherosclerosis and HTN. Increased expression of chemokines and adhesion molecules, immune cell infiltration, cytokine production, increased oxidative stress, and activation of pro-inflammatory signaling pathways in arteries from atherosclerotic or hypertensive rodents is evidence for a role of vascular inflammation in the pathophysiology of atherosclerosis and hypertension [202, 203].

Inflammation involves a complex series of events that begins with the activation of the endothelium as a result of an injury, infection or other stimuli, which can include Ang II or ET-1 [204-206]. Subsequent events leads to increase in vascular permeability, leukocyte extravasation and tissue repair [207]. Under physiological conditions, this process is tightly regulated and reversible. Activation and set up of inflammatory responses is followed by a resolution phase whereby inflammation is down-regulated. However, in pathological conditions, inflammatory responses are not regulated and persist to cause tissue damage.

Induction of inflammatory responses leading to plaque formation in atherosclerosis has been well described. The concept of low-grade vascular inflammation in HTN has however evolved over the last two decades or so, and may share similarities with the initial steps observed in atherosclerosis [208]. In

this section, the key cellular and molecular mechanisms involved in vascular inflammation will be described in context of atherosclerosis and HTN.

7.1 Immune cells

Detection of immune cell infiltrates in the vasculature during atherosclerosis and HTN was first suggestive of their role in the progression of these diseases. More recently, evidence from genetic or pharmacological targeting of specific subsets of immune cells or their functions have broadened our understanding of their role in the pathophysiology of vascular pathology in atherosclerosis and HTN. Immune cells can contribute to vascular damage by producing ROS and other pro-inflammatory mediators such as cytokines [209].

The immune system is broadly divided into innate and adaptive immunity [210, 211]. Innate immunity is the dominant host defense that is triggered non-specifically in response to stimuli including external pathogens or endogenous damage signals. Cells of the innate immune system include monocytes and macrophages, antigen-presenting cells (APCs, including dendritic cells), mast cells, eosinophils, basophils, and natural killer (NK) cells. Innate cells either respond to pathogen-associated or damage signals themselves, or process them as antigens for the activation of adaptive immunity. Adaptive immunity refers to specific immune response and results from immunological memory. T and B lymphocytes participate in adaptive immunity, performing a variety of functions. B lymphocytes produce antibodies against specific antigens in affected cells to label them for later clearance by phagocytes or complement activation. For the purpose of this thesis, only monocyte/macrophages, antigen-presenting cells and T cells will be described in context of CVD. The evidence provided here is not meant to be exhaustive but to give a general idea of the literature supporting a role for various immune cell subsets in the progression of atherosclerosis and HTN. The various immune cells and their hematopoietic origin are illustrated in Figure I-5.

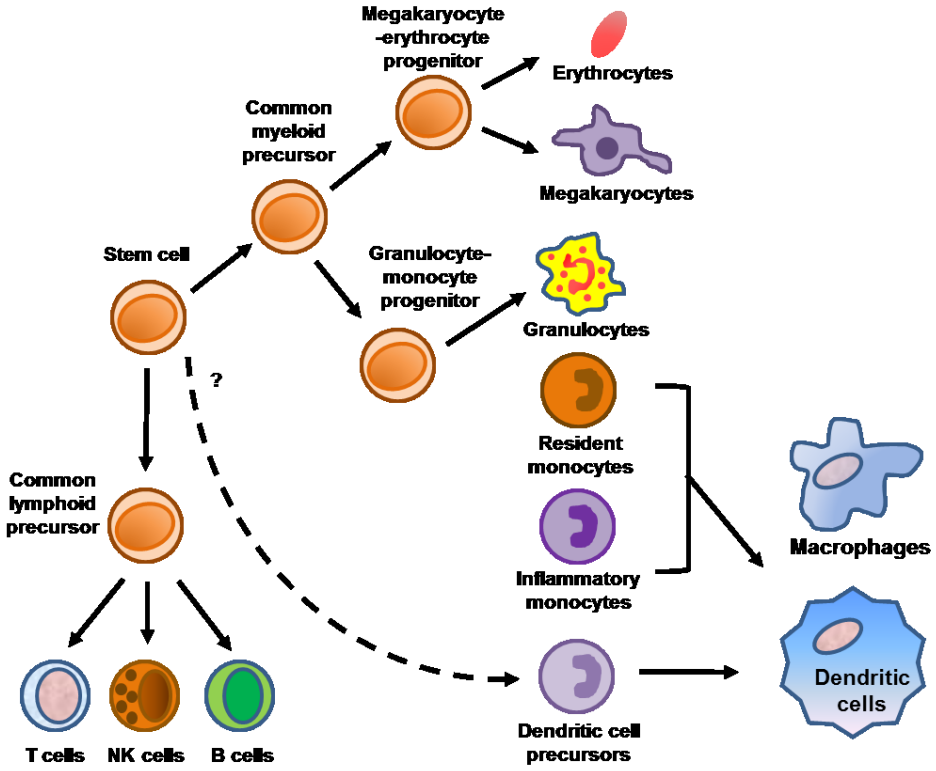

Figure I-5: Immune cells and their origin. Adapted from Imhof *et al.* [212].

7.1.1 Monocytes and macrophages

Monocytes are cells of the innate immunity that originate in the bone marrow from hematopoietic stem cells via a series of differentiation stages, under the control of mainly macrophage-colony stimulating factor (M-CSF) [213]. Once formed, monocytes enter the circulation and form a systemic reservoir for tissue-specific innate cells. Circulating monocytes respond and are attracted to chemical signals released locally to infiltrate into tissues, a process known as chemotaxis, and differentiate into macrophages and dendritic cells. Macrophages are identifiable via their specific expression of proteins including cluster of differentiation (CD)-14, CD11b, F4/80 (mice), Mac-1/Mac-3, and CD68 [214]. Dendritic cells express CD11c. Together, monocytes, macrophages, and dendritic cells contribute to inflammatory responses by performing phagocytosis, antigen presentation, ROS production, and cytokine release.

Monocytes and macrophages are a heterogeneous population of cells consisting of various activation states, which may interchange depending on the surrounding microenvironment [213, 215]. Murine monocytes are generally divided into inflammatory Ly6C$^+$ monocytes (similar to human CD14$^+$ classical monocytes) or patrolling Ly6C$^-$ monocytes (similar to human CD16$^+$ alternate monocytes). Like monocytes, macrophages also exhibit functional diversity. Of the several subsets, two are most important. Macrophages can polarize towards a pro-inflammatory/killing phenotype (M1) in response to cytokines interferon (IFN)-γ and TNF-α, or an immune-modulatory/wound healing phenotype (M2) in response to IL-4. M1 macrophages have upregulated expression of proteins such as iNOS and major histocompatibility complex (MHC)-II, and produce ROS and pro-inflammatory cytokines such as interleukin (IL)-1β, IL-12, IL-6, and TNF-α. M2 macrophages express CD206 (mannose receptor) and sometimes arginase (Arg)-1, and produce IL-10. Inflammatory Ly6C$^+$ monocytes have been hypothesized to be precursors to M1-type macrophages in tissues while Ly6C$^-$ monocytes acquire an M2-type phenotype [213, 216, 217], although trans-differentiation from inflammatory monocytes into M2 macrophages has also been observed [218, 219]. It is possible that differentiation of infiltrating monocytes is influenced by the microenvironment that they face.

The role of monocytes/macrophages in lipid uptake, foam cell formation, vascular inflammation and development and progression of atherosclerotic lesions has been extensively studied and reviewed in the literature [220], and was also alluded to in section 4.2. During atherosclerosis, Ly6C$^+$ inflammatory monocytes preferentially infiltrate into the vascular wall and differentiate into macrophages that resemble the M1 phenotype. These macrophages uptake modified lipoproteins via scavenger receptors and other mechanisms to become foam cells. Accumulation of oxidized lipids and other cellular debris causes many macrophages to apoptose. If these apoptotic cells are not cleared by neighboring phagocytes, they may undergo secondary necrosis, which leads to the formation of necrotic core in atherosclerotic lesions. Although Ly6C^{high} monocytes have been most implicated for their atherogenic potential, recruitment of Ly6C^{low} may

also be important [221]. Although ET-1 is known to induce potent vascular inflammatory signaling, a demonstration of a link between enhanced ET-1 signaling and increased atherogenic monocyte/macrophage infiltration in the aorta is lacking. Moreover, it is unknown if ET-1 can alter systemic proportions of monocyte subsets towards the more pro-atherosclerotic $Ly6C^{high}$ monocytes. ET-1-induced vascular monocyte/macrophage infiltration could contribute to AAA formation; however this has never been shown before.

A role for monocyte/macrophages in HTN has also been identified. It has been previously shown that osteopetrotic mice, which have a mutation within the M-CSF gene and accordingly a generalized deficiency of macrophage subpopulations, exhibit blunted vascular remodeling and oxidative stress when they are infused with Ang II [222], treated with DOCA-salt [223], or when they have endothelium specific overexpression of ET-1 [224]. In a mouse model where Lysozyme M^+ monocytes express the diphtheria toxin receptor, Wenzel *et al.* demonstrated that toxin-mediated depletion of circulating monocytes attenuates Ang II-induced HTN, vascular remodeling and oxidative stress, and up-regulation of pro-inflammatory mediators and macrophage infiltration [224]. Adoptive transfer of monocytes but not neutrophils restored the Ang II phenotype in these mice following depletion. Recently, a protective role for macrophages in salt-sensitive HTN was described in studies conducted by Machnik *et al.* [225, 226]. They showed that, following salt-loading or DOCA salt treatment, macrophages accumulate in the skin and secrete vascular endothelial growth factor C (VEGF-C) to stimulate subcutaneous lymphatic proliferation and promote interstitial Na^+ clearance. Clodronate liposome-mediated depletion of macrophages reduced macrophage infiltration, failure of interstitial Na^+ buffering, leading to salt-sensitive blood pressure elevation. These differing roles of monocytes/macrophages may be mediated by different subsets described above, although the exact roles of inflammatory vs patrolling monocytes and M1 vs M2 macrophages in HTN remains to be clarified. The role of different subsets of T cells on monocyte and macrophage polarization in context of HTN is also unknown.

7.1.2 Antigen presenting cells

Antigen presentation by a specialized subset of innate cells, the APCs, is a key step for the activation of adaptive immunity including T cells. Dendritic cells are the most potent APCs, although macrophages can also perform this function [227]. APCs activate T cells by providing an activation signal, which involves presentation of the antigenic peptides via the MHC-I or II molecules to the T cell receptor, and simultaneous co-stimulatory signals [228]. Costimulatory signals, such as interaction between CD28 and CD40 ligand (CD40L) on T cells with B7 ligands (CD80 and CD86) and CD40 on APCs respectively, provide strong stimulus for T cell activation and expansion.

The role of antigen presentation by APCs in the progression of atherosclerosis is supported by evidence showing that genetic disruption of B7 costimulatory molecules blunts atherosclerosis in *Ldlr*$^{-/-}$ mice [229]. Moreover, mice lacking the MHC-II-associated protein invariant chain, CD74, also exhibit reduced atherosclerosis [230]. Dendritic cells have been detected near T cells within unstable plaques [231-233]. In the aortic wall of *Apoe*$^{-/-}$ mice, Koltsova *et al.* [234] recently demonstrated that fluorescent-labelled CD11c^{+} cells interact with and activate CD4^{+} T cells (discussed further on), leading to cell proliferation and secretion of IFN-γ and TNF-α. These pro-inflammatory cytokines then enhanced uptake of modified LDL in macrophages.

Recently, Vinh *et al.* [235] showed a role for T cell-costimulation by B7 ligands in the development of HTN. In their study, pharmacological inhibition of the B7-CD28 axis blunted Ang II and DOCA-salt induced HTN, also preventing T cell activation and aortic T cell infiltration. Mice lacking B7 ligands CD80 and CD86 presented a similar blunting effect in Ang II-induced HTN, which was restored by bone marrow transplant from wild-type mice. Activated dendritic cells (CD11c^{+}CD86^{+}) were increased in secondary lymphoid organs of hypertensive mice. It is unknown whether macrophages play a similar antigen presenting function to activate T cells in HTN.

7.1.3 T cells

T lymphocytes are cells of the adaptive immunity that express the T cell receptor (TCR) consisting of two TCR chains, a CD3 co-receptor, and a ζ-chain accessory molecule [236]. During development in the thymus, T cells undergo further differentiation to express $CD4^+$ or $CD8^+$, which are co-receptors for the TCR complex and mediate activation of downstream signaling pathways when the TCR engages with an antigen presented by APCs. Stimulation by antigen presentation, co-stimulation and cytokines polarizes the naïve $CD4^+$ T helper (Th) cells into predominantly Th1, Th2, T regulatory lymphocytes (Treg), or Th17 subsets, each of which produce their own panel of cytokines and perform specific functions (Figure I-6). $CD8^+$ T cells differentiate into cytotoxic T cells upon activation.

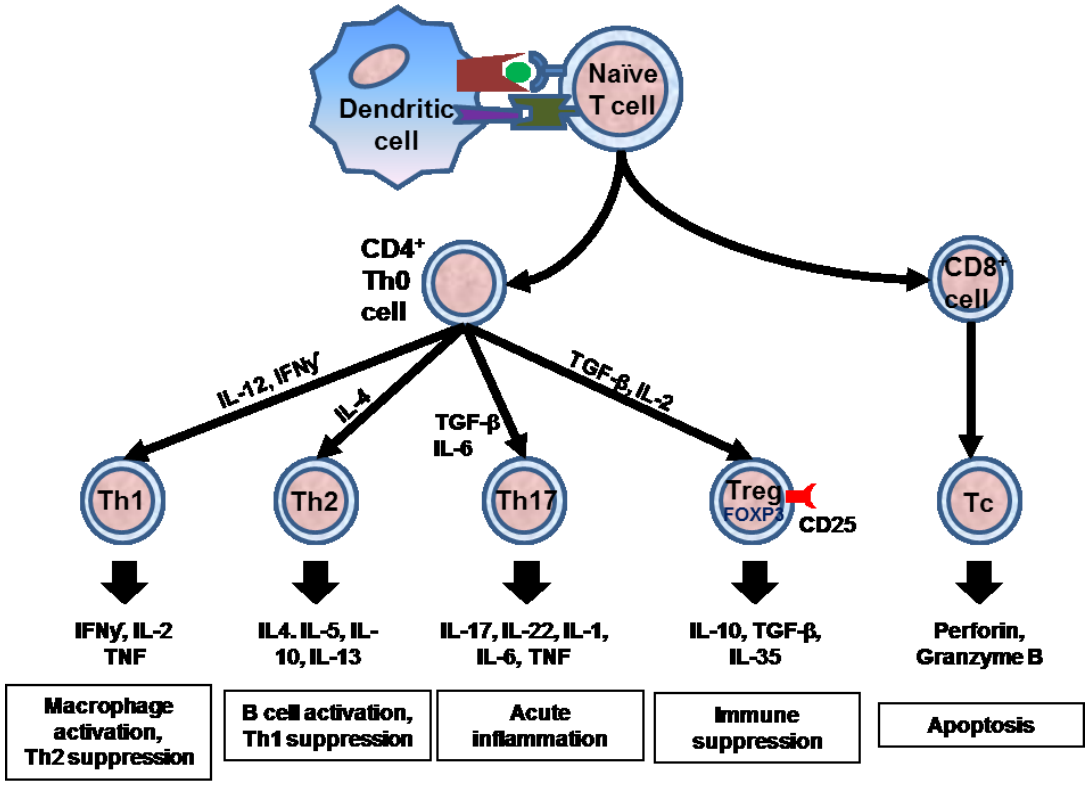

Figure I-6: Various subsets of T cells, differentiation signals, and their functions. Adapted from Idris-Khodja *et al.* [236].

A role for T cells has been demonstrated in atherosclerosis and HTN. Mice deficient in T and B cells exhibit significantly blunted atherosclerotic lesion development [237, 238]. Adoptive transfer of $CD4^+$ T cells from *Apoe* $^{-/-}$ mice into immunodeficient *Apoe*$^{-/-}$/*scid* mice has been shown to restore atherosclerotic plaque development to levels comparable to immunocompetent controls [239]. Ang II-induced hypertension, vascular dysfunction, and oxidative stress was shown to be blunted in recombination activating gene-1 knockout mice (*Rag1*$^{-/-}$), which are deficient in T and B cells [240]. The Ang II-induced vascular phenotype in these immunodeficient mice was restored by the adoptive transfer of $CD3^+$ T cells from wild-type mice. Whereas this evidence implicates T cells in the vascular pathology of atherosclerosis and HTN, the roles of various subsets of T cells are still under investigation.

7.1.3.1 Th1/Th2 response

In the presence of cytokines IL-12 and IFN-γ, naïve $CD4^+$ T cells polarize towards Th1 phenotype [236, 241, 242]. Polarized Th1 cells produce pro-inflammatory cytokines IFN-γ, IL-2, TNF-α and TNF-β, and participate in cell-mediated defense against intracellular microorganisms, macrophage activation, and suppression of Th2 response. IL-4 polarizes naïve $CD4^+$ T cells into Th2 cells, which produce IL4, IL-5, IL-10, and IL-13. Th2 cytokines suppress Th1-type responses and activate B cell-mediated immunoglobulin production. IL-4 suppresses Th1 polarization whereas IL-10 counteracts Th1 cytokine production [243]. Therefore, Th1 response is weak during Th2 polarized response and vice versa.

Vascular pathology observed in atherosclerosis and HTN has been associated with a shift in Th1/Th2 balance towards the former. Studies have shown that Th cells in atherosclerotic lesions polarize towards Th1 phenotype with increased IFN-γ and IL-2 production whereas Th2 cytokines IL-4 andIL-10 are less detectable [244]. As well, cells within the lesions are known to produce Th1 stimulating cytokines such as IL-12 [244]. Deficiency of IFN-γ or its receptor reduced lesion development, and increased plaque collagen content in atherosclerosis-prone mice [245, 246], while intra-peritoneal IFN-γ infusion enhances lesion development [245]. Whether ET-1 contributes to activation of effector T cells and polarization towards Th1 phenotype during atherosclerosis and AAA formation is unknown. In the context of HTN, Ang II-infused rats have been shown to exhibit increased Th1-mediated responses, evidenced by increased production of Th1 cytokine IFN-γ, and decreased Th2 mediated responses in an AT_{1a}R-dependent manner [247, 248]. Knockout of IFN-γ in mice blunted Ang II-induced vascular dysfunction independently of blood pressure effects [249]. Deficiency of chemokine ligand 16 (CXCL16), which binds to C-X-C chemokine receptor type 6 characteristically found on Th1-type T cells, prevents Ang II-induced infiltration of macrophages and T cells in the kidney [250]. Thus, polarization towards Th1-type responses may be important in the progression of

both atherosclerosis and HTN. It must be noted, however, that other studies have implicated IL-4 in the development of HTN and IFN-γ in the maintenance of normal blood pressure in hypertensive mice [251, 252]. This discrepancy may be due to use of different models of HTN or species in these studies.

7.1.3.2 Treg response

Treg are anti-inflammatory T cells that suppress the activity of T effector subsets (Th1, Th2, Th17) and other immune cells. Treg normally develop in the thymus (natural [n]Treg), but T cells can also be induced in the periphery to become Treg (induced [i]Treg) [253]. Several subsets of T cells exhibit T cell-suppressive activity, but regulatory activity has been described to be most in cells expressing CD4, the IL-2 receptor alpha chain (CD25), and the transcription factor forkhead box P3 (FOXP3). Treg also express cytotoxic T-lymphocyte-associated antigen 4 (CTLA-4), L-selectin, CD134 (OX40), and glucocorticoid-induced tumor necrosis factor receptor (GITR). Several studies support a role for FOXP3 as the master regulator of Treg development and function [254]. FOXP3 interacts with other transcription factors such as nuclear factor activated in T cells (NFAT) and acute myeloid leukemia 1 (AML1), represses genes involved in T cell activation such as IL-2, and induces expression of CD25 and CTLA-4 [255]. Mutation in the FOXP3 gene results in the autoimmune disorder Immunodysregulation polyendocrinopathy enteropathy X-linked (IPEX) syndrome in humans and Scurfy phenotype in mice [253]. Regulatory function has also been observed in activated CD8+ cells during inflammatory processes [256, 257].

7.1.3.2.1 Mechanisms of Treg action

Treg exert their immune-suppressive effects via several mechanisms (Figure I-7). Treg produce anti-inflammatory cytokines IL-10, TGF-β, and IL-35. IL-10 signaling via its receptor suppresses cytokine secretion by macrophages, Th1 and Th2 cells, promotes cell survival, and impairs APC activity [258, 259].

TGF-β can induce generation of T suppressor cells in the periphery [260, 261], but is not required for nTreg activity [262]. Besides inhibiting immune cells, TGF-β also suppresses proliferation and migration, and stimulates apoptosis of VSMCs and ECs [263]. However, TGF-β has a dual role in the vasculature in that it can also induce fibrosis. IL-35 is a relatively novel anti-inflammatory cytokine that is known to inhibit Th17 development [264].

Treg express galectin-1, which binds to CD45 and other glycoproteins on immune cells and promotes cell-cycle arrest, apoptosis, and inhibition of pro-inflammatory cytokine release [265]. Treg also eliminate activated T effector cells by producing granzyme A and B, which induce apoptosis in target cells via mechanisms that remain to be fully elucidated [266, 267]. Treg inactivate extracellular pro-inflammatory ATP released during tissue damage via CD39, which works with CD73 to degrade ATP and produce adenosine [268, 269]. Adenosine acts via A_{2A} adenosine receptors to inhibit T effector cells.

Treg also inhibit T effector activation by limiting APC responses. *In vitro*, it has been shown that the expression of co-stimulatory molecules on dendritic cells is downregulated by Treg partially via the anti-inflammatory signaling of TGF-β [270]. Moreover, CTLA-4 expressed on the surface of Treg blocks co-stimulation by interacting with B7 ligands (CD80 and CD86) on dendritic cells, which leads to reduced expression of these ligands [271]. Treg also interact with dendritic cells via Neuropillin-1, thereby preventing the interaction of the latter with T effector cells [272]. Finally, fibrinogen-like protein 2 (FGL2) produced by Treg inhibits dendritic cell maturation and proliferation [273].

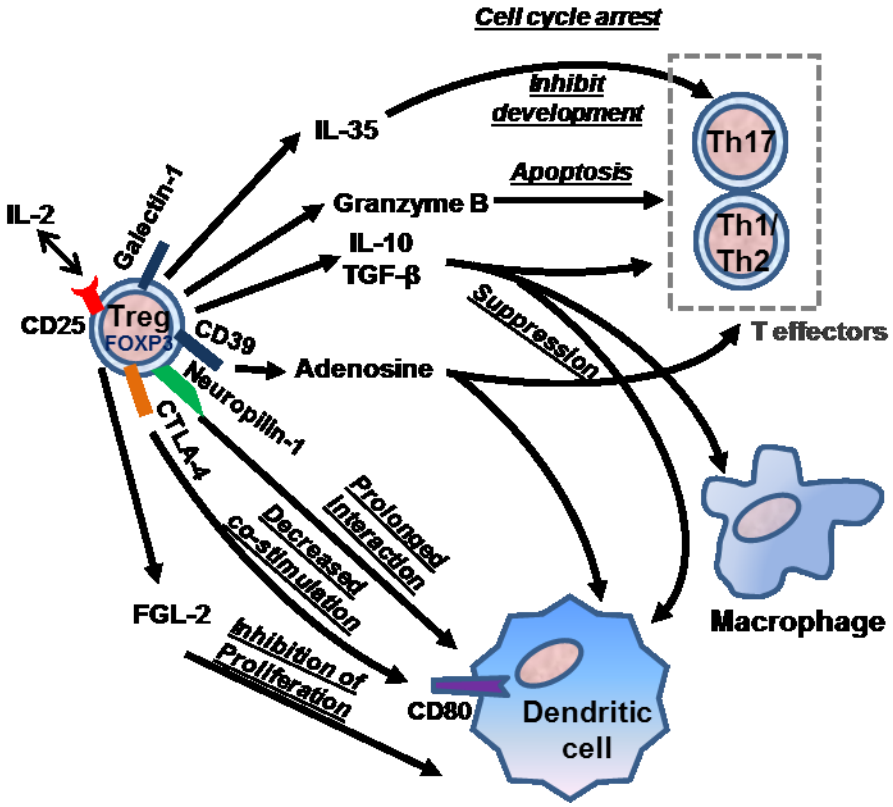

Figure I-7: Mechanisms of Treg action. Adapted from Schiffrin [274].

7.1.3.2.2 Treg and cardiovascular disease

Depletion of Treg by anti-CD25 antibody was shown to enhance atherosclerosis lesion size, inflammation, and vulnerability in Apoe$^{-/-}$ mice [275]. Apoe$^{-/-}$ mice adoptively transferred with CD4^{+}CD25^{+} Treg population exhibited reduced lesion size compared to mice injected with saline or CD4^{+}CD25^{-} T effector cells [275, 276]. The production of IL-10 and TGF-β by Treg is important for their anti-atherogenic effects. Disrupting the function or gene for either cytokine in atherosclerosis-prone mouse models accelerated lesion development (studies reviewed in [277]). Recently, Klingenberg *et al.* [278] elegantly demonstrated a mechanistic role for transcription factor FOXP3 in Treg-mediated athero-protection. In their study, lethally irradiated Ldlr-/- mice were transplanted with bone marrow from DEREG mice, which expresses the diphtheria toxin

receptor under control of the FOXP3 promoter. Diphtheria toxin-mediated depletion of $FOXP3^+$ Treg in transplanted mice enhanced atherosclerosis without increasing vascular inflammation. These mice exhibited altered lipoprotein metabolism and clearance, resulting in increased cholesterol-rich particles in the circulation, which explained the exaggeration in plaque formation.

A protective role for Treg during HTN was first suggested using consomic rats, which had chromosome 2 from normotensive Brown Norway rats on a genetic background of the hypertensive Dahl salt-sensitive rats [279]. Chromosome 2 contains many pro-inflammatory genes, including IL-2, IL6, fibroblast growth factor 2, and vascular cell adhesion molecule (VCAM)-1 [280]. The vessels from consomic rats exhibited reduced production of pro-inflammatory cytokines, compared with Dahl salt-sensitive rats, which was associated with enhanced aortic expression of FOXP3 and increased $CD4^+CD25^+$ and $CD8^+CD25^+$ lymphocytes and their activity [279]. Adoptive transfer of $CD4^+CD25^+$ Treg was shown to blunt HTN, small artery stiffness, $\bullet O_2^-$ production, and infiltration of vascular immune cells in Ang II-infused mice [281]. In a previous study, Ang II-induced cardiac remodeling was reversed by $CD4^+CD25^+$ Treg transfer in a blood pressure independent manner [282]. Aldosterone-infused mice adoptively transferred with CD4+ CD25+ Treg exhibited reduced small artery remodeling and oxidative stress, and vascular and renal immune cell infiltration without changing blood pressure [283]. IL-10-deficient mice (*Il10*$^{-/-}$) treated with Ang II exhibited increased $\bullet O_2^-$ production and enhanced impairment of acetylcholine-induced relaxation in vessels compared with wild-type mice [284]. Systolic blood pressure, nicotinamide adenine dinucleotide phosphate (NADPH) oxidase activity and endothelium-dependent relaxation was improved in AngII-infused *Il10*$^{-/-}$ mice receiving cultured Treg from control mice [285]. Together, this evidence provides preliminary support for a protective role for Treg in HTN via IL-10 production. However, this does not conclusively prove the protective role of Treg in HTN and associated vascular injury since adoptive transfer of Treg could have had pharmacological effects that are non-physiological. To unambiguously demonstrate the role of Treg in HTN,

the use of a model in which this regulatory component of adaptive immunity is absent is mandatory. This demonstration has never been provided before.

7.1.3.3 Th17 response

Th17 cells are a relatively novel subset of $CD4^+$ T helper cells [286]. Cytokines TGF-β and IL-6 promote Th17 polarization whereas IL-23 plays a role in the maintenance of Th17 cells. Th17 cells and Treg can interchange phenotypes, depending on the ensuing cytokine milieu, since TGF-β also induces differentiation of naïve T helper cells into Treg. The presence of absence of IL-6 is critical in determining whether naïve or effector T cells differentiate into Treg or Th17 cells. Th17 cells produce cytokines such as IL-17 and IL-22 and participate in acute inflammatory responses against extracellular bacteria and fungi. Th17 cells are key contributors to chronic inflammation associated with autoimmune diseases. IL-17 can mediate strong pro-inflammatory responses by promoting leukocyte proliferation and chemotaxis [287]. As well, IL-17 can be anti-inflammatory by inhibiting expression of adhesion molecules and chemoattractants on fibroblasts [288]. Increased plasma concentrations of IL-17 in coronary artery disease patients suggests a pro-atherogenic role for Th17 cells in atherosclerosis [289]. However, experimental studies in atherosclerosis have yielded conflicting results on the roles of Th17 cells and IL-17 signaling in disease progression [290]. This discrepancy may be due to the dual role of IL-17 described above.

Ang II- [291] and DOCA-salt-induced [292] HTN is associated with increased Th17 cell activity. IL-17 knockout mice (*IL-17*$^{-/-}$) infused with Ang II exhibit blunted HTN, superoxide production and aortic collagen deposition, stiffening and T cell infiltration [291, 293]. Placental ischemic rats have been shown to have increased numbers of Th17 cells [294]. Administration of IL-17 soluble receptor C in reduced-uterine perfusion pressure (RUPP) rats, a model of preeclampsia, reduced HTN, oxidative stress, and circulating Th17 cells [295].

Together, this evidence supports a pathological role for Th17 cells and IL-17 in HTN.

7.1.3.4 Cytotoxic T cells

$CD8^+$ cells polarize to cytotoxic T cells upon activation by APCs [296]. Cytotoxic T cells secrete pro-inflammatory cytokines IFN-γ and TNF-α, and perform cytolytic activity in target cells by producing perforin and granzyme B. Perforin binds to target cell membranes, forming a pore through which granzyme B enters the cell and induces apoptosis [296]. Cytotoxic T cells can also trigger apoptosis via the Fas ligand on $CD8^+$ cells, which binds to FAS on target cells to initiate apoptotic signals [296]. Accumulation of cytotoxic T cells has been reported to occur from early stages in mouse lesions [297, 298] and in advanced human plaques [237]. Kyaw *et al.* [299] recently demonstrated that antibody-mediated depletion of $CD8^+$ cells in HFD-fed *Apoe*$^{-/-}$ mice reduced atherosclerosis, macrophage accumulation, necrotic cores, and expression of pro-inflammatory cytokines IL-1β and IFN-γ. Transfer of $CD8^+$ T cells into lymphocyte-deficient *Apoe*$^{-/-}$ mice restored plaque progression and pro-inflammatory responses. The role of cytotoxic T cells in HTN and associated vascular injury is less well understood. Adoptive transfer of wild-type bone marrow into inhibitor of differentiation 2 knockout mice, which are deficient in specialized $CD8^+$ dendritic cells, natural killer cells and $CD8^+$ T memory lymphocytes, was unable to restore Ang II-mediated pressor responses, suggesting that cytotoxic T cells do not play a role in Ang II-induced HTN [300]. In another study, Ang II-induced arteriolar thrombosis in cremaster arterioles was found to be blunted in *Rag1*$^{-/-}$ and $CD4^+$ T cell-deficient mice, while $CD8^+$ T cell-deficient mice had an intermediate phenotype [301]. Thus, $CD8^+$ T cells may participate to some extent in Ang II-induced microvascular thrombosis.

Studies mentioned above suggest an important role for several immune cells in the vascular pathology associated with atherosclerosis and HTN.

Inflammatory response in the vascular wall begins with recruitment of immune cells to target regions.

7.2 The inflammatory response

In atherosclerosis, accumulation of oxidized LDL within the vascular wall is thought to be the primary initiator of inflammatory responses that leads to plaque formation [302]. Mechanisms that initiate vascular inflammatory responses observed in HTN are less well understood [303]. However, certain elements of the inflammatory response are common to the vascular pathology in both atherosclerosis and HTN, suggesting that similar mechanisms may be involved. In this section, the general features of leukocyte infiltration and initiation of the vascular inflammatory cascade will be described, and evidence for involvement of some of these features in CVD provided.

Leukocyte trafficking is an important mechanism of immune surveillance that allows immune cells to migrate between peripheral tissues and provide immune responses where required [304]. Immune cell infiltration involves a sequence of steps mediated by various interactions with ECs.

7.2.1 Leukocyte capturing, rolling and firm adhesion

Leukocyte infiltration is initiated by pro-inflammatory stimuli such as chemokines secreted by affected vascular cells, especially ECs (Figure I-8). Chemokines are secondary mediators of inflammation that stick to glycosaminoglycans on the surface of ECs and bind to specific receptors on immune cells to initiate leukocyte recruitment [305]. Perhaps the most studied chemokine is monocyte chemoattractant protein (MCP)-1, which binds to chemokine receptor (CC) R2 to promote the recruitment of monocytes, and T and B cells to the vascular wall [306]. MCP-1 has been shown to be upregulated in the vascular wall during both atherosclerosis [307] and HTN [308]. IL-8, produced by homed macrophages and other cells in the vascular wall, is another

important chemotactic factor that causes migration of neutrophils to the sites of inflammation [306].

Leukocyte capturing is followed by cell rolling, which occurs due to dissociation of old bonds and the formation of new bonds between ECs and infiltrating immune cells [309]. Leukocyte rolling is mediated by interaction between special adhesion molecules called selectins and their respective ligands. These adhesion molecules include P-selectin, E-selectin, and L-selectin. The expression of P-selectin and E-selectin is upregulated on ECs during inflammatory conditions, while L-selectin is constitutively expressed by leukocytes [310]. Whereas our understanding of the involvement of L-selectin in CVD is incomplete, knockout studies have revealed a role for P-selectin and E-selectin in atherosclerosis progression [311]. As well, soluble forms of P-selectin and E-selectin have been shown to be increased in patients with HTN and may contribute to vascular damage by facilitating leukocyte recruitment [312].

Following cell rolling, leukocytes undergo firm adhesion to the inflamed ECs. This step involves the interaction between integrins expressed on infiltrating leukocytes and their ligands on ECs. Integrins studied most include lymphocyte function-associated antigen-1 (LFA-1) and very late antigen-4 (VLA-4) that bind to their ligands intracellular adhesion molecule-1 (ICAM-1) and VCAM-1, respectively. Inflammatory mediators such as TNF-α increase the expression of both ICAM-1 and VCAM-1 on ECs [313]. Vascular injury during atherosclerosis and HTN is associated with upregulation of ICAM-1 and VCAM-1 expression [279, 314].

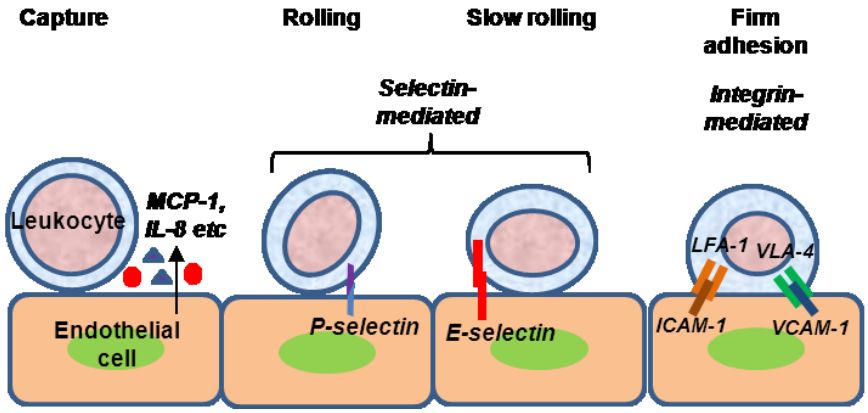

Figure I-8: Steps in leukocyte recruitment.

Integrin-immunoglobulin complex formation also triggers intracellular signaling pathways. Binding of VCAM-1 to VLA-4 leads to activation of Rac1 and p38 mitogen-activated protein kinase (p38 MAPK), ROS production and actin skeleton rearrangement [315, 316]. ROS can cause the proteolytic degradation of junctions between ECs via the induction of MMP activity [315]. Moreover, downstream signaling by ICAM-1 mediates intracellular Ca^{2+} release and Rho GTPase activation, which can break down homophilic interactions [317]. Collectively, these signaling pathways increase endothelial permeability to facilitate leukocyte transmigration.

7.2.2 Leukocyte transmigration

Intracellular free Ca^{2+} concentrations regulate leukocyte transmigration to the sub-endothelial layer. Increase in free Ca^{2+} indirectly results in unfolding of myosin II and retraction of endothelial cell [318]. Leukocyte transmigration is the least well understood step of the leukocyte recruitment cascade, and occurs either via the paracellular pathway or the transcellular pathway (Figure I-9). The pathway adopted by infiltrating immune cells is likely influenced by the stimulus for migration, the prevailing inflammatory conditions and the vascular bed involved [319].

Most of leukocyte transmigration occurs via the paracellular route [320]. This pathway involves the destabilization of cell-cell junctions followed by migration of leukocytes through inter-endothelial contacts. The molecules that regulate leukocyte transmigration via the paracellular pathway include vascular endothelial (VE)-cadherin, platelet-endothelial adhesion molecule-1 (PECAM-1), CD99 and the junctional adhesion molecules (JAM)-A, -B, and -C. VE-cadherins on neighboring ECs complex together in a Ca^{2+}-dependent manner to maintain endothelial junction integrity [321]. Proteolytic cleavage of the extracellular domain of VE-cadherins decreases junctions between ECs thereby increasing vascular permeability [322]. As well, binding of leukocytes to the luminal side of ECs can stimulate downstream signaling that results in the destabilization and disassembly of VE-cadherin complexes [323, 324]. Leukocytes then migrate through the gaps that are formed, facilitated by homophilic or heterophilic interactions between adhesion molecules PECAM-1, CD99, and the JAMs on ECs and infiltrating immune cells [325-327].

A fraction of leukocyte transmigration occurs through the endothelium at non-junctional sites, which is referred to as the transcellular pathway. Transcellular migration occurs specifically where the endothelium is thin and is dependent on intracellular events triggered by LFA-1 binding to ICAM-1 [328, 329]. Interaction of LFA-1 with ICAM-1 stimulates translocation of ICAM-1 to regions that are rich in caveolae (vasiculo-vacuolar organelles) and F-actin (cytoskeleton), forming an intracellular channel via which caveolae transports leukocytes along with caveolin-1 through ECs [329].

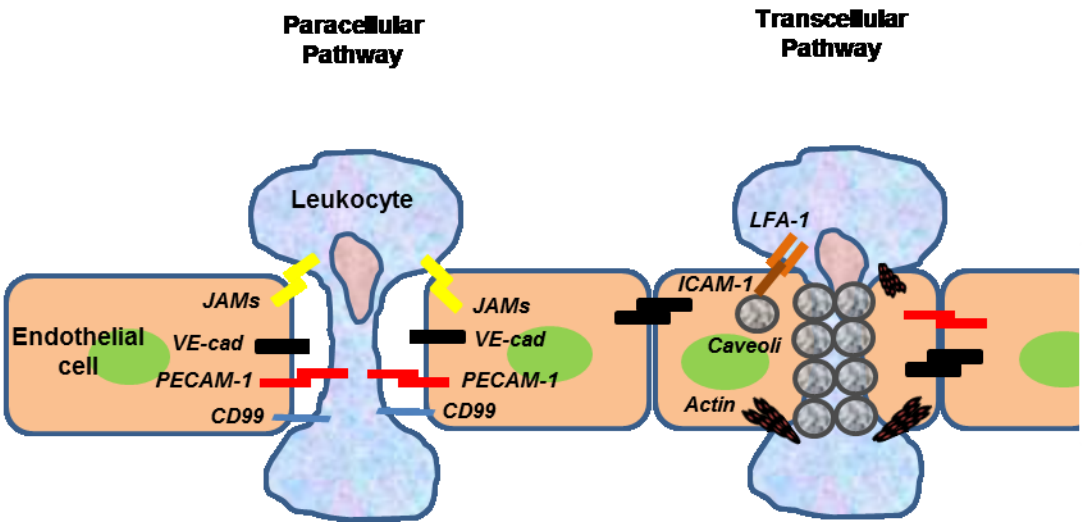

Figure I-9: Pathways of leukocyte transmigration through the endothelium. Figure adapted from Ley *et al.* [309].

7.2.3 Inflammatory responses within the vascular wall

Following transmigration through the endothelial layer, leukocytes migrate within the vascular wall. Chemoattractants such as RANTES (CC-chemokine ligand 5, CCL5), IL15, MCP-1, and IL-8 are produced by ECs, VSMCs and/or macrophages to attract and facilitate the migration of immune cells that express the corresponding receptors for these molecules. RANTES attracts cells expressing CCR1 and CCR5 including macrophages, dendritic cells, lymphocytes, and natural killer cells [238]. IL-15 is released in response to IFN-γ and stimulates the migration of T cells [330]. MCP-1, as discussed previously, attracts macrophages and lymphocytes that express CCR2. Finally, IL-8 is a chemoattractant for cells expressing CX-chemokine receptor (CXCR) 1 and CXCR2 including leukocytes [331].

Within the medial layer, leukocytes undergo differentiation, growth or activation [238]. Monocytes differentiate into mature macrophages and produce a range of pro-inflammatory cytokines. T cells undergo peripheral activation by dendritic cells and macrophages to differentiate into Th1 or Th2 phenotype,

depending on the ensuing cytokine microenvironment. Activated T cells also produce pro-inflammatory cytokines. Pro-inflammatory mediators in turn have multiple effects on the vasculature. Cytokines enhance expression of adhesion molecules (endothelial cell activation), disrupt cell-cell junctions to increase vascular permeability, increase MMP expression to promote extracellular matrix remodeling, and also stimulate VSMC migration and proliferation [202, 238, 332].

T cells also undergo differentiation into the anti-inflammatory Treg when they are activated by immature dendritic cells [238, 333]. Treg counteract Th1 and Th2 responses to reduce the pro-inflammatory cytokine microenvironment. Macrophages can also elicit anti-inflammatory properties by producing cytokines such as IL-10 and TGF-β that further blunt Th1 responses and induce Treg differentiation. Anti-inflammatory mechanisms serve to moderate inflammatory responses, and play a role in resolution of inflammation after injury repair [334]. The role of anti-inflammatory macrophages in context of vascular inflammation in atherosclerosis and HTN is still unclear.

7.3 Oxidative stress

ROS are biologically active derivatives of O_2 that are known to be important regulators of vascular function by modulating cell growth, apoptosis, inflammation, and extracellular matrix production [335]. Oxidative stress is the consequence of imbalance in pro-oxidant and anti-oxidant capacities in favor of the former, resulting in excess ROS. There is ample evidence that oxidative stress contributes to the progression of hypertension and atherosclerosis [335-337]. Anti-oxidants counter the development of atherosclerosis [338], and reduce blood pressure in experimental [339] and human HTN [340]. Oxidative stress can upregulate intracellular inflammatory signaling pathways and modify proteins, lipids, and DNA resulting in altered structure and function [341]. Oxidative stress is a potent inductor of endothelial dysfunction, vascular inflammation, and vascular remodeling.

Oxidative stress occurs predominantly as a consequence of increased production of $\bullet O_2^-$, which can be further converted to other forms of ROS including hydrogen peroxide (H_2O_2), hypochlorus acid (HOCl) and hydroxyl radicals (•OH) or reactive nitrogen species such as $ONOO^-$ (Figure I-10) [342]. $\bullet O_2^-$ has a short half-life and is quickly converted into H_2O_2 by the enzyme copper/zinc superoxide dismutase. H_2O_2 is then converted into water, a reaction that is catalyzed by catalase, glutathione peroxidase or thioredoxin reductase. As well, H_2O_2 can be catalyzed to HOCl by the enzyme myeloperoxidase, or be transformed to •OH in the presence of Fe^{3+}. As mentioned previously, $\bullet O_2^-$ can also react with NO to form $ONOO^-$. $ONOO^-$ can interact directly or indirectly with lipids, DNA, and proteins to trigger a range of cellular responses from minor modulation in cell signaling to excessive oxidative injury that causes necrosis or apoptosis [343]. $ONOO^-$ generation is a hallmark pathogenic mechanism in chronic inflammatory diseases, CVDs, and cancer.

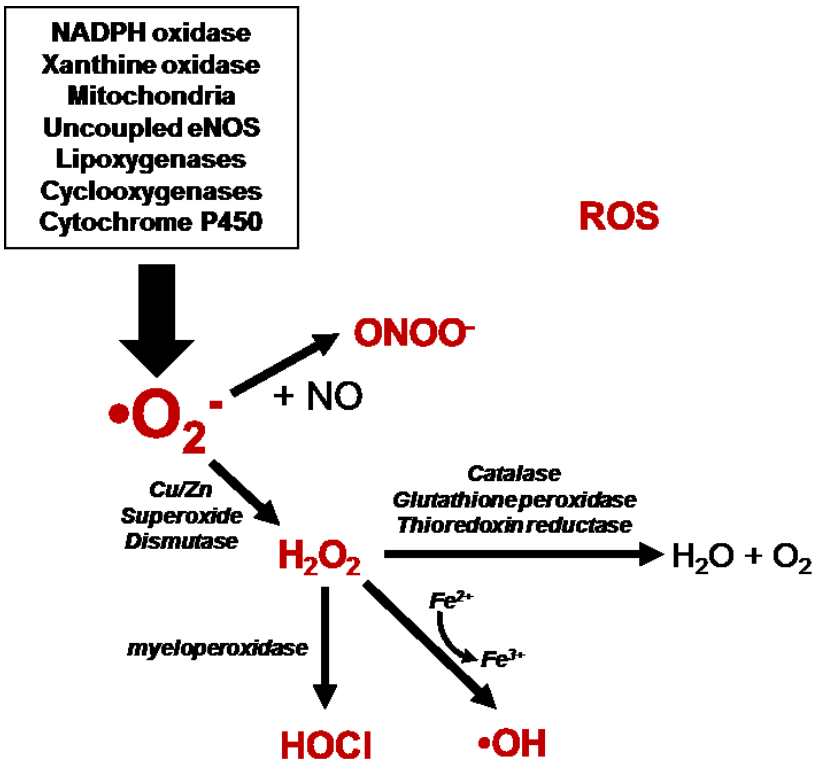

Figure I-10: ROS and their sources. Adapted from Madamanchi *et al.* [109].

Both vascular and immune cells contribute to ROS formation in the vasculature via the activity of several enzymes. The major sources of vascular ROS include NADPH oxidase, xanthine oxidoreductase, uncoupled eNOS, and the mitochondria. COX, lipoxygenases, and cytochrome P450 are other enzymes that also contribute to ROS production but to a lesser extent.

7.3.1 NADPH Oxidase

NADPH oxidase is the major source of $\bullet O_2^-$ production in vascular and immune cells. This enzyme generally consists of a heterodimer of two membrane-bound subunits, $gp91^{phox}$ and $p22^{phox}$, and up to three cytosolic components $p47^{phox}$, $p67^{phox}$ and G-protein rac1 or rac2 that regulate the activity of the enzyme [344]. The cytoplasmic subunits are recruited upon activation to the membrane-bound $gp91^{phox}/p22^{phox}$ heterodimer to form a multi-protein complex of NADPH oxidase that produces $\bullet O_2^-$. $gp91^{phox}$, otherwise known as Nox, is the catalytic subunit of the enzyme and exists as different isoforms (Nox1, Nox2, Nox 3, Nox4 and Nox5) depending on cell type. Nox2 and all other components of the enzyme are present in phagocytic cells, ECs and adventitial fibroblasts [344-346]. VSMCs, on the other hand, have the $gp91^{phox}$ homologues Nox1, Nox2, Nox4 and/or Nox5 (present only in humans) depending on the vascular bed studied [344]. In addition, VSMCs do not appear to possess the cytosolic subunit $p67^{phox}$ [347]. Vascular oxidases produce several orders of magnitude less $\bullet O_2^-$ than phagocytic oxidases [348].

Production of $\bullet O_2^-$ by NADPH oxidase occurs in normal metabolism, but sustained activation can ensue in response to agonists such as Ang II and ET-1 [349-351]. Oxidative stress as a consequence of sustained NADPH oxidase activity is important in progression of atherosclerosis and HTN. Hypercholesterolemic *Apoe*$^{-/-}$ mice lacking the $p47^{phox}$ gene exhibited significantly fewer lesions in their descending aortas compared with *Apoe*$^{-/-}$ mice [352]. Treatment of hypercholesterolemic rabbits prone to atherosclerosis with

AT_1R antagonists normalized vascular NADPH oxidase activity and reduced early plaque formation [353], suggesting that Ang II-induced NADPH oxidase activity plays an important role in the early stages of atherosclerosis. In context of HTN, deletion of the Nox1 gene, which is expressed in VSMCs, blunted Ang II-induced blood pressure rise [354]. Beyond the activity of vascular oxidases, NADPH oxidase in immune cells also play an important role in pathophysiology of vascular diseases. Guzik *et al.* demonstrated that while reconstitution of T cells into immunodeficient *Rag1*$^{-/-}$ mice restored Ang II-induced HTN and vascular dysfunction, adoptive transfer of T cells lacking the $p47^{phox}$ subunit was unable to fully reinstate the Ang II phenotype [240]. Thus, NADPH oxidase activity may be critically involved in the vascular damage observed in the course of progression of atherosclerosis and HTN.

7.3.2 Xanthine oxidoreductase

Xanthine oxidoreductase (XOR) is a molybdoflavoenzyme consisting of two interchangeable forms, xanthine dehydrogenase (XDH) and xanthine oxidase (XO). XOR generates $\bullet O_2^-$ while catalyzing the conversion of hypoxanthine and xanthine to uric acid. Transcription factors NFκB and activator protein (AP)-1 regulate the activity of XOR. Pro-inflammatory stimuli including lipopolysaccharide and cytokines as well as phosphorylation by p38 MAPK upregulate the expression of XOR [355]. XO exists in plasma and ECs but not in VSMCs [337].

XOR is an important source of oxidative stress under pathophysiological conditions. Ang II increases the expression and activity of XO in cultured ECs [356]. Increased activity of XO was associated with endothelial dysfunction as a consequence of enhanced vascular $\bullet O_2^-$ production by the enzyme [357]. XO inhibitor oxypurinol normalized $\bullet O_2^-$ production in the vessels of hypercholesterolemic rabbits [358]. In coronary artery disease patients, endothelial XO expression and activity were shown to be increased [357, 359, 360], and were correlated with endothelial dysfunction [357]. In animal models of

genetic and salt-sensitive HTN, XO inhibitors allopurinol and oxypurinol prevented blood pressure rise [361]. Treatment with ET_AR antagonist was shown to reduce XO-mediated $\bullet O_2^-$ production in mesenteric arteries of DOCA-salt rats, indicating that ET-1 signaling activates XO in salt-induced HTN [362].

7.3.3 Mitochondria

Mitochondria are important organelles that produce energy in the form of adenosine triphosphate (ATP) through oxidative phosphorylation [109]. Electron transport carriers within the mitochondria transfer electrons from NADH or FADH2 to molecular oxygen, forming ATP in the process. The electron transport chain consists of complex I (NADH-ubiquinone oxidoreductase), complex II (succinate-ubiquinone oxidoreductase), complex III (ubiquinol-cytochrome c reductase), and complex IV (cytochrome c oxidase). Normally, some electrons escape the electron transport chain to form $\bullet O_2^-$, which is immediately sequestered by mitochondrial superoxide dismutase (SOD2). Under pathophysiological conditions, however, uncoupling of the electron transport chain leads to increased $\bullet O_2^-$ production by complexes I and III [363, 364].

Enhanced mitochondrial ROS formation may contribute to the progression of atherosclerosis and HTN. Atherosclerosis development in *Apoe*$^{-/-}$ mice was correlated with mitochondrial DNA damage [365], which occurs as a consequence of enhanced mitochondrial ROS production [366]. Moreover, *Apoe*$^{-/-}$ mice deficient in SOD2 exhibited increased early mitochondrial DNA damage as well as an accelerated atherogenesis [365]. Partial or complete SOD2 deficiency was also associated with salt-sensitive hypertension and accelerated renal senescence [367]. However, the direct evidence for exactly how mitochondrial ROS contributes to the development of atherosclerosis and HTN is lacking. Mitochondrial ROS act as signal-transducing molecules that provoke endothelial dysfunction, enhance infiltration and activation of inflammatory cells, and increase apoptosis of ECs and VSMCs [368]. It is likely that the role of

mitochondrial ROS in these processes enables them to contribute to vascular pathology in CVD.

7.3.4 Other sources of ROS

Other enzymes can also produce ROS in the vasculature, Uncoupled eNOS is a major source of $\bullet O_2^-$ that has already been described in the previous section. The inducible COX2 is another source of ROS that is increased during inflammatory responses. COX2 is implicated in the pathogenesis of atherosclerosis and HTN. Selective COX-2 inhibition has been shown to reduce atherosclerosis in female *Apoe*$^{-/-}$ mice [369]. Moreover, deletion of the COX-2 gene resulted in blunted Ang II-induced oxidative stress and hypertension [370]. Lipoxygenases can also contribute to vascular ROS during atherosclerosis and HTN. Activated T cells require lipoxygenases for the production of ROS [371]. Disruption of the 12/15-lipoxygenase gene diminished atherosclerosis in ApoE-deficient mice [372], and inhibition of lipoxygenase pathway reduced blood pressure in renovascular hypertensive rats [373]. The role of cytochrome P450 superfamily in cardiovascular physiology and disease is less well understood. However, evidence from inhibition studies suggest a role for cytochrome P450 in enhancing endothelial dysfunction in coronary artery disease patients [374], as well as in the development of Ang II-induced HTN [375].

7.3.5 Oxidative stress, inflammation and vascular damage

ROS can mediate inflammatory responses in the vasculature in a number of ways (Figure I-11) [340]. Intracellular ROS activate redox-sensitive transcription factors (NFκB, AP-1 and hypoxia-inducible factor-1 (HIF-1)) to upregulate the expression of pro-inflammatory cytokines, chemokines and adhesion molecules. ROS can also enhance the activity of several kinases that influence cell proliferation and growth. Inactivation of phosphatases through

oxidation by ROS further amplifies signaling via kinases. Activation of MMPs and TIMPs by ROS can lead to extracellular matrix remodeling thereby altering the vascular structure and mechanical properties. ROS can affect vasoactivity directly by stimulating Ca^{2+} and K^{+} channels on the plasma membrane or indirectly by reducing NO bioavailability. ROS can also cause cell cycle arrest, which may influence cell growth and apoptosis. Uncontrolled activation of redox-sensitive cellular responses as a result of enhanced ROS production could therefore contribute to vascular inflammation and damage observed in atherosclerosis and HTN [340]. It is, however, unknown if ET-1-induced ROS production is a mechanism that contributes to atherosclerosis progression and AAA formation.

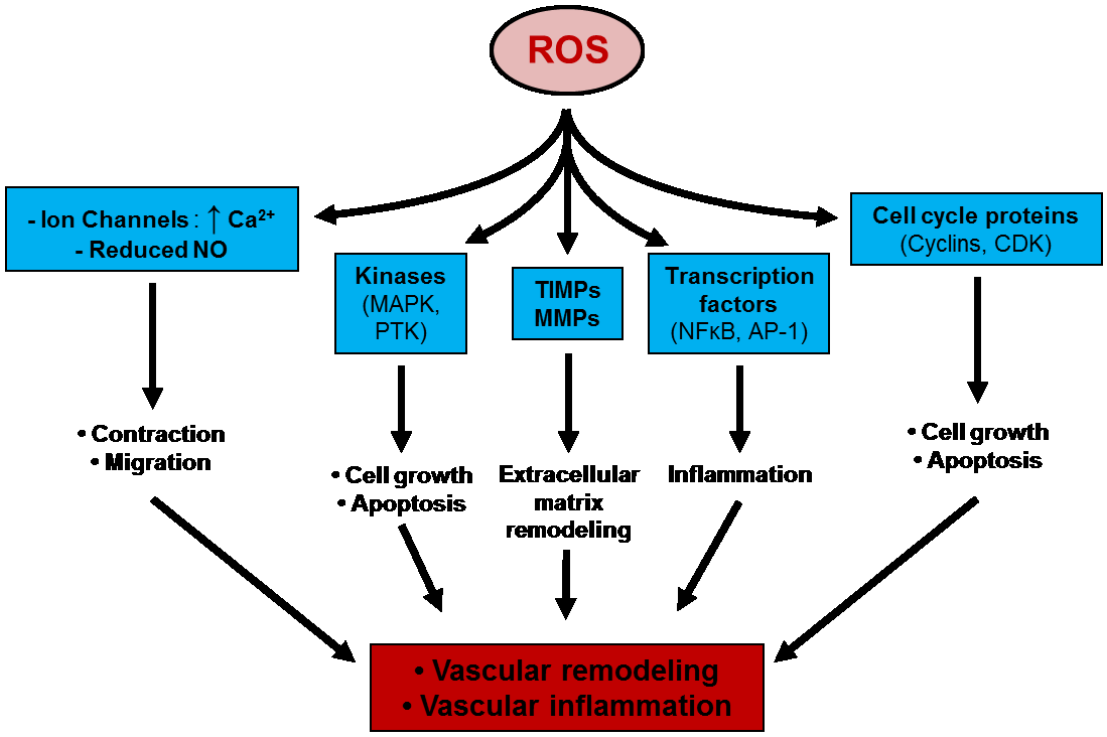

Figure I-11: Redox-dependent signaling pathways leading to vascular inflammation and damage. Adapted from Paravicini and Touyz [340].

7.4 Signaling pathways in vascular inflammatory responses

During inflammatory conditions, activation of signal transduction pathways propagate vascular inflammatory responses. Signal transduction pathways involved in vascular inflammation are complex and interlinked, and are mediated by the activity of multiple factors that include kinase families such as MAPK and phosphoinositide 3-kinase (PI3K), transcription factors (e.g. NFκB) and nuclear receptors (e.g. mineralocorticoid receptor (MR) and peroxisome proliferator-activated receptors (PPARs)). Some of these factors will be briefly described here to reflect the importance of signaling pathways in vascular inflammation.

7.4.1 Kinases

Kinases are enzymes that catalyze the transfer of phosphate groups from high-energy, phosphate-donating molecules to specific substrates [376]. The activity of these enzymes are critical for several cellular processes including metabolism, cell signaling, protein regulation, cellular transport, and secretion. MAPK and PI3K are two super-families of kinases that are important mediators in vascular inflammatory responses.

MAPK are member of the serine/threonine kinases and consist of seven sub-families [377]. Extracellular signal regulated kinase (ERK) 1/2, p38 MAPK, and c-jun N-terminal protein kinase (JNK)/stress-activated protein kinase (SAPK) are the three major classes of MAPK in mammals. Activation of MAPK is dependent on upstream activation of threonine/tyrosine kinases by small G proteins and other molecules. Stimuli that engage the MAPK signaling pathways include growth factors, peptides such as Ang II and ET-1, and pro-inflammatory mediators (e.g. cytokines) [378-381]. The activity of MAPK is associated with hypertrophy, proliferation, contraction and inflammatory responses in vascular cells [378, 382, 383]. MAPK signaling pathways are also important in immune cells. p38 MAPK is a critical mediator of leukocyte endothelial transmigration and production of inflammatory mediators [378]. Peritoneal macrophages treated with

oxidized LDL exhibited enhanced signaling through ERK1/2, p38 MAPK and JNK [384], suggesting a role for MAPK signaling in foam cell formation during atherosclerosis. Treatment of macrophages with JNK inhibitors [384] or p38 MAPK inhibitors [385] blocked oxidized LDL-induced foam cell formation. In context of HTN, p38 MAPK inhibition has been shown to blunt endothelial dysfunction and blood pressure rise in Ang II-infused [386] and diabetic [387] rats.

PI3K constitutes a lipid kinase family divided into three classes [388]. Classes IA and IB are expressed in the heart and the vasculature, whereas Class II is expressed in cardiac and hepatic tissues. PI3K are activated either by GPCRs, in response to stimuli such as Ang II and ET-1, or by tyrosine kinase receptors [388, 389]. Upon activation, PI3K phosphorylates phosphatidylinositols to yield lipid byproducts that can activate another important signaling mediator protein kinase B (PKB/Akt). The PI3K/Akt/PKB signaling axis mediates several cellular responses including proliferation, differentiation, chemotaxis, and survival [390]. Activity of PI3K is associated with vascular remodeling [391] and endothelial dysfunction [392]. As well, PI3K signaling plays an important role in inflammatory responses in vascular and immune cells. PI3K signaling has been implicated in T cell activation and neutrophil migration [393], macrophage migration and pro-inflammatory cytokine production [394, 395], and expression of VCAM-1 and ICAM-1 in ECs [396]. The PI3K/Akt signaling also indirectly activates NFκB, a strong pro-inflammatory transcription factor that will be discussed next.

7.4.2 Transcription factors

The transcription factor NFκB is a critical mediator of inflammatory responses. NFκB functions as a heterodimer, with the p50/p65 complex most abundantly found [397]. In its inactive state, NFκB is bound to the natural inhibitor of kappa B (IκB), which sequesters the transcription factor in the cytosol by preventing its translocation into the nucleus. Under inflammatory conditions, IκB

is phosphorylated by IκB kinase (IKK) and degraded by the proteasome, leaving NFκB free to translocate to the nucleus. Within the nucleus, NFκB upregulates the expression a many pro-inflammatory genes, which include chemokines and chemoattractants, adhesion molecules, cytokines, MMPs, iNOS, COX2, and MHC class I and II molecules, in a stimulus and cell-type specific manner [398, 399]. Other functions of NFκB include control of cell survival, differentiation and proliferation [399, 400]. Multiple signaling pathways mediated by cytokines, ROS and GPCRs can lead to NFκB activation. Vasoactive peptides such as Ang II and ET-1 are known to activate vascular NFκB [97, 401].

NFκB activity is strongly implicated in CVD, including atherosclerosis and HTN. Endothelium-specific inhibition of NFκB p65 activation led to decreased expression of adhesion molecules, cytokines and chemokines, reduced macrophage infiltration, and blunted plaque development in the aorta of *Apoe*$^{-/-}$ mice [402]. In advanced atherosclerotic lesions, nuclear localization of NFκB was observed in not only ECs but also VSMCs, macrophages and T cells [403]. In addition, NFκB activation in ECs has been associated with hypertension, and endothelial cell-specific NFκB suppression attenuated hypertension-induced renal damage [404].

Other transcription factors that are involved in inflammatory responses include AP-1 and NFAT, which play a role in cell differentiation and proliferation, and pro-inflammatory cytokine production [405-408].

7.4.3 Nuclear receptors

Nuclear receptors are transcription factors broadly divided into three families: steroid (e.g. MR) and thyroid hormone receptors, orphan receptors and adopted orphan receptors (PPARs) [409]. Upon binding of their ligand, nuclear receptors translocate from the cytoplasm, where they exist in complexes with chaperone proteins, into the nucleus to exert pro-inflammatory or anti-inflammatory effects, depending on the receptor family studied. Only the MR and PPARs will be briefly described here for completeness.

The main physiological function of MR is in the kidneys to regulate salt-water balance. However, MR activation has also been demonstrated to contribute to tissue oxidative stress and vascular inflammation [410]. Some of the target genes of MR include ACE and ET-1, which are involved in inflammatory responses. The pro-inflammatory activity of MR has been implicated in CVD. Activation of MR by aldosterone, one of the best known agonists, increases blood pressure and induces vascular inflammation, remodeling, hypertrophy, and fibrosis in animal models [411, 412]. Antagonism of MR has been shown to reduce blood pressure and vascular damage in human [413] and experimental HTN [414]. Aldosterone infusion in *Apoe*$^{-/-}$ mice increased early atherosclerosis and promoted an inflammatory plaque phenotype [415]. Moreover, MR antagonism improved endothelial function and reduced $\bullet O_2^-$ production in diet-induced atherosclerosis [416]. Together, this evidence shows that MR signaling contributes to vascular inflammation and damage during atherogenesis and HTN.

PPARs are a family of adopted orphan receptors that exist as three isoforms: PPARα, PPARβ/δ and PPARγ. Upon ligand binding, PPARs interact with the nuclear receptor 9-cis retinoic acid receptor (RXR) and other co-activators to exert various effects [417]. PPARα has anti-inflammatory effects in vascular tissues that include interaction and repression of the pro-inflammatory transcriptional activity of NFκB and AP-1 [418], and reduction in the activity of vascular NADPH oxidase [419]. PPARβ/δ, which is expressed ubiquitously, has both deleterious and anti-inflammatory properties. While this PPAR can stimulate endothelial cell proliferation and angiogenesis [420], its effects also include reduction of expression or activity of MCP-1 and NFκB in macrophages and ECs [421, 422] as well as decrease in ROS generation in the vasculature [422]. PPARγ is most well-known for regulating genes that are involved in adipogenesis and insulin sensitivity [423, 424]. In addition, PPARγ is a strong suppressor of vascular inflammation, can mediate a range of anti-inflammatory effects in ECs, VSMCs, and immune cells in a cell-type specific manner [425]. The anti-inflammatory properties of PPARγ have been particularly well studied in context of CVD. Disruption of endothelial PPARγ enhanced diet-induced atherogenesis

in *LDL-R*$^{-/-}$ mice [426]. Treatment with PPARγ agonist rosiglitazone suppressed vascular inflammation and development of atherosclerosis in *LDL-R*$^{-/-}$ mice fed a Western-type diet [427] and in diabetic *Apoe*$^{-/-}$ mice [428]. Recent clinical trials have also demonstrated the beneficial effects of PPARγ agonists in preventing atherosclerotic disease [429, 430]. Inducible inactivation of PPARγ exaggerated Ang II-induced vascular remodeling, vascular inflammation, and endothelial dysfunction [431]. The protective role of VSMC PPARγ in Ang II-induced vascular injury could be mediated in part by regulation of Ang II stimulated MAPK and PI3K signaling pathways by the nuclear receptor [432].

8. Experimental animal models

Experimental animal models of atherosclerosis and HTN have been developed to mimic the human forms of these diseases. Pharmacological, genetic, and surgical manipulations of animal models help to dissect the underlying pathophysiological mechanisms that contribute to the progression of CVD. In this section, the animal models used for the research presented in this thesis will be briefly described.

8.1 Induction of atherosclerosis: the *Apoe*$^{-/-}$ mouse model

Mice are inherently resistant to the development of atherosclerosis as a result of rapid murine hepatic LDL clearance and HDL being the main carrier of cholesterol in the plasma [433, 434]. Mouse models of atherosclerosis have therefore been developed by disrupting a critical anti-atherogenic gene product involved in cholesterol metabolism. One of the most widely used murine models of atherosclerosis is the *Apoe*$^{-/-}$ mouse. These mice have spontaneous elevations of total plasma cholesterol and triglycerides and reduced HDL. Atherosclerotic plaque development in this mouse model resembles that of natural history of atherosclerosis progression in humans. Chow-fed *Apoe*$^{-/-}$ mice exhibit development of fatty streaks in the proximal aorta in as early as 3 months of age,

with intermediate lesions occurring around 15 weeks and advanced fibrous plaques appearing at 20 weeks of age [435]. The development of atherosclerosis in *Apoe*$^{-/-}$ mice is accelerated by a Western-type diet. Atherosclerotic plaques in *Apoe*$^{-/-}$ mice increase in both complexity and size with age [436]. Vascular remodeling, including wall calcification and thinning and elastic lamina fragmentation as well as inflammation are characteristic of atherosclerotic plaques in this mouse model [433, 436]. AAA formation in *Apoe*$^{-/-}$ mice is induced when the RAAS is activated such as by Ang II infusion [437].

Our lab previously generated transgenic mice overexpressing ET-1 in the endothelium (eET-1 mice) [135]. These mice exhibited increased expression of genes associated with lipid metabolism in the vascular wall. We further crossed eET-1 with *Apoe*$^{-/-}$ mice to yield eET-1/ *Apoe*$^{-/-}$ mice. eET-1/ *Apoe*$^{-/-}$ mice have exaggerated plaque development compared to their *Apoe*$^{-/-}$ counterparts, suggesting a role for ET-1 in atherosclerosis progression. However, it is unclear whether ET-1 contributes to atherosclerosis progression beyond increasing lipid metabolism genes by also enhancing vascular inflammation.

8.2 Induction of hypertension: Ang II infusion

Various animal models are used to mimic and understand the heterogeneous etiology of human HTN [438]. Models of HTN include renovascular, renal parenchymal, pharmacologically-induced, environmentally-induced, and genetic models. Ang II-induced HTN in rodents is one of the most frequently used models to understand the pathophysiology of essential HTN associated with an activated RAAS. HTN is induced by Ang II infusion using osmotic mini-pumps to deliver the vasoactive peptide at a constant rate. Blood pressure elevation in this model is a consequence of VSMC contraction, sodium retention, activation of central and peripheral nervous systems, and increased synthesis of aldosterone [439]. Vascular pathology in Ang II-induced HTN is characterized by inward remodeling, endothelial dysfunction, and chronic low-grade inflammation [152, 182, 207]. Increased expression of adhesion

molecules, infiltration of immune cells, and enhanced ROS production signifies the inflammation in the vasculature in this model. Cardiac hypertrophy and renal damage are also observed in this form of HTN [440, 441].

9. Hypothesis and objectives

Under physiological conditions, inflammation is a highly regulated process. Pro-inflammatory and pro-oxidative mechanisms are counterbalanced to prevent tissue injury. The observation of vascular inflammatory responses in atherosclerosis and HTN suggests that homeostatic control of inflammation is impaired during disease progression. Autoimmune conditions are characterized by aberrant pro-inflammatory activation signals that persistently induce an inflammatory response and loss of anti-inflammatory moderation such as the immunosuppressive function of Treg. It is likely that analogous pathological mechanisms that result in chronic low-grade vascular inflammation are occurring during atherosclerosis and HTN. Ang II and ET-1 have been implicated in the pathophysiology of vascular damage in atherosclerosis and HTN. Both, Ang II and ET-1 are potent inducers of inflammation, and can promote activation and migration of pro-inflammatory immune cells into the vasculature. The vascular protective effect of increasing Treg population by adoptive transfer has been demonstrated in experimental models of atherosclerosis and HTN, suggesting that loss of Treg immune-moderation could be a contributing factor to enhanced vascular inflammatory responses during CVD. With this evidence in mind, we hypothesize that:

Dysregulated activation of immune-inflammatory mechanisms contributes to the progression of vascular damage in atherosclerosis and HTN

The main objectives of this thesis include:

- To determine whether ET-1 signaling enhances aortic injury and resistance artery dysfunction by promoting immune-inflammatory

responses in hyperlipidemia-induced atherosclerosis. We will use *Apoe*$^{-/-}$ mice with endothelium-restricted overexpression of ET-1 as a model of enhanced ET-1 signaling in atherosclerosis.

- To determine whether deficiency of anti-inflammatory Treg exaggerates microvascular injury by promoting immune-inflammatory responses in Ang II-induced HTN. We will use T and B cell-deficient *Rag1*$^{-/-}$ mice adoptively transferred with wild-type or FOXP3-deficient T cells, which lack Treg.

CHAPTER II: Activation of vascular immune-inflammatory responses by ET-1 signaling contributes to the progression of atherosclerosis and development of aortic abdominal aneurysms in hypercholesterolemic Apoe$^{-/-}$ mice

Hypothesis and objectives

Enhanced ET-1 signaling has been associated with the severity of atherosclerosis and incidence of aortic abdominal aneurysms (AAAs) in clinical and experimental studies. We previously showed that enhanced endothelial ET-1 expression exaggerates atherosclerosis in *Apoe*$^{-/-}$ mice [135]. However, mechanistic evidence of how ET-1 contributes to aortic injury in hyperlipidemic conditions is lacking. Transgenic mice overexpressing ET-1 specifically in the endothelium exhibit enhanced vascular inflammatory responses, characterized by increased infiltration of immune cells and enhanced oxidative stress production [135]. ET-1 can enhance vascular •O2^{-} production by activating enzymes NADPH oxidase and XO. Moreover, ET-1 can also stimulate various pro-inflammatory signaling pathways within vascular cells. In immune cells, ET-1 promotes migration and production of pro-inflammatory mediators [99-101]. It is possible to propose that vascular inflammatory responses induced by ET-1 signaling plays a role in the progression of atherosclerosis and development of AAAs under hyperlipidemic conditions. Therefore, we hypothesize that:

Activation of vascular immune-inflammatory responses by ET-1 signaling contributes to the progression of atherosclerosis and development of AAAs in hypercholesterolemic Apoe$^{-/-}$ *mice.*

The specific objectives of this study include:

- To characterize plasma lipids, aortic atherosclerotic plaques and AAA in our previously established model of exaggerated atherosclerosis as a result of endothelial ET-1 overexpression in hypercholesterolemic (HFD-fed) *Apoe*$^{-/-}$ mice.
- To determine whether ET-1-exaggerated atherosclerotic vascular injury is associated with enhanced vascular immune-inflammatory responses.

- To determine whether ET-1-exaggerated atherosclerotic vascular injury is associated with enhanced expression of activation/pro-inflammatory markers in splenic T cell subsets and monocytes.
- To identify potential vascular inflammatory mechanism(s) induced by ET-1 that could explain the enhanced atherosclerotic aortic injury.

Endothelin-1 overexpression exacerbates atherosclerosis and induces aortic aneurysms in apolipoprotein e knockout mice

Melissa W. Li*, Muhammad Oneeb Rehman Mian*, Tlili Barhoumi, Asia Rehman, Koren Mann, Pierre Paradis, Ernesto L. Schiffrin

Lady Davis Institute for Medical Research (M.W.L., M.O.R.M., T.B., A.R., K.M., P.P., E.L.S.), Department of Medicine (E.L.S.), and Department of Oncology (K.M.), Sir Mortimer B. Davis-Jewish General Hospital, McGill University, Montréal, Québec, Canada.

Published in:
Arteriosclerosis, Thrombosis, and Vascular Biology. 2013; 33: 2306-2315

*These authors contributed equally

The manuscript is presented here according to the instructions of the journal in which it was published. The main manuscript is followed by the Online Supplemental material (including the expanded materials and methods section).

Abstract

Objective: Endothelin (ET)-1 plays a role in vascular reactive oxygen species production and inflammation. ET-1 has been implicated in human atherosclerosis and abdominal aortic aneurysm (AAA) development. ET-1 overexpression exacerbates high-fat diet–induced atherosclerosis in apolipoprotein $E^{-/-}$ (*Apoe*$^{-/-}$) mice. ET-1–induced reactive oxygen species and inflammation may contribute to atherosclerosis progression and AAA development.

Approach and Results: Eight-week-old male wild-type mice, transgenic mice overexpressing ET-1 selectively in endothelium (eET-1), *Apoe*$^{-/-}$ mice, and eET-1/*Apoe*$^{-/-}$ mice were fed high-fat diet for 8 weeks. eET-1/*Apoe*$^{-/-}$ had a 45% reduction in plasma high-density lipoprotein ($P<0.05$) and presented ≥2-fold more aortic atherosclerotic lesions compared with *Apoe*$^{-/-}$ ($P<0.01$). AAAs were detected only in eET-1/*Apoe*$^{-/-}$ (8/21; $P<0.05$). Reactive oxygen species production was increased ≥2-fold in perivascular fat, media, or atherosclerotic lesions in the ascending aorta and AAAs of eET-1/*Apoe*$^{-/-}$ compared with *Apoe*$^{-/-}$ ($P<0.05$). Monocyte/macrophage infiltration was enhanced ≥2.5-fold in perivascular fat of ascending aorta and AAAs in eET-1/*Apoe*$^{-/-}$ compared with *Apoe*$^{-/-}$ ($P<0.05$). $CD4^+$ T cells were detected almost exclusively in perivascular fat (3/6) and atherosclerotic lesions (5/6) in ascending aorta of eET-1/*Apoe*$^{-/-}$ ($P<0.05$). The percentage of spleen proinflammatory Ly-$6C^{hi}$ monocytes was enhanced 26% by ET-1 overexpression in *Apoe*$^{-/-}$ ($P<0.05$), and matrix metalloproteinase-2 was increased 2-fold in plaques of eET-1/*Apoe*$^{-/-}$ ($P<0.05$) compared with *Apoe*$^{-/-}$.

Conclusions: ET-1 plays a role in progression of atherosclerosis and AAA formation by decreasing high-density lipoprotein, and increasing oxidative stress, inflammatory cell infiltration, and matrix metalloproteinase-2 in perivascular fat, vascular wall, and atherosclerotic lesions.

Keywords: cholesterol, HDL, elastin, fibronectin, inflammation, monocytes, oxidative stress, T lymphocytes

Introduction

Endothelin (ET)-1 is a 21-aa peptide discovered in endothelium but also produced by many other tissues. It is one of the most potent endogenous vasoconstrictors [1]. ET-1 plays an important role in the pathophysiology of cardiovascular disease by causing vascular damage [2, 3]. We have previously generated transgenic mice overexpressing ET-1 selectively in endothelium (eET-1) that exhibit increased ET-1 plasma levels, endothelial dysfunction and vascular remodeling, oxidative stress, and inflammation [4, 5]. ET-1 has also been implicated in the progression of atherosclerosis. ET-1 may participate in atherosclerosis by acting as a mitogen on vascular smooth muscle cells and potentiating cytokine release in atherosclerotic lesions [6-9], or by mediating vascular inflammation and neointima formation [10, 11]. Plasma and coronary artery ET-1 levels are elevated in early and advanced atherosclerosis in humans, and there is a relationship between plasma ET immune reactivity and severity of atherosclerosis [12, 13]. Aortic ET-1 levels are increased in Western diet–induced atherosclerosis in apolipoprotein E knockout (*Apoe*$^{-/-}$) mice [14] and low-density lipoprotein receptor knockout (*Ldlr*$^{-/-}$) mice [15]. Consistent with these observations, the development of atherosclerosis has been shown to be reduced by mixed $ET_{A/B}$ and selective ET_A receptor antagonists in Western-type diet–fed *Apoe*$^{-/-}$ mice [14, 16], *Ldlr*$^{-/-}$ mice [15], and hamsters [17].

Recently, we reported using DNA microarrays that eET-1 mice present changes in the expression of genes involved in lipid biosynthesis in the vascular wall [18]. In pilot experiments, to demonstrate the biological significance of this alteration in gene expression, we found that increased ET-1 expression in the endothelium of *Apoe*$^{-/-}$ mice exacerbates high-fat diet (HFD)–induced lipid–containing lesions in the descending thoracic aorta. However, it remains unclear how increased ET-1 expression worsens atherosclerosis progression in HFD-fed *Apoe*$^{-/-}$ mice.

Inflammation in PVAT may play a role in atherosclerosis [19, 20]. Angiotensin (Ang) II and aldosterone induce oxidative stress and T lymphocyte

and monocyte/macrophage infiltration in PVAT [21-23]. It is unknown, however, whether ET-1 has similar effects.

ET-1 plasma levels are increased in patients with abdominal aortic aneurysms (AAAs) [24-26]. Patients with larger AAAs displayed higher levels of ET-1 [25, 26]. Accordingly, a role for ET-1 has been suggested in the development of AAAs in humans. Whether ET-1 overexpression indeed causes AAAs has not been demonstrated.

We hypothesized that ET-1–induced PVAT and vascular oxidative stress and inflammation contribute to the progression of atherosclerosis and increased incidence of AAAs. To test this hypothesis, we crossed eET-1 with *Apoe*$^{-/-}$ mice, to determine whether ET-1 overexpression exaggerates HFD-induced atherosclerosis in the latter, and establish whether this is associated with enhanced PVAT and vascular oxidative stress and inflammation, and whether increased incidence of AAAs will occur.

Materials and methods

Materials and Methods are available in detail in the online-only Supplement.

Results

Physiological Parameters

HFD decreased body weight gain by 8%, 9%, 21%, and 24% in wild-type (WT), eET-1, *Apoe*$^{-/-}$, and eET-1/*Apoe*$^{-/-}$ mice, respectively (Table II-S1 in the online-only Data Supplement). This was not attributable to decreased growth because tibia length (TL) was similar in all groups. The eET-1/*Apoe*$^{-/-}$ mice presented a 20% increase in heart weight and heart weight/TL compared with WT. HFD decreased heart weight and heart weight/TL by ≈10% in WT and eET-1 mice and 25% in *Apoe*$^{-/-}$ and eET-1/*Apoe*$^{-/-}$ mice. HFD decreased kidney weight by 32% and 56% and kidney weight/TL by 31% and 37% in *Apoe*$^{-/-}$ and eET-

1/*Apoe*$^{-/-}$ mice, respectively. HFD resulted in increased spleen weight and spleen weight/TL by 38% in eET-1 mice. Spleen weight/TL was increased by 9% in *Apoe*$^{-/-}$ mice, and spleen weight and spleen weight/TL were augmented by 14% in eET-1/*Apoe*$^{-/-}$ mice fed a HFD compared with regular chow.

As previously reported [4, 5] circulating ET-1 levels were >10-fold higher in eET-1 mice (Figure II-1A) compared with WT mice fed a regular chow. The increase in plasma ET-1 was not affected by crossing eET-1 with *Apoe*$^{-/-}$ mice or by the diet. Systolic blood pressure (BP) and heart rate were not affected by genotype or diet (Figure II-1B; Figure II-S2 in the online-only Data Supplement). However, when regular chow and HFD groups were combined, systolic BP was 10 to 15 mm Hg higher in eET-1, *Apoe*$^{-/-}$, and eET-1/*Apoe*$^{-/-}$ compared with WT mice (Figure II-1B). Plasma cholesterol was unaltered in eET-1 mice but was increased 2.6- and 3-fold in *Apoe*$^{-/-}$ and eET-1/*Apoe*$^{-/-}$, respectively, compared with WT mice fed a regular chow (Figure II-1C). HFD increased plasma cholesterol 1.5- and 1.8-fold in WT and eET-1 mice, respectively. As expected, HFD increased plasma cholesterol 7-fold in *Apoe*$^{-/-}$ mice, which was not affected by ET-1 overexpression. Triglyceride levels were unaffected by ET-1 overexpression, Apoe knockout, or both in regular chow–fed animals (Figure II-S3 in the online-only Data Supplement). However, triglyceride levels were decreased ≈50% in WT and eET-1/*Apoe*$^{-/-}$ mice and tended to be lower in eET-1 and *Apoe*$^{-/-}$ mice in HFD-fed animals compared with regular chow. High-density lipoprotein (HDL) levels were unchanged by ET-1 overexpression, Apoe knockout, or both in regular chow–fed animals (Figure II-1D). HDL levels were unaffected by the HFD in WT, eET-1, or *Apoe*$^{-/-}$ mice but were decreased 45% in eET-1/*Apoe*$^{-/-}$ mice.

ET-1 Overexpression Exacerbated HFD-Induced Atherosclerosis and Triggered AAA Formation in *Apoe*$^{-/-}$ Mice

HFD-induced atherosclerotic lesions were characterized in cyrosections of aortic sinus and 4 cryosections at 80-μm intervals of ascending aorta. No atherosclerotic lesions were detected in the aortic sinus and ascending aorta

sections of WT or eET-1 mice (Figure II-2A and II-2B). Minor lipid deposition was observed in the aortic sinus of 2 of 9 WT and 3 of 9 eET-1 mice (Figure II-S4 in the online-only Data Supplement). Atherosclerotic lesions were detected in cryosections of aortic sinus and ascending aorta of HFD-fed *Apoe*$^{-/-}$ mice. HFD-induced an additional 2- and 6-fold increase in lesion size in the aortic sinus and ascending aorta, respectively, of eET-1/*Apoe*$^{-/-}$ mice compared with *Apoe*$^{-/-}$ mice. Atherosclerotic plaques in aortic arch sections of HFD-fed *Apoe*$^{-/-}$ and eET-1/*Apoe*$^{-/-}$ mice were further characterized by determining collagen distribution. Atherosclerotic plaques were observed in all 8 eET-1/*Apoe*$^{-/-}$ mice examined compared with 3 of 7 *Apoe*$^{-/-}$ mice ($P<0.05$). Plaques in eET-1/*Apoe*$^{-/-}$ mice contained necrotic cores surrounded by a fibrous cap (Figure II-S6 in the online-only Data Supplement).

AAAs were found at the suprarenal level in 8 of 21 eET-1/*Apoe*$^{-/-}$ mice fed a HFD (Figure II-3A; Table II-1). No AAAs were detected in the other groups fed a regular chow or HFD. All AAAs were associated with atherosclerosis plaques (Figure II-3A). Aortic circumference at the suprarenal aortic level was 2-fold greater in eET-1/*Apoe*$^{-/-}$ mice with AAAs than in other groups fed a HFD (Figure II-3B). Stretching and fragmentation of elastin was detected only in AAAs of eET-1/*Apoe*$^{-/-}$ mice (Figure II-4A). The media collagen fraction was decreased 57% in HFD-fed *Apoe*$^{-/-}$ mice, which was not further changed by ET-1 overexpression (Figure II-S5 in the online-only Data Supplement). Fibronectin expression in the media tended to decrease in HFD-fed *Apoe*$^{-/-}$ mice, and was decreased by 42% in HFD-fed eET-1/*Apoe*$^{-/-}$ mice (Figure II-4B).

ET-1 Overexpression in HFD-Fed *Apoe*$^{-/-}$ Mice Exacerbated Superoxide Production in Ascending and AAAs

In HFD animals, reactive oxygen species (ROS) generation measured as dihydroethidium fluorescence tended to be higher in the media and PVAT of ascending and abdominal suprarenal aorta in eET-1 compared with WT mice (Figure II-5A and II-5B). ROS production was increased 4.6- and 3.3-fold in the media and PVAT of ascending aorta, respectively, in *Apoe*$^{-/-}$ compared with WT

mice (Figure II-5A). ROS production was also detected in atherosclerotic plaques of *Apoe*$^{-/-}$ mice. The increase in ROS production was exaggerated 2.7-fold in the media and 1.9-fold in the PVAT and atherosclerotic lesions in eET-1/*Apoe*$^{-/-}$ compared with *Apoe*$^{-/-}$ mice. Similar changes in ROS generation were observed in abdominal suprarenal aorta (Figure II-5B). ROS production was increased ≥6-fold in the media and PVAT in *Apoe*$^{-/-}$ compared with WT mice. This was further elevated 3.4- and 2.8-fold in the media and PVAT, respectively, in eET-1/*Apoe*$^{-/-}$ compared with *Apoe*$^{-/-}$ mice. Comparable levels of ROS were detected in atherosclerotic plaques at the level of abdominal suprarenal aorta and ascending aorta in eET-1/*Apoe*$^{-/-}$ mice (Figure II-5A and II-5B).

ET-1 Overexpression in HFD-Fed *Apoe*$^{-/-}$ Mice Exacerbated Vascular Inflammation in Ascending and Abdominal Suprarenal Aorta

Monocyte/macrophage infiltration, measured in HFD-fed animals, was minimal in the ascending aorta of WT and eET-1 mice (Figure II-6A). Monocyte/macrophage infiltration was detected in 2%, 8%, and 52% of the surface of media, PVAT, and atherosclerotic plaques, respectively, in *Apoe*$^{-/-}$ mice. In the ascending aorta of eET-1/*Apoe*$^{-/-}$ mice, monocyte/macrophage infiltration was further increased 5.2- and 8.3-fold in the media and PVAT, respectively, compared with *Apoe*$^{-/-}$ mice. The level of monocyte/macrophage infiltration in atherosclerotic lesions was similar in eET-1/Apoe$^{-/-}$ and *Apoe*$^{-/-}$ mice. In abdominal suprarenal aorta of *Apoe*$^{-/-}$ mice, monocyte/macrophage infiltration was detected in ≥12% of the surface of the media and PVAT (Figure II-6B). This was further exaggerated 2.6-fold in the PVAT but not in the media of abdominal suprarenal aorta in eET-1/*Apoe*$^{-/-}$ mice compared with *Apoe*$^{-/-}$ mice. Similar levels of monocyte/macrophages were found in atherosclerotic lesions at the level of the abdominal suprarenal aorta and ascending aorta in eET-1/*Apoe*$^{-/-}$ mice (Figure II-6A and II-6B).

$CD4^+$ cells, measured in HFD-fed animals, were undetectable in ascending or abdominal suprarenal aorta of WT and eET-1 mice (Table II-2). Very few $CD4^+$ cells were found in ascending aortic plaques of *Apoe*$^{-/-}$ mice.

$CD4^+$ infiltration was present more frequently in ascending and abdominal suprarenal aorta sections of eET-1/*Apoe*$^{-/-}$ mice. CD4+ cells were detected in ascending aorta sections of media in 3 of 6 and PVAT in 5 of 6 eET-1/*Apoe*$^{-/-}$ mice (Figure II-6C; Table II-2). $CD4^+$ cell infiltration was also found in abdominal suprarenal aortic plaques of 4 of 6 eET-1/*Apoe*$^{-/-}$ mice (Figure II-6D; Table II-2). However, few $CD4^+$ cells were detected in PVAT.

ET-1 Overexpression in HFD-Fed *Apoe*$^{-/-}$ Mice Exacerbated Spleen Proinflammatory Ly-6C^{hi} Monocytes but Did Not Affect Plasma Cytokine Levels or T Cell Subsets

Plasma interleukin (IL)-6 was decreased by 61%, whereas tumor necrosis factor-α and monocyte chemotactic protein-1 tended to be lower, and IL-10 was unchanged in HFD-fed eET-1 compared with WT mice (Figure II-S7 in the online-only Data Supplement). Plasma tumor necrosis factor-α, IL-6, and monocyte chemotactic protein-1 levels were unchanged, whereas IL-10 tended to be increased in *Apoe*$^{-/-}$ compared with WT mice. ET-1 overexpression in *Apoe*$^{-/-}$ mice did not further alter the levels of IL-6, monocyte chemotactic protein-1, and IL-10, and tended to decrease tumor necrosis factor-α compared with *Apoe*$^{-/-}$ mice. The percentage of spleen $CD3^+$ T cells tended to be decreased in *Apoe*$^{-/-}$ and eET-1/*Apoe*$^{-/-}$ compared with WT mice (Figure II-S8 in the online-only Data Supplement). The percentage of spleen $CD4^+$ T cells was unaffected by either ET-1 overexpression, Apoe knockout, or both. The percentage of spleen $CD8^+$ T cells was decreased by 41% in *Apoe*$^{-/-}$ compared with WT mice, and tended to be increased in eET-1/*Apoe*$^{-/-}$ compared with *Apoe*$^{-/-}$ mice. The percentage of spleen anti-inflammatory $CD4^+CD25^+FOXP3^+$ T regulatory cells was increased 2-fold in *Apoe*$^{-/-}$ and eET-1/*Apoe*$^{-/-}$ compared with WT mice. The percentage of spleen-activated $CD4^+CD69^+$ T cells was increased 3.3-fold in *Apoe*$^{-/-}$ and eET-1/*Apoe*$^{-/-}$ compared with WT mice. The percentage of spleen-activated $CD8^+CD69^+$ T cells was 2.4-fold higher in *Apoe*$^{-/-}$ compared with WT mice, and tended to be further increased in eET-1/*Apoe*$^{-/-}$ mice. The percentage of spleen proinflammatory Ly-6C^{hi} monocytes was increased 1.7-fold in *Apoe*$^{-/-}$ compared

with WT mice, and was further increased 26% in eET-1/ *Apoe*$^{-/-}$ mice (Figure II-S9 in the online-only Data Supplement). ET-1 overexpression alone did not alter spleen T cell and monocyte subtype profiles.

ET-1 Overexpression Increased Matrix Metalloproteinase-2 Expression in Atherosclerotic Plaques

There was a 2-fold increase in matrix metalloproteinase-2 (MMP2) expression in atherosclerotic plaques of ascending aorta in eET-1/*Apoe*$^{-/-}$ compared with *Apoe*$^{-/-}$ mice (Figure II-S10 in the online-only Data Supplement).

Discussion

Our study extends our previous findings by demonstrating that increased expression of ET-1 in endothelium, in addition to exaggerating HFD-induced atherosclerosis [18], triggers AAA formation in *Apoe*$^{-/-}$ mice, an atherosclerosis-prone model that resembles human disease. These phenomena were associated with decreased plasma HDL, elevated oxidative stress in the media, plaque, and PVAT, increased monocyte/macrophage infiltration primarily in the PVAT, $CD4^+$ T cell infiltration in plaque and PVAT, and greater percentage of spleen proinflammatory Ly-$6C^{hi}$ monocytes. Our findings provide support to the hypothesis that ET-1 overexpression worsens the progression of atherosclerosis and contributes to the pathogenesis of AAAs via pro-oxidant and inflammatory mechanisms, and lowering of HDL.

Plasma ET immunoreactivity in patients with early and advanced atherosclerosis has been shown to be >2-fold higher than in healthy subjects [12, 13], and has been correlated with the extent of atherosclerosis, indicating a possible role of ET-1 in atherogenesis. Animal studies have shown that ET-1 is increased in plasma and the vessel wall from *Apoe*$^{-/-}$ [14, 16] and *Ldlr*$^{-/-}$ mice [15], and in pigs [27] fed a HFD. Increased ET-1 expression in the vascular wall has also been associated with atherosclerosis development in 1-year-old *Apoe*$^{-/-}$ mice fed a regular chow [26, 28]. In the present study, 8 weeks of HFD induced an increase in plasma ET-1 levels in WT and *Apoe*$^{-/-}$ mice, but this was not

sufficient to accelerate the development of atherosclerosis. The increase in plasma ET-1, however, did not reach the levels observed in previous pig and human studies. Consistent with our previous reports, both eET-1 and eET-1/*Apoe*$^{-/-}$ mice demonstrated 10-fold elevation in plasma ET-1 [4, 29]. However, only eET-1/*Apoe*$^{-/-}$ mice presented advanced atherosclerosis. This suggests that increased ET-1 levels exaggerate the progression of atherosclerosis only in conditions predisposed toward the development of atherosclerosis. In agreement with this, it has been shown that ET-1 infusion inducing a similar increase in plasma levels caused worsening of the intimal hyperplastic response after mechanical injury in rats [11]. Interestingly, plasma ET immunoreactivity is higher in patients with AAAs and correlates with AAA size, suggesting a role for ET-1 in AAA pathogenesis [25, 26]. In this study, exaggeration of atherosclerosis in HFD-fed eET-1/*Apoe*$^{-/-}$ mice was accompanied by increased incidence of AAAs, indicating that elevated ET-1 levels could contribute to the development of AAAs in an atherosclerotic setting.

We found a minor increase in total plasma cholesterol in HFD-fed WT and eET-1 mice. A similar increase in cholesterol levels was previously reported in WT C57BL/6 mice fed the same HFD as in this study for 12 or 18 weeks [30, 31]. It has also been shown that the increase in plasma cholesterol reaches a plateau after ≈2 weeks of HFD feeding [31]. Therefore, it is not surprising that the plasma cholesterol levels were increased in HFD-fed WT and eET-1 mice, which are on a C57BL/6 background. A large increase in plasma cholesterol was observed in HFD-fed *Apoe*$^{-/-}$ and eET-1/*Apoe*$^{-/-}$ mice. However, aggravation of atherosclerotic lesions and formation of AAAs occurred only in eET-1/*Apoe*$^{-/-}$ mice. This was accompanied by a decrease in plasma HDL. HDL levels are inversely correlated with the risk for coronary vascular disease [32, 33]. HDL mediates the reverse transport of cholesterol from the vasculature to the liver [33]. It has also been shown that, in addition to apolipoprotein A-I, HDL carry several proteins including α1-antitrypsin with anti-elastase activity, which can counteract the development of AAAs [34]. Therefore, it is plausible that ET-1 overexpression–induced decrease in HDL contributed to the enhanced damaging

effects of increased plasma cholesterol on the induction of atherosclerosis and triggering of AAAs, as observed in HFD-fed eET-1/*Apoe*$^{-/-}$ mice. Further studies are required to determine the mechanisms by which ET-1 overexpression decreases plasma HDL.

Previous studies have shown that the development of atherosclerosis in *Apoe*$^{-/-}$ mice can be accelerated by Ang II infusion [35] or deoxycorticosterone acetate-salt treatment [36]. Although Weiss *et al.* [35] and others have demonstrated that BP elevation by norepinephrine (40 mm Hg) does not accelerate the development of atherosclerosis to the same extent as Ang II (40–60 mm Hg), elevated BP may contribute to development of atherosclerotic lesions. In the present study, BP was unaltered by ET-1 overexpression, Apoe knockout, the combination of both, or by HFD feeding. A 10 to 15 mm Hg BP rise was found in eET-1, *Apoe*$^{-/-}$, and eET-1/*Apoe*$^{-/-}$ mice compared with WT mice only when regular chow and HFD data were combined. Thus, exacerbation of atherosclerosis and triggering of AAAs found in HFD-fed eET-1/*Apoe*$^{-/-}$ mice occurred in absence of significant BP elevation. This new animal model combining genetically modified mice overexpressing human ET-1 on a genetic background of atherosclerosis-prone *Apoe*$^{-/-}$ provides novel evidence that pathological effects of ET-1 on atherosclerosis and AAA development are BP-independent.

AAAs were observed in ≈40% of the eET-1/*Apoe*$^{-/-}$ mice fed a HFD, whereas none were detected in the other groups of mice. AAAs were observed at the suprarenal aortic level, as reported previously for Ang II–infused *Apoe*$^{-/-}$ mice 37-39]. As observed in humans, AAAs in HFD-fed eET-1/*Apoe*$^{-/-}$ mice were characterized by elastin breaks and flattening, and decreased media collagen fraction [40]. However, a decrease in media collagen fraction was also observed in HFD-fed *Apoe*$^{-/-}$ mice. Consequently, although collagen degradation lowers aortic tensile strength and therefore weakens the aortic wall [41], it predisposes to but is not sufficient for AAA development in *Apoe*$^{-/-}$ mice. Incidentally, ET-1 overexpression in *Apoe*$^{-/-}$ mice caused a decrease in media fibronectin

expression that could contribute to the development of AAAs by further weakening the aortic wall.

Recently, Suen *et al.* [42] reported that treatment with a mixed $ET_{A/B}$ receptor antagonist reduced Ang II–induced atherosclerosis in young (4 weeks) but not in old (6 months) *Apoe*$^{-/-}$ mice fed a Western-type diet, and failed to protect against Ang II–triggered AAAs. It is possible that blocking ET receptors only partially inhibits Ang II–mediated vascular inflammation and signaling pathways involved in the development of atherosclerosis and aneurysms. It is also possible that the increase in ET-1 expression might be suboptimal to induce AAAs in this model because Ang II did not cause a significant increase in plasma ET-1. Therefore, our findings suggest a novel mechanism of AAAs mediated by ET-1. The exact mechanism for aneurysm formation remains to be established. However, it is likely that oxidative stress and low-grade inflammation triggered by ET-1 overexpression [5] aggravate oxidative stress and inflammation already present in *Apoe*$^{-/-}$ mice, thereby playing a role in development of aneurysms.

We have previously reported that blood vessels in eET-1 mice are characterized by increased oxidative stress compared with WT mice [4]. Our current data show that ET-1 overexpression exaggerates ROS generation not only in the vascular wall but also in atherosclerotic plaques and PVAT in ascending aorta and AAAs of eET-1/*Apoe*$^{-/-}$ mice. This enhancement of oxidative stress could be attributable to increased activity of reduced nicotinamide adenine dinucleotide oxidase or uncoupling of endothelial NO synthase, or both [43, 44]. Kuhlencordt *et al.* [45] previously showed that double *Apoe* and *Nos3* knockout mice on a Western style diet exhibit increases in atherosclerotic lesions compared with *Apoe*$^{-/-}$ mice. In addition, Gao *et al.* [46] demonstrated a role for tetrahydrobiopterin deficiency–induced endothelial NO synthase uncoupling causing $\bullet O_2^-$ production and reduced NO availability in AAA formation. Ang II–induced AAAs are increased in hyperphenylalaninemia (hph)-1 mice deficient in endothelial NO synthase cofactor tetrahydrobiopterin biosynthetic enzyme guanosine triphosphate cyclohydrolase 1, which can be prevented by restoring tetrahydrobiopterin levels by treatment with folic acid or

endothelium-targeted dihydrofolate reductase gene therapy. These data are consistent with our findings, suggesting a key role of ET-1–induced oxidative stress in the development of atherosclerosis and AAA formation. In addition, our results suggest a participation of ET-1–induced ROS production by PVAT in atherosclerosis and AAA development.

The concept that atherosclerosis is an inflammatory disease is now well accepted [47-50]. Monocyte/macrophage and T cell infiltration play roles in the pathogenesis of atherosclerosis [51] and AAA formation [52]. ET-1 can also be produced by macrophages [53], which could further contribute to inflammation. Heavy ET-1 staining has been reported in foam cells within atherosclerotic lesions, and in vascular smooth muscle cells of the intima and media [28]. Here, ET-1 overexpression exaggerated monocyte/macrophage infiltration primarily in the PVAT of ascending aorta and AAAs in eET-1/*Apoe*$^{-/-}$ compared with *Apoe*$^{-/-}$ mice. However, monocyte/macrophage infiltration was equally high in plaques from eET-1/*Apoe*$^{-/-}$ and *Apoe*$^{-/-}$ mice. Because atherosclerotic plaques are larger in eET-1/*Apoe*$^{-/-}$ compared with *Apoe*$^{-/-}$ mice, and the cell infiltration is expressed as percentage of total surface, these data can also be interpreted as eET-1/*Apoe*$^{-/-}$ mice having more atherosclerotic plaque monocytes/macrophages. Interestingly, ET-1 overexpression exaggerated the increase in the percentage of spleen proinflammatory Ly-6C^{hi} monocytes in *Apoe*$^{-/-}$ mice, suggesting that there is an increase in circulating proinflammatory Ly-6C^{hi} monocytes that can contribute to the increase in monocyte/macrophage infiltration in the PVAT and, hence, to the development of atherosclerotic plaques. It should be noted that the monocyte subtype profile was unchanged by ET-1 overexpression in absence of *Apoe* knockout. MMP2, which could be secreted by macrophages, was higher in plaques from eET-1/*Apoe*$^{-/-}$ than from *Apoe*$^{-/-}$ mice. The increase in MMP2 could contribute to plaque development and rupture, and AAA formation. However, the mechanisms by which ET-1 overexpression increases MMP2 expression in the plaques are unknown and could be mediated in part by monocytes and macrophages. It has been shown that the severity of atherosclerosis is reduced in *Apoe*$^{-/-}$ mice that are lacking

functional monocyte/macrophages [54] or are deficient in MMP2 [55]. Recently, we reported that ET-1 overexpression–induced vascular remodeling and oxidative stress, which is associated with monocyte/macrophage infiltration in the adventitia and PVAT, is prevented by crossing eET-1 with mice carrying an osteopetrotic mutation in the macrophage colony–stimulating factor (*Csf1*$^{Op/+}$) gene [29]. Increased expression of ET-1 in endothelial cells of eET-1/*Apoe*$^{-/-}$ mice could act in paracrine fashion to stimulate the production of proinflammatory monocytes in the periphery, increase the recruitment of monocytes to atherosclerotic plaques, and promote the differentiation of monocytes into macrophages. Whether ET-1 overexpression directly increases the expression of MMP2 in macrophages remains to be determined.

In this study, the eET-1 mice did not present signs of systemic inflammation because plasma cytokines and spleen T cells and monocyte subtype profiles were unaltered. *Apoe*$^{-/-}$ mice fed a HFD for 8 weeks presented low levels of systemic inflammatory mediators. Plasma tumor necrosis factor-α, IL-6, monocyte chemotactic protein-1, and IL-10 levels were unchanged, and the percentage of spleen-activated $CD4^+CD69^+$, $CD8^+CD69^+$ T cells, and $CD4^+CD25^+FOXP3^+$ T regulatory cells, which are suppressor T cells, were elevated. The increase in T regulatory cells could probably be a compensatory mechanism counteracting the increase in activated T cells. ET-1 overexpression did not change the plasma cytokine levels and the T cell profile and, therefore, did not alter the systemic inflammation in *Apoe*$^{-/-}$ mice. $CD4^+$ T cell infiltration was barely detectable in atherosclerotic plaques of *Apoe*$^{-/-}$ mice. ET-1 overexpression induced $CD4^+$ T cell infiltration in atherosclerotic plaques and PVAT in ascending aorta, and in plaques in AAAs of eET-1/*Apoe*$^{-/-}$ mice on HFD. $CD8^+$ T cells could not be detected in media, atherosclerotic plaque or PVAT of *Apoe*$^{-/-}$ or eET-1/*Apoe*$^{-/-}$ mice (data not shown). Interestingly, crossing *Apoe*$^{-/-}$ mice with severe combined immunodeficiency (*Scid*) mice lacking T and B cells has been shown to reduce atherosclerosis. Adoptive transfer of $CD4^+$ T cells abolished this protection and increased atherosclerotic lesions in immunodeficient *Apoe*$^{-/-}$ mice [56]. Therefore, previous data are consistent with

our findings and suggest an important role for ET-1–induced infiltration of monocyte/macrophages and $CD4^+$ T cells in development of atherosclerosis and AAA formation. In addition, our results indicate an important role for ET-1–induced inflammatory cell infiltration in PVAT for both atherosclerosis and AAA development. However, the mechanisms of ET-1–induced T cell infiltration remain to be determined.

There is evidence that PVAT plays a role in atherosclerosis [19, 20]. In humans and mice, PVAT presents a higher inflammatory state compared with subcutaneous and epididymal fat [57]. HFD induced ROS production in PVAT, which caused endothelial dysfunction [58]. PVAT is a source of vascular inflammatory cells that play a role in hypertension and vascular damage [22]. PVAT surrounding atherosclerotic aorta has chemotactic properties through secretion of cytokines, thereby attracting macrophages and T cells [59]. Accumulation of macrophages and T cells at the interface between PVAT and adventitia of human atherosclerotic aorta has been previously reported. In *Apoe*$^{-/-}$ mice fed HFD, PVAT transplantation next to the common carotid artery, a site normally devoid of atherosclerotic lesions, impairs vascular relaxation and causes local formation of an atherosclerotic plaque [60]. So far, there has been no evidence of a role of PVAT in AAA formation. However, the previously cited results are consistent with our finding that increased ET-1 enhances ROS production and monocyte/macrophage and $CD4^+$ T cell infiltration in PVAT, which then plays a role in progression of atherosclerosis and in AAA formation.

Recently, we showed that there was an increase in expression of genes associated with lipid biogenesis, including elongation of very long chain fatty acids family member 6 (*Elovl6*) that is responsible for the final step in saturated fatty acid synthesis, which could lead to excess accumulation of lipids within the vascular wall and, hence, contribute to vascular remodeling, endothelial dysfunction, and development of atherosclerosis [18]. Saito *et al.* [61] have suggested a role for ELOVL6-induced elongation of saturated and monounsaturated fatty acids in foam cell formation and atherosclerosis progression. In their study, Western diet–induced atherosclerotic lesions and

monocyte/macrophage infiltration were reduced in irradiated *Ldlr*$^{-/-}$ mice transplanted with bone marrow cells from *Elovl6*$^{-/-}$ versus cells from WT mice. It is possible that higher levels of ET-1 might increase the expression of *Elovl6* in macrophages resulting in exaggeration of foam cell formation, progression of atherosclerosis, and development of AAA formation.

A limitation of the present study is that the eET-1 mice presented a greater increase in plasma levels of ET-1 than that observed in humans with atherosclerosis or aneurysms. However, by achieving greater increase in ET-1 expression, and thereby exaggerating the activity of a biological system such as ET-1, we were able to reveal the underlying pathophysiological mechanisms by which ET-1 contributes to the development of atherosclerosis and aneurysms. Nevertheless, additional studies might be necessary to confirm the importance for humans of the present findings.

Conclusions and Perspectives

We have demonstrated that ET-1 overexpression exerts a potent proatherogenic effect and triggers AAA formation in *Apoe*$^{-/-}$ mice on a HFD, possibly through pro-oxidant and inflammatory mechanisms and decrease in HDL. We also suggest that PVAT plays a prominent role. Clinically, our results underscore the importance of ET-1 in human atherosclerosis and AAA formation. ET_A or $ET_{A/B}$ receptor blockers and ET converting enzyme inhibitors could be potential pharmacological candidates for treatment of atherosclerosis and prevention of growth of AAAs. In support, Yoon *et al.* [62] have recently showed that long-term ET_A receptor blocker treatment attenuates the progression of coronary plaques in patients with early atherosclerosis.

Acknowledgements

We are grateful to Marie-Ève Deschênes, Adriana Cristina Ene, Nourredine Idris-Khodja, Christian Young (Flow cytometry facility), and Lilian Canetti (Research Pathology Facility) for excellent technical assistance.

Sources of Funding

T. Barhoumi was supported by La société québécoise d'hypertension artérielle. This work was supported by the Canadian Institutes of Health Research (CIHR) grant 37917, a Canada Research Chair (CRC) on Hypertension and Vascular Research from the CIHR/government of Canada CRC program, and by the Canada Fund for Innovation, all to E.L. Schiffrin. K. Mann is supported by CIHR grant 115000 and is a Junior 2 Chercheur Boursier of the Fonds de recherche du Québec - Santé.

Disclosures

None.

Significance

A role for the vasoconstrictor peptide, endothelin-1, has been suggested in the development atherosclerosis and aneurysms in humans and animal models. In this study, we show that overexpressing endothelin-1 in the endothelium of apolipoprotein E knockout (*Apoe*$^{-/-}$) mice fed a high-fat diet exaggerated the development of atherosclerosis and triggered abdominal aortic aneurysms. This was associated with increased vascular oxidative stress and immune cell infiltration, mostly monocytes/macrophages, which could be mediated in large part by perivascular fat. An exaggerated increase in spleen proinflammatory Ly-6C^{hi} monocytes was also present, which could contribute to the monocyte/macrophage infiltration in perivascular fat and ultimately in the atherosclerotic plaque. A decrease in plasma high-density lipoprotein, which is a risk factor for coronary vascular disease, also accompanied endothelin-1–induced exaggeration of atherosclerosis and abdominal aortic aneurysms. This could contribute to atherosclerotic plaque enlargement and abdominal aortic aneurysms development. These observations establish the mechanisms whereby endothelin-1 could contribute to atherosclerosis and abdominal aortic aneurysms in humans.

References

1. **Yanagisawa M, Kurihara H, Kimura S, Tomobe Y, Kobayashi M, Mitsui Y, Yazaki Y, Goto K, Masaki T**. A novel potent vasoconstrictor peptide produced by vascular endothelial cells. *Nature*. 1988; 332:411–415.

2. **Rautureau Y, Schiffrin EL**. Endothelin in hypertension: an update. *Curr Opin Nephrol Hypertens*. 2012; 21:128–136.

3. **Schiffrin EL**. Vascular endothelin in hypertension. *Vascul Pharmacol*. 2005; 43:19–29.

4. **Amiri F, Virdis A, Neves MF, Iglarz M, Seidah NG, Touyz RM, Reudelhuber TL, Schiffrin EL**. Endothelium-restricted overexpression of human endothelin-1 causes vascular remodeling and endothelial dysfunction. Circulation. 2004; 110:2233–2240.

5. **Amiri F, Paradis P, Reudelhuber TL, Schiffrin EL**. Vascular inflammation in absence of blood pressure elevation in transgenic murine model overexpressing endothelin-1 in endothelial cells. *J Hypertens*. 2008; 26:1102–1109.

6. **Brown KD, Littlewood CJ**. Endothelin stimulates DNA synthesis in Swiss 3T3 cells. Synergy with polypeptide growth factors. *Biochem J*. 1989; 263:977–980.

7. **Hirata Y, Takagi Y, Fukuda Y, Marumo F**. Endothelin is a potent mitogen for rat vascular smooth muscle cells. *Atherosclerosis*. 1989; 78:225–228.

8. **Komuro I, Kurihara H, Sugiyama T, Yoshizumi M, Takaku F, Yazaki Y**. Endothelin stimulates c-fos and c-myc expression and proliferation of vascular smooth muscle cells. *FEBS Lett*. 1988; 238:249–252.

9. **Yoshizumi M, Kim S, Kagami S, Hamaguchi A, Tsuchiya K, Houchi H, Iwao H, Kido H, Tamaki T**. Effect of endothelin-1 (1-31) on extracellular signal-regulated kinase and proliferation of human coronary artery smooth muscle cells. *Br J Pharmacol*. 1998; 125:1019–1027.

10. **Anggrahini DW, Emoto N, Nakayama K, Widyantoro B, Adiarto S, Iwasa N, Nonaka H, Rikitake Y, Kisanuki YY, Yanagisawa M, Hirata K**.

Vascular endothelial cell-derived endothelin-1 mediates vascular inflammation and neointima formation following blood flow cessation. *Cardiovasc Res*. 2009; 82:143–151.

11. **Trachtenberg JD, Sun S, Choi ET, Callow AD, Ryan US**. Effect of endothelin-1 infusion on the development of intimal hyperplasia after balloon catheter injury. *J Cardiovasc Pharmacol*. 1993; 22 suppl 8:S355–S359.

12. **Lerman A, Edwards BS, Hallett JW, Heublein DM, Sandberg SM, Burnett JC Jr**.. Circulating and tissue endothelin immunoreactivity in advanced atherosclerosis. *N Engl J Med*. 1991; 325:997–1001.

13. **Lerman A, Holmes DR Jr., Bell MR, Garratt KN, Nishimura RA, Burnett JC Jr.**. Endothelin in coronary endothelial dysfunction and early atherosclerosis in humans. *Circulation*. 1995; 92:2426–2431.

14. **Barton M, Haudenschild CC, d'Uscio LV, Shaw S, Münter K, Lüscher TF**. Endothelin ETA receptor blockade restores NO-mediated endothelial function and inhibits atherosclerosis in apolipoprotein E-deficient mice. *Proc Natl Acad Sci U S A*. 1998; 95:14367–14372.

15. **Babaei S, Picard P, Ravandi A, Monge JC, Lee TC, Cernacek P, Stewart DJ**. Blockade of endothelin receptors markedly reduces atherosclerosis in LDL receptor deficient mice: role of endothelin in macrophage foam cell formation. *Cardiovasc Res*. 2000; 48:158–167.

16. **Iwasa S, Fan J, Miyauchi T, Watanabe T**. Blockade of endothelin receptors reduces diet-induced hypercholesterolemia and atherosclerosis in apolipoprotein E-deficient mice. *Pathobiology*. 2001; 69:1–10.

17. **Kowala MC, Rose PM, Stein PD, Goller N, Recce R, Beyer S, Valentine M, Barton D, Durham SK**. Selective blockade of the endothelin subtype A receptor decreases early atherosclerosis in hamsters fed cholesterol. *Am J Pathol*. 1995; 146:819–826.

18. **Simeone SM, Li MW, Paradis P, Schiffrin EL**. Vascular gene expression in mice overexpressing human endothelin-1 targeted to the endothelium. *Physiol Genomics*. 2011; 43:148–160.

19. **Campbell KA, Lipinski MJ, Doran AC, Skaflen MD, Fuster V, McNamara CA**. Lymphocytes and the adventitial immune response in atherosclerosis. *Circ Res*. 2012; 110:889–900.

20. **Stern N, Marcus Y**. Perivascular fat: innocent bystander or active player in vascular disease? *J Cardiometab Syndr*. 2006; 1:115–120.

21. **Barhoumi T, Kasal DA, Li MW, Shbat L, Laurant P, Neves MF, Paradis P, Schiffrin EL**. T regulatory lymphocytes prevent angiotensin II-induced hypertension and vascular injury. *Hypertension*. 2011; 57:469–476.

22. **Guzik TJ, Hoch NE, Brown KA, McCann LA, Rahman A, Dikalov S, Goronzy J, Weyand C, Harrison DG**. Role of the T cell in the genesis of angiotensin II induced hypertension and vascular dysfunction. *J Exp Med*. 2007; 204:2449–2460.

23. **Kasal DA, Barhoumi T, Li MW, Yamamoto N, Zdanovich E, Rehman A, Neves MF, Laurant P, Paradis P, Schiffrin EL**. T regulatory lymphocytes prevent aldosterone-induced vascular injury. *Hypertension*. 2012; 59:324–330.

24. **Flondell-Sité D, Lindblad B, Kölbel T, Gottsäter A**. Cytokines and systemic biomarkers are related to the size of abdominal aortic aneurysms. *Cytokine*. 2009; 46:211–215.

25. **Flondell-Sité D, Lindblad B, Gottsäter A**. High levels of endothelin (ET)-1 and aneurysm diameter independently predict growth of stable abdominal aortic aneurysms. *Angiology*. 2010; 61:324–328.

26. **Treska V, Wenham PW, Valenta J, Topolcan O, Pecen L**. Plasma endothelin levels in patients with abdominal aortic aneurysms. *Eur J Vasc Endovasc Surg*. 1999; 17:424–428.

27. **Lerman A, Webster MW, Chesebro JH, Edwards WD, Wei CM, Fuster V, Burnett JC Jr.**. Circulating and tissue endothelin immunoreactivity in hypercholesterolemic pigs. *Circulation*. 1993; 88:2923–2928.

28. **Kobayashi T, Miyauchi T, Iwasa S, Sakai S, Fan J, Nagata M, Goto K, Watanabe T**. Corresponding distributions of increased endothelin-B receptor expression and increased endothelin-1 expression in the aorta of apolipoprotein E-deficient mice with advanced atherosclerosis. *Pathol Int*. 2000; 50:929–936.

29. **Javeshghani D, Barhoumi T, Idris-Khodja N, Paradis P, Schiffrin EL**. Reduced macrophage-dependent inflammation improves endothelin-1-induced vascular injury. *Hypertension*. 2013; 62:112–117.

30. **Paigen B**. Genetics of responsiveness to high-fat and high-cholesterol diets in the mouse. *Am J Clin Nutr*. 1995; 62:458S–462S.

31. **Zhang SH, Reddick RL, Burkey B, Maeda N**. Diet-induced atherosclerosis in mice heterozygous and homozygous for apolipoprotein E gene disruption. *J Clin Invest*. 1994; 94:937–945.

32. **Badimon L, Vilahur G**. LDL-cholesterol versus HDL-cholesterol in the atherosclerotic plaque: inflammatory resolution versus thrombotic chaos. *Ann N Y Acad Sci*. 2012; 1254:18–32.

33. **Sorci-Thomas MG, Thomas MJ**. High density lipoprotein biogenesis, cholesterol efflux, and immune cell function. *Arterioscler Thromb Vasc Biol*. 2012; 32:2561–2565.

34. **Ortiz-Muñoz G, Houard X, Martín-Ventura JL, Ishida BY, Loyau S, Rossignol P, Moreno JA, Kane JP, Chalkley RJ, Burlingame AL, Michel JB, Meilhac O**. HDL antielastase activity prevents smooth muscle cell anoikis, a potential new antiatherogenic property. *FASEB J*. 2009; 23:3129–3139.

35. **Weiss D, Kools JJ, Taylor WR**. Angiotensin II-induced hypertension accelerates the development of atherosclerosis in apoE-deficient mice. *Circulation*. 2001; 103:448–454.

36. **Weiss D, Taylor WR**. Deoxycorticosterone acetate salt hypertension in apolipoprotein E-/- mice results in accelerated atherosclerosis: the role of angiotensin II. *Hypertension*. 2008; 51:218–224.

37. **Daugherty A, Manning MW, Cassis LA**. Angiotensin II promotes atherosclerotic lesions and aneurysms in apolipoprotein E-deficient mice. *J Clin Invest*. 2000; 105:1605–1612.

38. **Daugherty A, Cassis LA**. Mouse models of abdominal aortic aneurysms. *Arterioscler Thromb Vasc Biol*. 2004; 24:429–434.

39. **Manning MW, Cassis LA, Daugherty A**. Differential effects of doxycycline, a broad-spectrum matrix metalloproteinase inhibitor, on angiotensin

II-induced atherosclerosis and abdominal aortic aneurysms. *Arterioscler Thromb Vasc Biol*. 2003; 23:483–488.

40. **Ailawadi G, Eliason JL, Upchurch GR Jr.**. Current concepts in the pathogenesis of abdominal aortic aneurysm. *J Vasc Surg*. 2003; 38:584–588.

41. **Cho BS, Roelofs KJ, Ford JW, Henke PK, Upchurch GR Jr.**. Decreased collagen and increased matrix metalloproteinase-13 in experimental abdominal aortic aneurysms in males compared with females. *Surgery*. 2010; 147:258–267.

42. **Suen RS, Rampersad SN, Stewart DJ, Courtman DW**. Differential roles of endothelin-1 in angiotensin II-induced atherosclerosis and aortic aneurysms in apolipoprotein E-null mice. *Am J Pathol*. 2011; 179:1549–1559.

43. **Li L, Fink GD, Watts SW, Northcott CA, Galligan JJ, Pagano PJ, Chen AF**. Endothelin-1 increases vascular superoxide via endothelin(A)-NADPH oxidase pathway in low-renin hypertension. *Circulation*. 2003; 107:1053–1058.

44. **Sedeek MH, Llinas MT, Drummond H, Fortepiani L, Abram SR, Alexander BT, Reckelhoff JF, Granger JP**. Role of reactive oxygen species in endothelin-induced hypertension. *Hypertension*. 2003; 42:806–810.

45. **Kuhlencordt PJ, Gyurko R, Han F, Scherrer-Crosbie M, Aretz TH, Hajjar R, Picard MH, Huang PL**. Accelerated atherosclerosis, aortic aneurysm formation, and ischemic heart disease in apolipoprotein E/endothelial nitric oxide synthase double-knockout mice. *Circulation*. 2001; 104:448–454.

46. **Gao L, Siu KL, Chalupsky K, Nguyen A, Chen P, Weintraub NL, Galis Z, Cai H**. Role of uncoupled endothelial nitric oxide synthase in abdominal aortic aneurysm formation: treatment with folic acid. *Hypertension*. 2012; 59:158–166.

47. **Libby P, Ridker PM, Hansson GK**. Inflammation in atherosclerosis: from pathophysiology to practice. *J Am Coll Cardiol*. 2009;54:2129–2138

48. **Ross R**. Atherosclerosis–an inflammatory disease. *N Engl J Med*. 1999; 340:115–126.

49. **Binder CJ, Chang MK, Shaw PX, Miller YI, Hartvigsen K, Dewan A, Witztum JL**. Innate and acquired immunity in atherogenesis. *Nat Med*. 2002; 8:1218–1226.

50. **Glass CK, Witztum JL**. Atherosclerosis. the road ahead. *Cell*. 2001; 104:503–516

51. **Stoll G, Bendszus M**. Inflammation and atherosclerosis: novel insights into plaque formation and destabilization. *Stroke*. 2006; 37:1923–1932.

52. **Shimizu K, Mitchell RN, Libby P**. Inflammation and cellular immune responses in abdominal aortic aneurysms. *Arterioscler Thromb Vasc Biol*. 2006; 26:987–994.

53. **Ehrenreich H, Anderson RW, Fox CH, Rieckmann P, Hoffman GS, Travis WD, Coligan JE, Kehrl JH, Fauci AS**. Endothelins, peptides with potent vasoactive properties, are produced by human macrophages. *J Exp Med*. 1990; 172:1741–1748

54. **Smith JD, Trogan E, Ginsberg M, Grigaux C, Tian J, Miyata M**. Decreased atherosclerosis in mice deficient in both macrophage colony-stimulating factor (op) and apolipoprotein E. *Proc Natl Acad Sci U S A*. 1995; 92:8264–8268.

55. **Kuzuya M, Nakamura K, Sasaki T, Cheng XW, Itohara S, Iguchi A**. Effect of MMP-2 deficiency on atherosclerotic lesion formation in apoE-deficient mice. *Arterioscler Thromb Vasc Biol*. 2006; 26:1120–1125.

56. **Zhou X, Nicoletti A, Elhage R, Hansson GK**. Transfer of CD4(+) T cells aggravates atherosclerosis in immunodeficient apolipoprotein E knockout mice. *Circulation*. 2000; 102:2919–2922.

57. **Chatterjee TK, Stoll LL, Denning GM, Harrelson A, Blomkalns AL, Idelman G, Rothenberg FG, Neltner B, Romig-Martin SA, Dickson EW, Rudich S, Weintraub NL**. Proinflammatory phenotype of perivascular adipocytes: influence of high-fat feeding. *Circ Res*. 2009; 104:541–549.

58. **Ketonen J, Shi J, Martonen E, Mervaala E**. Periadventitial adipose tissue promotes endothelial dysfunction via oxidative stress in diet-induced obese C57Bl/6 mice. *Circ J*. 2010; 74:1479–1487.

59. **Henrichot E, Juge-Aubry CE, Pernin A, Pache JC, Velebit V, Dayer JM, Meda P, Chizzolini C, Meier CA**. Production of chemokines by perivascular

adipose tissue: a role in the pathogenesis of atherosclerosis? *Arterioscler Thromb Vasc Biol*. 2005; 25:2594–2599.

60. **Öhman MK, Luo W, Wang H, Guo C, Abdallah W, Russo HM, Eitzman DT**. Perivascular visceral adipose tissue induces atherosclerosis in apolipoprotein E deficient mice. *Atherosclerosis*. 2011; 219:33–39.

61. **Saito R, Matsuzaka T, Karasawa T, et al**. Macrophage Elovl6 deficiency ameliorates foam cell formation and reduces atherosclerosis in low-density lipoprotein receptor-deficient mice. *Arterioscler Thromb Vasc Biol*. 2011; 31:1973–1979.

62. **Yoon MH, Reriani M, Mario G, Rihal C, Gulati R, Lennon R, Tilford JM, Lerman LO, Lerman A**. Long-term endothelin receptor antagonism attenuates coronary plaque progression in patients with early atherosclerosis. *Int J Cardiol*. January 3, 2013. doi: 10.1016/j.ijcard.2012.12.001. http://www.internationaljournalofcardiology.com/article/S0167-5273%2812%2901629-4/abstract. Accessed July 30, 2013.

Figures and tables

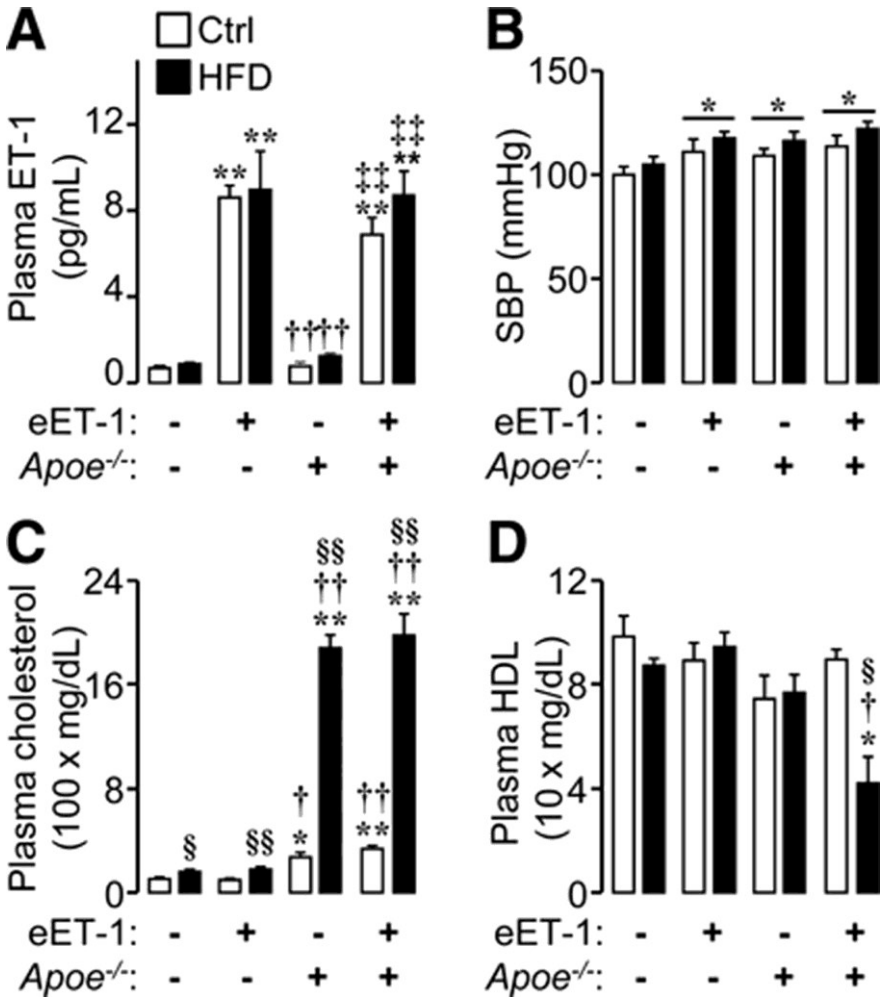

Figure II-1: Plasma endothelin (ET)-1 (**A**), systolic blood pressure (SBP; **B**), and plasma total cholesterol (**C**) and high-density lipoprotein (HDL; **D**) levels were determined in 16-week-old wild-type (WT), transgenic mice overexpressing ET-1 selectively in endothelium (eET-1), Apoe$^{-/-}$, and eET1/Apoe$^{-/-}$ mice fed a high-fat diet (HFD) or regular chow (Ctrl) for 8 weeks starting at age 8 weeks. Values are mean±SEM, n=6 to 13 for **A**, 6 to 10 for **B**, and 7 to 12 for **C** and **D**. **P*<0.05 and ***P*<0.001 vs WT on same diet, †*P*<0.05 and ††*P*<0.001 vs eET-1, ‡*P*<0.05 and ‡‡*P*<0.001 vs Apoe$^{-/-}$ on same diet and §*P*<0.05 and §§*P*<0.001 vs Ctrl.

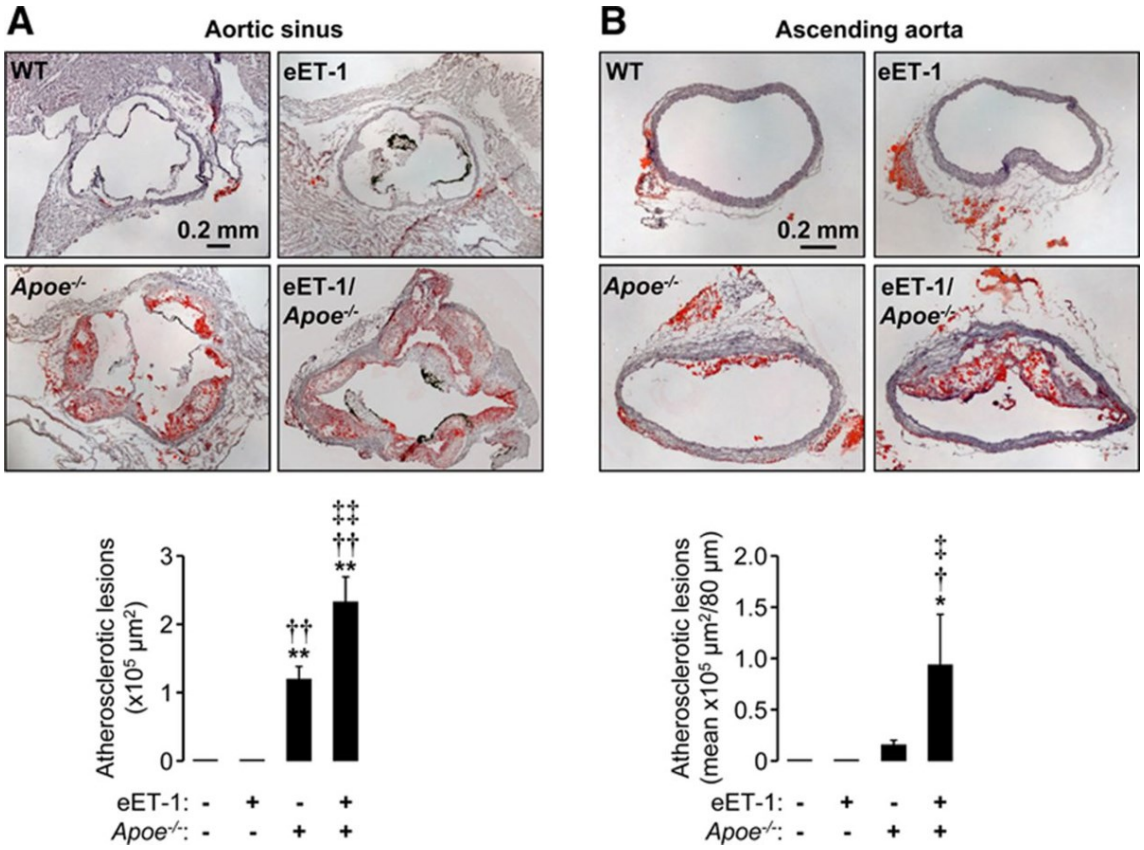

Figure II-2: Endothelin (ET)-1 overexpression exacerbated high-fat diet–induced aortic atherosclerosis in *Apoe*$^{-/-}$ mice. Atherosclerotic lesion areas were determined by oil red O staining in aortic sinus (**A**) and ascending aorta cryosections (**B**) of same groups as in Figure II-1. Representative images of oil red O–stained and Mayer's hematoxylin–counterstained aortic sinus (**A**) and ascending aorta cryosections (**B**) are shown. Lesion sizes were calculated as µm2 for the aortic sinus and mean µm2 of 4 sections at 80-µm intervals of ascending aorta. Values are mean±SEM, n=9 to 11 for **A** and 4 to 5 for **B**. **P*<0.01 and ††*P*<0.001 vs wild type (WT), †*P*<0.01 and ††*P*<0.001 vs transgenic mice overexpressing ET-1 selectively in endothelium (eET-1) and ‡*P*<0.05 vs *Apoe*$^{-/-}$.

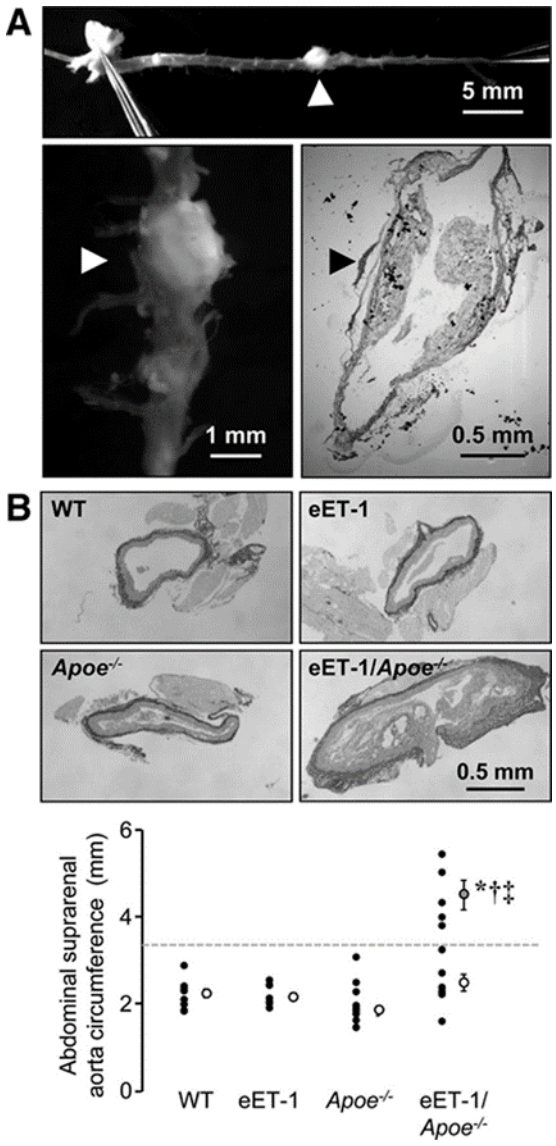

Figure II-3: Endothelin (ET)-1 overexpression increased incidence of abdominal aortic aneurysms (AAAs) in *Apoe*$^{-/-}$ mice fed a high-fat diet. **A**, Example of AAAs in transgenic mice overexpressing ET-1 selectively in endothelium (eET-1)/*Apoe*$^{-/-}$ mouse is presented. The top left picture shows whole aorta containing AAAs. A magnification of AAAs is presented in bottom left picture. The **bottom right** picture shows an oil red O-stained section of AAAs. Arrowheads indicate AAAs. Incidence of AAAs is shown in Table II-S1. **B**, The abdominal suprarenal aorta circumference was determined in the same groups as in Figure II-1. Representative images of Sirius red-stained aorta sections and abdominal

suprarenal aorta circumference for each individual (closed circle) and mean circumference for wild type (WT), eET-1, *Apoe*$^{-/-}$, and eET1/*Apoe*$^{-/-}$ with normal circumference (open circle), and eET1/*Apoe*$^{-/-}$ with circumference >1.5-fold of WT mean circumference indicated by the dashed gray line (gray-filled circle) are shown. Values are mean±SEM, n=8 to 13. **P*<0.001 vs WT, †*P*<0.001 vs eET-1, and ‡*P*<0.001 vs *Apoe*$^{-/-}$.

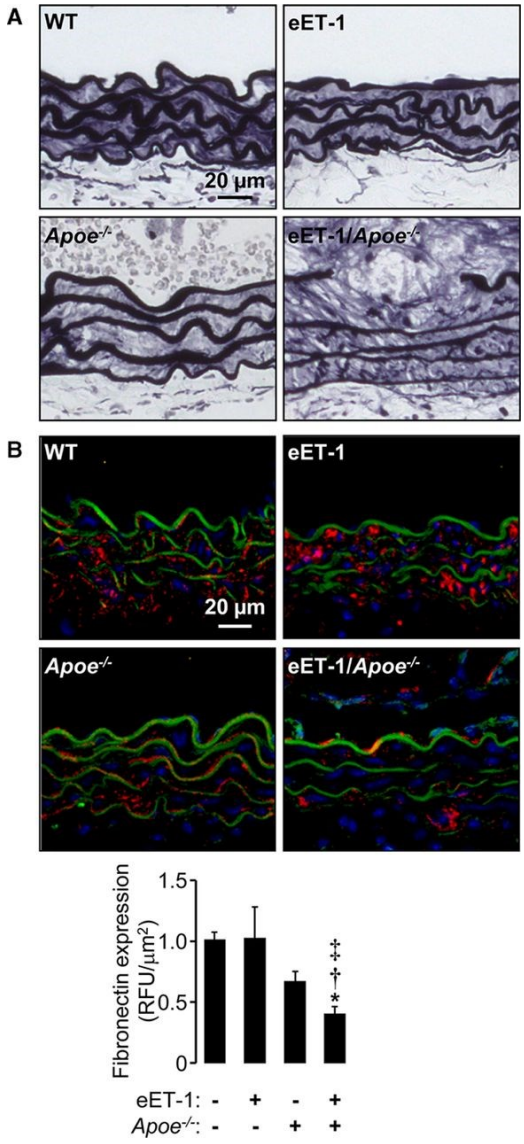

Figure II-4: Endothelin (ET-1) overexpression–induced abdominal aortic aneurysms are associated with elastic laminae disruption and flattening and decreased media fibronectin expression. The structure of elastin (**A**) and expression of fibronectin (**B**) were determined in abdominal suprarenal aorta of the same groups as in Figure II-1. Representative images of Verhoeff's elastic–stained sections (**A**) and fibronectin immunofluorescence (red; **B**) are shown. Blue and green fluorescence represent nuclear DAPI staining and autofluorescence of elastin, respectively. RFU indicates relative fluorescence units. Values are mean±SEM, n=4 to 5 for **A** and 4 to 6 for **B**. **P*<0.001 vs wild

type (WT), †P<0.001 vs transgenic mice overexpressing ET-1 selectively in endothelium (eET-1), and ‡P<0.001 vs *Apoe*$^{-/-}$.

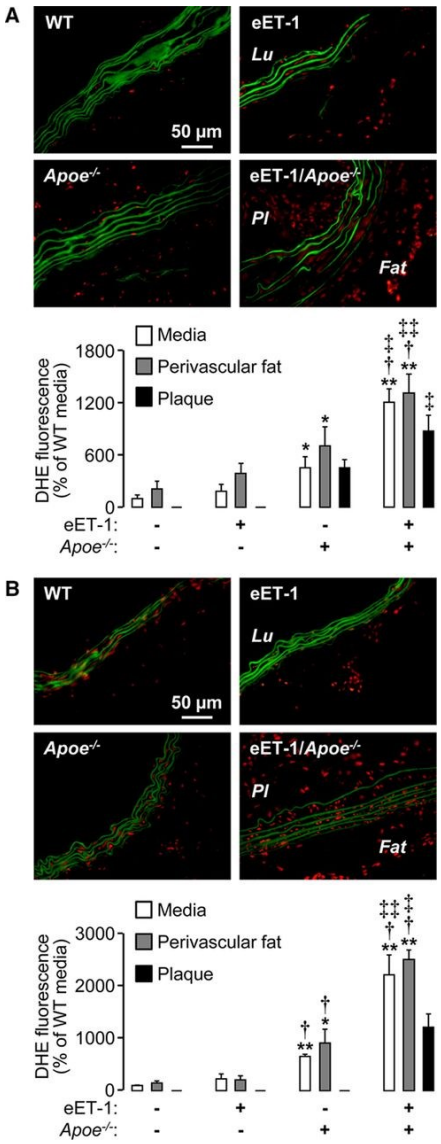

Figure II-5: Endothelin (ET-1) overexpression exacerbated high-fat diet–induced reactive oxygen species (ROS) production in ascending and abdominal suprarenal aorta of *Apoe*$^{-/-}$ mice. ROS were determined using dihydroethidium (DHE) staining in ascending (**A**) and abdominal suprarenal (**B**) aortic sections of the same groups as in Figure II-1. Representative images of DHE-stained ascending (**A**) and abdominal suprarenal (**B**) aortic sections with quantification of DHE fluorescence in media, perivascular fat, and atherosclerotic plaques are shown. Red fluorescence indicates DHE fluorescence, and green fluorescence represents the autofluorescence of elastin. The lumen (Lu), plaque (PI), and

perivascular fat (Fat) are indicated. Values are mean±SEM, n=4 to 6 for **A** and 4 to 5 for **B**. **P*<0.05 and ***P*<0.01 vs wild type (WT), †*P*<0.05 vs transgenic mice overexpressing ET-1 selectively in endothelium (eET-1), and ‡*P*<0.05 and ‡‡*P*<0.01 vs *Apoe*$^{-/-}$.

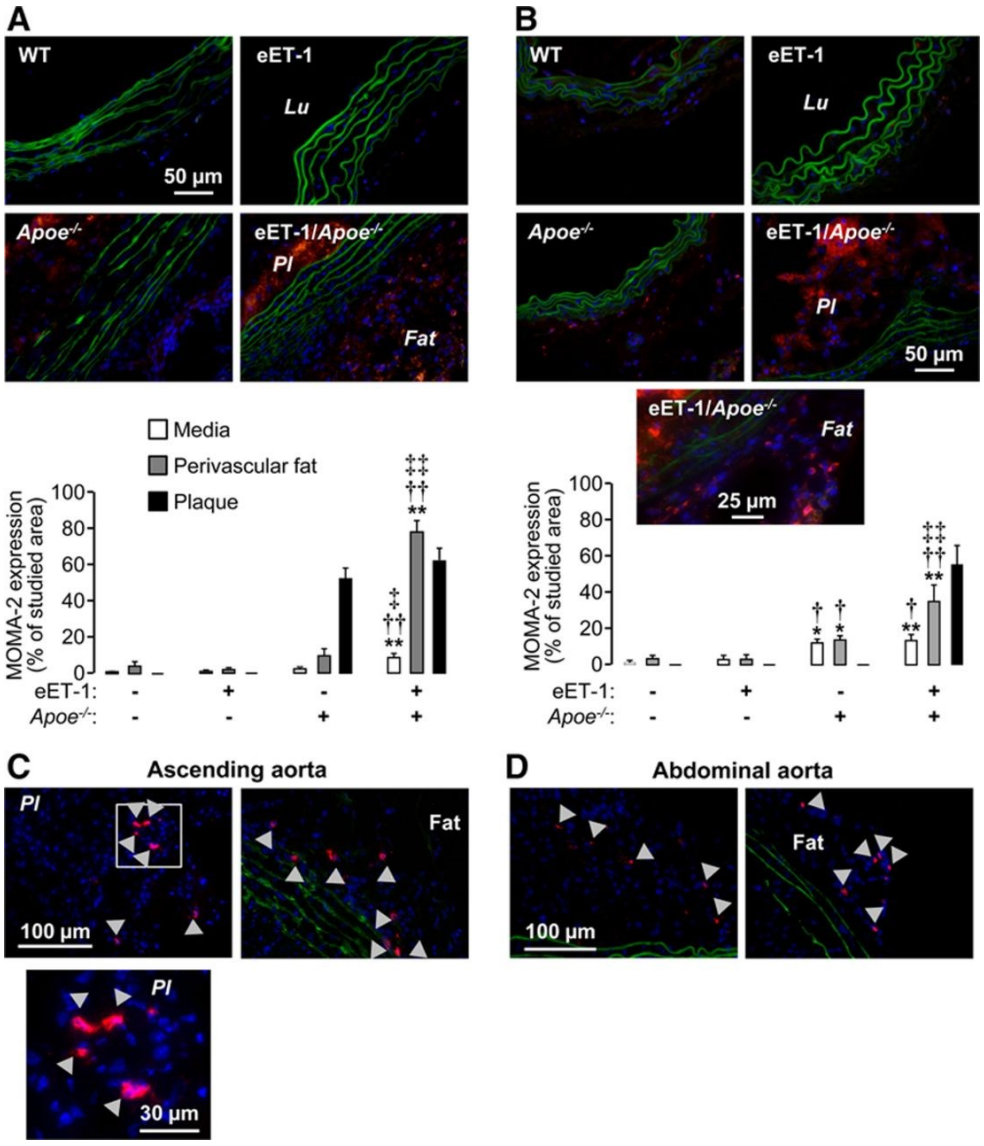

Figure II-6: Endothelin (ET-1) overexpression exaggerated high-fat diet–induced monocyte/macrophage and $CD4^+$ T cell infiltration in perivascular fat of ascending and abdominal suprarenal aorta of *Apoe*$^{-/-}$ mice. Infiltration of monocytes/macrophages (**A** and **B**; red fluorescence) and $CD4^+$ T cells (**C** and **D**; red fluorescence) was determined by immunofluorescence in ascending (**A** and **C**) and abdominal suprarenal (**B** and **D**) aortic sections of same groups as in Figure II-1. Representative images of monocyte/macrophage (MOMA-2)–stained ascending (**A**) and abdominal suprarenal (**B**) aortic sections with quantification of percentage of MOMA-2 staining per area in media, perivascular fat, and plaques

are presented. Representative MOMA-2 staining in the plaque, media, and perivascular fat of transgenic mice overexpressing ET-1 selectively in endothelium (eET-1)/*Apoe*$^{-/-}$ mice is shown in 2 separate images using different exposures. Representative images of CD4^{+} cell infiltration in plaques and perivascular fat of ascending aorta and in plaque (**C**) and perivascular fat of abdominal suprarenal aorta (**D**) of eET1/*Apoe*$^{-/-}$ mice. Frequency of occurrence of CD4^{+} cell infiltration in ascending and abdominal suprarenal aortic perivascular fat and atherosclerotic plaques is shown in Table II-S2. Blue and green represent nuclear DAPI staining and autofluorescence of elastin, respectively. Lu indicates lumen; and PI, plaque. Values are mean±SEM, n=4 to 5 for **A** and **B**. **P*<0.05 and ***P*<0.01 vs wild type (WT), †*P*<0.05 and ††*P*<0.01 vs eET-1, and ‡*P*<0.05 and ‡‡*P*<0.01 vs *Apoe*$^{-/-}$.

Table II-1: ET-1 overexpression increased the prevalence of abdominal aortic aneurysm in *Apoe*$^{-/-}$ mice.

Groups	Ctrl	HFD*
WT	0/7	0/15
eET-1	0/6	0/17
Apoe$^{-/-}$	0/8	0/20
eET-1/*Apoe*$^{-/-}$	0/9	8/21

The prevalence of abdominal aortic aneurysm was determined in 16-week old wild-type (WT), eET-1, *Apoe*$^{-/-}$ and eET1/*Apoe*$^{-/-}$ mice fed regular chow (Ctrl) or a high-fat diet (HFD) for 8 weeks. Values are ratios of number of animals with aneurysms over total number of mice studied. *Higher rate of abdominal aortic aneurysm in eET-1/*Apoe*$^{-/-}$ with $P<0.01$ by χ^2.

Table II-2: $CD4^+$ cell infiltration in ascending and abdominal suprarenal aortic perivascular fat and atherosclerotic plaques of wild-type, eET-1, *Apoe*$^{-/-}$ and eET1/*Apoe*$^{-/-}$ mice fed a high-fat diet.

	Ascending aorta		Abdominal aorta	
Groups	Perivascular fat*	Plaques*	Perivascular fat	Plaques
WT	0/6	NP	0/5	NP
eET-1	0/6	NP	0/4	NP
Apoe$^{-/-}$	0/5	1/6	0/5	NP
eET-1/*Apoe*$^{-/-}$	3/6	5/6	2/6	4/6

$CD4^+$ cell infiltration was determined in 16-week old wild-type (WT), eET-1, *Apoe*$^{-/-}$ and eET1/*Apoe*$^{-/-}$ mice fed a high-fat diet for 8 weeks. Values are ratios of number of animals with $CD4^+$ cells over total number of mice studied. NP, no plaques. *Greater $CD4^+$ cell infiltration in eET-1/*Apoe*$^{-/-}$, $P<0.05$ by χ^2.

Expanded Materials and Methods

Generation of eET-1/*Apoe*$^{-/-}$ mice and study design

The study was approved by the Animal Care Committee of the Lady Davis Institute for Medical Research and McGill University, followed recommendations of the Canadian Council for Animal Care and was in agreement with the Guide for the Care and Use of Laboratory Animals published by the US National Institutes of Health. C57BL/6 transgenic mice overexpressing the human ET-1 (eET-1) driven by the *Tie2* promoter conferring endothelial-specific expression were described previously [1]. It should be noted that the human ET-1 signal peptide is very well conserved and the peptide processing sites necessary for the maturation of the proET-1 and the mature ET-1 peptide are identical to those found in mouse ET-1 (Figure II-SI in the online-only Data Supplement) [2]. C57BL/6 *Apoe*$^{-/-}$ mice were obtained from The Jackson Laboratory (B6.129P2-Apoe$^{tm1Unc/J}$, Bar Harbor, ME, USA). The eET-1/*Apoe*$^{-/-}$ mice were generated by crossing eET-1 mice with *Apoe*$^{-/-}$ mice and then eET-1/*Apoe*$^{+/-}$ mice with eET-1/*Apoe*$^{-/-}$ mice. Eight-week old male wild-type (WT), eET-1, *Apoe*$^{-/-}$, and eET-1/*Apoe*$^{-/-}$ mice were fed a high-fat, cholesterol rich diet (35% fat, 1.25% cholesterol, D12336, Research Diets Inc., New Brunswick, NJ, US) (n = 11-15) or regular chow (n = 9-13) for 8 weeks.

At the end of the protocol, systolic blood pressure was measured by the tail-cuff method using a MC4000 blood pressure analysis system (Hatteras Instruments, Cary, NC, USA). Body weight was measured and mice anesthetized with 3% isoflurane (mixed with O_2 at 1 L/mL, depth of anesthesia confirmed by rear foot squeezing). One mL of blood was collected by cardia puncture, on heparin for measurement of plasma cholesterol, high-density lipoprotein (HDL) and triglycerides or on EDTA for ET-1 and cytokines. In one group of animals, the whole aorta was excised from the root to the iliac bifurcation for study of abdominal aortic aneurysms (AAA), and heart, kidneys and spleen were harvested and weighed. Tibia length was measured. In another group of mice, the top part of the heart and thoracic aorta with perivascular fat (PVAT) were

dissected to characterize atherosclerotic plaques, and the abdominal suprarenal aorta with PVAT was collected to study AAA. The spleen was used to determine T cells and monocyte subtype profiles. Atherosclerotic plaques, reactive oxygen species (ROS) production, and monocyte/macrophage and $CD4^+$ cell infiltration were determined in cryosections of aortic sinus and ascending aorta. Matrix metalloproteinase-2 (MMP2) expression was determined in cryosections of ascending aorta. Collagen content was examined in paraffin sections of aortic arch and abdominal suprarenal aorta. Elastin structure and fibronectin expression were determined in paraffin sections of the abdominal suprarenal aorta.

Quantification of atherosclerosis and abdominal aortic aneurysm

To study atherosclerotic plaques in the aortic sinus and ascending aorta, the top part of the heart and a section of ascending aorta were embedded in VWR Clear Frozen Section Compound (VWR International, West Chester, PA, USA). Five μm cryosections of aortic sinus and four cryosections at 80-μm intervals of ascending aorta were air-dried for 30 min and fixed 5 min with 4% paraformaldehyde (PFA) solution in phosphate buffered saline (PBS). Sections were rinsed in three changes of distilled water, immersed in 100% propylene glycol for 5 min, and then stained with pre-warmed Oil Red O solution (Electron Microscopy Sciences, Hatfield, PA, USA) for 10 min at 60 °C. Excess stain was removed with 85% propylene glycol for 5 min, after which the sections were rinsed with two changes of distilled water and then counterstained with Mayer's hematoxylin (Sigma-Aldrich, St Louis, MO, USA) for 10 min. The sections were washed thoroughly in running tap water, adjusted to RT, for 3 min, and then mounted using aqueous mounting medium (Thermo Scientific, Pittsburgh, PA, USA).

To study abdominal aortic aneurysms, a section of the abdominal suprarenal aorta was embedded in Tissue-Tek OCT (Sakura, Torrance, CA, USA). Five μm cryosections were fixed for 5 min in 4% PFA followed by rinsing

with water. The sections were stained with 0.5% oil red O working solution for 30 min. The sections were rinsed 3 times for 5 min with water and mounted with Immu-Mount mounting solution (Thermo Scientific, Pittsburgh, PA). In a second set of samples, sections of the abdominal suprarenal aorta were fixed in 4% PFA at 4°C for 48 h and embedded in paraffin. Sections were stained with Sirius red as indicated below.

Images were captured with Infinity capture imaging software (Luminera Corp., Ottawa, ON, Canada). Atherosclerotic plaques and abdominal suprarenal aorta circumference at abdominal aortic aneurysm level were quantified using ImageJ [3]. The atherosclerotic plaques were expressed in μm^2 for aortic sinus and in mean μm^2 of the four sections at 80-μm intervals for ascending aorta.

Reactive oxygen species production

Dihydroethidium (DHE) was used to evaluate the in situ production of reactive oxygen species (ROS) as previously described [4]. Ascending and abdominal suprarenal aortas containing the perivascular fat were embedded in Tissue-Tek OCT. Five μm sections of unfixed frozen ascending and abdominal suprarenal aorta were thawed, air dried for 30 min at RT and incubated in DHE (2 μmol/l) at RT for 5 min. Fluorescent images were captured as above using a CY3 filter. The fluorescence was quantified in media, perivascular fat and plaque separately using ImageJ. DHE fluorescence per unit of surface was normalized to fluorescence in the media of wild-type (WT) mice acquired on the same day and expressed as % of WT media. This was done to eliminate any variation due to changes in the oxidative environment on any given day.

Monocyte/macrophage and $CD4^+$ cell infiltration and fibronectin and matrix metalloproteinase-2 expression

Infiltration of monocyte/macrophage (MOMA-2) and $CD4^+$ cells (CD4) in ascending aorta and abdominal suprarenal aorta, and the expression of MMP2 in the ascending aorta were determined by immunofluorescence microscopy on 5 μm cryostat sections. Fibronectin expression in abdominal suprarenal aorta was

determined in 5 μm paraffin sections. All the aortic sections contained perivascular fat. Tissue cryosections were air-dried for 30 min and then fixed in 4% paraformaldehyde for 20 min at RT (for MOMA-2, and MMP2) or in ice cold acetone for 10 min at RT (for CD4). Thereafter, sections were washed with PBS twice for 5 min. Sections were blocked for 1 h at RT with TBS (50 mM Tris pH 7.4, 150 mM NaCl) containing 1% bovine serum albumin, 0.4% Triton X-100 and 20% fetal bovine serum for MOMA-2 and CD4 or PBS containing 10% normal donkey serum (Jackson ImmunoResearch Laboratories, West Grove, PA) for MMP2. Sections were incubated overnight at 4°C with a rat anti-monocyte/macrophagespecific antigen MOMA-2 (1:50, Abcam, Cambridge, MA) or a rat anti-CD4 (1:20, BD Biosciences, Mississauga, ON, Canada) antibody in TBS blocking solution, or with a goat anti-MMP2 antibody (1:50, Santa Cruz Biotechnology, Santa Cruz, CA), or normal goat IgG as negative control for MMP2 immunofluorescence in PBS. The sections were washed 3 times with TBS containing 0.1 % Tween-20 (TBST) for MOMA-2 and CD4 or with PBS for MMP2. Sections were incubated with Alexa Fluor® 555 goat anti-rat (1/200) (Invitrogen Corp., Carlsbad, CA, USA), Alexa Fluor® 568 goat anti-rat (1:400) or Alexa Fluor® 555 donkey anti-goat (1:200) antibody for 1 h at RT, and then washed 3 times with TBST for MOMA-2 and CD4 or with PBS for MMP2. Sections were mounted with Vectashield containing 4',6-diamidino-2-phenylindole (DAPI) (Vector Laboratories, Burlingame, CA, USA) or stained with 3 μM DAPI (Invitrogen) in PBS, washed 3 times with PBS and mounted with Fluoromount (Sigma-Aldrich). Paraffin sections were deparaffinized with two 5 min xylene baths, rehydrated in successive 3 min baths of ethanol (100%, 100%, 95%, 90%, 80%, 70% and 50%) followed by 5 min incubation in PBS. Sections were blocked with 10% normal goat serum (NGS) for 1 h, and then incubated with rabbit anti-mouse fibronectin antibody (1:200, EMD Millipore, Billerica, MA, USA) overnight at 4 ºC. Sections were then washed three times using TBST and incubated with Alexa® Fluor 568 goat anti-rabbit antibody (1:200, Life Technologies, Burlington, ON, Canada) for 1 h at RT. After, sections were counterstained with DAPI and mounted as above. Images were captured using a fluorescent microscope Leica

DM2000 (Leica Microsystems, Richmond Hill, ON, Canada) and analyzed with ImageJ. MOMA-2 expression and $CD4^+$ cells were determined in the media, perivascular fat and atherosclerotic lesions separately. MOMA-2 was expressed as % of studied area and presence or absence of $CD4^+$ cells determined. MMP2 was determined in atherosclerotic plaques, and expressed as the relative fluorescence unit (RFU) per μm^2 of atherosclerotic lesion.

Collagen content and elastin structure

Collagen content in abdominal suprarenal aortic media and in aortic arch atherosclerotic plaques was determined in 5 µm paraffin sections as follows. Paraffin sections were deparaffinized with two 5 min xylene baths, rehydrated in successive 3 min baths of ethanol (100%, 100%, 95%, 95% and 70%) followed by 5 min incubation in water. Sections were stained with 0.1% Sirius red solution (Sigma-Aldrich, St. Louis, MO, USA) prepared in saturated picric acid for 60 min at RT. Excess stain was removed by rinsing in 100 mM acetic acid for 3 min. Sections were then de-hydrated in successive 3 min baths of ethanol (95%, 100%, 100% and 100%) and immersed in two baths of xylene for 3 min. Sections were then mounted using Eukitt Mounting Medium (Electron Microscopy Sciences, Hatfield, PA, USA). Images were acquired by light microscopy using a Leica DM2000 microscope, and analyzed by color RGB thresholding using Northern Eclipse software (EMPIX Imaging, Missisauga, ON, Canada). Abdominal suprarenal aorta media collagen fraction was defined as the ratio of the media stained area to the total media area and expressed as a percentage.

Elastin structure in abdominal suprarenal aortic media was determined in 5 µm paraffin sections as follows. Paraffin sections were deparaffinized with two 2 min xylene baths, rehydrated in successive 1 min baths of ethanol (100%, 95%, 90% and 70%) followed by 3 min incubation in water. Sections were stained with freshly prepare Verhoeff's solution for 30 min at RT. Verhoeff's stain was made by mixing 2.5 part of of 0.17 M hematoxylin BSC (Fisher Scientific, Fair Lawn, NJ, USA) in ethanol, 1 part of 10% ferric chloride solution (Fisher, Fair Lawn, NJ, USA) and 1 part of Lugol solution (Sigma-Aldrich). Excess stain was

differentiated using 2% ferric chloride solution for ~3 min. Sections were then washed in running tap water for 30 sec at RT, and dipped in 5% sodium hyposulphite solution (Fisher Scientific). Sections were then dehydrated in successive 3 min baths of ethanol (70%, 90%, 95% and 100%) and, and cleared by immersing in three changes of xylene for 1 min each. Sections were then mounted and imaged as above.

Flow cytometry profiling of splenic T cells and monocytes

Profile of T cells and monocyte subtypes was determined by flow cytometry as follows. The technique of monocyte profiling has previously been described [5]. Single splenocyte suspension was obtained by releasing the splenocytes by forcing pieces of spleen through a 70 μm nylon mesh cell strainer (BD Biosciences, Durham, NC, USA) pre-wet with PBS supplemented with 5% fetal bovine serum (FBS) with the back of a 3 mL syringe plunger. The cell strainer was washed with PBS/5% FBS to flush the cells through the nylon mesh. The two previous steps were repeated until only connective tissue remained in the cell strainer. Cells were centrifuged at 300 x g for 10 min at RT. Cells were resuspended in 5 mL of Red Blood Cell lysis buffer (Sigma-Aldrich) and incubated at RT for 3 min with occasional gentle mixing to eliminate red blood cells. The mixture was diluted with 30 mL of PBS/5% FBS, filtered through a 70 μm nylon mesh cell strainer, and centrifuged at 300 x g for 5 min at RT. Cells were resuspended in 2 mL of PBS/5% FBS and counted using a Z2 Coulter® Counter (Beckman-Coulter, Mississauga, ON, Canada). Two million cells were stained with a fixable viability dye eFluor® 506 (eBioscience, San Diego, CA, USA) in PBS, incubated with rat anti-mouse CD16/CD32 Fc receptor block (clone 2.4G2, BD Biosciences), and stained with specific antibodies or appropriate isotype control antibodies in PBS/5% FBS. Specific antibody-fluorochrome staining panel and example of the general gating procedure used for analysis are included in Table II-S2 and Figure II-S8 in the online-only Data Supplement for profiling of T cells and Table II-S3 and Figure II-S9 in the online-only Data Supplement for profiling of monocytes. Flow cytometry was performed on the the

BD LSRFortessa cell analyzer (BD Biosciences). Fluorescence minus one controls were used to determine fluorescence background and positivity. Data analysis was performed using FlowJo software (Tree Star Inc., Ashland, OR, USA). Data are expressed as indicated in Figure. VIII and IX legends in the online-only Data Supplement.

Plasma determinations

Blood samples were centrifugation at 1,000 x g for 15 min at 4°C to remove blood cells followed by a centrifugation at 10,000 x g for 10 min at 4°C to remove platelets. Plasma samples were stored at -80°C until tested. Plasma cholesterol, triglycerides and HDL were measured using a J&J Vitros 250 chemistry analyzer by Diagnostic Research Support Services at the Comparative Medicine and Animal Resource Centre of McGill University. The concentration of ET-1 was determined in plasma on EDTA using a human ET-1 QuantiGlo ELISA Kit (R&D Systems Inc., Minneapolis, MN, USA). Plasma levels of interleukin (IL)-6, IL-10, monocyte chemotactic protein-1 (MCP-1) and tumor necrosis factor (TNF)-α were measured using micro-bead multiplex immunoassays on a Bio-Plex 200 (Bio-Rad Laboratories).

Statistical analysis

Data are shown as means ± SEM. Comparisons were made by one- or two-way ANOVA as appropriate, followed by a Student–Newman–Keuls or Dunnett's T3 post-hoc test, as appropriate. Comparisons between two groups were made using an unpaired t-test. Percent prevalence was compared using a chi-square test or a Fisher Exact test, as appropriate. A value of $P<0.05$ was considered significant.

References

1. **Amiri F, Paradis P, Reudelhuber TL, Schiffrin EL**. Vascular inflammation in absence of blood pressure elevation in transgenic murine model

overexpressing endothelin-1 in endothelial cells. *J Hypertens*. 2008; 26:1102-1109.

2. **Chan TS, Lin CX, Chan WY, Chung SS, Chung SK**. Mouse preproendothelin-1 gene. cDNA cloning, sequence analysis and determination of sites of expression during embryonic development. *Eur J Biochem*. 1995;234: 819-826.

3. **Rasband WS**. ImageJ. *ImageJ, U S National Institutes of Health, Bethesda, Maryland, USA*, 1997-2011 2012; Available at: URL: imagej.nih.gov/ij/.

4. **Viel EC, Benkirane K, Javeshghani D, Touyz RM, Schiffrin EL**. Xanthine oxidase and mitochondria contribute to vascular superoxide anion generation in DOCA-salt hypertensive rats. *Am J Physiol Heart Circ Physiol*. 2008; 295:H281-H288.

5. **Swirski FK, Libby P, Aikawa E, Alcaide P, Luscinskas FW, Weissleder R, Pittet MJ**. Ly-6C^{hi} monocytes dominate hypercholesterolemia-associated monocytosis and give rise to macrophages in atheromata. *J Clin Invest*. 2007; 117:195-205.

Supplemental figures and tables

Table II-S1: Body and organ weights of animals.

Description	**WT**		**eET-1**		***Apoe*$^{-/-}$**		**eET-1/*Apoe*$^{-/-}$**	
Diet	**Ctrl**	**HFD**	**Ctrl**	**HFD**	**Ctrl**	**HFD**	**Ctrl**	**HFD**
n	16	19	8	15	10	25	7	13
BW (g)	30.3 ± 0.9	27.9 ± 0.6§	30.1 ± 1.1	27.4 ± 0.7§	30.8 ± 0.6	24.4 ± 1.2**,‡‡,§§	30.0 ± 0.6	22.9 ± 0.4**,‡‡,§§
TL (mm)	18.2 ± 0.2	18.0 ± 0.2	17.8 ± 0.1	17.5 ± 0.2	17.8 ± 0.1	17.5 ± 0.1	18.2 ± 0.2	17.6 ± 0.1
HW (mg)	129 ± 4	117 ± 3§	137 ± 5	121 ± 4§	138 ± 4	103 ± 2*,†,§§	155 ± 13*	112 ± 4§§
HW/TL (mg/mm)	7.1 ± 0.2	6.5 ± 0.1	7.7 ± 0.3	7.0 ± 0.2	7.7 ± 0.2	5.9 ± 0.1*,††,§§	8.5 ± 0.8*	6.4 ± 0.2§§
KW (mg)	368 ± 11	366 ± 8	365 ± 15	353 ± 9	396 ± 13	269 ± 11**,††,§§	404 ± 18	249 ± 20**,††,§§
KW/TL (mg/mm)	20.2 ± 0.5	20.4 ± 0.4	20.5 ± 0.9	20.5 ± 0.5	22.2 ± 0.7	15.4 ± 0.6**,††,§§	22.3 ± 1.1	14.1 ± 0.6**,††,§§
SW (mg)	78 ± 12	85 ± 5	67 ± 7	92 ± 6§	98 ± 9	105 ± 5	107 ± 11†	123 ± 8**,†
SW/TL (mg/mm)	4.3 ± 0.6	4.7 ± 0.2	3.8 ± 0.4	5.3 ± 0.4§	5.5 ± 0.5	6.0 ± 0.3*	5.9 ± 0.6	6.7 ± 0.5*

Body and organ weights were determined in 16-week old wild-type (WT), eET-1, *Apoe*$^{-/-}$ and eET-1/*Apoe*$^{-/-}$ mice fed a regular chow (Ctrl) or a high-fat diet (HFD) for 8 weeks starting at 8 weeks of age. Values are means ± SEM, *P<0.05 and **P<0.01 vs. WT, †P<0.05 and ††P<0.01 vs. eET-1, ‡P<0.05 and ‡‡P<0.01 vs. *Apoe*$^{-/-}$, §P<0.05 and §§P<0.01 vs. Ctrl. BW, body weight; TL, tibia length; HW, heart weight; KW, kidney weight; SW, spleen weight.

Table II-S2: Antibodies for flow cytometry profiling of T cells.

Antibodies	Description	Clone, company
CD3	A700-conjugated rat anti-mouse CD3 antibody	17A2, eBioscience
CD3 isotype	A700-conjugated rat IgG2b κ isotype control antibody	eB149/10H5, eBioscience
CD4	PerCP-e710-conjugated rat anti-mouse CD4 antibody	RM4-5, eBioscience
CD4 isotype	PerCP-e710-conjugated rat IgG2a κ isotype control antibody	eBR2a, eBioscience
CD8a	APC-e780-conjugated rat anti-mouse-CD8a antibody	53-6.7, eBioscience
CD8a isotype	APC-e780-conjugated rat IgG2a κ isotype control antibody	eBR2a, eBioscience
CD25	e450-conjugated rat anti-mouse-CD25 antibody	PC61.5, eBioscience
CD25 isotype	e450-conjugated rat IgG1 κ isotype control antibody	eBRG1, eBioscience
FOXP3	APC-conjugated rat anti-mouse-FOXP3 antibody	FJK-16s, eBioscience
FOXP3 isotype	APC-conjugated rat IgG2a κ isotype control antibody	eBR2a, eBioscience
CD69	PE-conjugated hamster anti-mouse CD69 antibody	H1.2F3, BD Biosciences
CD69 isotype	PE-conjugated hamster IgG1 λ1 isotype control antibody	G235-2356, BD Biosciences

A700, Alexa Fluor® 700, APC, allophycocyanin, APC-e780, APC-eFluor® 780, e450, eFluor® 450, FOXP3, transcription factor X-linked forkhead/winged helix, PE, phycoerythrin, PerCPe710, PerCP-eFluor® 710.

Table II-S3: Antibodies for flow cytometry profiling of monocytes.

Antibodies	Description	Clone, company
CD90	PE-conjugated rat anti-mouse CD90.2 (Thy-1.2) antibody	53-2.1, eBioscience
CD90 isotype	PE-conjugated rat IgG2a κ isotype control antibody	eBR2a, eBioscience
B220	PE-conjugated rat anti-human/mouse CD45R (B220) antibody	RA3-6B2, eBioscience
B220 isotype	PE-conjugated rat IgG2a κ isotype control antibody	eBR2a, eBioscience
CD49b	PE-conjugated anti-mouse CD49b (Integrin alpha 2) antibody	DX5, eBioscience
CD49b isotype	PE-conjugated rat IgG2M κ isotype control antibody	eBRM, eBioscience
NK1.1	PE-conjugated mouse anti-mouse NK1.1 antibody	PK136, BD Biosciences
NK1.1 isotype	PE-conjugated mouse IgG2a κ isotype control antibody	G155-178, BD Biosciences
Ly-6G	PE-conjugated rat anti-Ly-6G (Gr-1) antibody	RB6-8C5, eBioscience
Ly-6G isotype	PE-conjugated rat IgG2b κ isotype control antibody	eB149/10H5, eBiosciences
CD11b	APC-conjugated rat anti-mouse CD11b antibody	M1/70, eBioscience
CD11b isotype	APC-conjugated rat IgG2b κ Isotype control	eB149/10H5, eBioscience
Ly-6C	eFluor® 450 conjugated anti-mouse Ly-6C antibody	HK1.4, eBioscience
Ly-6C isotype	Not available	eBioscience

APC, allophycocyanin, PE, phycoerythrin. No antibody was used in replacement of Ly-6C isotype control antibody since this latter was not available.

Figure II-S1: Alignment of the human and mouse preproendothelin-1 amino acid sequence. Human and mouse amino acid sequences were obtained from UCSC Genome Bioinformatics web site (http://www.genome.ucsc.edu/) and the sequences were compared using the multiple sequence alignment software ClustalW2 (http://www.ebi.ac.uk/Tools/msa/clustalw2/#). An asterisk (*) indicates positions which have a single, fully conserved residue. A colon (:) indicates conservation between groups of strongly similar properties with a scoring > 0.5 in the Gonnet PAM 250 matrix. A period (.) indicates conservation between groups of weakly similar properties with a scoring ≤ 0.5 in the Gonnet PAM 250 matrix.

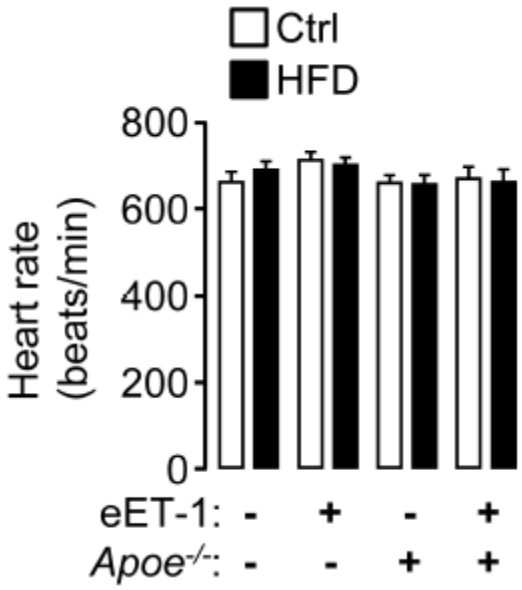

Figure II-S2: Heart rate was determined in 16-week old wild-type (WT), eET-1, *Apoe*$^{-/-}$ and eET1/*Apoe*$^{-/-}$ mice fed a high-fat diet (HFD) or regular chow (Ctrl) for 8 weeks starting at age 8 weeks. Values are means ± SEM, n = 6 for WT, 9 for eET-1, 9 for *Apoe*$^{-/-}$ and 9 for eET1/*Apoe*$^{-/-}$ mice fed regular chow, and 6 for WT, 8 for eET-1, 10 for *Apoe*$^{-/-}$ and 6 for eET1/*Apoe*$^{-/-}$ mice fed HFD.

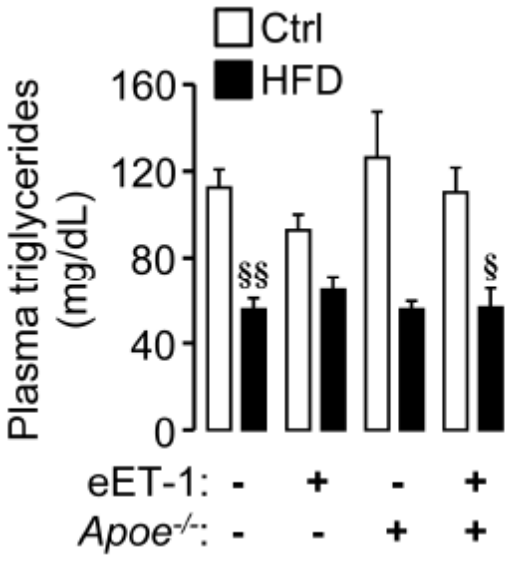

Figure II-S3: Plasma triglyceride levels were determined in 16-week old wild-type (WT), eET-1, *Apoe*$^{-/-}$ and eET-1/*Apoe*$^{-/-}$ mice fed a regular chow (Ctrl) or a high-fat diet (HFD) for 8 weeks starting at 8 weeks of age. Values are means ± SEM, n = 7 for WT, 7 for eET-1, 9 for *Apoe*$^{-/-}$ and 8 for eET1/*Apoe*$^{-/-}$ mice fed a regular chow, and 9 for WT, 12 for eET-1, 8 for *Apoe*$^{-/-}$ and 11 for eET1/*Apoe*$^{-/-}$ mice fed a HFD. §P<0.05 and §§P<0.001 vs. Ctrl.

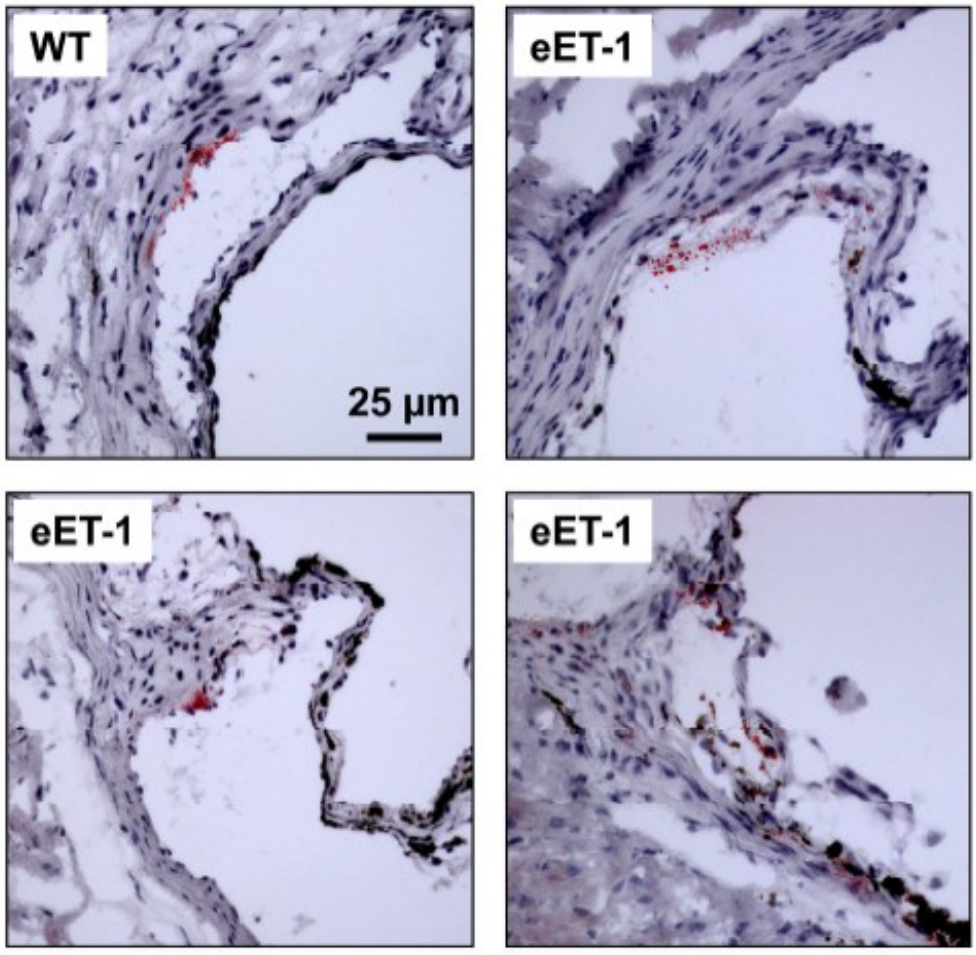

Figure II-S4: Representative images of oil red O-stained and Mayer's hematoxylin counterstained aortic sinus of wild-type (WT) and eET-1 mice.

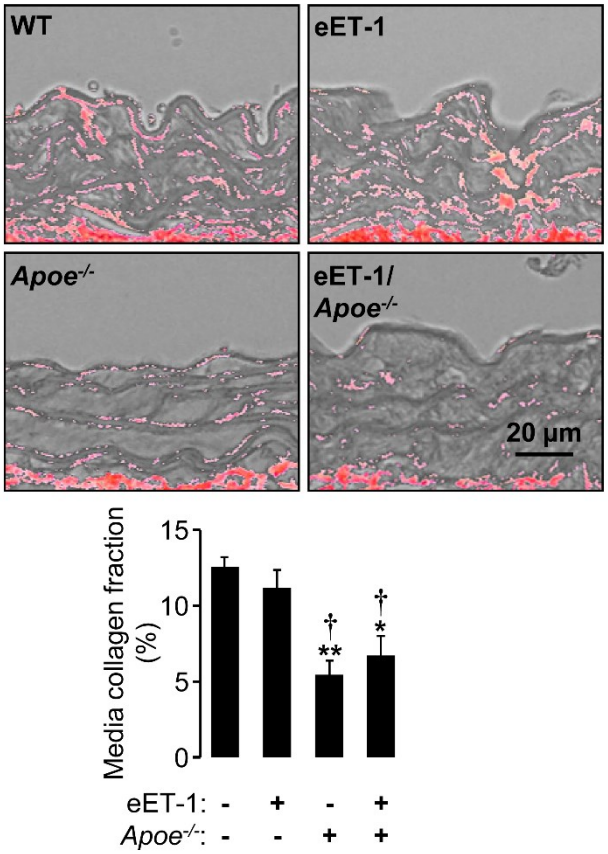

Figure II-S5: Collagen content is decreased to the same extent in *Apoe*$^{-/-}$ and eET-1*Apoe*$^{-/-}$ mice. Collagen content was determined in the media of abdominal suprarenal aorta by Sirius red staining in 16-week old wild-type (WT), eET-1, *Apoe*$^{-/-}$ and eET-1/*Apoe*$^{-/-}$ mice fed a high-fat diet (HFD) for 8 weeks starting at 8 weeks of age. Representative RGB thresholded images of Sirius red-stained sections of abdominal suprarenal aorta. Collagen was quantified as the % of red staining contained in the aortic media in the RGB thresholded images. Values are means ± SEM, n = 4 for WT, 3 for eET-1, 5 for *Apoe*$^{-/-}$ and 6 for eET1/*Apoe*$^{-/-}$ mice. **P*<0.05 and ***P*<0.01 vs. WT and †*P*<0.05 vs. eET-1.

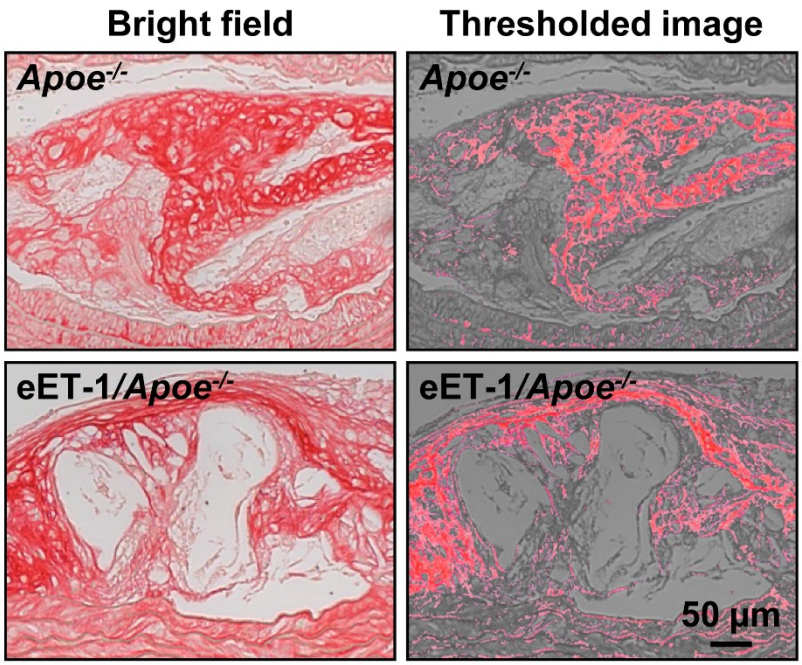

Figure II-S6: Collagen content was determined in atherosclerosis plaques of aortic arch of 16-week old *Apoe*$^{-/-}$ and eET-1/*Apoe*$^{-/-}$ mice fed a high-fat diet (HFD) for 8 weeks starting at 8 weeks of age. Representative bright field and RGB thresholded images of Sirius red stained sections are shown. Collagen is visualized as the red staining contained in the aortic media and the plaques in the RGB thresholded images. n = 7 for *Apoe*$^{-/-}$ and 8 for eET-1/*Apoe*$^{-/-}$ mice.

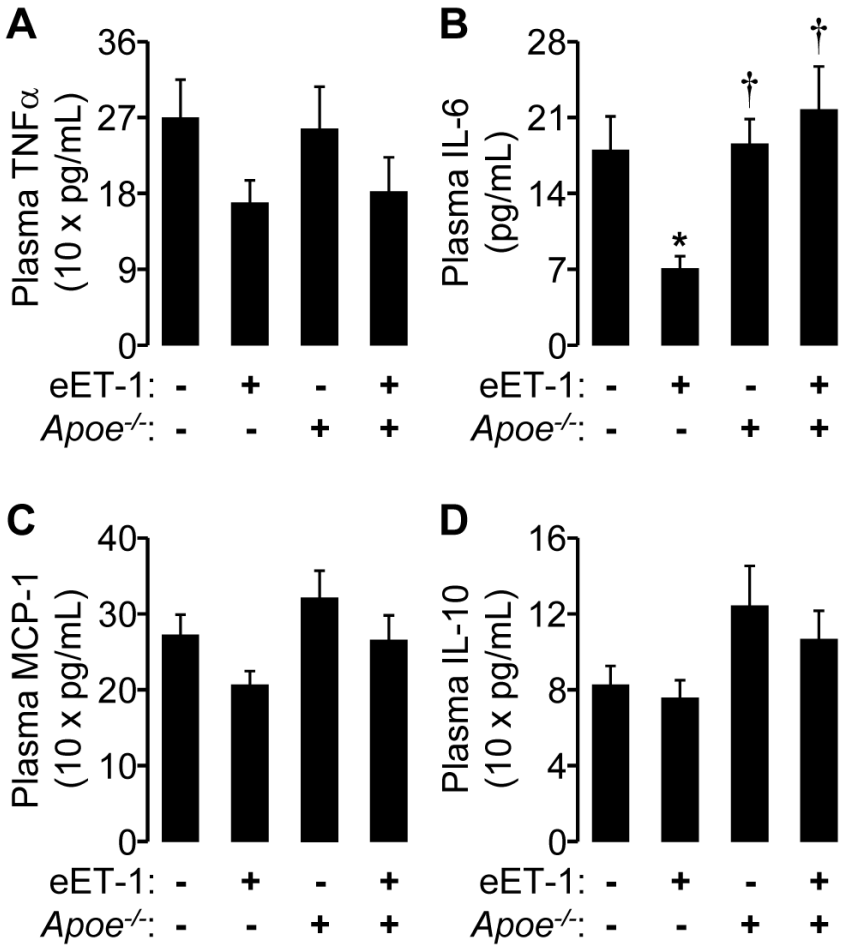

Figure II-S7: ET-1 overexpression did not alter plasma cytokine levels in *Apoe*$^{-/-}$ mice. Plasma levels of tumor necrosis factor (TNF)-α (A), interleukin (IL)-6 (B), monocyte chemotactic protein-1 (MCP-1, C) and IL-10 (D) were measured in 16-week old wild-type (WT), eET-1, *Apoe*$^{-/-}$ and eET1/*Apoe*$^{-/-}$ mice fed a high-fat diet for 8 weeks. Values are means ± SEM, n = 7 for WT, 8 for eET-1, 9 for *Apoe*$^{-/-}$ and 12 for eET1/*Apoe*$^{-/-}$ mice. *P<0.01 vs. WT and †P<0.01 vs. eET-1.

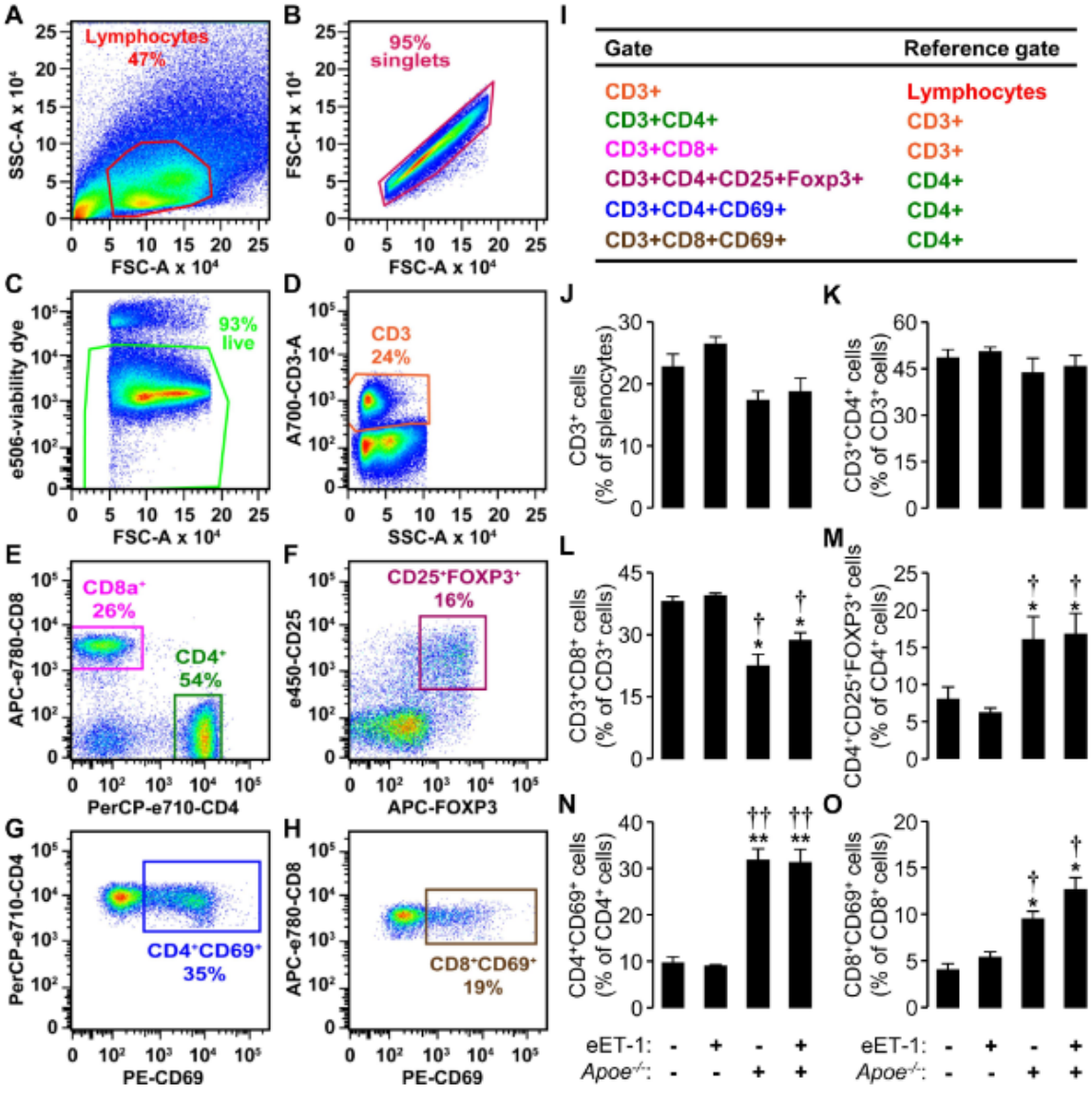

Figure II-S8: Flow cytometry profiling of splenic T cells. The profile of $CD3^+$, $CD4^+$, $CD8^+$, $CD4^+CD25^+FOXP3^+$, $CD4^+CD69^+$ and $CD8^+CD69^+$ cells were determined by flow cytometry in the spleen of 16-week old wild-type (WT), eET-1, *Apoe*$^{-/-}$ and eET1/*Apoe*$^{-/-}$ mice fed a high-fat diet for 8 weeks. Splenocytes were stained with Fixable Viability Dye eFluor® 506 (e506), Alexa Fluor® 700 (A700)-conjugated anti-mouse CD3, PerCP-eFluor® 710 (PerCP-e710)-conjugated anti-mouse CD4, allophycocyanin (APC)-eFluor® 780 (APC-e780)-conjugated antimouse CD8a, eFluor® 450 (e450)-conjugated anti-mouse CD25, phycoerythrin (PE)-conjugated hamster anti-mouse CD69 and APC-conjugated

anti-mouse Foxp3 antibodies, and analyzed by flow cytometry. Fluorophores were respectively excited and analyzed with appropriate laser and bandpass filter (BP) (e450: 405 nm with 450/50 BP, e506: 405 nm with 525/50 BP, A700: 640 nm with 730/45 BP, PerCP-eFluor® 710: 488 nm with 695/40 BP, APC-e780: 640 nm with 780/60 BP, APC: 640 nm with 670/14 BP, PE: 561 nm with 582/15 BP). Representative Flow cytometry profile of splenocytes (A-H) with the gating strategy (I) and the % of cells are showed for an eET-1/*Apoe*$^{-/-}$ mouse. A. Lymphocytes were gated in the side scatter (SSC)/forward scatter (FSC) plot. B. Singlet lymphocytes were gated using FSC height (FSC-H) over FSC area (FSCA). C. Live lymphocytes were gated in the viability dye/FSC-A plot. D. $CD3^+$ cells were gated in the CD3/SSC-A plot. E. $CD3^+CD4^+$ and $CD3^+CD8^+$ were gated in the CD8/CD4 plot from the $CD3^+$ cells population. F. Gated $CD3^+CD4^+$ cells were further characterized for CD25 and FOXP3 expression in the CD25/FOXP3 plot. Gated $CD3^+CD4^+$ and $CD3^+CD8^+$ cells were further examined for CD69 expression in CD4/CD69 (G) and CD8/CD69 (H) plots, respectively. The % $CD3^+$ cells in lymphocytes (J), % of $CD4^+$ (K) and $CD8^+$ (L) cells in $CD3^+$ cells, % of $CD4^+CD25^+FOXP3^+$ cells in $CD4^+$ cells (M), % of $CD4^+CD69^+$ cells in $CD4^+$ cells (N) and $CD8^+CD69^+$ cells in $CD8^+$ cells (O) are presented. Values are means ± SEM, n = 3 for WT, 4 for eET-1, 5 for *Apoe*$^{-/-}$ and 7 for eET1/*Apoe*$^{-/-}$ mice. **P*<0.05 and ***P*<0.001 vs. WT and †*P*<0.05 and ††*P*<0.001 vs. eET-1.

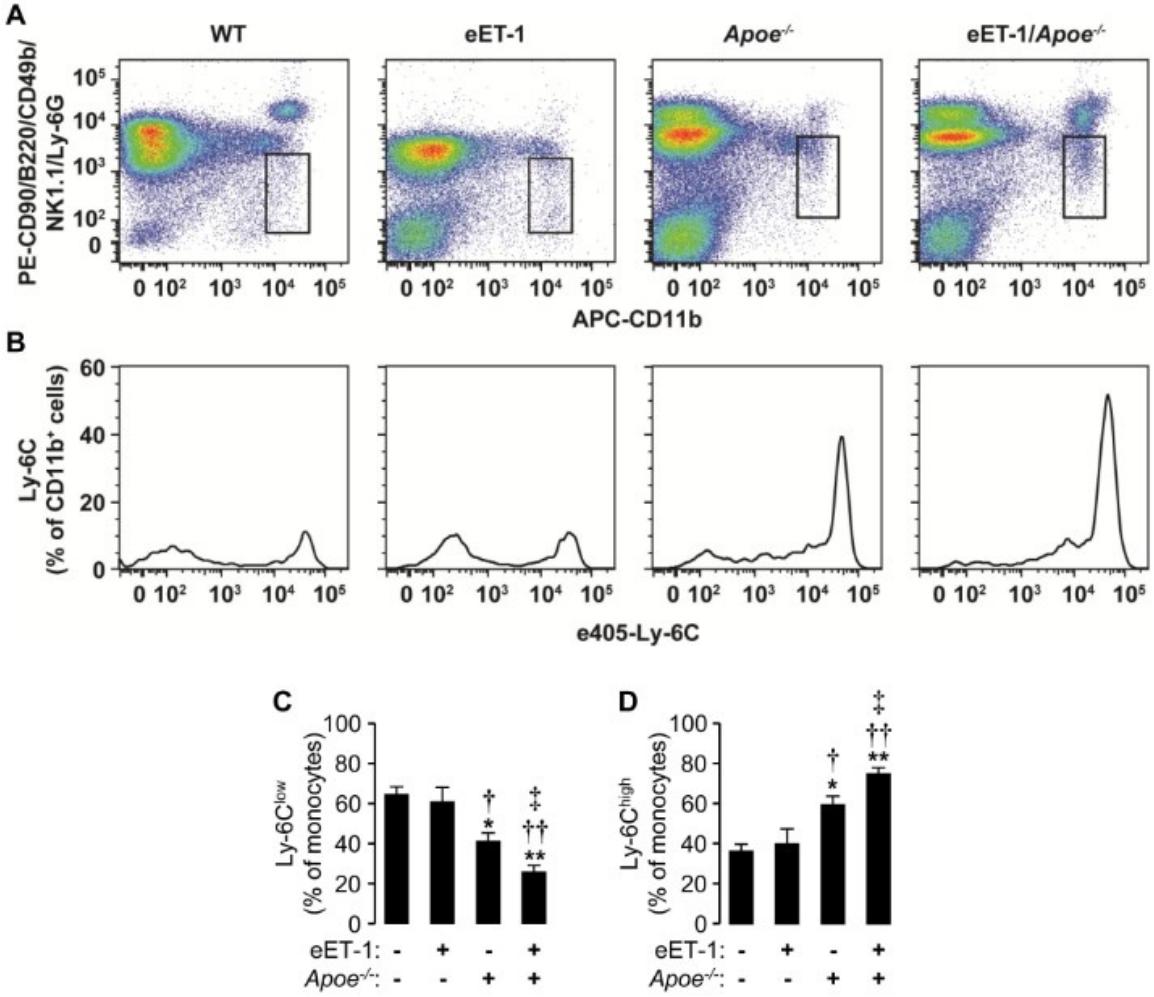

Figure II-S9: Flow cytometry profiling of splenic monocytes. The profile of monocytes and monocyte subset Ly-6C^{hi} in the spleen of 16-week old wild-type (WT), eET-1, *Apoe*$^{-/-}$ and eET1/*Apoe*$^{-/-}$ mice fed a high-fat diet for 8 weeks was determined by flow cytometry as previously described [3]. Splenocytes were stained with Fixable Viability Dye eFluor® 506 (e506), phycoerythrin (PE)-conjugated rat anti-mouse CD90.2 (T cells), PE-conjugated rat human/mouse B220 (B cells), PE-conjugated anti-mouse CD49b (NK cells), PE-conjugated mouse anti-mouse NK1.1 (NK cells), PE-conjugated rat anti-Ly-6G (granulocytes), allophycocyanin (APC)- conjugated rat anti-mouse CD11b (myeloid cells) and eFluor® 450 conjugated anti-mouse Ly-6C (monocyte subsets) antibodies, and analyzed by flow cytometry. Fluorophores were

respectively excited and analyzed with appropriate laser and bandpass filter (BP) (PE: 561 nm with 582/15 BP, APC-e780: 640 nm with 780/60 BP, e450: 405 nm with 450/50 BP, e506: 405 nm with 525/50 BP). As presented in Table II-S3, lymphocytes were gated in the side scatter (SSC)/forward scatter (FSC) plot, singlet lymphocytes were gated using FSC height (FSC-H) over FSC area (FSC-A) and live lymphocytes were gated in the viability dye/FSC-A plot. Monocytes ($CD11b^{hi}CD90^{lo}B220^{lo}CD49b^{lo}NK1\text{-}1^{lo}Ly\text{-}6G^{lo}$) were gated in CD90 B220 CD49b NK1-1 Ly-6G/CD11b plot (A), which was further divided into Ly-6Clo (B and D) and Ly-6Chi subsets (B and E). Representative dot plots (A) and histograms (B) for WT, eET-1, *Apoe*$^{-/-}$ and eET1/*Apoe*$^{-/-}$ mice fed a HFD are shown. Values are means ± SEM, n = 9 for WT, 5 for eET-1, 5 for *Apoe*$^{-/-}$ and 9 for eET1/*Apoe*$^{-/-}$ mice. **P*<0.05 and ***P*<0.001 vs. WT, †*P*<0.05 and ††*P*<0.001 vs. eET-1 and ‡ *P*<0.05 vs. *Apoe*$^{-/-}$ mice.

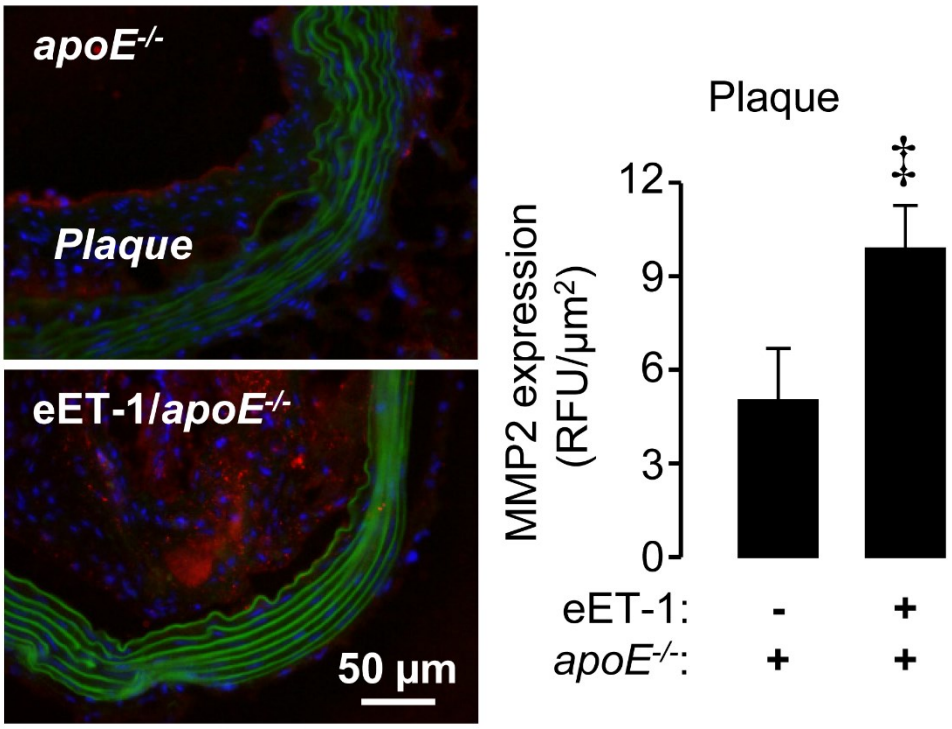

Figure II-S10: ET-1 overexpression increased MMP2 expression in aortic atherosclerotic plaques of *Apoe*$^{-/-}$ mice. MMP2 expression was determined by immunofluorescence in ascending aortic sections of 16-week old *Apoe*$^{-/-}$ and eET1/*Apoe*$^{-/-}$ mice fed a high-fat diet for 8 weeks. Representative images of MMP2-stained ascending aortic sections of *Apoe*$^{-/-}$ and eET1/*Apoe*$^{-/-}$ mice with quantification of relative fluorescence unit (RFU)/µm^2 of atherosclerotic plaque are presented. Blue, green and red fluorescence represent nuclear DAPI staining, autofluorescence of elastin and MMP2 staining, respectively. Values are means ± SEM, n = 5. ‡P<0.05 vs. *Apoe*$^{-/-}$.

CHAPTER III: Endothelial ET-1 overexpression in Apoe$^{-/-}$ mice induces a worsening of endothelium-dependent relaxation in resistance arteries

Hypothesis and objectives

Endothelial dysfunction is associated with the development of atherosclerosis. One of the key features of endothelial dysfunction is impaired endothelium-dependent relaxation (EDR). EDR is a consequence of activation of pathways mediated by several endothelium-derived relaxing factors, including NO and EDHF. Impaired EDR has been reported in several vascular beds in atherosclerosis [191]. Decreases in NO-mediated EDR in conduit vessels of *Apoe*$^{-/-}$ mice were restored by ET_AR blockade [132, 442]. In resistance arteries, an EDHF mechanism may substitute reduced NO-mediated EDR [443]. Although ET-1 is known to impair endothelium relaxation [200], exactly how ET-1 modifies resistance artery EDR pathways during development of atherosclerosis has not been studied. In the study addressed in chapter II, we observed that ET-1-exaggerated atherosclerosis in *Apoe*$^{-/-}$ mice was associated with enhanced vascular inflammatory responses, including increased ROS production. ROS can contribute to endothelial dysfunction in several ways, which were alluded to in section 6 of chapter I. Since *Apoe*$^{-/-}$ mice with endothelial ET-1 overexpression exhibit enhanced vascular ROS production, we hypothesize that:

Endothelial ET-1 overexpression in Apoe$^{-/-}$ *mice will induce a worsening of EDR in resistance arteries.*

The specific objectives of this study include:

- To determine whether ET-1-exaggerated atherosclerosis is associated with worsening of EDR in resistance arteries.
- To characterize the role of ET-1 on various EDR pathways in atherosclerosis.

Preservation of endothelium-dependent relaxation in atherosclerotic mice with endothelium-restricted endothelin-1overexpression.

Muhammad Oneeb Rehman Mian*, Nourredine Idris-Khodja*, Melissa W. Li, Avshalom Leibowitz, Pierre Paradis, Yohann Rautureau, Ernesto L. Schiffrin.

Lady Davis Institute for Medical Research (M.O.R.M., N.I.K., M.W.L., A.L., P.P., Y.R., E.L.S.), and Department of Medicine (E.L.S.), Sir Mortimer B. Davis-Jewish General Hospital, McGill University, Montreal, Quebec, Canada.

Published in:
Journal of Pharmacology and Experimental Therapeutics. *2013; 347(1):30-37*

*These authors contributed equally

The manuscript is presented here according to the instructions of the journal in which it was published. The main manuscript (including the expanded materials and methods section) is followed by the Online Supplemental material.

Abstract

In human atherosclerosis, which is associated with elevated plasma and coronary endothelin (ET)-1 levels, ET_A receptor antagonists improved coronary endothelial function. Mice overexpressing ET-1 specifically in the endothelium (eET-1) crossed with atherosclerosis-prone apolipoprotein E knockout mice (*Apoe*$^{-/-}$) exhibit exaggerated high-fat diet (HFD)-induced atherosclerosis. Since endothelial dysfunction often precedes atherosclerosis development, we hypothesized that mice overexpressing endothelial ET-1 on a genetic background deficient in apolipoprotein E (eET-1/*Apoe*$^{-/-}$) would have severe endothelial dysfunction. In order to test this hypothesis, we investigated endothelium-dependent relaxation (EDR) to acetylcholine in eET-1/*Apoe*$^{-/-}$ mice. EDR in mesenteric resistance arteries from 8- and 16-week-old mice fed a normal or HFD was improved in eET-1/*Apoe*$^{-/-}$ compared to *Apoe*$^{-/-}$ mice. NO synthase (NOS) inhibition abolished EDR in *Apoe*$^{-/-}$. EDR in eET-1/*Apoe*$^{-/-}$ was resistant to NOS inhibition irrespective of age or diet. Inhibition of cyclooxygenase, the cytochrome P450 pathway and endothelium-dependent hyperpolarization (EDH) resulted in little or no inhibition of EDR in eET-1/*Apoe*$^{-/-}$, compared to wild-type (WT) mice. In eET-1/*Apoe*$^{-/-}$ mice, blocking of EDH or soluble guanylate cyclase (sGC) in addition to NOS inhibition, decreased EDR by 36 and 30% respectively. The activation of 4-aminopyridine sensitive voltage-dependent potassium channels (K_v) during EDR was increased in eET-1/*Apoe*$^{-/-}$ compared to WT mice. We conclude that increasing eET-1 in mice that develop atherosclerosis results in decreased mutual dependence of endothelial signaling pathways responsible for EDR, and that NOS-independent activation of sGC and increased activation of K_v are responsible for enhanced EDR in this model of atherosclerosis associated with elevated endothelial and circulating ET-1.

Introduction

Endothelin (ET)-1 is an endothelium-derived contracting peptide with potent vasoconstrictor effects. Endothelin type A (ET_A) and type B (ET_B) receptors are responsible for its physiological effects on the vasculature. In vascular smooth muscle cells (VSMC), ET_A activation and, to a lesser extent, ET_B activation can induce contraction and proliferation of VSMC, although the main role of ET_B is in the endothelium to stimulate release of vasorelaxant agents [nitric oxide (NO) and prostacyclin (PGI_2)] [1]. ET-1 is involved in the pathophysiology of cardiovascular disease. In hypertension, ET-1 induces hypertrophic remodeling of small arteries [2-4]. In the coronary circulation there is a correlation between the severity of atherosclerosis and plasma ET-1 concentration [5]. ET-1 antagonists have been shown to decrease the size of atheroma in humans [6]. In a mouse model of endothelial ET-1 overexpression (eET-1), we showed that ET-1 is associated with vascular injury characterized by enhanced vascular remodeling, increase in reactive oxygen species formation, and inflammation [7, 8]. In eET-1 mice we demonstrated an increase in expression of genes associated with lipid synthesis in the vasculature [9]. This change in gene expression was associated with an exacerbation of high-fat diet(HFD)-induced aortic atherosclerotic lesions when eET-1 mice were crossed with apolipoprotein E knock-out mice (*Apoe*$^{-/-}$), a model to study progression of atherosclerosis [10]. We proposed that eET-1-induced lipids synthesis could be involved in its pro-atherosclerotic effect [9].

Endothelial dysfunction is associated with the development of atherosclerosis [11, 12]. One of the main consequences of endothelial dysfunction is impairment of endothelium-dependent relaxation (EDR) [11]. EDR is dependent on the activation of several signaling pathways resulting in the production of endothelium-derived relaxing factors (EDRFs) by endothelial cells and leading to relaxation of VSMC. These signaling pathways include production of NO by endothelial nitric oxide synthase (eNOS), PGI_2 by cyclooxygenase (COX), and epoxyeicosatrienoic acids (EETs) by the cytochrome P 450

epoxygenase [13]. Endothelium-dependent hyperpolarization (EDH) [14] is an additional vasorelaxation mechanism involving the activation of endothelial small (SK_{Ca}) and intermediate conductance (IK_{Ca}) of calcium-activated potassium channels (K_{Ca}), which are known to be inhibited by apamin and TRAM-34 [1-[(2-chlorophenyl)diphenylmethyl]-1***H***-pyrazole], respectively [15]. Opening of SK_{Ca} and IK_{Ca} increases extracellular potassium, which activates inward rectifier K^+ channels (K_{ir}) and the Na^+/K^+ exchanger to hyperpolarize and relax VSMC [16]. In general, endothelium signaling pathways lead to the activation of several classes of K^+ channels that are important effectors of EDR as they are responsible for repolarization of membrane potential and the decrease in calcium concentrations in VSMC [17].

In conduit vessels of *Apoe*$^{-/-}$ mice, there is a decrease of NO-mediated EDR [18] that is restored by blockade of ET_A receptor [19, 20]. In resistance arteries, decreased NO-mediated EDR may be substituted by an EDH mechanism [21]. Although it is known that ET-1 impairs EDR, a specific role of ET-1 on EDR signaling pathways during development of atherosclerosis is unknown. We examined EDR in *Apoe*$^{-/-}$ mice overexpressing eET-1 (eET-1/*Apoe*$^{-/-}$) and observed that these mice have a restored EDR compared to *Apoe*$^{-/-}$ mice. This enhanced EDR in eET-1/*Apoe*$^{-/-}$ mice was predominantly resistant to NOS, COX and EDH inhibitors. Therefore, we investigated the mechanisms for the restoration of EDR in eET-1/*Apoe*$^{-/-}$ mice, which exhibit transgenic overexpression of ET-1, resulting in high levels of ET-1 in endothelial cells and in the circulation.

Materials and Methods

Generation of eET-1/*Apoe*$^{-/-}$ mice and procedures

Protocols were approved by the Animal Care Committees of the Lady Davis Institute for Medical Research and McGill University, followed the guidelines of the Canadian Council for Animal Care, and were in agreement with the recommendations for the Care and Use of Laboratory Animals published by

the US National Institutes of Health. Mice were housed in the Lady Davis Institute for Medical Research Animal Facility. Transgenic mice generated in our laboratory and overexpressing human preproET-1 (eET-1) in endothelial cells were described previously [7]. Human ET-1 is processed similarly to the endogenous protein as the consensus sequences necessary for the maturation of the prepropeptide are identical in mice and humans [22]. Apolipoprotein E knockout (*Apoe*$^{-/-}$) mice were obtained from The Jackson Laboratories (B6.129P2-Apoe$^{tm1Unc/J}$, Bar Harbor, ME, USA). *Apoe*$^{-/-}$ mice were crossed with eET-1 mice to obtain eET-1/*Apoe*$^{-/-}$ mice. An additional cross of eET-1/*Apoe*$^{-/-}$ with *Apoe*$^{-/-}$ mice produced the mice used in the present experiments. Eight-week-old male eET-1, *Apoe*$^{-/-}$, eET-1/*Apoe*$^{-/-}$, and littermate wild-type (WT) mice were used for experiments or were fed either a high-fat, cholesterol-rich diet (HFD; 35% fat, 1.25% cholesterol, D12336, Research Diets Inc., New Brunswick, NJ, US) or regular chow (normal diet, ND) for 8 weeks. All mice were on C57BL/6 genetic background.

Drugs

Apamin and TRAM-34 were purchased from Tocris Bioscience (Minneapolis, MN). Acetylcholine (ACh), 4-aminopyridine (4-AP), iberiotoxin (Ibtx), $BaCl_2$, fluconazole, L-NAME (N^{ω}-Nitro-L-arginine methyl ester) hydrochloride, sodium salt of meclofenamic acid (meclo), norepinephrine (NE), ODQ (1*H*- [1, 2, 4]oxadiazolo[4, 3-a]quinoxalin-1-one) and TEA were purchased from Sigma-aldrich (St. Louis, MO). 14,15-epoxyeicosa-5(*Z*)-enoic acid (14,15-EE5ZE) was purchased from Cayman Chemical (Ann Arbor, MI). Stock solutions (10^{-2} M) of ODQ and TRAM-34 were made in ethanol. Stock solution (6.7×10^{-3} M) of fluconazole was made in DMSO. All the other products were dissolved in water.

Collection of tissues and study of vascular reactivity on a pressurized myograph

Second order mesenteric vessels were dissected and mounted on a pressurized myograph system to study vascular reactivity, as previously described [23, 24]. Mice were anesthetized using isoflurane, and the complete mesenteric arterial bed was collected and placed in cold Krebs' solution, pH 7.4, containing (in mM): NaCl (120), $NaHCO_3$ (25), KCl (4.7), KH_2PO_4 (1.18), $MgSO_4$ (1.18), $CaCl_2$ (2.5), EDTA (0.026) and glucose (5.5). Second-order mesenteric arteries (150-250 μm, 2 mm long sections) were cleaned of surrounding fat, mounted on glass micropipettes on a pressurized myograph, and perfused with Krebs' solution at an intraluminal pressure of 45 mmHg. Pressurized vessels were kept in a chamber with a superfusion flow of warmed (37°C) and oxygenated (95% air–5% CO_2) control solution (Krebs') or Krebs' containing the pharmacological agents. After mounting, vessels were equilibrated for 60 min in Krebs solution. The lumen diameter was measured using a computer-based video imaging system (Living Systems Instrumentation, Burlington, VA). All vessels were initially constricted with Krebs solution containing 10^{-5} M NE and 120 mM KCl. Only vessels constricting at least 60% of the initial resting diameter were used for further studies. Viable vessels were used to perform concentration-response curves to NE, or were pre-constricted in presence of 5 x 10^{-5} M NE to study concentration-responses to ACh or sodium nitroprusside (SNP). For some concentration-response studies, vessels were pretreated with inhibitors before NE constriction, as indicated in Table III-1. In presence of inhibitors, preconstriction levels were similar between different strains. Vessels were allowed to rest for 30-40 minutes with Krebs' superfusion between concentration-response studies. For studies in presence of 14,15-EE5ZE, response to a single concentration of ACh (10^{-6} M) was obtained on NE pre-constricted arteries.

Data analysis

The percentage of contraction is expressed relative to the diameter of the lumen of the vessel in the resting state before application of the first

concentration of NE. The percentage of relaxation is expressed relative to the pre-constriction induced by NE. Results are presented as means ± S.E.M.; *n* refers to the number of experimental animals. pEC_{50} and area-under-the-curve (AUC) values of concentration-response curves were calculated using Sigma Plot 12.0 (Systat Software Inc. Chicago, IL). The effects of strain, diet or pharmacological inhibitors were analyzed by comparing the AUCs, pEC_{50}s, and E_{max} of concentration-response curves using one-way ANOVA with Sigma Plot 12.0. Unless otherwise specified, only statistical analyses of the AUCs of concentration-response curves are discussed or represented. E_{max} differences of concentration-response curves were calculated as the difference between the percentage of maximum relaxation of each curve. The effect of apamin + TRAM-34 treatment in WT and eET-1/*Apoe*$^{-/-}$ was determined using two-way analysis of variance for repeated measures. *P* values less than 0.05 were considered significant.

Results

eET-1 restores EDR in atherosclerotic mice.

NE-induced contraction of mesenteric arteries from 8-week-old mice and 16-week-old mice on ND or HFD was similar in WT, eET-1, *Apoe*$^{-/-}$ and eET-1/*Apoe*$^{-/-}$ mice (Figure III-S1 and Figure III-S2A). EDR to ACh 10^{-4} M in mesenteric arteries of 8-week-old (E_{max}: 84.2 ± 6.5%), 16-week-old ND (82.5 ± 5.6%) and HFD wild-type (WT) mice (88.0 ± 2.6%) was comparable (Figure III-1A, III-1B; Figure III-S2B). Eight-week- (Figure III-S2B) and 16-week-old (Figure III-1A) eET-1 mice presented similar ACh-induced vasorelaxation when fed an ND (E_{max}: 72 ± 7.4%) compared with WT mice (82.5 ± 5.6%). ACh-induced vasorelaxation was significantly inhibited in eET-1 mice fed a HFD (eET-1: 51.8 ± 5.6%, WT 88.0 ± 2.6%, $P<0.05$). In *Apoe*$^{-/-}$ mice, relaxation was decreased by 30.5% in 8-week-old (Figure III-S2B) and by 43.5 and 64.2 % (Figure III-1A, III-1B) in 16-week-old mice fed a ND or HFD, respectively, compared with the corresponding WT mice ($P<0.01$). In *Apoe*$^{-/-}$ mice overexpressing eET-1 (eET-

1/*Apoe*-/-), ACh-induced EDR was restored at 8 weeks (74.0 ± 13.0%, Figure III-S2B), 16 weeks ND (88.3 ± 4.2%, Figure III-1A), and 16 weeks HFD (70.9 ± 9.8%, Figure III-1B), compared with *Apoe*$^{-/-}$ mice (P<0.01). NO-dependent, endothelium-independent relaxation of VSMC in response to the NO donor SNP was similar in WT, eET-1, *Apoe*$^{-/-}$, eET-1/ *Apoe*$^{-/-}$ mice at 8 weeks (Suppl. Fig.2C), and 16 weeks on ND (Figure III-1C). In 16-week-old mice fed a HFD, WT, eET-1 and eET-1/*Apoe*$^{-/-}$ presented similar SNP-induced relaxation (Figure III-1D). Only arteries from *Apoe*$^{-/-}$ mice presented a decreased sensitivity to SNP (pEC_{50}: 5.7 ± 0.1), compared with WT (6.3 ± 0.1) (P<0.01, Figure III-1D). However, E_{max} values were not significantly different (WT, 98.1 ± 1.2%, *Apoe*$^{-/-}$, 87.2 ± 5.8%, Figure III-1D).

EDR in mesenteric arteries from eET-1/*Apoe*$^{-/-}$ is resistant to eNOS inhibition.

In 16-week-old mice fed a ND, eNOS inhibition by L-NAME predominantly abolished the maximal ACh-induced EDR in WT (E_{max}=2.8 ± 0.4%), eET-1 (E_{max}=3.5 ± 1.1%) and *Apoe*$^{-/-}$ (E_{max}=10.4 ± 5.5%) mice (Figure III-2A). In contrast, ACh-induced EDR in eET-1/*Apoe*$^{-/-}$ was resistant to L-NAME (E_{max}=68.6 ± 9.9%, P<0.01 vs *Apoe*$^{-/-}$). Similar results were found for the 4 groups of mice at 8-weeks, (Figure III-S2D) and in 16-week-old mice on HFD (Figure III-2B).

Remodeling of EDRF and EDH-mediated EDR in eET-1/*Apoe*$^{-/-}$ mice.

By use of specific pharmacological inhibitors, we studied the role of signaling pathways involved in ACh-induced EDR in 16-week-old WT and eET-1/*Apoe*$^{-/-}$ mice fed an ND. In WT mice, incubation with meclofenamate, an inhibitor of COX1, decreased maximal EDR to ACh by 27.0% to 55.7 ± 3.1% (P<0.05 vs vehicle-treated, Figure III-3A). In contrast, maximal EDR to ACh was preserved in mesenteric arteries from eET-1/*Apoe*$^{-/-}$ mice incubated with meclofenamate (E_{max}=83.3 ± 7.8%, Figure III-3B), compared with control conditions. Similarly, fluconazole, which inhibits synthesis of epoxyeicosatrienoic acids (EETs) by cytochrome P450, tended to decrease ACh-induced EDR in WT

mice (Figure III-3C, nonsignificant), but did not alter it in eET-1/*Apoe*$^{-/-}$ mice (E_{max}=83.7 ± 16.3%, Figure III-3D). Incubation with 14,15-EE5ZE, an antagonist of EETs [25], decreased vasorelaxation to ACh (10^{-6} M) to the same extent in WT (15.7%) and eET-1/*Apoe*$^{-/-}$ mice (18.3%), without, however, achieving significance but essentially confirming fluconazole results and the minor role of the EET signaling pathway in enhanced EDR to ACh observed in eET-1/*Apoe*$^{-/-}$ mice. (Figure III-S3)

We next investigated the role of endothelial hyperpolarization mediated by IK_{Ca} and SK_{Ca} activation in EDR. Apamin and TRAM-34 incubation inhibited maximal EDR to ACh by 46 % in WT (Figure III-3E). In eET-1/*Apoe*$^{-/-}$ mice, apamin and TRAM-34 did not modify maximal EDR but induced a shift to the right of the concentration-relaxation curve to ACh from a pEC_{50} of 7.0 ± 0.2 to 6.1 ± 0.2 (For pEC_{50}, P<0.05, Figure III-3F, Table III-S1). In presence of apamin + TRAM-34, ACh-induced relaxation was greater in eET-1/*Apoe*$^{-/-}$ than in WT mice (P<0.01). $BaCl_2$ + ouabain were used to inhibit VSMC hyperpolarization activated by the potassium cloud formed by the activation of endothelial IK_{Ca} and SK_{Ca} [26]. In WT and in eET-1/*Apoe*$^{-/-}$ mice, $BaCl_2$ + ouabain decreased maximal ACh-induced EDR by 30% to 52.1 ± 2.5% and 20% to 62.4 ± 10.3%, respectively (both P<0.01 versus vehicle, Figure III-3G-H).

In eET-1/*Apoe*$^{-/-}$ mice fed an HFD, we performed additional experiments using apamin and TRAM-34 in addition to L-NAME. In presence of L-NAME, maximal EDR to ACh was 82.8 ± 8.4%. The addition of apamin + TRAM-34 + L-NAME decreased maximal EDR to ACh by 36.3 % to 43.0 ± 8.3% (Figure III-4A, P<0.01 vs L-NAME alone). We also examined the role of soluble guanylate cyclase (sGC) on EDR independent of eNOS activation. Addition of the sGC inhibitor ODQ to L-NAME decreased EDR to ACh by 30.6 % to 48.6 ± 19.2% (Figure III-4B, P<0.01 vs L-NAME alone, Table III-S2).

The role of 4-AP-sensitive K_v channels mediating ACh-induced EDR is enhanced in eET-1/*Apoe*$^{-/-}$ mice.

Several classes of K^+ channels mediate EDR [27]. We used selective inhibitors of different classes of K^+ channel to investigate their involvement in 16-week-old ND WT and eET-1/*Apoe*$^{-/-}$ mice. We first tested TEA, an inhibitor of voltage-dependent (K_v) and calcium-dependent potassium channels (K_{Ca}) [17]. TEA inhibited maximal EDR to ACh by 28.3% to 54.3 ± 10.6% in WT mice (P<0.05, Figure III-5A). In eET-1/*Apoe*$^{-/-}$ mice, TEA inhibition also decreased maximal ACh-induced EDR by 14.8% to 73.5% (P<0.05, Figure III-5B). We then studied the effect of iberiotoxin (Ibtx), a selective inhibitor of large conductance K_{Ca} (BK_{Ca}), and 4-aminopyridine (4-AP), a selective inhibitor of K_v. In WT mice, Ibtx inhibited maximal EDR to ACh by 50.5% to 38 ± 13.6% (P<0.05, Fig. 5C), whereas 4-AP did not significantly modify EDR (E_{max}=69.3 ± 8.2%, Fig. 5E), compared with control. In contrast, both Ibtx and 4-AP significantly inhibited maximal ACh-induced EDR by ~38 % in eET-1/*Apoe*$^{-/-}$ mice. (P<0.05 for both; Figure III-5D and F).

Inward rectifier potassium channels (Kir) are important regulators of the resting membrane potential and are activated by an increase in extracellular potassium concentration [27]. We used $BaCl_2$ at 100 μM to investigate selectively the role of K_{ir}. EDR to ACh was significantly inhibited by $BaCl_2$ in WT (reduction of 31.3 %, P<0.05) (Figure III-5G). In eET-1/*Apoe*$^{-/-}$ mice, K_{ir} function appeared relatively preserved with a nonsignificant reduction of 24.1% in the amplitude of the response (Figure III- 5H).

Discussion

Our findings indicate that overexpression of eET-1 in *Apoe*$^{-/-}$ mice unexpectedly restores EDR in a model of eET-1 mediated exacerbation of atherosclerosis. This restoration of endothelial function is associated with remodeling of endothelial signaling pathways mediating ACh-induced EDR. We found that overexpressing eET-1 in *Apoe*$^{-/-}$ mice makes ACh-induced EDR more

resistant to eNOS, COX, cytochrome P450, and EDH inhibition compared with WT. We propose that this endothelial remodeling could be explained by a decrease in mutual dependence between endothelial signaling pathways. The reduction of ACh-induced EDR in vessels treated with sGC inhibitor and L-NAME (Figure III-4B) suggests that eNOS-independent activation of sGC is involved in ACh-induced EDR in eET-1/*Apoe*$^{-/-}$.

Unlike in the aorta and other conduit arteries, neither atheroma nor the early-occurring fatty streaks develop in small mesenteric resistance arteries and would not be expected nor are found in *Apoe*$^{-/-}$ and in eET-1/*Apoe*$^{-/-}$ used in this study. The use of small mesenteric arteries is an established model to study reactivity of arteries involved in the control of microvascular regional blood flow, which can be affected by endothelial dysfunction in atherosclerosis. In aortae of *Apoe*$^{-/-}$ mice, reduction in EDR is dependent on increased production of superoxide that reduces NO bioavailability [18, 19, 28]. A decrease in EDR has been reported in mesenteric arteries of *Apoe*$^{-/-}$ mice fed a Western-type diet for 30 weeks [20]. In the latter study and in 16-week-old *Apoe*$^{-/-}$ mice on HFD in the present work, decreased EDR was accompanied by a diminished endothelium-independent vasorelaxation in response to a NO donor, suggesting that there is a decreased NO relaxant response of VSMC in *Apoe*$^{-/-}$ mice. In other studies, however, no modification of ACh-induced EDR in mesenteric arteries was observed in 10-16-week old *Apoe*$^{-/-}$ mice [21, 29, 30]. It is important to point out that our study design differed from these other studies. For example, we used NE to pre-contract vessels whereas Morikawa *et al.* [29] used prostaglandin F2α, and Beleznai *et al.* [21] and Ding *et al.* [30] used phenylephrine. Dysfunction in α_2-adrenoceptor-mediated EDR has been reported in *Apoe*$^{-/-}$ mice [31]. The absence of α_2-adrenoceptor stimulation by NE in phenylephrine-and prostaglandin F2α-pre-constricted arteries could be related to the impaired EDR observed.

In our study, the application of L-NAME (10^{-4} M) abolished EDR in WT and *Apoe*$^{-/-}$ mice. Whereas some groups have reported similar findings [32, 33], others have shown that in mesenteric arteries from WT [29, 34] and *Apoe*$^{-/-}$ mice

[21], EDR to ACh is resistant to eNOS inhibition. Such discrepancies could be explained by different housing conditions, intestinal microbiota differences, or technical aspects of myography.

We did not observe impairment of endothelial function in 8-weeks-old eET-1 mice, and only a minor impairment at 16 weeks, in contrast to other reports [35] and our own previous work [36, 37]. Loss of endothelial dysfunction in eET-1 mice in this study could have been caused by additional backcrossing into the C57BL/6 background or by accidental selection of mice resistant to eET-1–induced endothelial dysfunction [38].

Atherosclerosis development in eET-1/*Apoe*$^{-/-}$ mice was much more extensive than in *Apoe*$^{-/-}$ mice at comparable ages [9]. Since endothelial dysfunction occurs early in the development of atherosclerosis, we hypothesized that eET-1 overexpression in *Apoe*$^{-/-}$ would induce a worsening of endothelial dysfunction. Unexpectedly, we observed that EDR was fully restored in eET-1/*Apoe*$^{-/-}$ mice, compared to *Apoe*$^{-/-}$ mice, at all endpoints. This vasorelaxation was resistant to L-NAME inhibition. ODQ co-incubation with L-NAME decreased ACh-induced EDR, indicating that there was eNOS-independent activation of sGC. Several mechanisms can account for this finding. It has been previously shown that NO stores can mediate EDR [39, 40]. Nitrite and nitrate are endogenous sources of NO as they can be reduced to form bioactive nitrogen oxides [41]. The heme containing proteins, myoglobin, hemoglobin, xanthine oxidase and cytochrome P450 enzyme system, generate NO from nitrite and nitrate. Nitrite- and nitrate-dependent generation contributes to endothelium-dependent, eNOS-independent regulation of vascular tone [42]. *S*-nitrosothiols, derived in part from *S*-nitrosoglutathione, have also been shown to be an eNOS-independent source of NO that could account for ACh-mediated NO release [43]. Carbon monoxide, an endogenous weak activator of sGC produced by heme oxygenases 2 and 3 [44], could also be involved in eNOS-independent, sGC-mediated EDR [44]. In eET-1/*Apoe*$^{-/-}$ mice, superoxide production by aorta is significant (unpublished observations). Uncoupled eNOS produces superoxide that can be reduced to hydrogen peroxide by superoxide dismutase [45]. NOS-

derived hydrogen peroxide has been shown to be involved in EDR [45]. Hydrogen peroxide can mediate dimerization and activation of G-kinase [46] by means of disulfide bridge formation [47-49]. Heterodimerization of α and β subunits of sGC is augmented in presence of enhanced oxidative stress [50]. Hydrogen peroxide-mediated dimerization and activation of sGC could therefore be involved in L-NAME-resistant EDR. It has also been proposed that residual NOS activation in response to ACh could occur in presence of L-NAME [47-49]. Since we observed complete inhibition of EDR in WT, eET-1 and *Apoe*$^{-/-}$ mice, decreased affinity of eNOS for L-NAME or an increased concentration of L-arginine, which can compete with L-NAME, could play a role in L-NAME-resistant eNOS activation in eET-1/*Apoe*$^{-/-}$ mice.

Because the eNOS pathway involved in EDR was altered in eET-1/*Apoe*$^{-/-}$ mice compared with WT mice, we investigated other endothelial pathways mediating relaxation. By use of specific pharmacological inhibitors, we found that COX and, to a lesser extent, cytochrome P450 pathways/EETs were involved in EDR in WT mice. In contrast, no involvement of COX and cytochrome P450 pathways was found in eET-1/*Apoe*$^{-/-}$ mice. As inhibition of EDRF pathways was unable to modify EDR in eET-1/*Apoe*$^{-/-}$, we investigated EDH mechanisms mediated by endothelial hyperpolarization /K^+ cloud[26]. In WT mice, both ouabain + $BaCl_2$ and apamin + TRAM-34 efficiently inhibited EDR. In eET-1/*Apoe*$^{-/-}$ mice, ouabain + $BaCl_2$ inhibition was less effective than in WT mice, and there was a decreased sensitivity to ACh in presence of apamin + TRAM-34. Incubation with L-NAME + apamin + TRAM-34 potentiated the inhibition of EDR (Figure III-4A). This suggests that eNOS- and EDH- signaling mechanisms are less mutually dependent in eET-1/*Apoe*$^{-/-}$ mice than in WT mice.

Potassium channels are major regulators of vascular tone in EDR. We hypothesized that changes in various potassium channels involved in EDR accompanied remodeling of endothelial function in eET-1/*Apoe*$^{-/-}$ mice compared with WT mice. In presence of TEA, a non-selective inhibitor of K_v and BK_{Ca} [17], EDR was inhibited to the same extent in WT and eET-1/*Apoe*$^{-/-}$ mice. We then looked at the specific roles of BK_{Ca} and Kv using selective inhibitors, Ibtx and 4-

AP, respectively. Ibtx induced similar inhibition in both strains of mice, but the inhibitory effect of 4-AP was potentiated in eET-1/*Apoe*$^{-/-}$ mice compared with WT. Consistent with our results using $BaCl_2$ + ouabain, blockade of K_{ir} with $BaCl_2$ induced a more pronounced inhibition in WT than in eET-1/*Apoe*$^{-/-}$ mice (Figure III-5G-H). Therefore, we conclude that increase in K_v and decrease in K_{ir} contributes to remodeling of endothelial signaling pathways in eET-1/*Apoe*$^{-/-}$ mice. Inhibition of EDR by 4-AP is a hallmark of nitroxyl (HNO) action. HNO activates sGC to induce vasorelaxation [51]. In a model of vessel injury (angiotensin II-treated mice), HNO-mediated relaxation has been shown to be inhibited by 4-AP, whereas in sham mice. HNO donor-induced relaxation is insensitive to 4-AP [52]. As L-NAME resistant EDR is partially inhibited by ODQ in eET-1/*Apoe*$^{-/-}$ mice, it will be necessary in the future to investigate the role of HNO in 4-AP-sensitive EDR in these mice.

Overall, our studies demonstrate that in a model of atherosclerosis, exacerbation of atherosclerosis induced by overexpression of eET-1 is accompanied by preservation and remodeling of endothelial signaling pathways and K^+ channels mediating EDR. ET-1 overexpression induces development of compensatory mechanisms in arteries of eET-1/*Apoe*$^{-/-}$ mice, which allows eNOS, EDH mechanisms or the COX pathway to mediate independently EDR.

Acknowledgments

We are grateful to Marie-Ève Deschênes and Heather Mlynarski for animal care.

Authorship contributions

Participated in research design: Mian, Idris-Khodja, Li, Paradis, Rautureau, Schiffrin.

Conducted experiments: Mian, Idris-Khodja, Li, Leibowitz, Rautureau.

Performed data analysis: Mian, Idris-Khodja, Li, Leibowitz, Paradis, Rautureau, Schiffrin.
Wrote or contributed to the writing of the manuscript: Mian, Idris-Khodja, Paradis, Rautureau, Schiffrin.

Footnotes

This work was supported by the Canadian Institutes of Health Research (CIHR) [Grant 37917]; a Canada Research Chair (CRC) on Hypertension and Vascular Research from the CIHR/government of Canada CRC program, and by the Canada Fund for Innovation [Grant 202891]; all to ELS.

Part of this work has been previously presented as an oral presentation: Rautureau Y, Li MW, Leibowitz A, Paradis P, Schiffrin EL (2010) Remodeling of endothelial function in atherosclerotic mice overexpressing endothelial endothelin-1 at the *Scientific Sessions 2010 of the Council for High Blood Pressure Research of the American Heart Association*, Washington, DC. Li MW, Ebrahimian T, Paradis P, Schiffrin EL (2009) Effect of Endothelin-1 Overexpression on Vascular Structure and Function of Apolipoprotein E Knockout Mice *The eleventh International conference on endothelin,* Montreal, QC, Canada.

References

1. **Rautureau Y, Schiffrin EL**. Endothelin in hypertension: an update. *Curr Opin Nephrol Hypertens.* 2012; 21(2):128-36.

2. **Schiffrin EL, Lariviere R, Li JS, Sventek P**. Enhanced expression of the endothelin-1 gene in blood vessels of DOCA-salt hypertensive rats: correlation with vascular structure. *J Vasc Res.* May; 33(3):235-48.

3. **Schiffrin EL**. Vascular endothelin in hypertension. *Vascul Pharmacol.* 2005; 43(1):19-29.

4. **Li JS, Lariviere R, Schiffrin EL**. Effect of a nonselective endothelin antagonist on vascular remodeling in deoxycorticosterone acetate-salt hypertensive rats. Evidence for a role of endothelin in vascular hypertrophy. *Hypertension.* 1994; 24(2):183-8.

5. **Lerman A, Holmes DR, Jr., Bell MR, Garratt KN, Nishimura RA, Burnett JC, Jr**. Endothelin in coronary endothelial dysfunction and early atherosclerosis in humans. *Circulation.* 1995; 92(9):2426-31.

6. **Yoon MH, Reriani M, Mario G, Rihal C, Gulati R, Lennon R, Tilford JM, Lerman LO, Lerman A**. Long-term endothelin receptor antagonism attenuates coronary plaque progression in patients with early atherosclerosis. *Int J Cardiol.* 2013.

7. **Amiri F, Virdis A, Neves MF, Iglarz M, Seidah NG, Touyz RM, Reudelhuber TL, Schiffrin EL**. Endothelium-restricted overexpression of human endothelin-1 causes vascular remodeling and endothelial dysfunction. *Circulation.* 2004; 110(15):2233-40.

8. **Amiri F, Paradis P, Reudelhuber TL, Schiffrin EL**. Vascular inflammation in absence of blood pressure elevation in transgenic murine model overexpressing endothelin-1 in endothelial cells. *J Hypertens.* 2008; 26(6):1102-9.

9. **Simeone SM, Li MW, Paradis P, Schiffrin EL**. Vascular gene expression in mice overexpressing human endothelin-1 targeted to the endothelium. *Physiol Genomics.* 2011; 43(3):148-60.

10. **Plump AS, Smith JD, Hayek T, Aalto-Setala K, Walsh A, Verstuyft JG, Rubin EM, Breslow JL**. Severe hypercholesterolemia and atherosclerosis in apolipoprotein E-deficient mice created by homologous recombination in ES cells. *Cell.* 1992; 71(2):343-53.

11. **Freiman PC, Mitchell GG, Heistad DD, Armstrong ML, Harrison DG**. Atherosclerosis impairs endothelium-dependent vascular relaxation to acetylcholine and thrombin in primates. *Circ Res.* 1986; 58(6):783-9.

12. **Ross R**. The pathogenesis of atherosclerosis: a perspective for the 1990s. *Nature.* 1993; 362(6423):801-9.

13. **Vanhoutte PM, Shimokawa H, Tang EH, Feletou M**. Endothelial dysfunction and vascular disease. *Acta Physiol (Oxf).* 2009; 196(2):193-222.

14. **Feletou M, Vanhoutte PM**. Endothelium-dependent hyperpolarization: no longer an f-word! *J Cardiovasc Pharmacol.* 2013; 61(2):91-2.

15. **Feletou M, Vanhoutte PM, Weston AH, Edwards G**. EDHF and endothelial potassiun channels: IKCa and SKCa. *Br J Pharmacol.* 2003; 140(1):225.

16. **Edwards G, Feletou M, Weston AH**. Endothelium-derived hyperpolarising factors and associated pathways: a synopsis. *Pflugers Arch.* 2010; 459(6):863-79.

17. **Cox RH**. Molecular determinants of voltage-gated potassium currents in vascular smooth muscle. *Cell Biochem Biophys.* 2005; 42(2):167-95.

18. **D'Uscio LV, Baker TA, Mantilla CB, Smith L, Weiler D, Sieck GC, Katusic ZS**. Mechanism of endothelial dysfunction in apolipoprotein E-deficient mice. *Arterioscler Thromb Vasc Biol.* 2001; 21(6):1017-22.

19. **Barton M, Haudenschild CC, D'Uscio LV, Shaw S, Munter K, Luscher TF**. Endothelin ETA receptor blockade restores NO-mediated endothelial function and inhibits atherosclerosis in apolipoprotein E-deficient mice. *Proc Natl Acad Sci U S A.* 1998; 95(24):14367-72.

20. **D'Uscio LV, Barton M, Shaw S, Luscher TF**. Chronic ET(A) receptor blockade prevents endothelial dysfunction of small arteries in apolipoprotein E-deficient mice. *Cardiovasc Res.* 2002; 53(2):487-95.

21. **Beleznai T, Takano H, Hamill C, Yarova P, Douglas G, Channon K, Dora K**. Enhanced K(+)-channel-mediated endothelium-dependent local and conducted dilation of small mesenteric arteries from ApoE(-/-) mice. *Cardiovasc Res.* 2011; 92(2):199-208.

22. **Chan TS, Lin CX, Chan WY, Chung SS, Chung SK**. Mouse preproendothelin-1 gene. cDNA cloning, sequence analysis and determination of sites of expression during embryonic development. *Eur J Biochem.* 1995; 234(3):819-26.

23. **Diep QN, El MM, Cohn JS, Endemann D, Amiri F, Virdis A, Neves MF, Schiffrin EL**. Structure, endothelial function, cell growth, and inflammation in blood vessels of angiotensin II-infused rats: role of peroxisome proliferator-activated receptor-gamma. *Circulation.* 2002; 105(19):2296-302.

24. **Leibovitz E, Ebrahimian T, Paradis P, Schiffrin EL**. Aldosterone induces arterial stiffness in absence of oxidative stress and endothelial dysfunction. *J Hypertens.* 2009; 27(11):2192-200.

25. **Gauthier KM, Deeter C, Krishna UM, Reddy YK, Bondlela M, Falck JR, Campbell WB**. 14,15-Epoxyeicosa-5(Z)-enoic acid: a selective epoxyeicosatrienoic acid antagonist that inhibits endothelium-dependent hyperpolarization and relaxation in coronary arteries. *Circ Res.* 2002; 90(9):1028-36.

26. **Edwards G, Dora KA, Gardener MJ, Garland CJ, Weston AH**. K+ is an endothelium-derived hyperpolarizing factor in rat arteries. *Nature.* 1998; 396(6708):269-72.

27. **Ko EA, Han J, Jung ID, Park WS**. Physiological roles of K+ channels in vascular smooth muscle cells. *J Smooth Muscle Res.* 2008; 44(2):65-81.

28. **Laursen JB, Somers M, Kurz S, McCann L, Warnholtz A, Freeman BA, Tarpey M, Fukai T, Harrison DG**. Endothelial regulation of vasomotion in apoE-deficient mice: implications for interactions between peroxynitrite and tetrahydrobiopterin. *Circulation.* 2001; 103(9):1282-8.

29. **Morikawa K, Matoba T, Kubota H, Hatanaka M, Fujiki T, Takahashi S, Takeshita A, Shimokawa H**. Influence of diabetes mellitus,

hypercholesterolemia, and their combination on EDHF-mediated responses in mice. *J Cardiovasc Pharmacol.* 2005; 45(5):485-90.

30. **Ding H, Hashem M, Wiehler WB, Lau W, Martin J, Reid J, Triggle C**. Endothelial dysfunction in the streptozotocin-induced diabetic apoE-deficient mouse. *Br J Pharmacol.* 2005; 146(8):1110-8.

31. **Lee MY, Li H, Xiao Y, Zhou Z, Xu A, Vanhoutte PM**. Chronic administration of BMS309403 improves endothelial function in apolipoprotein E-deficient mice and in cultured human endothelial cells. *Br J Pharmacol.* 2011l; 162(7):1564-76.

32. **Andrews KL, Irvine JC, Tare M, Apostolopoulos J, Favaloro JL, Triggle CR, Kemp-Harper BK**. A role for nitroxyl (HNO) as an endothelium-derived relaxing and hyperpolarizing factor in resistance arteries. *Br J Pharmacol.* 2009; 157(4):540-50.

33. **Hosoya M, Ohashi J, Sawada A, Takaki A, Shimokawa H**. Combination therapy with olmesartan and azelnidipine improves EDHF-mediated responses in diabetic apolipoprotein E-deficient mice. *Circ J.* 2010; 74(4):798-806.

34. **Ohashi J, Sawada A, Nakajima S, Noda K, Takaki A, Shimokawa H**. Mechanisms for enhanced endothelium-derived hyperpolarizing factor-mediated responses in microvessels in mice. *Circ J.* 2012; 76(7):1768-79.

35. **Leung JW, Wong WT, Koon HW, Mo FM, Tam S, Huang Y, Vanhoutte PM, Chung SS, Chung SK**. Transgenic mice over-expressing ET-1 in the endothelial cells develop systemic hypertension with altered vascular reactivity. *PLoS One.* 2011; 6(11):e26994.

36. **Amiri F, Virdis A, Neves MF, Iglarz M, Seidah NG, Touyz RM, Reudelhuber TL, Schiffrin EL**. Endothelium-restricted overexpression of human endothelin-1 causes vascular remodeling and endothelial dysfunction. *Circulation.* 2004; 110(15):2233-40.

37. **Amiri F, Paradis P, Reudelhuber TL, Schiffrin EL**. Vascular inflammation in absence of blood pressure elevation in transgenic murine model overexpressing endothelin-1 in endothelial cells. *J Hypertens.* 2008; 26(6):1102-9.

38. **Javeshghani D, Barhoumi T, Idris-Khodja N, Paradis P, Schiffrin EL**. Reduced Macrophage-Dependent Inflammation Improves Endothelin-1-Induced Vascular Injury. *Hypertension.* 2013.

39. **Danser AH, de VR, Schoemaker RG, Saxena PR**. Bradykinin-induced release of nitric oxide by the isolated perfused rat heart: importance of preformed pools of nitric oxide-containing factors. *J Hypertens.* 1998; 16(2):239-44.

40. **Chauhan S, Rahman A, Nilsson H, Clapp L, MacAllister R, Ahluwalia A**. NO contributes to EDHF-like responses in rat small arteries: a role for NO stores. *Cardiovasc Res.* 2003; 57(1):207-16.

41. **Lundberg JO, Weitzberg E, Gladwin MT**. The nitrate-nitrite-nitric oxide pathway in physiology and therapeutics. *Nat Rev Drug Discov.* 2008; 7(2):156-67.

42. **Zhao Y, Vanhoutte PM, Leung SW**. Endothelial nitric oxide synthase-independent release of nitric oxide in the aorta of the spontaneously hypertensive rat. *J Pharmacol Exp Ther.* 2013; 344(1):15-22.

43. **Ng ES, Cheng ZJ, Ellis A, Ding H, Jiang Y, Li Y, Hollenberg MD, Triggle CR**. Nitrosothiol stores in vascular tissue: modulation by ultraviolet light, acetylcholine and ionomycin. *Eur J Pharmacol.* 2007; 560(2-3):183-92.

44. **Foresti R, Hammad J, Clark JE, Johnson TR, Mann BE, Friebe A, Green CJ, Motterlini R**. Vasoactive properties of CORM-3, a novel water-soluble carbon monoxide-releasing molecule. *Br J Pharmacol.* 2004; 142(3):453-60.

45. **Takaki A, Morikawa K, Tsutsui M, Murayama Y, Tekes E, Yamagishi H, Ohashi J, Yada T, Yanagihara N, Shimokawa H**. Crucial role of nitric oxide synthases system in endothelium-dependent hyperpolarization in mice. *J Exp Med.* 2008; 205(9):2053-63.

46. **Prysyazhna O, Rudyk O, Eaton P**. Single atom substitution in mouse protein kinase G eliminates oxidant sensing to cause hypertension. *Nat Med.* 2012; 18(2):286-90.

47. **Cohen RA, Plane F, Najibi S, Huk I, Malinski T, Garland CJ**. Nitric oxide is the mediator of both endothelium-dependent relaxation and hyperpolarization of the rabbit carotid artery. *Proc Natl Acad Sci U S A.* 1997; 94(8):4193-8.

48. **Leo MD, Siddegowda YK, Kumar D, Tandan SK, Sastry KV, Prakash VR, Mishra SK**. Role of nitric oxide and carbon monoxide in N(omega)-Nitro-L-arginine methyl ester-resistant acetylcholine-induced relaxation in chicken carotid artery. *Eur J Pharmacol.* 2008; 596(1-3):111-7.

49. **McCulloch AI, Bottrill FE, Randall MD, Hiley CR**. Characterization and modulation of EDHF-mediated relaxations in the rat isolated superior mesenteric arterial bed. *Br J Pharmacol.* 1997; 120(8):1431-8.

50. **Zheng X, Ying L, Liu J, Dou D, He Q, Leung SW, Man RY, Vanhoutte PM, Gao Y**. Role of sulfhydryl-dependent dimerization of soluble guanylyl cyclase in relaxation of porcine coronary artery to nitric oxide. *Cardiovasc Res.* 2011; 90(3):565-72.

51. **Bullen ML, Miller AA, Andrews KL, Irvine JC, Ritchie RH, Sobey CG, Kemp-Harper BK**. Nitroxyl (HNO) as a vasoprotective signaling molecule. *Antioxid Redox Signal.* 2011; 14(9):1675-86.

Wynne BM, Labazi H, Tostes RC, Webb RC. Aorta from angiotensin II hypertensive mice exhibit preserved nitroxyl anion mediated relaxation responses. *Pharmacol Res.* 2012; 65(1):41-7.

Figures and tables

Table III-1: List of pharmacological compounds used to study signaling pathways involved in EDR to ACh.

Compound	Concentration (mol/L)	Pretreatment period (min)	Target
4-AP	10^{-3}	30	Kv
Apamin	10^{-7}	20	SK_{Ca}
$BaCl_2$	10^{-4}	30	Kir
$BaCl_2$ + ouabain	3.10^{-5}	20	Kir
14,15-EE5ZE	10^{-5}	30	EETs
Fluconazole	5.10^{-5}	20	Cytochrome P450
Ibtx	10^{-7}	20	BK_{Ca}
L-NAME	10^{-4}	20	NOS
Meclofenamic acid	10^{-6}	20	COX 1
ODQ	10^{-6}	20	Soluble guanylate cyclase
Ouabain	10^{-3}	20	Na^+/K^+ pump
TEA	10^{-3}	30	K_{Ca}, K_v
TRAM-34	10^{-5}	20	IK_{Ca}

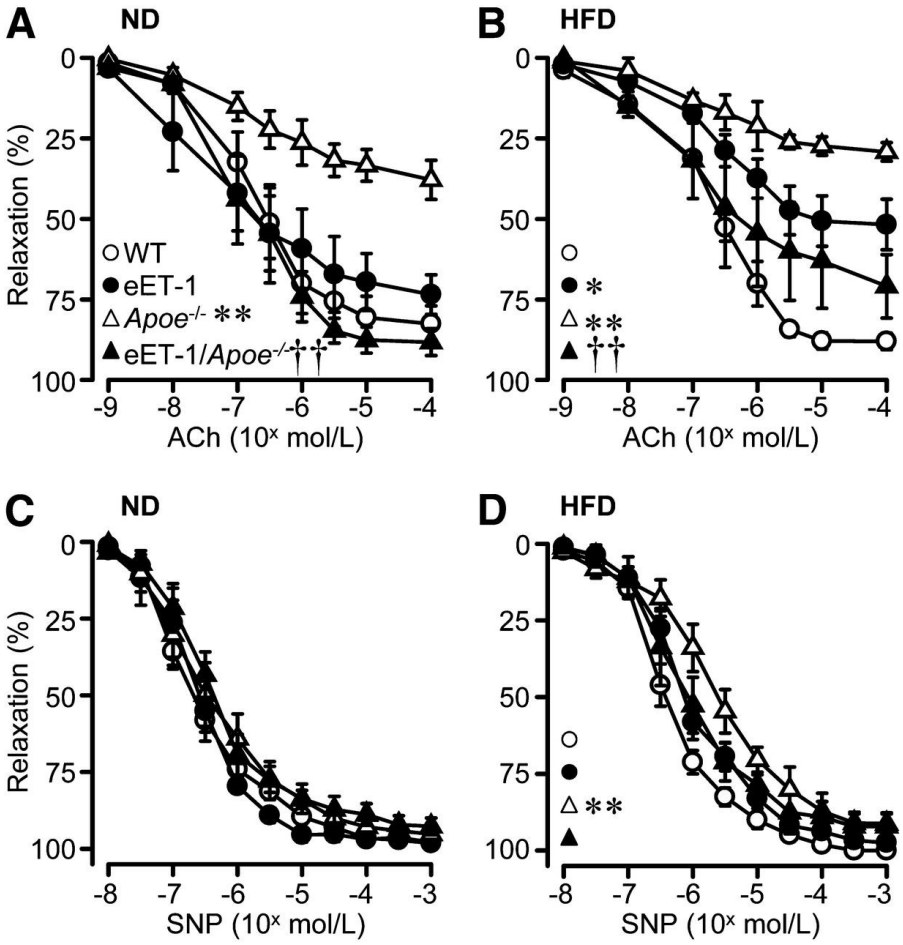

Figure III-1: ET-1 overexpression restores endothelium-dependent relaxation (EDR) in *Apoe*$^{-/-}$ mice. EDR to acetylcholine (ACh) (A and B) and endothelium-independent relaxation to sodium nitroprusside (SNP) (C and D) of mesenteric arteries from 16-week-old WT, eET-1, *Apoe*$^{-/-}$ and eET-1/*Apoe*$^{-/-}$ mice receiving either ND (A and C) or HFD (B and D) for 8 weeks. Values are means ± SEM. *P<0.05 and **P<0.01 vs. WT. †† P<0.01 vs. *Apoe*$^{-/-}$ within same diet groups, n = 3-6.

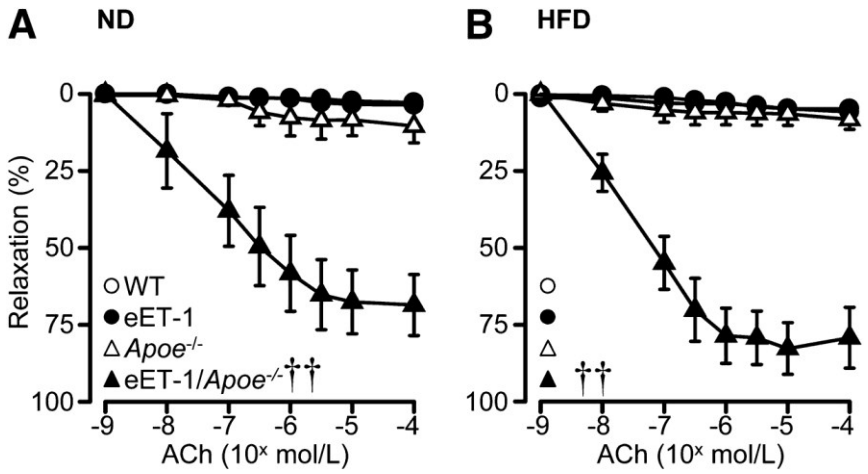

Figure III-2: ET-1 overexpression increases L-NAME-resistant EDR to ACh in *Apoe*$^{-/-}$ mice. EDR responses to ACh in the presence of L-NAME (NOS inhibitor) of mesenteric arteries from 16-week-old WT, eET-1, *Apoe*$^{-/-}$ and eET-1/*Apoe*$^{-/-}$ mice receiving either ND (A) or HFD, (B) for 8 weeks. Values are means ± SEM. ††P<0.01 vs. *Apoe*$^{-/-}$, n = 4-10.

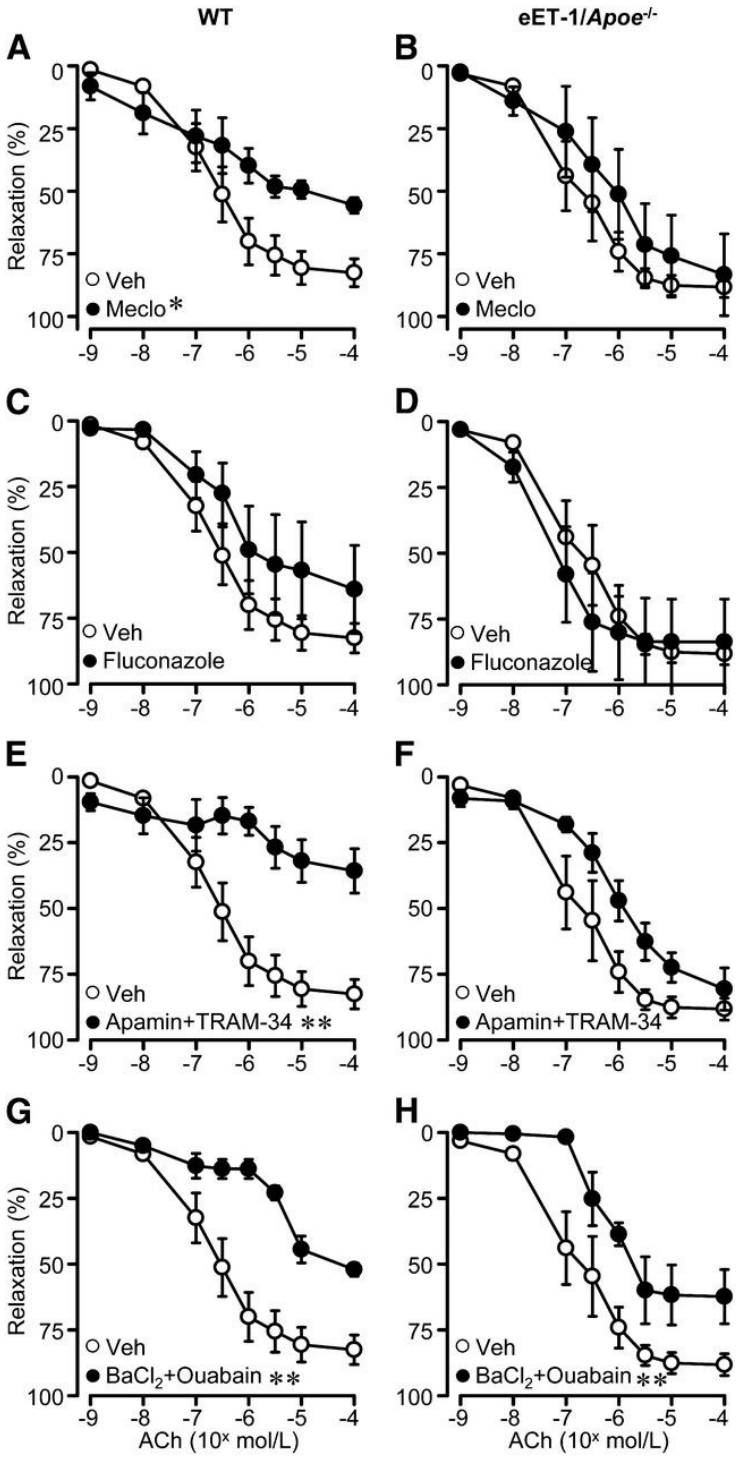

Figure III-3: Effect of COX-1, cytochrome P450, SK_{Ca} plus IK_{Ca}, Na^+/K^+-ATPase plus K_{ir} inhibition in eET-1/*Apoe*$^{-/-}$ compared with WT mice. EDR to ACh in mesenteric arteries from 16-week-old WT (A, C, E, and G) and eET-1/*Apoe*$^{-/-}$ (B, D, F, and H) mice receiving ND, in the presence of inhibitors of either COX-1

(meclofenamic acid, A and B), cytochrome P450 (fluconazole, C and D), SK_{Ca} plus IK_{Ca}, (apamin + TRAM-34, respectively, E and F) or K_{ir} plus Na^+/K^+-ATPase, ($BaCl_2$ + ouabain, respectively, G and H). Values are means ± SEM. **P*<0.05; ***P*<0.01 vs. vehicle, n = 4-6.

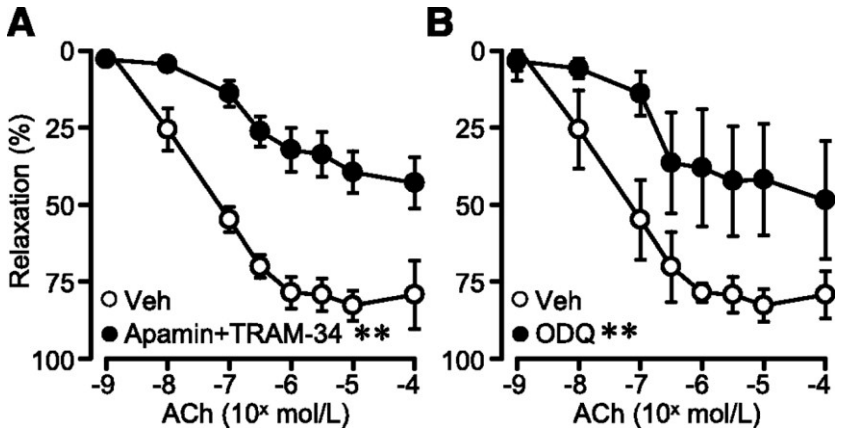

Figure III-4: L-NAME-resistant EDR, of mesenteric arteries from eET-1/*Apoe*$^{-/-}$ mice, is blunted by inhibitors of SK_{Ca} plus IK_{Ca} or sGC. EDR in mesenteric arteries from 16-week-old eET-1/*Apoe*$^{-/-}$ mice receiving HFD, in the presence of NOS inhibitor (L-NAME) plus either inhibitors of SK_{Ca} and IK_{Ca} (apamin + TRAM-34, respectively) or inhibitor of sGC. Values are means ± SEM. **P*<0.05 and ***P*<0.01 vs. vehicle, n = 4-9.

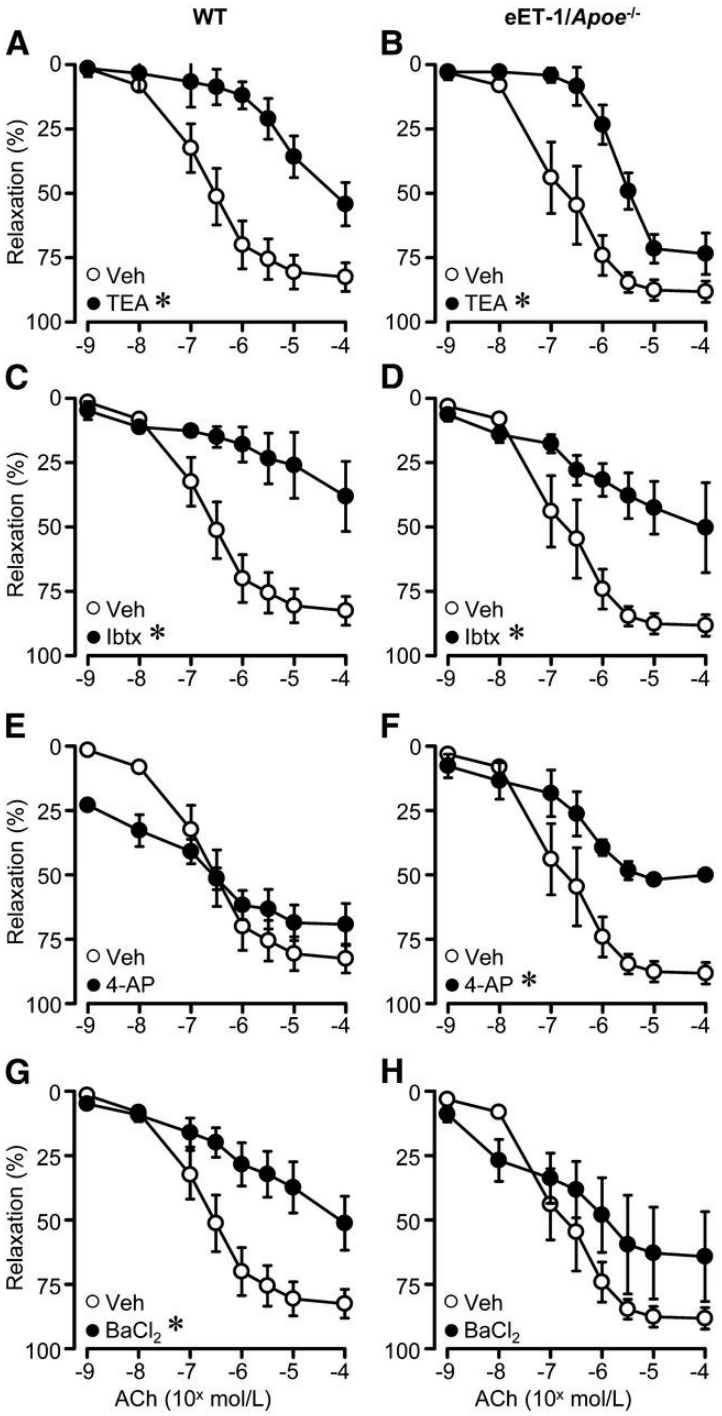

Figure III-5: 4-AP-sensitive K_v has an increased role mediating EDR in eET-1/*Apoe*$^{-/-}$ mice compared with WT mice. EDR to ACh in mesenteric arteries from 16-week-old WT (A, C, E, and G) and eET-1/*Apoe*$^{-/-}$ (B, D, F, and H) mice receiving ND, in the presence of the K_{Ca} and K_v inhibitor, TEA, (A and B), K_{ir} inhibitor ($BaCl_2$, C and D), BK_{Ca} inhibitor, iberiotoxin (Ibtx) (E and F) and K_v

inhibitor, 4-AP, (G and H). Values are means ± SEM. *P<0.05 and **P<0.01 vs. vehicle, n = 3-7

.

Supplemental figures and tables

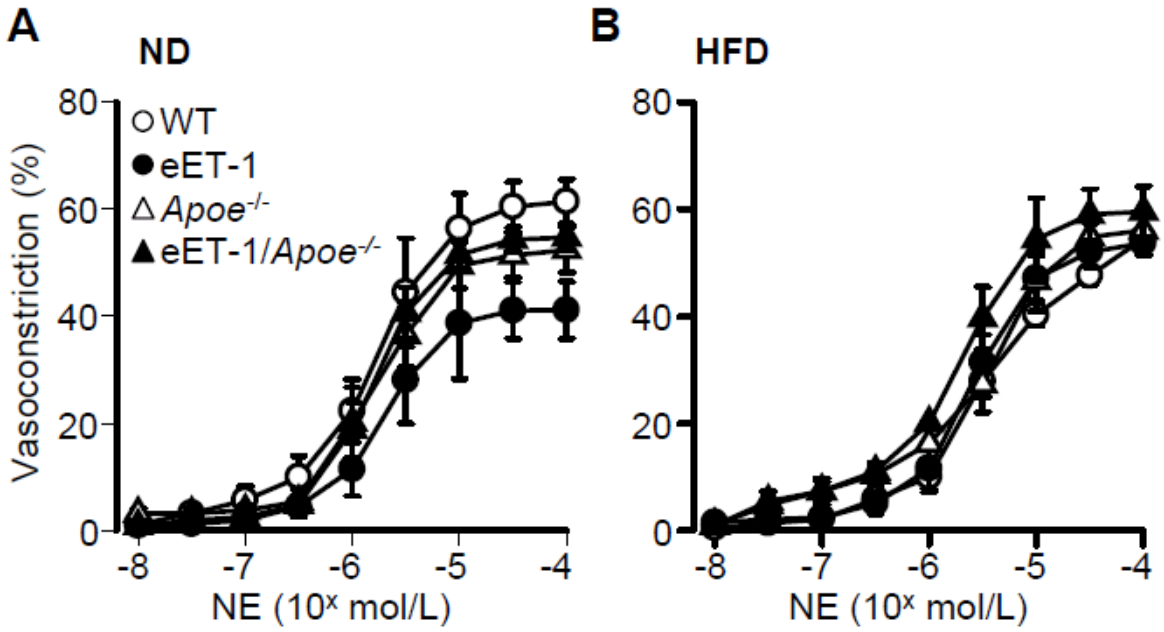

Figure III-S1: Contractile responses to norepinephrine (NE) of mesenteric arteries from 16-week-old wild type (WT), eET-1, *Apoe*$^{-/-}$ and eET-1/*Apoe*$^{-/-}$ mice, receiving normal diet (ND) (A) or high fat diet (HFD) (B) during 8 weeks, n = 3-6.

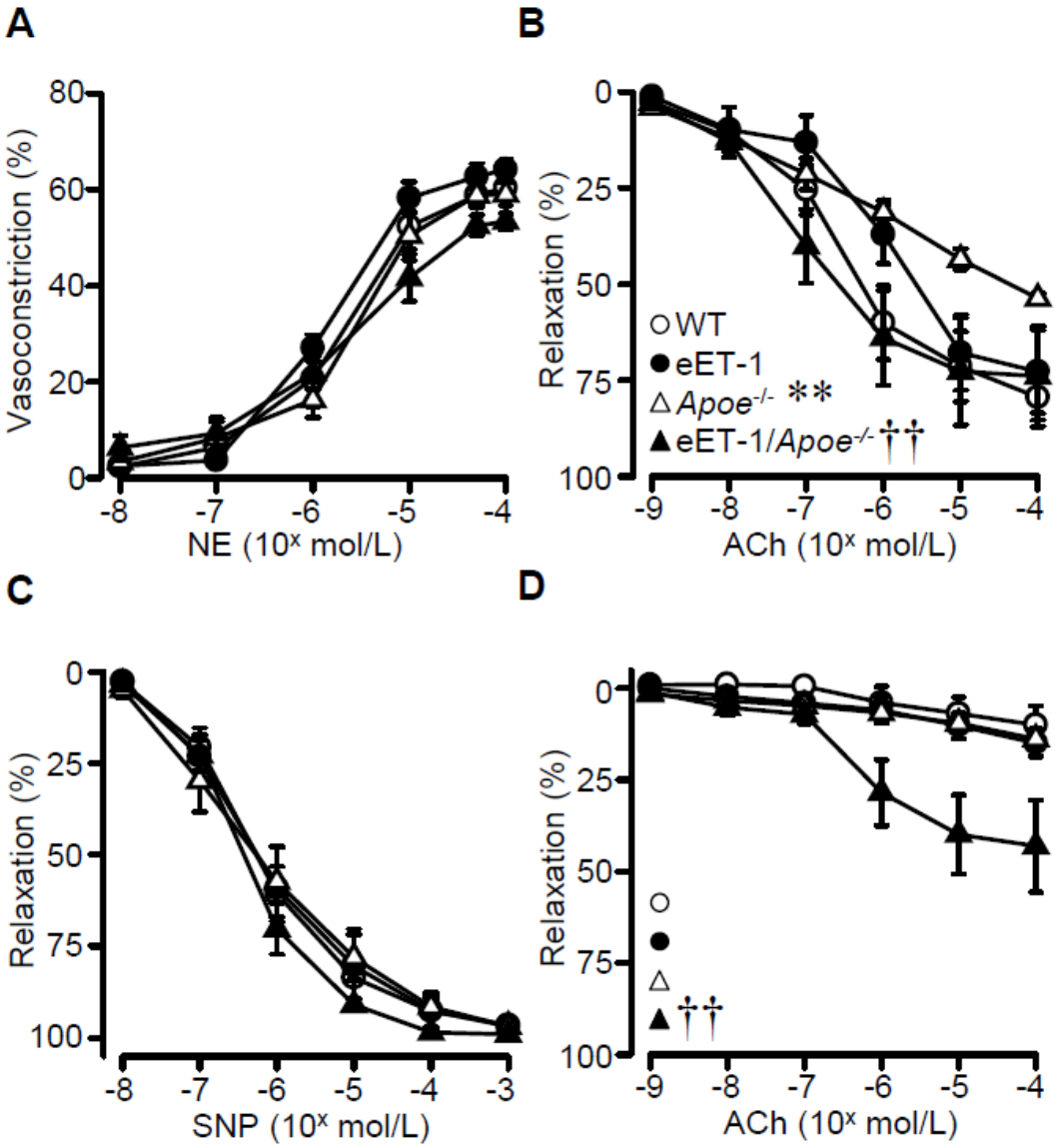

Figure III-S2: Contractile responses to NE (A), endothelium-dependent relaxation responses to acetylcholine (ACh) (B), endothelium-independent relaxation responses to sodium nitroprusside (SNP) (C) and endothelium-dependent responses to ACh in presence of L-NAME (D) of mesenteric arteries from 8-week-old WT, eET-1, *Apoe*$^{-/-}$ and eET-1/*Apoe*$^{-/-}$ mice receiving normal diet. Values are means ± SEM. ***P*<0.01 vs. WT, ††*P*<0.01 vs. *Apoe*$^{-/-}$, n = 4-8.

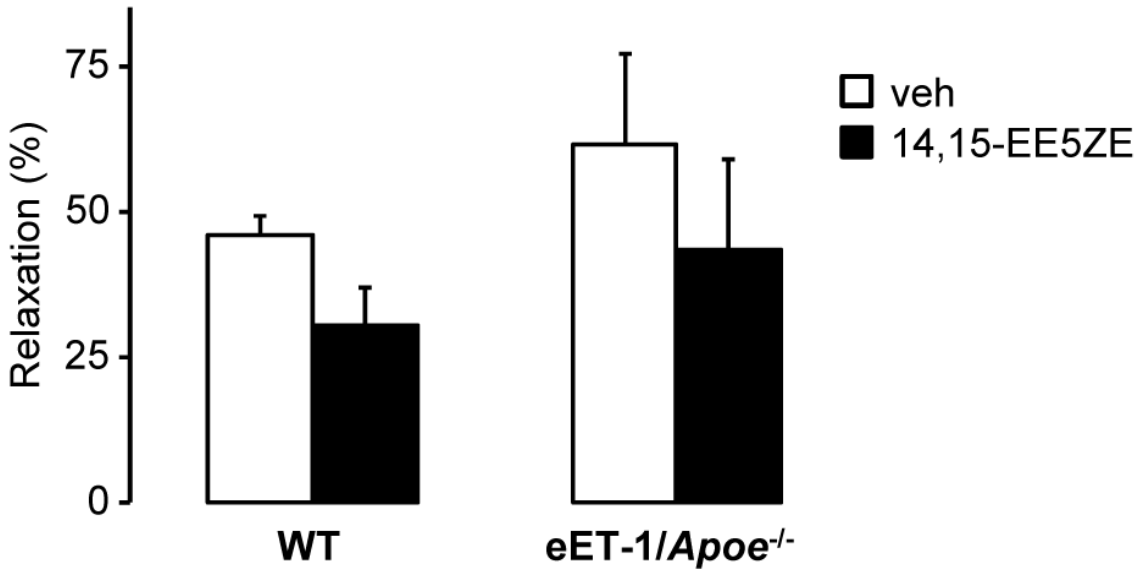

Figure III-S3: Endothelium-dependent relaxation to 10^{-6} M ACh in the absence and presence of 14,15-EE5ZE (10^{-5} M, antagonist of epoxyeicosatrienoic acids) of mesenteric arteries from 16-week-old WT and eET-1/*Apoe*$^{-/-}$ mice receiving normal diet. Values are means ± SEM, n = 4.

Table III-S1: pEC50, E_{max} and AUC of acetylcholine concentration-response curves in mesenteric arteries from 16-week-old WT and eET-1/*Apoe*$^{-/-}$ mice receiving normal diet, in the presence of indicated inhibitors. Values are means ± SEM. **P*<0.05 and ***P*<0.01 vs. vehicle, †*P*<0.05 and ††*P*<0.01vs. corresponding WT mice, n = 3-7.

Treatment	pEC50		E_{max}		AUC	
	WT	**eET-1/Apoe$^{-/-}$**	**WT**	**eET-1/Apoe$^{-/-}$**	**WT**	**eET-1/Apoe$^{-/-}$**
Vehicle	6.8 ± 0.2	7.0 ± 0.2	82.6 ± 5.6	88.3 ± 4.2	233.5 ± 28.0	259.2 ± 26.7
L-NAME	6.5 ± 1.5	7.3 ± 0.5	2.8 ± 0.5**	68.6 ± 10.0††	6.4 ± 01.9**	218.5 ± 47.4††
Meclofenamic acid	6.8 ± 1.1	6.3 ± 0.3	55.7 ± 3.1**	83.4 ± 7.8††	168.7 ± 33.1*	214.6 ± 28.5†
Fluconazole	6.5 ± 0.4	7.4 ± 0.4	64.1 ± 16.7	83.8 ± 16.3	160.6 ± 53.6	287.2 ± 64.2
Apamin + TRAM-34	5.7 ± 0.3**	6.1 ± 0.2*	35.8 ± 8.5**	80.7 ± 8.1††	104.4 ± 31.6**	190.9 ± 20.1
$BaCl_2$ + Ouabain	5.4 ± 0.3**	6.3 ± 0.2†	52.1 ± 2.5**	62.4 ± 10.3**	82.0 ± 19.1**	141.3 ± 26.1*†
TEA	5.1 ± 0.4**	5.7 ± 0.2**	54.3 ± 10.6	73.5 ± 20.0	84.1 ± 14.3*	138.2 ± 37.9*
$BaCl_2$	6.0 ± 0.4	6.7 ± 0.3	51.3 ± 10.5	64.2 ± 17.4	117.7 ± 26.2*	208.9 ± 59.0
Ibtx	5.3 ± 0.4**	6.4 ± 0.3†	38.2 ± 13.6*	50.3 ± 17.5*	90.0 ± 28.0*	136.4 ± 33.2*
4-AP	6.8 ± 0.4	6.4 ± 0.2	69.3 ± 08.2	50.1 ± 01.9**†	249.4 ± 19.4	152.1 ± 16.6*†

Table III-S2: pEC50, Emax and AUC of acetylcholine concentration-response curves in mesenteric arteries from 16-week-old eET-1/*Apoe*$^{-/-}$ mice receiving high-fat diet, in the presence of indicated inhibitors. Values are means ± SEM. ***P*<0.01 vs. L-NAME, n = 4-9.

Treatment	**eET-1/Apoe$^{-/-}$**		
	pEC50	**E_{max}**	**AUC**
L-NAME	7.7 ± 0.4	79.3 ± 9.9	282.0 ± 34.0
L-NAME + Apamin + TRAM-34	6.6 ± 0.3	43.0 ± 8.3**	113.6 ± 19.8**
L-NAME + ODQ	6.8 ± 0.4	48.6 ± 19.2	132.2 ± 52.5**

CHAPTER IV: Adoptive transfer of FOXP3-deficient (Scurfy) versus wild-type T cells will exacerbate Ang II-induced vascular damage in Rag1$^{-/-}$ mice

Hypothesis and objectives

Treg are a subset of T helper cells that a defined by their anti-inflammatory properties. Treg suppress the actions of T effector cells and other immune cells via several mechanisms that were mentioned previously in the introduction. The number and/or function of Treg in CVD may be affected. In our first study, we found an increase in $CD4^+CD25^+FOXP3^+$ Treg population in the spleens of *Apoe*$^{-/-}$ and eET-1/*Apoe*$^{-/-}$ mice but also an increase in numbers of spleen activated T cells and pro-inflammatory Ly-$6C^{hi}$ monocytes and enhanced vascular inflammatory responses. Whereas this numeric increase in Treg population may have been a compensatory response to enhanced systemic and vascular inflammation, concomitant increase in inflammatory responses suggests decreased suppressive capacity of Treg in this situation. In another study from our lab, cultured Treg isolated from high-fructose diet-fed rats, a metabolic syndrome-like model, were shown to produce less IL-10 also suggesting decreased Treg function [444]. This was associated with enhanced oxidative stress and expression of VCAM-1 and PECAM-1 in the aorta.

The protective effect of adoptive transfer of Treg on the vasculature has been previously demonstrated in animal models of atherosclerosis and HTN. Although these studies provide strong support of a protective effect of Treg in CVD, gain-of-function of Treg by increasing numbers could have produced non-physiological effects. A mechanistic understanding of the role of Treg could be revealed using a loss-of-function approach. As mentioned in the introduction, the transcription factor FOXP3 has been described as the master regulator of Treg maturation and function [254]. Mutations in the FOXP3 gene cause deficiency or absence of Treg in humans with immunodysregulation polyendocrinopathy enteropathy X-linked (IPEX) syndrome, and in mice with the Scurfy phenotype, which presents a lethal autoimmune syndrome [253]. In a human model of acute inflammation due to cardiac surgery, the proportion of $CD4^+FOXP3^+$ Treg and the expression of FOXP3 in $CD4^+CD25^{hi}CD127^{low}$ cells was increased, but the potential of Treg to suppress effector T cells was reduced [445]. Diphtheria toxin-

mediated depletion of FOXP3^{+} Treg in *Ldlr*$^{-/-}$ mice transplanted with bone marrow from DEREG mice was shown to enhance atherosclerosis by altering lipoprotein metabolism but without increasing vascular inflammation [278]. T effector lymphocytes contribute to vascular injury in Ang II-induced hypertension, but the role of Treg is unclear. Ang II-induced hypertension is blunted in T and B cell-deficient *Rag1*$^{-/-}$ mice, and restored with reconstitution of wild-type T cells [240]. Based on this evidence, we hypothesize that:

Adoptive transfer of FOXP3-deficient (Scurfy) versus wild-type T cells will exacerbate Ang II-induced vascular damage in Rag1$^{-/-}$ *mice.*

The specific objectives of this study include:

- To confirm whether Ang II-induced HTN and microvascular inflammation, dysfunction and remodeling are blunted in *Rag1*$^{-/-}$ mice.
- To determine whether reconstitution of wild-type T cells will restore Ang II-induced HTN and microvascular inflammation, dysfunction and remodeling in *Rag1*$^{-/-}$ mice.
- To determine whether reconstitution of Treg-deficient T cells will exaggerate HTN and microvascular inflammation, dysfunction and remodeling in *Rag1*$^{-/-}$ mice.
- To identify mechanism(s) by which Treg exert their vascular protective effect.

FOXP3$^+$ T regulatory cells blunt angiotensin II-induced microvascular injury by controlling innate and adaptive immune responses

Muhammad Oneeb Rehman Mian, Tlili Barhoumi, Marie Briet, Pierre Paradis and Ernesto L. Schiffrin

Lady Davis Institute for Medical Research (M.O.R.M., T.B., M.B., P.P., E.L.S.), and Department of Medicine (E.L.S.), Sir Mortimer B. Davis-Jewish General Hospital, McGill University, Montréal, Québec, Canada, and INSERM U1083 (M.B.), CNRS UMR 6214, Centre Hospitalo-Universitaire d'Angers, Université d'Angers, Angers, France

Submitted to:
Arteriosclerosis, Thrombosis, and Vascular Biology (March 2015)

The manuscript was prepared and is presented here according to the instructions of the journal to which it was submitted. The main manuscript is followed by the Online Supplemental material (including the expanded materials and methods section).

Abstract

Objective: T regulatory lymphocyte (Treg) adoptive transfer prevented angiotensin II-induced hypertension and microvascular injury. Scurfy mice are deficient in Treg due to a mutation in the transcription factor forkhead box P3 gene. Enhanced angiotensin II effects in absence of Treg would unambiguously demonstrate their vascular protective role. We hypothesized that adoptive transfer of Scurfy vs. wild-type T cells will exacerbate angiotensin II-induced microvascular damage in T and B cell-deficient recombination-activating gene 1 knockout (*Rag1*$^{-/-}$) mice.

Approach and Results: *Rag1*$^{-/-}$ were injected with vehicle, 10^7 T cells from wild-type or Scurfy mice or 10^6 wild-type Treg alone or with Scurfy T cells, and then infused or not with angiotensin II (490 ng/kg/min, s.c.) for 14 days. Angiotensin II increased systolic blood pressure in all the groups, but diastolic blood pressure only in wild-type and Scurfy groups. Angiotensin II induced endothelial dysfunction and oxidative stress in perivascular adipose tissue (PVAT) in mesenteric artery of wild-type T cell-injected *Rag1*$^{-/-}$, whereas these were exaggerated in Scurfy T cell-injected *Rag1*$^{-/-}$. Angiotensin II enhanced microvascular remodeling and stiffness in vehicle- and Scurfy T cell-injected *Rag1*$^{-/-}$. Angiotensin II increased monocyte chemotactic protein-1 expression in the vascular wall and PVAT, monocyte/macrophage infiltration and pro-inflammatory polarization in PVAT and the renal cortex, and T cell infiltration in the renal cortex only in Scurfy T cell-injected *Rag1*$^{-/-}$. Wild-type Treg co-injection with vehicle or Scurfy T cells prevented or reduced the effects of angiotensin II.

Conclusion: Treg counteract angiotensin II-induced microvascular injury by modulating innate and adaptive immune responses.

Keywords: Hypertension, innate immunity, adaptive immunity, oxidative stress

Introduction

Innate and adaptive immunity play a role in the development and progression of angiotensin (Ang) II-induced hypertension, vascular dysfunction and remodeling, and target-organ damage [1,2]. We and others have shown that monocytes and macrophages, which are key innate immune cells, participate in the development of experimental hypertension. Ang II-induced hypertension, and endothelial dysfunction, vascular remodeling and oxidative stress in small resistance arteries, were prevented in osteopetrotic mice that have a mutation within the macrophage colony-stimulating factor gene (*Csf1*) and an associated decrease in functional monocyte/macrophages due to the deficiency in CSF1 [3]. Similarly, selective reduction of monocytes using low-dose diphtheria toxin in mice with inducible expression of the diphtheria toxin receptor in lysozyme M-positive myelomonocytic cells attenuated Ang II-induced blood pressure (BP) rise and aortic damage [4]. Guzik *et al.* have demonstrated that T lymphocytes are adaptive immune cells that contribute to the development of experimental hypertension by showing that mice with inactivation of the recombination-activating gene 1 (*Rag1*$^{-/-}$), which lack T and B lymphocytes, have blunted hypertension, aortic endothelial dysfunction, vascular remodeling and oxidative stress in response to Ang II [5]. Reconstitution with T but not B lymphocytes from wild-type (WT) mice restored the Ang II responses in *Rag1*$^{-/-}$ mice.

T regulatory lymphocytes (Treg) are a subset of T lymphocytes characterized by expression of the transcription factor forkhead box P3 (FOXP3). They exert immune-suppressive actions on T lymphocytes such as T helper (T_h)1, T_h2 and T_h17, and other immune cells such as dendritic cells, monocytes and macrophages [1,2,6-8]. The immune-suppressive effect of Treg is mediated mainly by two cytokines, transforming growth factor-β and interleukin (IL)-10. Mutations in the *Foxp3* gene have been shown to cause deficiency or absence of Treg in humans with immunodysregulation polyendocrinopathy enteropathy X-linked (IPEX) syndrome, and in the Scurfy (Sf) mouse, which presents a lethal autoimmune syndrome [7].

We and others have identified a protective role for Treg in animal models of hypertension. We previously showed that chromosome 2-dependent modulation of immune responses in genetic hypertension involves Treg [9]. Hypertensive Dahl salt-sensitive rats exhibited vascular inflammation and BP elevation, which was associated with dysfunctional Treg. Consomic SSBN2 rats, in which chromosome 2 from normotensive Brown Norway rats has been introgressed on a Dahl salt genome background, presented with decreased hypertension, reduced aortic vascular and systemic inflammation, and improved Treg function compared to Dahl salt-sensitive rats. Recently, we observed that Ang II-induced BP elevation, mesenteric artery (MA) endothelial dysfunction and vascular remodeling, oxidative stress and inflammation in aorta of WT mice were associated with a decrease in Treg numbers in the kidney [10]. Adoptive transfer of WT $CD4^+CD25^+$ T cells, a subset of Treg, reduced or prevented Ang II-induced hypertension and microvascular injury. Matrougui *et al*. observed that Ang II-induced BP rise, coronary arteriolar endothelial dysfunction and inflammation and apoptosis of spleen Treg, were reduced by adoptive transfer of Treg [11]. Although the above studies provide strong support of a protective effect of Treg on hypertension and vascular injury, Treg gain-of-function could have produced non-physiological effects. However, a mechanistic understanding of the role of Treg in Ang II-induced hypertension and vascular damage could be revealed using a loss-of-function approach.

Given the critical role that the master transcription factor FOXP3 plays in driving maturation of naïve T lymphocytes into Treg, we investigated the role of Treg in hypertension by examining whether FOXP3 deficiency exacerbates hypertension and vascular damage mediated by Ang II via absence of Treg and its putative effect on innate and adaptive immune cells. To do so, we studied Ang II-induced hypertension, microvascular injury, oxidative stress, inflammation and monocyte/macrophage polarization in *Rag1*$^{-/-}$ mice reconstituted or not with T lymphocytes isolated from WT versus FOXP3-deficient Sf mice. In addition, to prove that the worsening of Ang II-induced hypertension and microvascular

damage is due to the absence of FOXP3$^+$ Treg, we assessed the end points in *Rag1*$^{-/-}$ mice after adoptive transfer of WT Treg alone or with Sf T cells.

Materials and Methods

Materials and methods are available in the online-only Data Supplement.

Results

T cell purity and efficiency of WT and Treg-deficient T cell and WT Treg adoptive transfers

The purity of the preparations of WT and Sf T cells used for adoptive transfer and the efficiency of WT and FOXP3$^+$ Treg-deficient Sf T cell and WT Treg adoptive transfers in *Rag1*$^{-/-}$ mice was assessed by flow cytometry at the end of the study (Supplemental Results and Fig. IV-S1 in the online-only Data Supplement). A single injection of 10^7 WT T cells in *Rag1*$^{-/-}$ restored 50% of CD3$^+$ T cell population and 100% of CD3$^+$CD4$^+$FOXP3$^+$ Treg compared to WT mice. Adoptive transfer of 10^7 Sf T cells restored 129% of CD3$^+$ T cells but not CD3$^+$CD4$^+$FOXP3$^+$ Treg. Co-injection of 10^6 WT CD4$^+$CD25$^+$ Treg in vehicle (Veh)- or Sf T cell-injected *Rag1*$^{-/-}$ mice caused the population of CD3$^+$CD4$^+$FOXP3$^+$ Treg to double compared to WT mice.

Body and tissue weights of experimental groups

These are presented in the Online Data Supplement.

Ang II effect on BP in *Rag1*$^{-/-}$ mice injected with WT T cells or Treg-deficient Sf T cells

Ang II induced a similar ~35 mmHg systolic BP (SBP) rise in Veh-, WT T cell- and Sf T cell-injected *Rag1*$^{-/-}$ mice (Fig. IV-1A). However, Ang II increased diastolic BP (DBP) by ~24 mmHg in WT T cell- and Sf T cell-injected *Rag1*$^{-/-}$ mice, whereas it tended to increase DBP in Veh-injected *Rag1*$^{-/-}$ mice (Fig. IV-

1B). Adoptive transfer of WT Treg blunted Ang II-induced SBP rise in Veh-injected *Rag1*$^{-/-}$ mice (Fig. IV-1A). Co-transfer of WT Treg delayed the onset of SBP rise and blunted DBP rise caused by Ang II in Sf T cell-injected *Rag1*$^{-/-}$ mice (Fig. IV-1).

Effect of Treg on Ang II-induced MA endothelial dysfunction and oxidative stress

There was no difference in the vasoconstrictor responses of MA to NE between the groups (Fig IV-S2A-C in the online-only Data Supplement). Ang II treatment did not alter MA relaxation responses to acetylcholine in Veh-injected *Rag1*$^{-/-}$ mice co-injected or not with WT Treg (Fig. IV-2A). Adoptive transfer of WT T cells restored Ang II-induced impairment of acetylcholine-mediated relaxation (Fig. IV-2B). Ang II-induced endothelial dysfunction was exaggerated in Sf T cell-injected *Rag1*$^{-/-}$ mice, but co-injection of WT Treg reduced the Ang II-induced endothelial dysfunction in Sf T cell-injected *Rag1*$^{-/-}$ mice (Fig. IV-2C). Acetylcholine-mediated relaxation was abrogated by the nitric oxide (NO) synthase inhibitor N^{ω}-nitro-L-arginine methyl ester in all the groups (Fig IV-S2D-F in the online-only Data Supplement). Sodium nitroprusside (SNP) responses were generally unaffected by most interventions, except in Sf T cell group in which Ang II tended to decrease relaxation responses to SNP (Supplemental Results and Fig. IV-S2G-I in the online-only Data Supplement)

Ang II infusion did not affect reactive oxygen species (ROS) generation in absence of T cells (Fig. IV-2D and IV-S3 in the online-only Data Supplement). Ang II increased ROS generation in the PVAT of WT T cell-injected *Rag1*$^{-/-}$ mice. Transfer of Sf T cells exaggerated Ang II-induced ROS generation in both the vessel wall and PVAT. Ang II response was abrogated by co-transfer with WT Treg.

Effect of Treg on Ang II-induced MA stiffness, fibronectin expression and remodeling

Ang II treatment increased MA stiffness in Veh-injected *Rag1*$^{-/-}$ mice, as indicated by a leftward shift of the stress-strain curve with respect to control (Fig. IV-3A). This was also observed in Sf T cell-injected but not in WT T cell-injected *Rag1*$^{-/-}$ mice (Fig. IV-3B and C). Ang II-induced MA stiffness in Veh- and Sf T cell-injected *Rag1*$^{-/-}$ mice was prevented by co-injection of WT Treg.

Ang II treatment increased MA fibronectin expression, which contributes to vascular stiffening, in Veh- and Sf T cell-injected *Rag1*$^{-/-}$ mice but not in WT T cell-injected *Rag1*$^{-/-}$ mice. These effects were prevented by co-injection of WT Treg (Fig. IV-3D and IV-S4 in the online-only Data Supplement).

Ang II increased MA media-to-lumen ratio in Veh-injected *Rag1*$^{-/-}$ mice and media-to-lumen ratio and media cross-sectional area in Sf T cell-injected mice (Fig. IV-3E and F). These changes did not occur in *Rag1*$^{-/-}$ mice adoptively transferred with WT T cells, or in Veh- and Sf T cell-injected *Rag1*$^{-/-}$ mice co-injected with WT Treg.

Effect of Treg on Ang II-induced inflammation

Monocyte chemotactic protein-1 (MCP-1) expression in MA vascular wall and PVAT was similar in Veh-, WT T cell- and Sf T cell-injected *Rag1*$^{-/-}$ mice (Fig. IV-4A-C). Ang II increased MCP-1 expression in MA vascular wall and PVAT only in Sf T cell-injected *Rag1*$^{-/-}$ mice, which was prevented by WT Treg co-injection. Similarly, monocyte/macrophage infiltration in MA PVAT (Fig. IV-4D-F) and renal cortex (Fig. IV-S5A-C in the online-only Data Supplement) was comparable in Veh-, WT T cell- and Sf T cell-injected *Rag1*$^{-/-}$ injected mice. Ang II enhanced monocyte/macrophage infiltration in MA PVAT and renal cortex only in Sf T cell-injected *Rag1*$^{-/-}$ mice, and this was prevented by WT Treg co-injection.

Ang II treatment did not increase CD3 T cell infiltration in MA PVAT in any of the groups (Fig. IV-S6 in the online-only Data Supplement). However, there was a trend to a lower CD3 T cell infiltration in mice co-transferred with Sf T cells and WT Treg, compared to Ang II-treated Sf T cell-injected mice. CD3 infiltration was also detected in renal cortex of WT and Sf T cell-injected *Rag1*$^{-/-}$ mice but not in Veh-injected *Rag1*$^{-/-}$ mice (Fig. IV-S5D-F in the online-only Data Supplement). Ang II enhanced CD3 infiltration in the renal cortex of Sf T cell-injected *Rag1*$^{-/-}$ mice while this only tended to increase in WT T cell-injected *Rag1*$^{-/-}$ mice. Co-transfer of WT Treg with Sf T cells blunted Ang II-mediated CD3 infiltration in the renal cortex.

Effect of Treg on Ang II-induced monocyte/macrophage polarization

To further characterize the protective role of Treg in Ang II-induced hypertension, markers of pro-inflammatory (M1) and anti-inflammatory (M2) macrophage polarization [12] in MA PVAT were examined. M1 markers inducible nitric oxide synthase (iNOS) and major histocompatibility complex class II (MHC-II) were expressed respectively in 29% and 48% of infiltrating monocytes/macrophages in Veh-injected *Rag1*$^{-/-}$ mice (Fig. IV-5). Similar proportions of infiltrating monocytes/macrophages expressing these M1 markers were observed in WT T cell-injected *Rag1*$^{-/-}$ mice, but these proportions tended to be higher in Sf T cell-injected mice compared to WT T cell-injected *Rag1*$^{-/-}$ mice. Ang II did not change the proportion of infiltrating monocytes/macrophages expressing M1 markers in Veh- and WT T cell-injected *Rag1*$^{-/-}$ mice. However, Ang II increased the proportion of infiltrating monocyte/macrophages expressing iNOS or tended to augment those expressing MHC-II in Sf T cell-injected *Rag1*$^{-/-}$ mice, both effects prevented by WT Treg co-injection. The M2 markers mannose receptor (CD206) and arginase-1 (Arg-1) were expressed respectively in ~80% of infiltrating monocytes/macrophages in Veh-injected *Rag1*$^{-/-}$ mice. Proportions of infiltrating monocyte/macrophages expressing these M2 markers were similar in all groups.

In the renal cortex, the M1 marker iNOS was expressed in 5% of monocyte/macrophages whereas MHC-II was too low to be quantified (Fig. IV-6 and IV-S7 in the online-only Data Supplement). Similar proportions of infiltrating monocyte/macrophages expressing iNOS were observed in WT T cell- and Sf T cell-injected *Rag1*$^{-/-}$ mice, which was unaffected by Ang II treatment in Veh- or WT T cell-injected *Rag1*$^{-/-}$ mice. However, they increased in Sf T cell-injected *Rag1*$^{-/-}$ mice; effect prevented by WT Treg co-injection. M2 markers CD206 and Arg-1 were expressed in ~30% of infiltrating monocytes/macrophages in Veh- and WT T cell-injected *Rag1*$^{-/-}$ mice. Sf T cell-injected *Rag1*$^{-/-}$ mice presented similar proportions of infiltrating monocyte/macrophages expressing CD206, whereas those expressing Arg1 tended to be lower compared to WT T cell-injected *Rag1*$^{-/-}$ mice. Ang II did not affect the proportion of infiltrating monocyte/macrophages expressing CD206 and Arg1 in WT T cell-injected *Rag1*$^{-/-}$ mice or those expressing CD206 in Sf T cell-injected *Rag1*$^{-/-}$ mice. However, Ang II decreased the proportion of infiltrating monocyte/macrophages expressing Arg1 or CD206 in Sf T cell-injected *Rag1*$^{-/-}$ mice; result prevented by WT Treg co-injection and normalized compared to control Sf T cell-injected *Rag1*$^{-/-}$ mice.

Effect of adoptive transfer of Treg-deficient T cells in *Rag1*$^{-/-}$ and co-transfer of WT Treg on plasma cytokines

WT T cell-injected *Rag1*$^{-/-}$ mice presented higher plasma interferon γ (INFγ) and IL-17a but similar plasma levels of MCP-1, IL-6, tumour necrosis factor α (TNFα) and RANTES (regulated on activation, normal T cell expressed and secreted) compared to Veh-injected *Rag1*$^{-/-}$ mice (Fig. IV-S8A-G in the online-only Data Supplement). Plasma pro-inflammatory cytokines were unchanged by Ang II and WT Treg injection in Veh-injected *Rag1*$^{-/-}$ mice. Ang II decreased plasma IFNγ but did not affect other pro-inflammatory cytokines in WT T cell-injected *Rag1*$^{-/-}$ mice. Much higher plasma MCP-1, IFNγ, IL-6, TNFα, and RANTES but not IL-17a was observed in Sf T cell-injected *Rag1*$^{-/-}$ compared to WT T cell-injected *Rag1*$^{-/-}$ mice, which was unaffected by Ang II and normalized by WT Treg co-injection. The anti-inflammatory IL-10 plasma levels were similar

in Veh-, WT T cell- and Sf T cell-injected mice (Fig. IV-S8K in the online-only Data Supplement). Ang II treatment tended to reduce the plasma levels of IL-10 in all groups except mice co-injected with WT Treg.

Discussion

This study demonstrates for the first time that Treg counteract Ang II-induced resistance artery endothelial dysfunction and remodeling, oxidative stress and inflammation by modulating innate and adaptive immune responses. When adoptively transferred with Sf T cells lacking Treg, T and B cell-deficient *Rag1*$^{-/-}$ mice presented an exaggerated response to Ang II including pro-inflammatory polarization of monocyte/macrophages, compared to adoptive transfer of WT T cells, which contain Treg. In addition, co-transfer of Treg with Sf T cells not only blunted these enhanced effects, but as previously observed, [10] prevented all Ang II vascular detrimental actions and delayed BP rise. Furthermore, this study delineates a novel mechanism whereby Ang II induces hypertension and resistance artery remodeling in an innate immune cell-dependent manner in *Rag1*$^{-/-}$ mice, which could be counteracted by adoptive transfer of WT Treg.

Ang II caused similar SBP rise in *Rag1*$^{-/-}$ mice injected with Veh or WT T cells, but DBP rise was blunted in *Rag1*$^{-/-}$ mice injected with Veh compared to mice adoptively transferred with WT T cells, which resembles in part previous results of other investigators [5,13,14]. Although *Rag1*$^{-/-}$ were obtained from the same source, differences in housing conditions and gut microbiota or in the BP determination technique could, at least in part, explain some dissimilarities. Adoptive transfer of Sf T cells, which lack Treg, in *Rag1*$^{-/-}$ mice did not affect basal BP or exacerbate Ang II-induced SBP and DBP rise compared to mice injected with WT T cells. This suggests that depletion of Treg may not be sufficient to cause further BP elevation. Interestingly, a single injection of WT Treg completely prevented Ang II-induced SBP and DBP rise in *Rag1*$^{-/-}$ mice, whereas co-transfer of Sf T cells with Treg delayed the onset of Ang II-induced

SBP and DBP rise. This is in line with our previous findings [10] and those of Matrougui *et al*. [11] showing Treg adoptive transfer blunts Ang II-induced BP elevation in WT mice. The additional protection observed with the adoptive transfer of WT Treg might be explained in part by pharmacological effects, as injection of Treg into *Rag1*$^{-/-}$ mice resulted in a greater proportion of Treg in the spleen than found in WT T cell-injected *Rag1*$^{-/-}$ mice.

This study demonstrates for the first time that Treg contained within the T cell population counteract Ang II-induced MA endothelial dysfunction and oxidative stress. Ang II-induced endothelial dysfunction and oxidative stress have been shown to be T cell-dependent in the aorta [5]. In this study we observed a similar effect at the level of the microvasculature since Ang II did not alter MA endothelial function and oxidative stress in *Rag1*$^{-/-}$ mice, but adoptive transfer of T cells restored the endothelial dysfunction induced by Ang II. Adoptive transfer of Sf T cells (lacking Treg) into *Rag1*$^{-/-}$ mice exaggerated Ang II-induced MA endothelial dysfunction and ROS generation compared to *Rag1*$^{-/-}$ mice injected with WT T cells. Interestingly, co-injection of Sf T cells and WT Treg prevented the exaggeration of these detrimental effects of Ang II in *Rag1*$^{-/-}$ mice. Ang II-induced ROS production by immune cells might contribute to induction of endothelial dysfunction. Beneficial effects of Treg could be mediated by suppression of T cells involved in adaptive immunity, and innate immune cells such as monocyte/macrophages, both of which express Ang type 1 receptors and NADPH (reduced nicotinamide adenine dinucleotide) oxidase [13,15-17].

In *Rag1*$^{-/-}$ mice (with no T cells) Ang II induced eutrophic remodeling and stiffening, and increased fibronectin expression in MA. This finding in resistance arteries is different from aorta, in which Ang II-induced stiffness was blunted in *Rag1*$^{-/-}$ mice [14], which can be due to differences in Ang II-induced BP changes as well as the type of vessel studied. In the present study, there was a greater pulse pressure in Ang II-treated Veh-injected *Rag1*$^{-/-}$ mice. It is also possible that innate immune cell activation in the absence of Treg, which supress innate and adaptive immune responses (reviewed in [1,18,19]), could have contributed to the observed effects of Ang II in *Rag1*$^{-/-}$ mice. In support of this hypothesis,

adoptive transfer of WT T cells, which contain Treg, blunted vascular remodeling, stiffening and increased fibronectin expression in MA compared to the Veh injected *Rag1*$^{-/-}$ mice. Adoptive transfer of WT Treg in *Rag1*$^{-/-}$ mice prevented the Ang II-induced BP rise and resistance artery remodeling, beneficial effects which might be mediated by suppression of innate immune cells. Consistent with these data, Yang *et al.* [20] showed that coronary artery remodeling in a model of left ventricular pressure overload caused by transverse aortic constriction (TAC), was exaggerated in *Rag1*$^{-/-}$ compared to WT mice. Despite these changes, coronary artery function was preserved in *Rag1*$^{-/-}$ but not in WT mice undergoing TAC. It is plausible that in both studies Treg within the T cell population counteracted microvascular remodeling induced by Ang II independently of T cell activation. In contrast, in presence of Sf T cells that lack Treg but not in presence of WT T cells, Ang II induced hypertrophic remodeling and stiffening in MA of *Rag1*$^{-/-}$ mice, changes that were BP-independent. Ang II induced inflammation in Sf T cell-injected *Rag1*$^{-/-}$ mice but not in *Rag1*$^{-/-}$ mice injected with WT T cells. Inflammatory effects induced by Ang II in these mice were prevented when Sf T cells were co-transferred with WT Treg. This could have been mediated, at least in part, by Ang II through BP-dependent and T cell-independent mechanisms.

Macrophages exhibit considerable plasticity in their polarization and response, and the inflammatory state of macrophages at any given time depends on the expression of various pro-inflammatory M1 and anti-inflammatory M2 activation markers relative to one another. This study demonstrates for the first time that Treg control polarization of monocyte/macrophages infiltrating the MA PVAT and renal cortex. Injection of Sf T cells lacking Treg allowed Ang II to cause infiltrating monocytes/macrophages to polarize toward a pro-inflammatory phenotype, effects prevented or reduced when Sf T cells were co-transferred with WT Treg. M1 macrophages are characterized by enhanced production of ROS and pro-inflammatory cytokines compared to M2 macrophages [21]. Polarization of infiltrating macrophages towards a more M1 phenotype could contribute to the exaggerated increase in ROS production and vascular damage in Sf T cell-injected *Rag1*$^{-/-}$ mice treated with Ang II. Modulation of macrophage

polarization by Treg could be important for prevention of other cardiovascular diseases. Indeed, Treg control of monocyte/macrophages polarization has been demonstrated by loss- or gain-of-Treg function that impaired or improved, respectively, post-myocardial infarction healing [22].

Mice injected with Sf T cells had, in the absence of Treg, higher basal plasma levels of several pro-inflammatory cytokines, suggesting a more activated state of the adaptive immune response, and perhaps also of innate immune cells such as monocyte/macrophages [23]. Pro-inflammatory cytokines, including TNFα, IL-6, IL-17a, and IFNγ have been previously identified as important players in Ang II-induced hypertension and vascular damage [5,24-28]. In the present study, although Ang II induced monocyte/macrophage and $CD3^+$ T cell infiltration and pro-inflammatory polarization of monocyte/macrophages in Sf T cell-injected *Rag1*$^{-/-}$ mice, there was no further elevation in cytokine plasma levels. However, increased infiltration of pro-inflammatory immune cells may have resulted in higher local production of pro-inflammatory cytokines. Co-transfer of WT Treg blunted both elevation of plasma pro-inflammatory cytokines and MA PVAT infiltration of pro-inflammatory immune cells. This was not unexpected, as Treg are known to suppress pro-inflammatory immune cells [19]. *Rag1*$^{-/-}$ mice exhibited similar plasma IL-10 levels compared to WT and Sf T cell-injected mice, which could be explained by the fact that innate immune cells such as macrophages express high levels of this anti-inflammatory cytokine [29]. Ang II treatment tended to decrease plasma levels of the anti-inflammatory IL-10 in all treatment groups, which tended to be restored by co-injection of WT Treg in Veh- and Sf T cell-injected *Rag1*$^{-/-}$ mice. Treg exert their protective effects in part due to the production of IL-10, and decreases in IL-10 levels may contribute to enhanced inflammation and vascular damage. Kassan *et al*. [31] showed using *Il10* knockout mice that IL-10 released from Treg attenuated NADPH oxidase activity and improved MA endothelial function in Ang II-induced hypertension.

In conclusion, these results demonstrate a protective role of Treg that counteract development of microvascular injury induced by Ang II mediated by

supression of innate and adaptive immune responses, and by polarization of monocyte/macrophages toward an M2 anti-inflammatory phenotype.

Acknowledgements

We are grateful to Véronique Michaud and Adriana Cristina Ene for excellent technical assistance.

Sources of Funding

This work was supported by Canadian Institutes of Health Research (CIHR) grant 102606, a Canada Research Chair on Hypertension and Vascular Research from CIHR/Government of Canada, and the Canada Fund for Innovation (all to ELS).

Disclosures

None.

Significance

Our results unambiguously demonstrate a protective role of Treg contained within the T cell population, counteracting development of microvascular injury in a model of Ang II-induced hypertension, via supression of innate and adaptive immune responses. We have identified an additional mechanism whereby Treg exert vascular protective actions controlling polarization of infiltrating monocyte/macrophages. It remains to be determined whether it is possible to take advantage of the anti-inflammatory and immunosuppresive capability of Treg to develop immunomodulatory approaches for treatment of hypertension and associated vascular injury.

References

1. **Mian MO, Paradis P, Schiffrin EL**. Innate immunity in hypertension. *Current hypertension reports*. 2014; 16:413.

2. **Idris-Khodja N, Mian MO, Paradis P, Schiffrin EL**. Dual opposing roles of adaptive immunity in hypertension. *European heart journal*. 2014; 35:1238-1244.

3. **De Ciuceis C, Amiri F, Brassard P, Endemann DH, Touyz RM, Schiffrin EL**. Reduced vascular remodeling, endothelial dysfunction, and oxidative stress in resistance arteries of angiotensin ii-infused macrophage colony-stimulating factor-deficient mice: Evidence for a role in inflammation in angiotensin-induced vascular injury. *Arteriosclerosis, thrombosis, and vascular biology*. 2005; 25:2106-2113.

4. **Wenzel P, Knorr M, Kossmann S, Stratmann J, Hausding M, Schuhmacher S, Karbach SH, Schwenk M, Yogev N, Schulz E, Oelze M, Grabbe S, Jonuleit H, Becker C, Daiber A, Waisman A, Munzel T**. Lysozyme m-positive monocytes mediate angiotensin ii-induced arterial hypertension and vascular dysfunction. *Circulation*. 2011; 124:1370-1381.

5. **Guzik TJ, Hoch NE, Brown KA, McCann LA, Rahman A, Dikalov S, Goronzy J, Weyand C, Harrison DG**. Role of the t cell in the genesis of angiotensin ii induced hypertension and vascular dysfunction. *The Journal of experimental medicine*. 2007; 204:2449-2460.

6. **Kassan M, Wecker A, Kadowitz P, Trebak M, Matrougui K**. Cd4+cd25+foxp3 regulatory t cells and vascular dysfunction in hypertension. *Journal of hypertension*. 2013; 31:1939-1943.

7. **Valencia X, Lipsky PE**. Cd4+cd25+foxp3+ regulatory t cells in autoimmune diseases. *Nature clinical practice. Rheumatology*. 2007; 3:619-626.

8. **Taleb S, Tedgui A, Mallat Z**. Regulatory t-cell immunity and its relevance to atherosclerosis. *Journal of internal medicine*. 2008; 263:489-499.

9. **Viel EC, Lemarie CA, Benkirane K, Paradis P, Schiffrin EL**. Immune regulation and vascular inflammation in genetic hypertension. *American journal of physiology. Heart and circulatory physiology*. 2010; 298:H938-944.

10. **Barhoumi T, Kasal DA, Li MW, Shbat L, Laurant P, Neves MF, Paradis P, Schiffrin EL**. T regulatory lymphocytes prevent angiotensin ii-induced hypertension and vascular injury. *Hypertension*. 2011; 57:469-476.

11. **Matrougui K, Abd Elmageed Z, Kassan M, Choi S, Nair D, Gonzalez-Villalobos RA, Chentoufi AA, Kadowitz P, Belmadani S, Partyka M**. Natural regulatory t cells control coronary arteriolar endothelial dysfunction in hypertensive mice. *The American journal of pathology*. 2011; 178:434-441.

12. **Ricardo SD, van Goor H, Eddy AA**. Macrophage diversity in renal injury and repair. *The Journal of clinical investigation*. 2008; 118:3522-3530.

13. **Hoch NE, Guzik TJ, Chen W, Deans T, Maalouf SA, Gratze P, Weyand C, Harrison DG**. Regulation of t-cell function by endogenously produced angiotensin ii. *American journal of physiology. Regulatory, integrative and comparative physiology*. 2009; 296:R208-216.

14. **Wu J, Thabet SR, Kirabo A, Trott DW, Saleh MA, Xiao L, Madhur MS, Chen W, Harrison DG**. Inflammation and mechanical stretch promote aortic stiffening in hypertension through activation of p38 mitogen-activated protein kinase. *Circulation research*. 2014; 114:616-625.

15. **Jackson SH, Devadas S, Kwon J, Pinto LA, Williams MS**. T cells express a phagocyte-type nadph oxidase that is activated after t cell receptor stimulation. *Nature immunology*. 2004; 5:818-827.

16. **Nataraj C, Oliverio MI, Mannon RB, Mannon PJ, Audoly LP, Amuchastegui CS, Ruiz P, Smithies O, Coffman TM**. Angiotensin ii regulates cellular immune responses through a calcineurin-dependent pathway. *The Journal of clinical investigation*. 1999; 104:1693-1701.

17. **Yanagitani Y, Rakugi H, Okamura A, Moriguchi K, Takiuchi S, Ohishi M, Suzuki K, Higaki J, Ogihara T**. Angiotensin ii type 1 receptor-mediated peroxide production in human macrophages. *Hypertension*. 1999; 33:335-339.

18. **Kinsey GR, Sharma R, Huang L, Li L, Vergis AL, Ye H, Ju ST, Okusa MD**. Regulatory t cells suppress innate immunity in kidney ischemia-reperfusion injury. *Journal of the American Society of Nephrology : JASN*. 2009; 20:1744-1753.

19. **Schiffrin EL**. Immune mechanisms in hypertension and vascular injury. *Clinical science*. 2014; 126:267-274.

20. **Yang F, Dong A, Mueller P, Caicedo J, Sutton AM, Odetunde J, Barrick CJ, Klyachkin YM, Abdel-Latif A, Smyth SS**. Coronary artery remodeling in a model of left ventricular pressure overload is influenced by platelets and inflammatory cells. *PloS one*. 2012; 7:e40196.

21. **Pelegrin P, Surprenant A**. Dynamics of macrophage polarization reveal new mechanism to inhibit il-1beta release through pyrophosphates. *The EMBO journal*. 2009; 28:2114-2127.

22. **Weirather J, Hofmann UD, Beyersdorf N, Ramos GC, Vogel B, Frey A, Ertl G, Kerkau T, Frantz S**. Foxp3+ cd4+ t cells improve healing after myocardial infarction by modulating monocyte/macrophage differentiation. *Circulation research*. 2014; 115:55-67.

23. **Curfs JH, Meis JF, Hoogkamp-Korstanje JA**. A primer on cytokines: Sources, receptors, effects, and inducers. *Clinical microbiology reviews*. 1997; 10:742-780.

24. **Brands MW, Banes-Berceli AK, Inscho EW, Al-Azawi H, Allen AJ, Labazi H**. Interleukin 6 knockout prevents angiotensin ii hypertension: Role of renal vasoconstriction and janus kinase 2/signal transducer and activator of transcription 3 activation. *Hypertension*. 2010; 56:879-884.

25. **Han YL, Li YL, Jia LX, Cheng JZ, Qi YF, Zhang HJ, Du J**. Reciprocal interaction between macrophages and t cells stimulates ifn-gamma and mcp-1 production in ang ii-induced cardiac inflammation and fibrosis. *PloS one*. 2012; 7:e35506.

26. **Madhur MS, Lob HE, McCann LA, Iwakura Y, Blinder Y, Guzik TJ, Harrison DG**. Interleukin 17 promotes angiotensin ii-induced hypertension and vascular dysfunction. *Hypertension*. 2010; 55:500-507.

27. **Sriramula S, Haque M, Majid DS, Francis J**. Involvement of tumor necrosis factor-alpha in angiotensin ii-mediated effects on salt appetite, hypertension, and cardiac hypertrophy. *Hypertension*. 2008; 51:1345-1351.

28. **Zhang W, Wang W, Yu H, Zhang Y, Dai Y, Ning C, Tao L, Sun H, Kellems RE, Blackburn MR, Xia Y**. Interleukin 6 underlies angiotensin ii-induced hypertension and chronic renal damage. *Hypertension*. 2012; 59:136-144.

29. **Saraiva M, O'Garra A**. The regulation of il-10 production by immune cells. *Nature reviews. Immunology*. 2010; 10:170-181.

30. **Kassan M, Galan M, Partyka M, Trebak M, Matrougui K**. Interleukin-10 released by cd4(+)cd25(+) natural regulatory t cells improves microvascular endothelial function through inhibition of nadph oxidase activity in hypertensive mice. *Arteriosclerosis, thrombosis, and vascular biology*. 2011; 31:2534-2542.

Figures

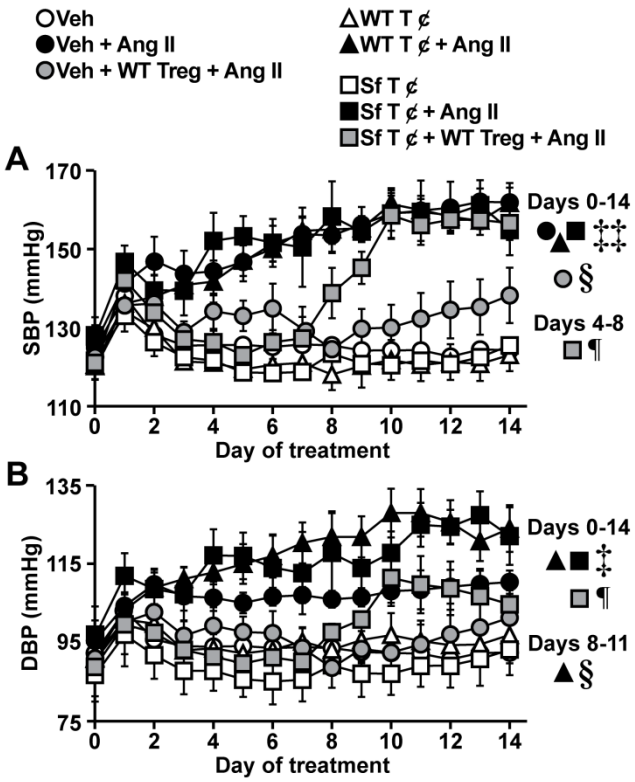

Figure IV-1: Adoptive transfer of Treg-deficient Scurfy (Sf) T cells (♀) in *Rag1*$^{-/-}$ mice did not exaggerate angiotensin (Ang) II-induced hypertension compared to wild-type (WT) T ♀, but injection of WT Treg alone or with Sf T ♀ blunted or delayed Ang II-induced hypertension in *Rag1*$^{-/-}$ mice. Systolic (A, SBP) and diastolic (B, DBP) blood pressure were measured by telemetry in *Rag1*$^{-/-}$ mice injected with vehicle (Veh), 10^7 WT T ♀ or Sf T ♀, or 10^6 Treg alone or with Sf T ♀, and 2 weeks later were infused or not with Ang II for 14 days. Values are means ± SEM, n = 3 – 6. ‡*P*<0.01 and ‡‡*P*<0.001 vs. respective control, §*P*<0.001 vs. Veh + Ang II for days 0 to 14 and ¶*P*<0.05 vs. Sf T ♀+ Ang II for days 4 to 8 in A and for days 0 to 14 for in B.

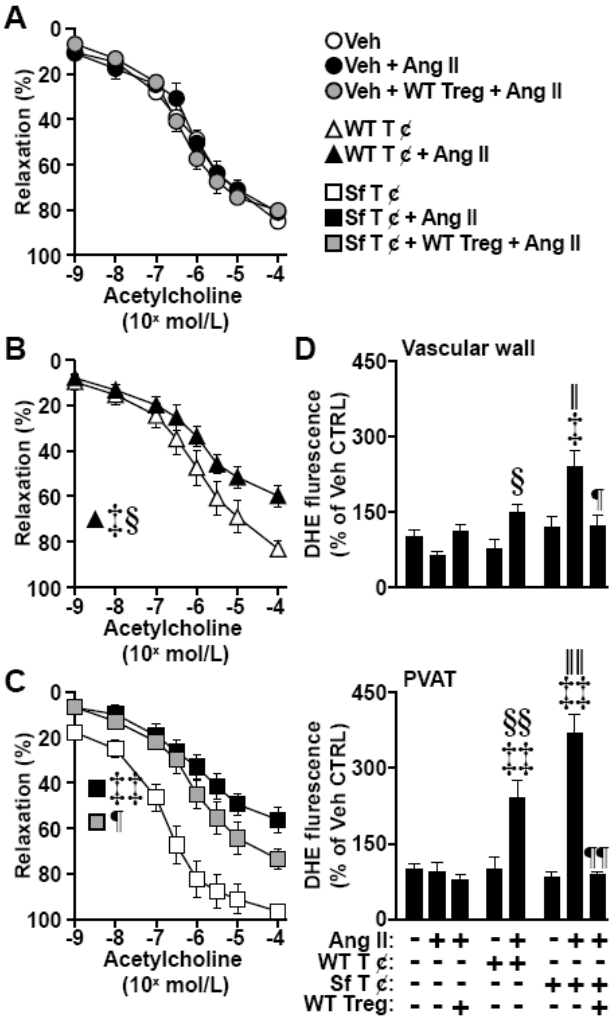

Figure IV-2: Adoptive transfer of Treg-deficient Scurfy (Sf) T cells (♀) exaggerated Ang II-induced endothelial dysfunction and reactive oxidative stress (ROS) generation in mesenteric artery compared to wild-type (WT) T ♀, which was reduced by co-transfer of WT Treg. Relaxation responses to acetylcholine (A-C) in mesenteric arteries and ROS generation in the mesenteric artery vascular wall and perivascular adipose tissue (PVAT) by dihydroethidium (DHE) staining (D) were determined in the same groups as in Figure 1. Data are means ± SEM, n = 7 – 11 for A-C and 5 – 7 for D. ‡*P*<0.05 and ‡‡*P*<0.001 vs. respective control, §*P*<0.05 01 and §§*P*<0.001 vs. vehicle (Veh) + Ang II, ǁ*P*<0.05 and ǁǁ*P*<0.01 vs. WT T ♀ + Ang II and ¶*P*<0.05 and ¶¶*P*<0.001 vs. Sf T ♀ + Ang II. The area-under-the-curve for last three points was used for comparison in A to C.

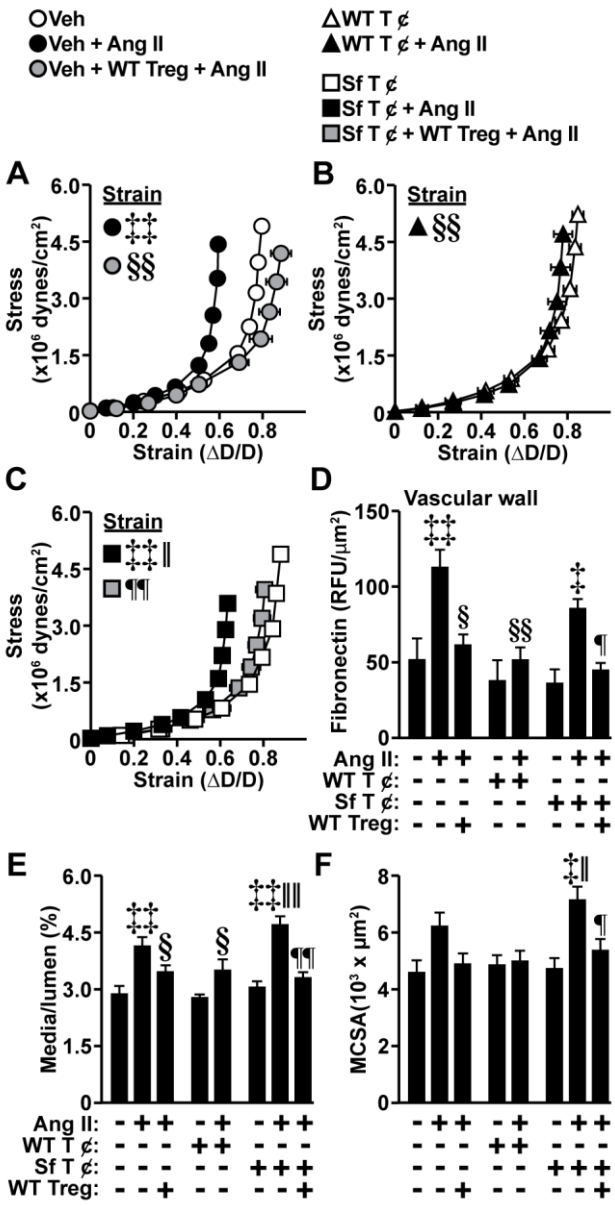

Figure IV- 3: Ang II increased mesenteric artery stiffening and fibronectin expression, and caused remodeling in *Rag1*$^{-/-}$ mice injected with vehicle (Veh) or Treg-deficient Scurfy (Sf) T cells (ɛ), but not when co-injection of wild-type (WT) Treg. Transfer of WT Treg alone or with Sf T ɛ prevented Ang II-induced increase in mesenteric artery stiffness and remodeling. Vascular stiffness (A, B and C), fibronectin expression (relative fluorescence units (RFU)) in the vascular wall (D), media/lumen (E) and media cross-sectional area (MCSA, F) were determined in mesenteric arteries of the same groups as in Fig. 1. Data are means ± SEM, n =

9 – 11 for A-C and E-F and 5 – 6 for D. ‡*P*<0.05 and ‡‡*P*<0.001 vs. respective control, §*P*<0.01 and §§*P*<0.001 vs. vehicle (Veh) + Ang II, ǁ*P*<0.01 and ǁǁ*P*<0.001 vs. WT T ♀ + Ang II, and ¶*P*<0.05 and ¶¶*P*<0.001 vs. Sf T ♀ + Ang II. Strain data measured at 140 mmHg were used for comparison.

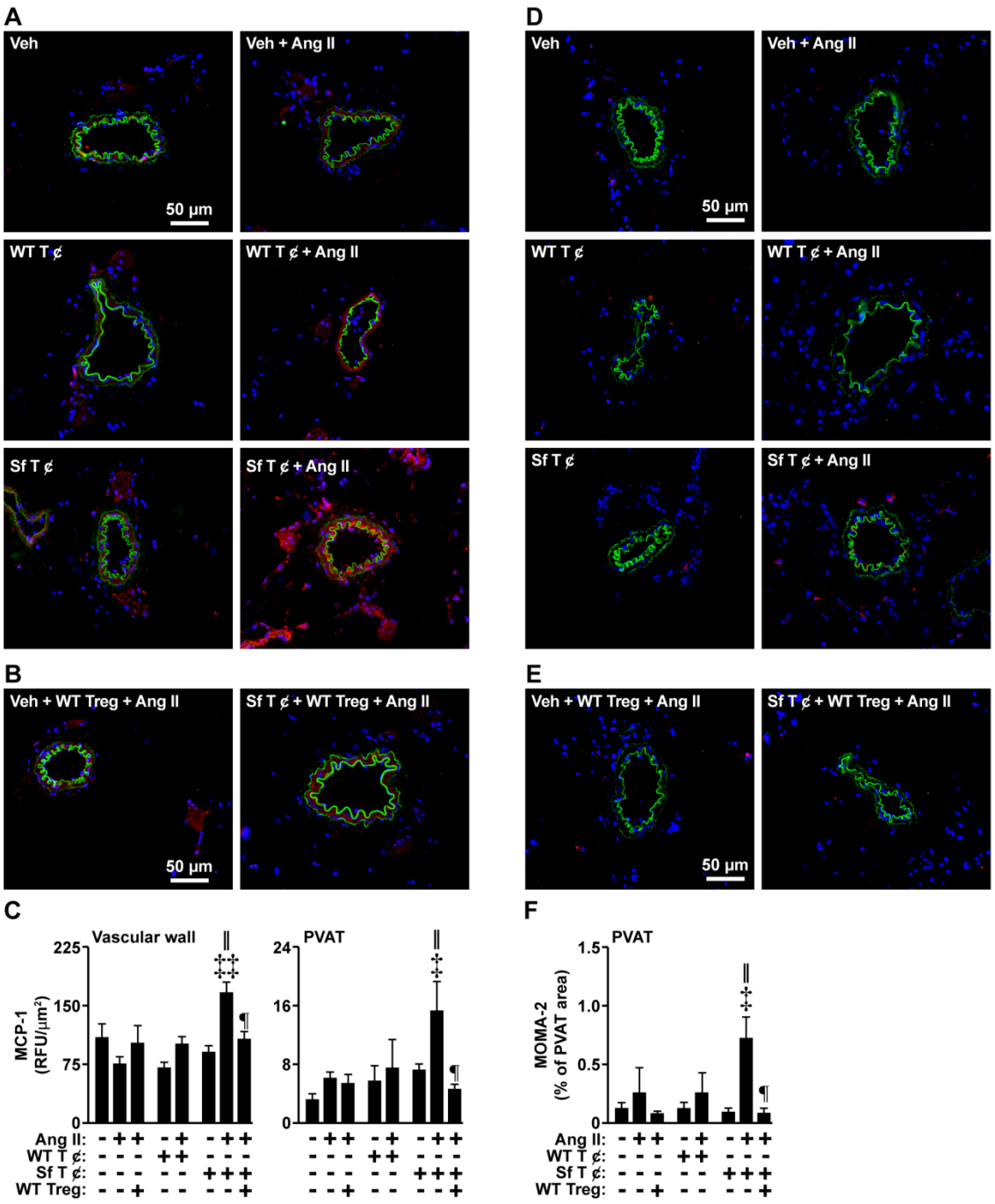

Figure IV-4: Adoptive transfer of Treg-deficient Scurfy (Sf) T cells (ɛ) to *Rag1*$^{-/-}$ mice allowed Ang II to induce increase in monocyte chemotactic protein-1 (MCP-1) expression in mesenteric artery vascular wall and perivascular adipose tissue (PVAT) (A-C) and monocyte/macrophage infiltration in mesenteric artery PVAT (D-F), but not when co-transferred with WT Treg. MCP-1 and

monocyte/macrophage infiltration (MOMA-2) were determined in the same groups as in Fig. 1. Representative MCP-1 (A and B) and MOMA-2 (D and E) fluorescence images (red fluorescence) of mesenteric artery sections of vehicle (veh), WT T ♀ and Sf T ♀-injected *Rag1*$^{-/-}$ treated or not with Ang II (A and D), and of *Rag1*$^{-/-}$ injected with Treg alone or with Sf T ♀ (B and F) and their quantification (C and F) are presented. Green and blue represent elastin autofluorescence and DAPI fluorescence, respectively. Data are means ± SEM, n = 5 – 7. ‡P<0.05 vs. respective control, ‡P<0.05 and ‡‡P<0.01 vs. respective control, ǁP<0.05 vs. WT T ♀ + Ang II and ¶P<0.05 vs. Sf T ♀ + Ang II.

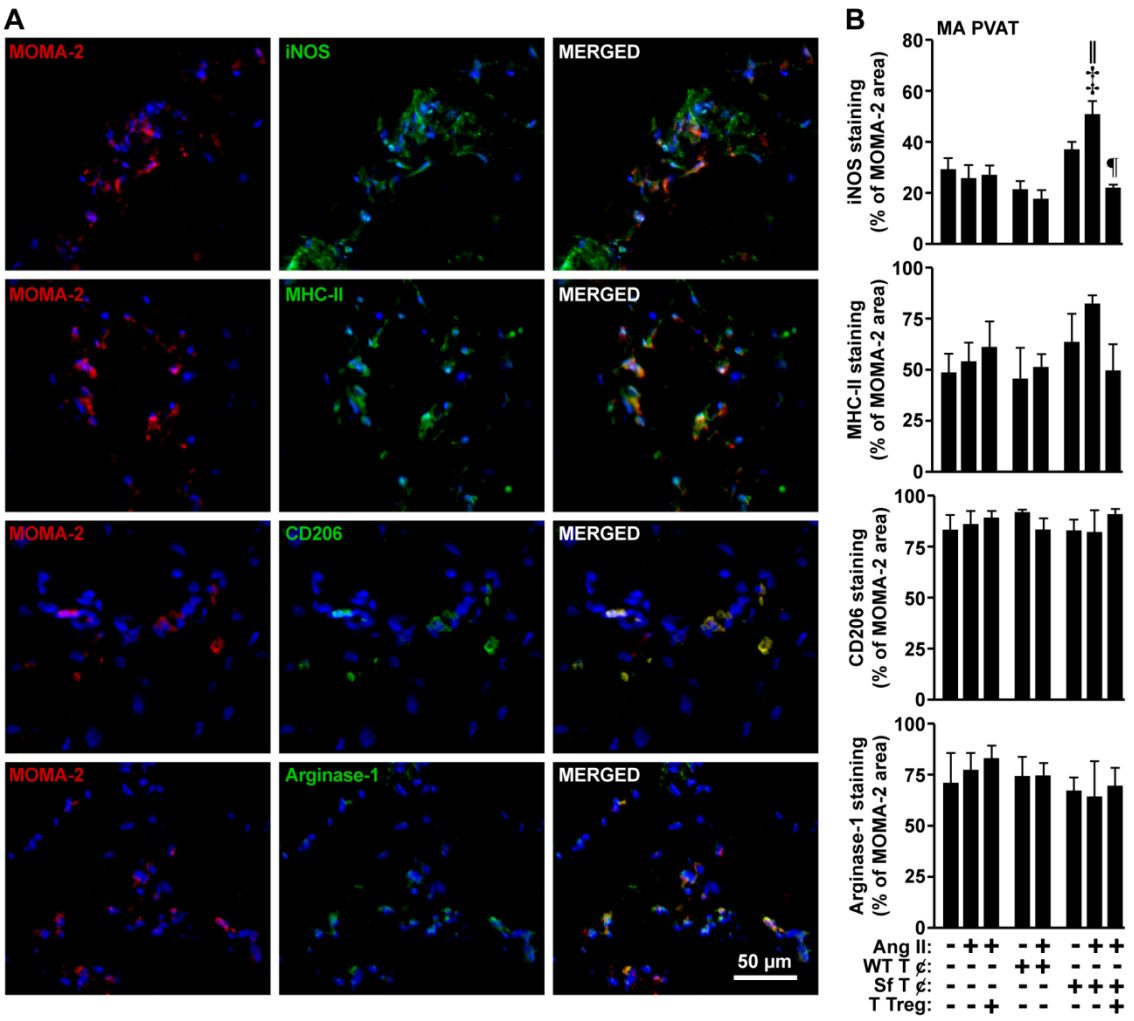

Figure IV-5: Ang II-induced monocytes/macrophages infiltrating the mesenteric artery perivascular adipose tissue (PVAT) to polarize toward a pro-inflammatory phenotype in *Rag1*$^{-/-}$ mice injected with Treg-deficient Scurfy (Sf) T cells (♀), but not when co-transferred with WT Treg. The expression of the pro-inflammatory M1 markers, inducible nitric oxide synthase (iNOS) and the major histocompatibility complex-II (MHC-II), and the anti-inflammatory M2 markers, mannose receptor (CD206) and arginase-1 (Arg-1), within monocytes/macrophages (MOMA-2) infiltrating the mesenteric artery PVAT was determined in the same groups as in Fig. 1. Representative immunofluorescence images of mesenteric arteries co-staining with MOMA-2 (in red) and iNOS, MHC-II, CD206 or Arg-1 (in green) are presented as independent and merged images

in A. Blue represents DAPI fluorescence. The area of each marker within MOMA-2 stained area was measured using color RGB thresholding and expressed as % of MOMA-2 area (B). Data are means ± SEM. ‡P<0.05 vs. respective control, ‖P<0.001 vs. WT T ♀ + Ang II, and ¶P<0.001 vs. Sf T ♀ + Ang II. n = 4 – 5.

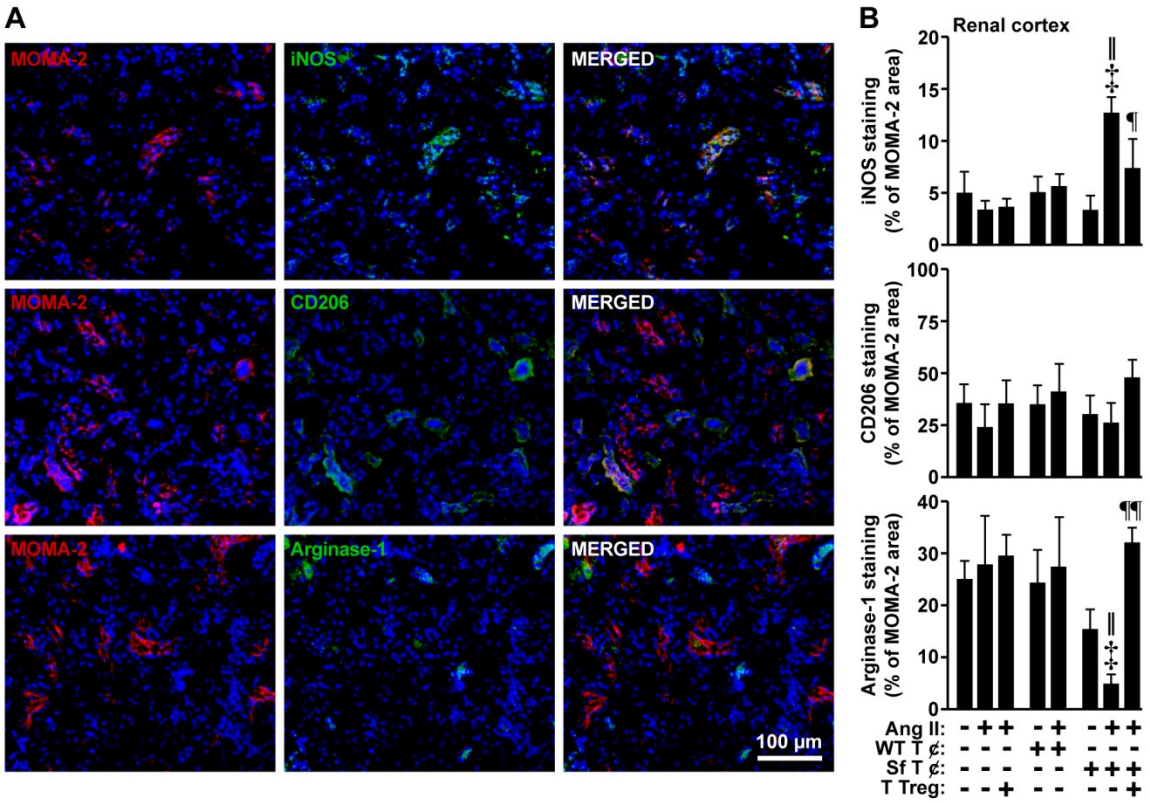

Figure IV- 6: Ang II induced monocyte/macrophages infiltrating the renal cortex to polarize toward a pro-inflammatory phenotype in *Rag1*$^{-/-}$ mice injected with Treg-deficient Scurfy (Sf) T cells (℄), but not when co-transferred with WT Treg. The expression of the pro-inflammatory M1 marker inducible nitric oxide synthase (iNOS), and the anti-inflammatory M2 markers, mannose receptor (CD206) and arginase-1 (Arg-1), within monocytes/macrophages (MOMA-2) infiltrating the renal cortex was determined in the same groups as in Fig. 1. Representative immunofluorescence images of renal cortex co-staining with MOMA-2 (in red) and iNos, CD206 or Arg-1 (in green) are presented as independent and merged images in A. Blue represents DAPI fluorescence. The area of each marker within MOMA-2 stained area was measured using color RGB thresholding and expressed as % of MOMA-2 area (B). Data are means ± SEM. ‡*P*<0.05 vs. respective control, ‖*P*<0.05 vs. WT T ℄ + Ang II, and ¶*P*<0.05 and ¶¶*P*<0.01 vs. Sf T ℄ + Ang II. n = 4 – 5.

Expanded Materials and Methods

Experimental design

The study was approved by the Animal Care Committee of the Lady Davis Institute and McGill University, and followed recommendations of the Canadian Council of Animal Care. Eight-week old C57BL/6J male recombination-activating gene-1 mice (*Rag1*$^{-/-}$, B6.129S7-*Rag1*^{tm1Mom}/J) and 3- to 5-week old C57BL/6J male wild-type (WT) mice were obtained from Jackson Laboratories (Bar Harbor, ME). Female mice heterozygous for the Scurfy mutation (B6.Cg-*Foxp3*$^{sf/x}$/J, Jackson Laboratories) were bred with WT male mice to produce 3- to 5-week old C57BL/6J male FOXP3$^+$ T regulatory cells (Treg)-deficient (B6.Cg-*Foxp3*$^{sf/y}$/J) Scurfy mice. Eleven-week old male *Rag1*$^{-/-}$ mice were injected IV via the tail vein with phosphate buffered saline (PBS) supplemented with 2% fetal bovine serum (FBS) (vehicle), 10^7 WT or Scurfy T cells, 10^6 CD4$^+$CD25$^+$ Treg alone or with 10^7 Scurfy T cells. Two weeks later, mice were anesthetized with 3% isoflurane mixed with O_2 at 1 L/min (depth of anesthesia confirmed by rear foot squeezing), the non-steroidal anti-inflammatory drug carprofen (20 mg/Kg) was administered SC to minimize the post-operation pain, then surgically implanted SC with ALZET osmotic minipumps (Durect) infusing angiotensin II (Ang II, 490 ng/kg/min) for 14 days, as recommended by the manufacturer. Control mice underwent sham surgery. Nine to 11 mice per group were used. In a subgroup of *Rag1*$^{-/-}$ mice, systolic (SBP) and diastolic blood pressure (DBP) was determined by telemetry as previously described.[1] In brief, 10-week old mice were anesthetized with isoflurane and injected with carprofen as above, and surgically instrumented with PA-C10 telemetery transmitters as recommended by the manufacturer (Data Sciences International, St. Paul, MN). Mice were allowed to recover for 7 days and carprofen administered as above once a day for the first three days, then treated as described above. SBP and DBP were determined every 5 min for 10 sec from two days before Ang II minipump or sham surgery until the mice were sacrificed. All mice were kept in sterile conditions. Five 13-week old WT C57BL/6

mice per group were treated or not with Ang II as above and used as reference for determination of T lymphocyte profile by flow cytometry.

Collection of tissues

At the end of the protocol, mice were weighed, anesthetized with isoflurane as above, and blood collected by cardiac puncture on EDTA for cytokine determination. Blood samples were centrifuged at 1,000 x *g* for 15 min at 4°C to remove blood cells, followed by centrifugation at 10,000 x *g* for 10 min at 4°C to remove platelets. Plasma samples were stored at -80°C until tested. The mesenteric artery (MA) vascular bed was dissected, and aorta, heart, lung, spleen, liver, kidneys and tibia were harvested in ice-cold PBS. Tissues were weighed and tibia length determined. Spleen was used for T cell profiling. Second-order MA were used for assessment of endothelial function and vessel mechanics and other sections of MA and kidney were embedded in VWR Clear Frozen Section Compound (VWR international, Edmonton, AL, Canada) for determination of ROS generation, expression of fibronectin and monocyte chemotactic protein-1 (MCP-1) or monocytes/macrophage and $CD3^+$ T cell infiltration. Sections of aorta were fixed with 4% paraformaldehyde for 48 h at 4°C and embedded in paraffin for quantification of collagen content. The remaining tissues were frozen in liquid nitrogen and stored at -80°C until used.

Isolation and adoptive transfer of T cells and/or Treg

T lymphocytes for each injection were isolated from one spleen of WT or Scurfy mouse using $CD3^+$ T cell-negative selection kit as per manufacturer's instructions (Stem Cell Technologies, Vancouver, BC, Canada). $CD4^+CD25^+$ T cells (Treg) for each injection were isolated from 3 spleens of 3-to-5 week old male WT C57BL/6J mice through $CD4^+$ T cell-negative selection followed by $CD25^+$ T cell-positive selection of splenocytes using the EasySep Mouse $CD4^+$ T Cell Pre-Enrichment and $CD25^+$ Positive Selection kits as per manufacturer's instructions (Stem Cell Technologies) as previously described.[1,2] Isolated WT or Scurfy T cells were washed and 10^7 cells were resuspended in 100 µl of PBS/2%

FBS for adoptive transfer. In some experiments, 10^6 Treg alone or together with 10^7 Scurfy T cells were resuspended in 100 µl of PBS/2% FBS for adoptive transfer. To perform adoptive transfer, mice were placed under a heat lamp to increase blood flow to the tail vein and then transferred to a holding device (AIMS restrainer). The lateral tail veins were identified and cells injected using a 0.5 ml syringe with a 26-gauge needle. The purity of isolated Treg using this technique has been previously determined by us.[2] Purity of T cells and efficiency of adoptive transfer at the time of sacrifice were determined by flow cytometry.

Determination of purity of isolated T cells and efficiency of adoptive transfer

T cells (10^6) isolated from spleen of WT and splenocytes (0.5-1 x 10^6) isolated from WT mice and *Rag1*$^{-/-}$ mice adoptively transferred with T cells, Treg or both, treated or not with Ang II, were resuspended in PBS/2% FBS. Cells were blocked with mouse BD Fc-Block™ (1:200, clone 2.4G2, BD Biosciences, Mississauga, ON, Canada) for 30 min at 4°C to avoid non-specific binding to mouse Fc-gamma receptors, stained for 1 h at 4°C with phycoerythrin (PE)-conjugated hamster anti-mouse CD3e (1:1000, clone 145-2C11, BD Biosciences) and allophycocyanin (APC)-conjugated rat anti-mouse CD4 antibody (1:2000, clone RM4-5, BD Biosciences), washed with PBS/2% FBS, fixed and permeabilized using the FOXP3 staining buffer set (eBioscience, San Diego, CA) as per manufacturer's instructions, and stained with fluorescein isothiocyanate (FITC)-conjugated rat anti-mouse FOXP3 antibody (1:1000, clone FJK-16s, eBioscience) for 1 h at 4°C. Additionally, cells were stained with PE-conjugated hamster anti-mouse IgG1k, APC-conjugated rat anti-mouse IgG2ak, and FITC-conjugated rat anti-mouse IgG2ak isotype control antibodies as per the above protocol to control for nonspecific staining. Cells were washed, resuspended with PBS/2% FBS, and analyzed using FACSCalibur™ flow cytometer (BD Biosciences) and FCS Express V3 software (De Novo Software, Los Angeles, CA).

Assessment of Endothelial Function and Vessel Mechanics

Second-order MA, of average lumen size ~220 μm, were dissected and mounted on a pressurized myograph as previously described.[3] Vessels were equilibrated for 45 min at 45 mmHg intraluminal pressure in Krebs solution (pH 7.4) containing (in mmol/L): 120 NaCl, 25 $NaHCO_3$, 4.7 KCl, 1.18 KH_2PO_4, 1.18 $MgSO_4$, 2.5 $CaCl_2$, 0.026 EDTA and 5.5 glucose, bubbled continuously with 95% air and 5% CO_2. Media and lumen diameters were measured by a computer-based video imaging system (Living Systems Instrumentation, Burlington, Virginia, USA). Contractile responses to cumulative concentrations of norepinephrine (10^{-8} to 10^{-4} mol/L) were determined. Endothelium-dependent and -independent relaxation was assessed by measuring the dilatory responses to cumulative concentrations of acetylcholine (10^{-9} to 10^{-4} mol/L) or sodium nitroprusside (SNP, 10^{-8} to 10^{-4} mol/L), respectively, in vessels precontracted with norepinephrine (5 x 10^{-5} mol/L). To evaluate the contribution of nitric oxide (NO) to the vascular response, the dose-response curve to acetylcholine was determined before and after a 30-min preincubation with the NO synthase inhibitor N^{ω}-nitro-L-arginine methyl ester (L-NAME, 10^{-4} mol/L). Thereafter, vessels were perfused with Ca^{2+}-free Krebs solution containing 10 mmol/L EGTA for 30 min to eliminate the tone. Media and lumen diameters were measured at 3, 10, 20, 30, 40, 45, 60, 80, 100, 120 and 140 mmHg intraluminal pressures. Media cross-sectional area, media/lumen, and stress and strain were calculated as previously described.[4]

Generation of reactive oxygen species (ROS)

Vascular and perivascular adipose tissue (PVAT) ROS production were assessed on 4-μm cryosections of MA by measuring fluorescence after incubation with the ROS-sensitive fluorescent dye dihydroethidium (DHE, 2 μmol/L) in the dark for 1 min at 37°C. Fluorescence was visualized and captured with a fluorescence microscope with a CY3 filter as previously described.[3] DHE fluorescence intensity per total surface area was quantified with ImageJ software (http://rsb.info.nih.gov/ij/).

Assessment of monocyte chemotactic protein-1 and fibronectin expression, monocyte/macrophage and CD3 T cell infiltration, and collagen content

Expression of monocyte chemotactic protein-1 (MCP-1) and fibronectin in MA, monocyte/macrophage (MOMA-2) and CD3 T cell infiltration in MA or kidney were determined by immunofluorescence microscopy on 4-µm cryostat sections. Monocyte/macrophage polarization was determined by co-staining for MOMA-2 and M1 (classically activated) macrophage markers inducible nitric oxide synthase (iNOS) or major histocompatibility complex class II (MHC-II), or M2 (alternatively activated) macrophage markers mannose receptor (CD206) or arginase-1 (Arg-1). Tissue cryosections were fixed in ice-cold acetone:methanol (1:1) mix for 10 min at room temperature (RT) (for fibronectin, MCP-1, MOMA-2, iNOS, MHC-II, CD206 and Arg-1) or air-dried for 30 min and fixed in 4% paraformaldehyde solution for 20 min at room temperature (RT) (for CD3). Thereafter, sections were washed with PBS twice for 5 min and twice with tris-buffered saline (TBS) containing 0.1% Tween-20 (TBST). Sections were blocked for 1 h at RT with TBST containing 10% normal goat serum (for fibronectin), or 10% normal donkey serum (for MCP-1), or containing 1% bovine serum albumin, 0.4% Triton X-100 and 20% fetal bovine serum (for MOMA-2, iNOS, MHC-II, CD206, Arg-1 and CD3). Sections were incubated overnight at 4°C with rabbit anti-mouse fibronectin antibody (1:100, EMD Millipore, Billerica, MA, USA), goat anti-mouse MCP-1 antibody (1:50, Santa Cruz Biotechnology, Santa Cruz, CA), rat anti-mouse MOMA-2 antibody (1:50, Abcam, Cambridge, MA), rabbit anti-mouse iNOS antibody (1:50, BD Biosciences), rabbit anti-mouse MHC-II antibody (1:125, Abcam), goat anti-mouse CD206 antibody (1:50, Santa Cruz Biotechnology), goat anti-mouse Arg-1 antibody (1:50, Santa Cruz Biotechnology), or rat anti-mouse CD3 antibody (1:100, eBiosciences, San Diego, CA). The sections were then washed 3 times with TBST, and incubated for 2 h at RT with Alexa® Fluor 647 goat anti-rabbit antibody (1:100, Life Technologies, Burlington, ON, Canada) for fibronectin, Alexa® Fluor 555 donkey

anti-goat antibody (1:150) for MCP-1, CD206 and Arg-1, Alexa® Fluor 647 goat anti-rat antibody (1:100) for MOMA-2, Alexa® Fluor 488 goat anti-rabbit antibody for iNOS and MHC-II, or Alexa® Fluor 555 goat anti-rat antibody (1:200) for CD3. Sections were then washed 3 times with TBST, counterstained with 4',6-diamidino-2-phenylindole (DAPI, 6 μM, Life Technologies) and mounted with Fluoromount (Sigma-Aldrich). Images were captured using a fluorescent microscope Leica DM2000 (Leica Microsystems, Richmond Hill, ON, Canada) and quantified with Image J software (National Institute of Mental Health, Bethesda, Maryland, USA). The expression of fibronectin and MCP-1 was determined in MA wall or PVAT and was presented as relative fluorescence unit (RFU) per μm^2. Monocyte/macrophage infiltration was analyzed in MA PVAT and kidney cortex by determining the area of MOMA-2 staining using color RGB thresholding, which was then expressed as % of studied area. Expression of M1 or M2 markers in infiltrating monocyte/macrophages was analyzed in MA PVAT and kidney cortex by determining the area of each marker within MOMA-2 stained area using color RGB thresholding, and the area of each marker expressed as % of MOMA-2 area. CD3 infiltration was quantified in kidney cortex and MA PVAT as the number of cells detected per μm^2.

Plama cytokines

Plasma levels of interleukin (IL)-6, IL-10, IL-17a, interferon γ (INFγ), monocyte chemotactic protein-1 (MCP-1), regulated on activation, normal T cell expressed and secreted (RANTES) and tumor necrosis factor α (TNFα) were measured using ProcartaPlex multiplex immunoassays (eBioscience) on a Bio-Plex 200 (Bio-Rad Laboratories).

Data Analysis

Results are presented as means ± SEM. BP data were compared with two-way analysis of variance (ANOVA) for repeated measures. Comparisons between multiple groups for other data and areas-under-the-curve for last three points of acetylcholine concentration-responses were by one-way ANOVA,

followed by a Student-Newman-Keuls post-hoc test. $P<0.05$ was considered statistically significant.

References

1. **Barhoumi T, Kasal DA, Li MW, Shbat L, Laurant P, Neves MF, Paradis P, Schiffrin EL**. T regulatory lymphocytes prevent angiotensin ii-induced hypertension and vascular injury. *Hypertension*. 2011; 57:469-476.

2. **Kasal DA, Barhoumi T, Li MW, Yamamoto N, Zdanovich E, Rehman A, Neves MF, Laurant P, Paradis P, Schiffrin EL**. T regulatory lymphocytes prevent aldosterone-induced vascular injury. *Hypertension*. 2012; 59:324-330.

3. **Leibovitz E, Ebrahimian T, Paradis P, Schiffrin EL**. Aldosterone induces arterial stiffness in absence of oxidative stress and endothelial dysfunction. *Journal of hypertension*. 2009; 27:2192-2200.

4. **Neves MF, Endemann D, Amiri F, Virdis A, Pu Q, Rozen R, Schiffrin EL**. Small artery mechanics in hyperhomocysteinemic mice: Effects of angiotensin ii. *Journal of hypertension*. 2004; 22:959-966.

Supplemental results

T cell purity and efficiency of WT and Treg-deficient T cell and WT Treg adoptive transfers

Flow cytometry analysis revealed that the purity of the preparations of wild-type (WT) and Scurfy (Sf) T cells used for adoptive transfer contained >85% $CD3^+$ T cells (Fig. S1A). The purity of WT $CD4^+CD25^+$ T regulatory cells (Treg) preparations has been previously determined.[1] The efficiency of WT and Treg-deficient Sf T cell and WT Treg adoptive transfers in recombination-activating gene 1 knockout (*Rag1*$^{-/-}$) mice was assessed by flow cytometry profiling at the end of the study the $CD3^+$ T cells, $CD3^+CD4^+$ T cells and $CD3^+CD4^+FOXP3^+$ Treg in the spleen of *Rag1*$^{-/-}$ mice treated or not with angiotensin (Ang) II and injected with vehicle (Veh), 10^7 WT or Sf T cells, 10^6 WT $CD4^+CD25^+$ Treg alone or with Sf T cells (Fig. S1B-G). As expected, the spleen of *Rag1*$^{-/-}$ mice was deficient in $CD3^+$ T cells whereas that of WT mice contained the expected proportion of $CD3^+$ T cells (23.5 ± 0.7% of splenocytes), $CD3^+CD4^+$ T cells (46.6 ± 1.8% of $CD3^+$ cells) and $CD3^+CD4^+FOXP3^+$ Treg (6.7 ± 0.4% of $CD3^+$ cells).

Body and organ weights

The body weight (BW) of Veh- and WT T cell-injected *Rag1*$^{-/-}$ mice was similar, whereas Sf T cell-injected *Rag1*$^{-/-}$ mice presented a slightly lower (8%) BW than that of WT T cell-injected *Rag1*$^{-/-}$ mice (Table S1). Ang II treatment and Treg adoptive transfer did not affect the BW. Tibia length (TL) was not unaltered by adoptive transfer of immune cells or Ang II treatment. The kidney weight-to-TL ratio was similar in all the groups. Spleen weight-to-TL ratio (SW/TL) was 1.3-fold higher in WT T cell-injected *Rag1*$^{-/-}$ mice compared to Veh-injected *Rag1*$^{-/-}$ mice, and 2.6-fold greater in Sf T cell-injected *Rag1*$^{-/-}$ mice compared to WT T cell-injected *Rag1*$^{-/-}$ mice. Ang II increased SW/TL ~1.5-fold in Veh- and Sf T cell-injected *Rag1*$^{-/-}$ mice, but not in WT T cell-injected *Rag1*$^{-/-}$ mice. Co-transfer of WT Treg decreased SW/TL by 64% in Ang II-treated Sf T cell-injected *Rag1*$^{-/-}$ mice.

The small increase in spleen weight observed in *Rag1*$^{-/-}$ mice injected with WT T cells compared to Veh-injected *Rag1*$^{-/-}$ mice can be explained by the reconstitution of T cells in these mice. The greater spleen weight observed in Sf T cell-injected *Rag1*$^{-/-}$ mice could also be expected because Sf T cells, which lack Treg immunosuppressive effects, proliferate more than WT T cells that include Treg. In support, Sf T cell-injected *Rag1*$^{-/-}$ mice tended to have more CD3^{+} T cells compared to *Rag1*$^{-/-}$ mice injected with WT T cells. Ang II increased spleen weight in Sf T cell-injected *Rag1*$^{-/-}$ mice could not be explained by a further increase in CD3^{+} T cells. It is possible that this was due to Ang II-induced proliferation of other immune cells such as monocyte/macrophages. Co-injection of WT Treg prevented Ang II-induced increase in spleen weight only in Sf T cell-injected *Rag1*$^{-/-}$ mice. This suggests that WT Treg counteracts Ang II-induced proliferation of T cells and other immune cells.

References

1. **Kasal DA, Barhoumi T, Li MW, Yamamoto N, Zdanovich E, Rehman A, Neves MF, Laurant P, Paradis P, Schiffrin EL**. T regulatory lymphocytes prevent aldosterone-induced vascular injury. *Hypertension*. 2012; 59:324-330.

Supplemental figures and tables

Table IV-S1: Body and tissue weights

Parameters	Veh	Veh + Ang II	Treg + Ang II	WT T ♀	WT T ♀ + Ang II	Sf T ♀	Sf T ♀ + Ang II	Sf T ♀ + Treg + Ang II
n	11	11	11	11	11	11	11	9
BW (g)	26.6 ± 0.6	26.7 ± 0.3	27.5 ± 0.3	28.6 ± 0.5	27.4 ± 0.4	26.3 ± 0.7†	26.6 ± 0.7	26.5 ± 0.3
TL (mm)	17.7 ± 0.1	17.4 ± 0.2	17.7 ± 0.2	17.4 ± 0.2	17.4 ± 0.1	17.4 ± 0.3	17.4 ± 0.3	17.5 ± 0.1
KW/TL (mg/mm)	18.0 ± 0.7	18.6 ± 0.7	17.4 ± 0.3	19.8 ± 0.7	17.6 ± 0.6	17.6 ± 0.3	18.2 ± 0.6	16.4 ± 0.6
SW/TL (mg/mm)	1.2 ± 0.1	1.9 ± 0.3‡‡	2.2 ± 0.3	1.6 ± 0.1**	2.0 ± 0.1	4.1 ± 1.0††	6.3 ± 1.0‡‖	2.3 ± 0.2¶¶

Body weight, tibia length (TL) and kidney (KW) and spleen (SW) weights were determined in *Rag1*$^{-/-}$ mice injected with vehicle (Veh), 10^7 wild-type (WT) or Scurfy (S) T cells (♀), 10^6 $CD4^+CD25^+$ Tregs alone or with Sf T ♀, and 2 weeks later were infused or not with angiotensin (Ang) II for 14 days. n, number. **P*<0.05 and ***P*<0.01 vs. Veh, †*P*<0.05 and ††*P*<0.01 vs. WT T ♀, ‡*P*<0.05 and ‡‡*P*<0.001 vs. respective control, §*P*<0.05 vs. Vehicle + Ang II, ‖*P*<0.001 vs. WT T ♀ + Ang II and ¶*P*<0.05 and ¶¶*P*<0.01 vs. Sf T ♀ + Ang II.

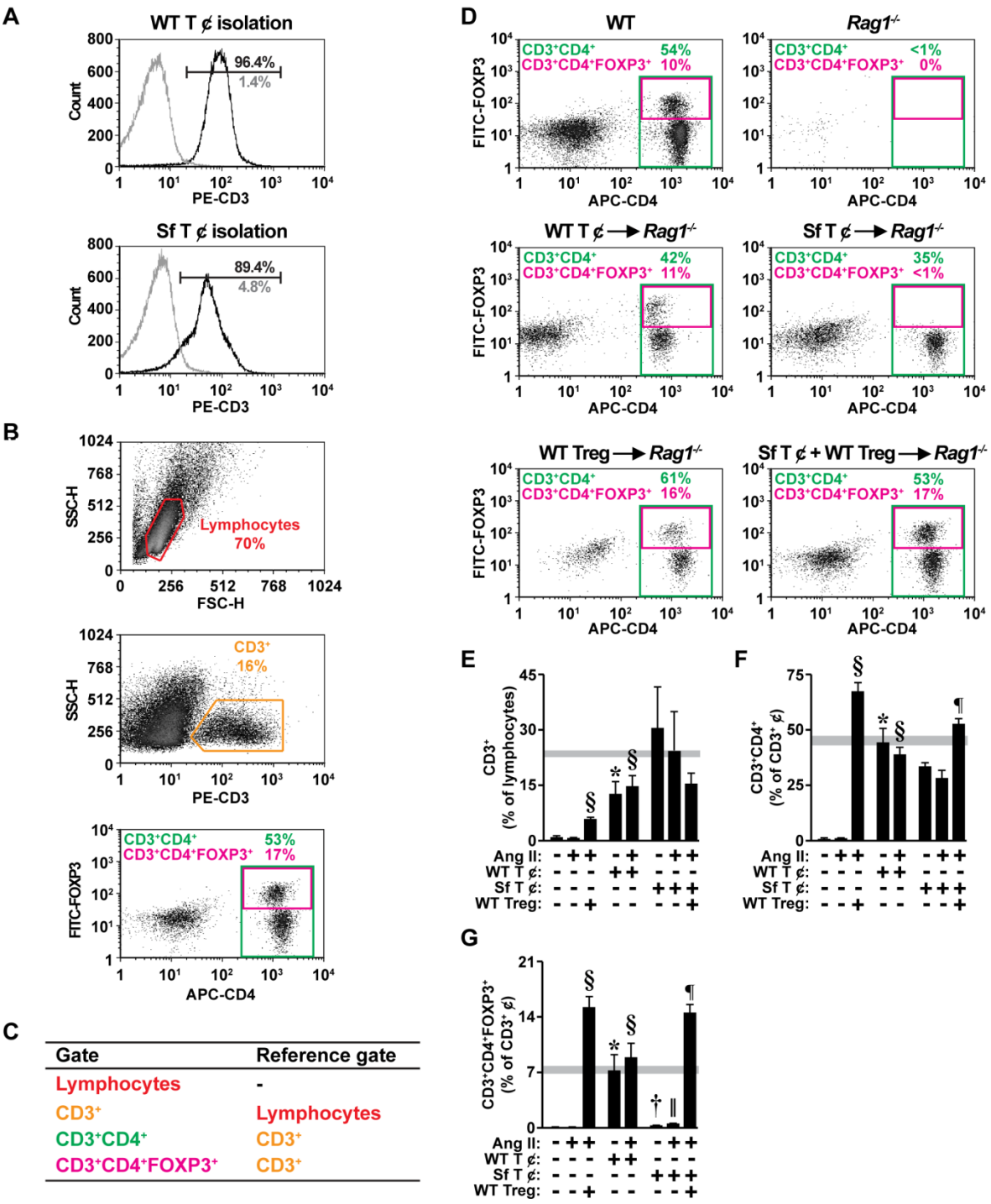

Figure IV-S1: Purity of isolated T cells (♀) and efficiency of T ♀ and Treg adoptive transfer were determined by flow cytometry. The % of $CD3^+$ T ♀ in splenocytes and T ♀ isolated from spleen of 3-5 week-old wild-type (WT) or Scurfy (Sf) mice (A) was determined by flow cytometry. Splenocytes were stained with

phycoerythrin (PE)-conjugated hamster anti-mouse CD3e and PE-conjugated hamster anti-mouse IgG1k isotype control antibodies, or subjected to negative selection to purify $CD3^+$ T cells, and then stained as above and analyzed by flow cytometry. Fluorophore was excited with a 488 nm laser and analyzed with a 586/24 bandpass filter (BP). All splenocytes were gated in the side scatter height (SSC-H)/forward scatter height (FSC-H) plot. $CD3^+$ cells were divided in a histogram and the % of $CD3^+$ T ♀ was calculated by substracting the overlapping isotype peak. Representative histograms indicating the % of $CD3^+$ ♀ for WT T cells or Sf T cells after isolation (in black) and the respective % of isotype overlap (in grey) are shown in A. The profile of $CD3^+$, $CD3^+CD4^+$, and $CD3^+CD4^+FOXP3^+$ cells in the the spleen of *Rag1*$^{-/-}$ mice injected with vehicle (Veh), 10^7 WT T ♀ or Sf T ♀, or 10^6 WT Treg alone or with Sf T ♀, and treated or not with angiotensin (Ang) II (B-G) were determined by flow cytometry. Splenocytes were stained with PE-conjugated hamster anti-mouse CD3e, allophycocyanin (APC)-conjugated rat anti-mouse CD4, and fluorescein isothiocyanate (FITC)-conjugated rat anti-mouse FOXP3 antibodies and analyzed by flow cytometry. Fluorophores were respectively excited and analyzed with appropriate laser and BP (FITC: 488 nm with 530/30 BP, PE: 488 nm with 586/24 BP and APC: 633 nm with 661/16 BP). Representative flow cytometry profile of splenocytes (B) with the gating strategy (C) and the % cells are shown from a *Rag1*$^{-/-}$ injected with Sf T cells and Treg. Lymphocytes were gated in the SSC-H/ FSC-H plot. $CD3^+$ cells were gated in the SSC-H/CD3 plot from the splenocyte population. $CD3^+CD4^+$ and $CD3^+CD4^+FOXP3^+$ cells were gated in the FOXP3/CD4 plot from the CD3 cells population. Representative FOXP3/CD4 plots for the different groups are shown (D). The % of $CD3^+$ cells in lymphocytes (E), and the % of $CD3^+CD4^+$ and $CD3^+CD4^+FOXP3^+$ cells in $CD3^+$ cells (F and G) are presented. Gray rectangles in E-G panels present the values of WT mice. Values are means ± SEM. ∗P<0.001 vs. Veh, **†**P<0.001 vs. WT T ♀, **§**P<0.001 vs. Veh + Ang II, ‖P<0.001 vs. WT T cells + Ang II and ¶P<0.001 vs. Sf T cells + Ang II. n = 3 for purity experiments, and n = 5-9 for flow cytometry profiling of T ♀.

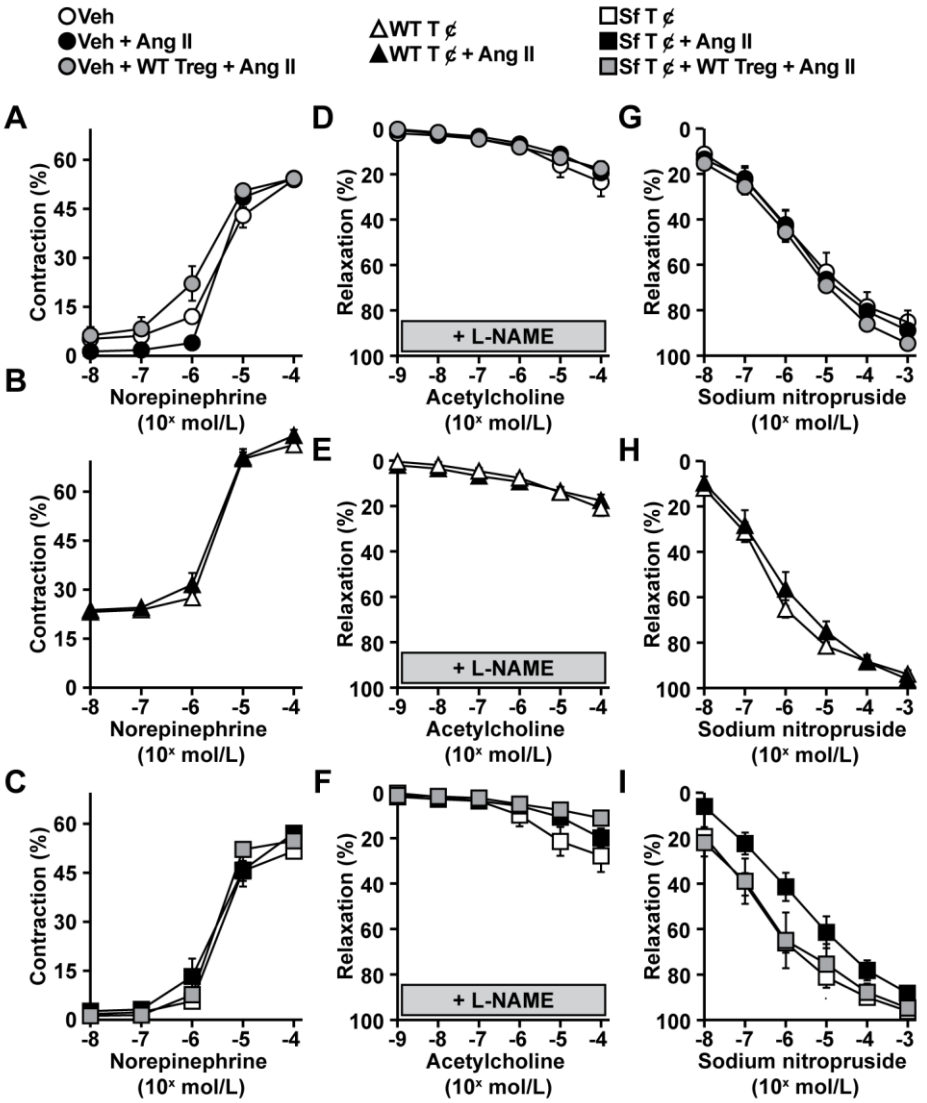

Figure IV-S2: Contractile responses to norepinephrine (A-C), and vasodilatory responses to acetylcholine in the presence of NO synthase inhibitor N^{ω}-nitro-L-arginine methyl ester (L-NAME, D-F) and to sodium nitroprusside (G-I) were determined in mesenteric arteries in *Rag1*$^{-/-}$ mice injected with vehicle (Veh), 10^7 wild-type (WT) T cells (♀) or Treg-deficient Scurfy (Sf) T ♀, or 10^6 WT Treg alone or with Sf T ♀, and 2 weeks later were infused or not with Ang II for 14 days. Data are means ± SEM, n = 7 – 10.

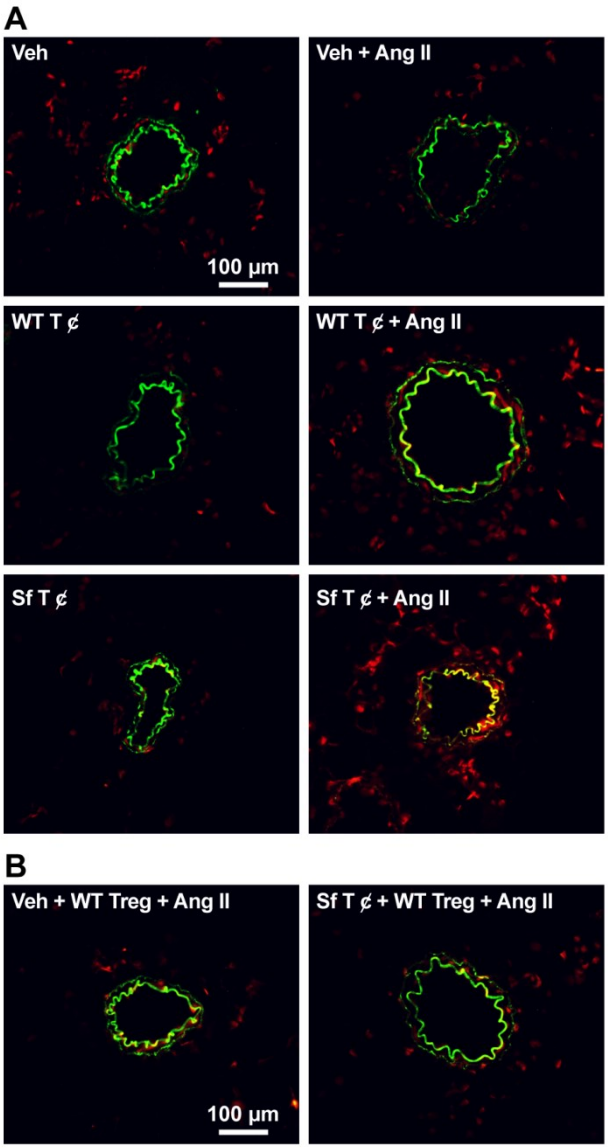

Figure IV-S3: Adoptive transfer of Treg-deficient Scurfy (Sf) T cells (¢) exaggerated Ang II-induced reactive oxidative stress (ROS) generation in mesenteric artery in mesenteric arteries compared to wild-type (WT) T ¢ (A and C), but not when co-transferred with WT Treg (B and C). ROS generation was determined in the mesenteric artery vascular wall and perivascular adipose tissue (PVAT) by dihydroethidium (DHE) staining (red fluorescence) in *Rag1*$^{-/-}$ mice injected with vehicle (Veh), 10^7 WT T ¢ or Sf T ¢, or 10^6 Treg alone or with Sf T ¢, and 2 weeks later were infused or not with Ang II for 14 days. Representative images of DHE stained mesenteric artery sections are shown in

A and B. The % of DHE fluorescence expressed as % of vehicle control (Veh CTRL) in vascular wall and PVAT is presented in C. Green represents elastin autofluorescence.

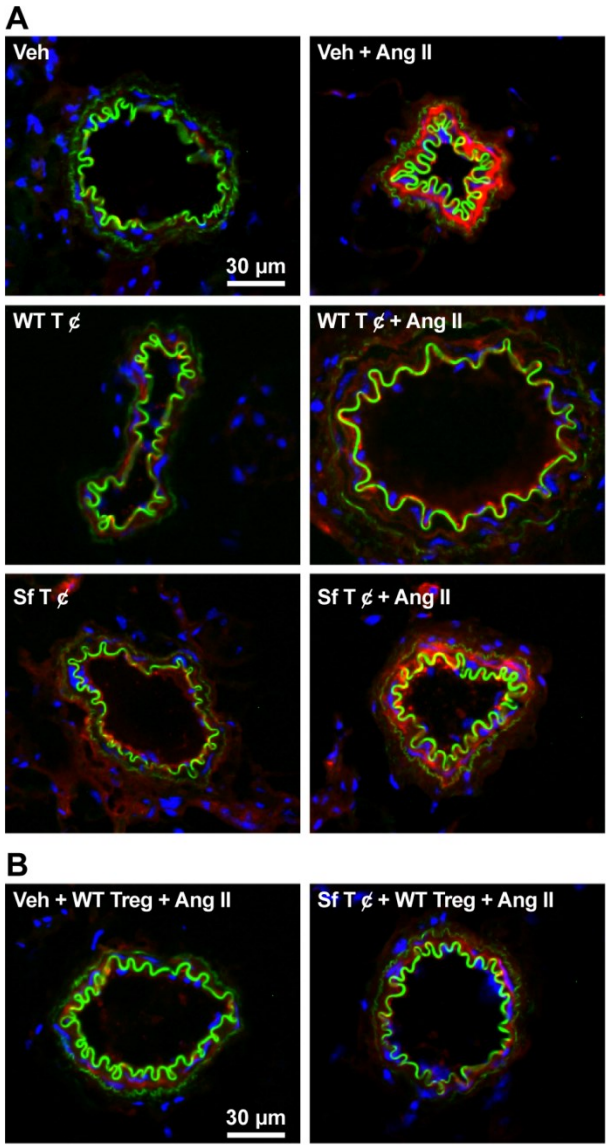

Figure IV-S4: Ang II increased mesenteric artery fibronectin expression in *Rag1*$^{-/-}$ injected with vehicle (Veh) or Treg-deficient Scurfy (Sf) T cells (¢), but not in mice injected with wild-type (WT) T ¢ (A, C). Transfer of WT Treg alone or with Sf T ¢ prevented Ang II-induced increase in fibronectin expression (B, C). Fibronectin expression (red fluorescence) was determined in mesenteric artery vascular wall of *Rag1*$^{-/-}$ mice injected with vehicle (Veh), 10^7 WT T ¢ or Sf T ¢, or 10^6 Treg alone or with Sf T ¢, and 2 weeks later were infused or not with Ang II for 14 days. Representative fibronectin fluorescence images (A and B) and

quantification (C) are presented. Green and blue represent elastin autofluorescence and DAPI fluorescence, respectively.

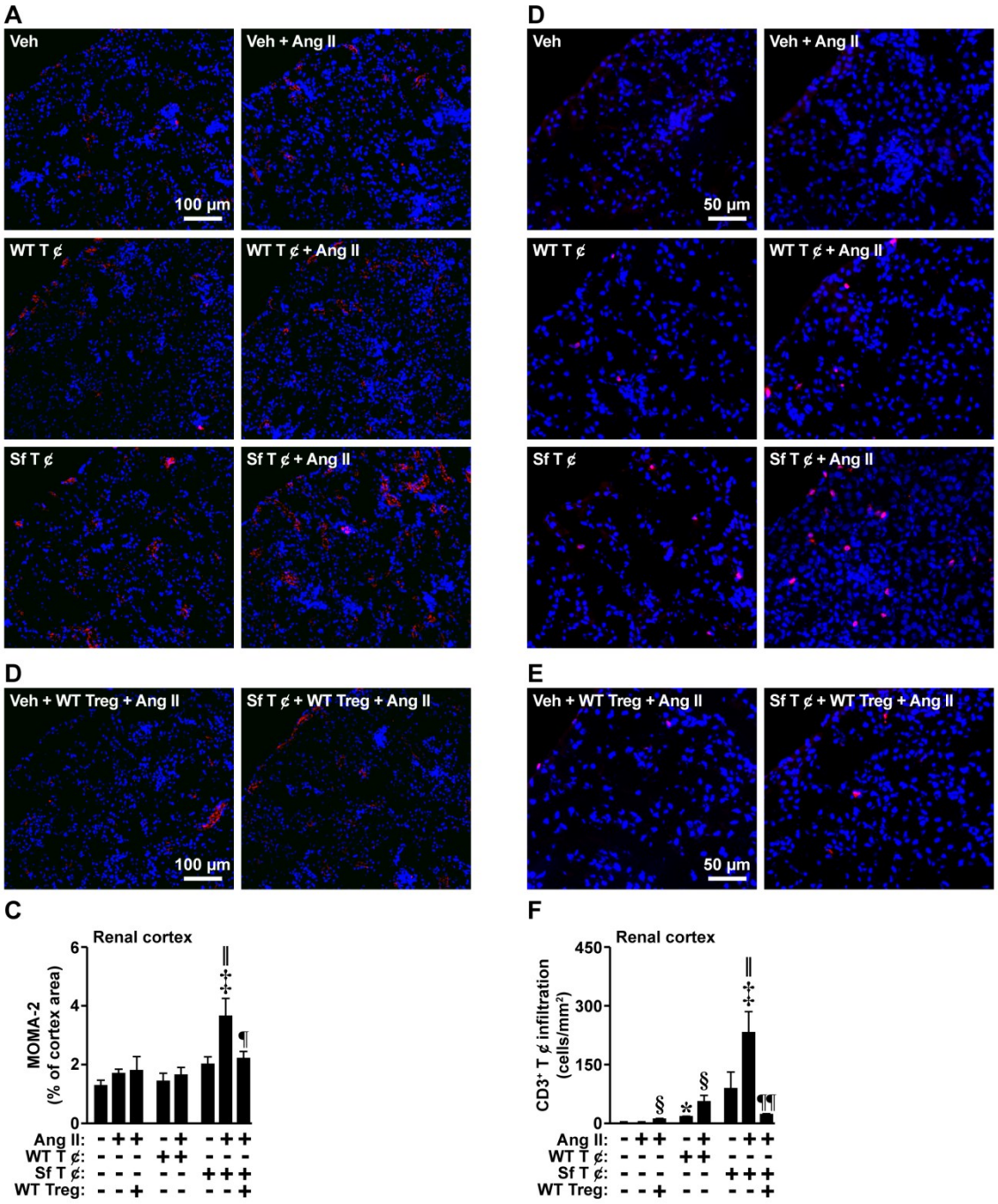

Figure IV-S5: Adoptive transfer of Treg-deficient Scurfy (Sf) T cells (♀) exaggerated Ang II-induced monocyte/macrophage infiltration (A-C) and CD3 T ♀ infiltration (D-F) in renal cortex compared to wild-type (WT) T ♀, but not when co-transferred with WT Treg. Monocyte/macrophage infiltration (MOMA-2) and CD3 T cell infiltration (in red) were determined in determined in *Rag1*$^{-/-}$ mice injected

with vehicle (Veh), 10^7 wild-type (WT) T ♀ or Sf T ♀, or 10^6 WT Treg alone or with Sf T ♀, and 2 weeks later were infused or not with Ang II for 14 days. Representative MOMA-2 (A and B) and CD3 (D and E) fluorescence images (red fluorescence) of renal cortex sections of vehicle (veh), WT T ♀ and Sf T ♀-injected *Rag1*$^{-/-}$ treated or not with Ang II (A and D), and of *Rag1*$^{-/-}$ injected with Treg alone or with Sf T ♀ (B and F) and their quantification (C and F) are presented. Green and blue represent elastin autofluorescence and DAPI fluorescence, respectively. Data are means ± SEM, n = 4 – 5. **P*<0.001 vs. Veh**, ‡***P***<0.05 vs. respective control, **§***P*<0.001 vs. Veh + Ang II, ǁ*P*<0.05 vs. WT T ♀ + Ang II, and **¶***P*<0.01 vs. Sf T ♀ + Ang II.

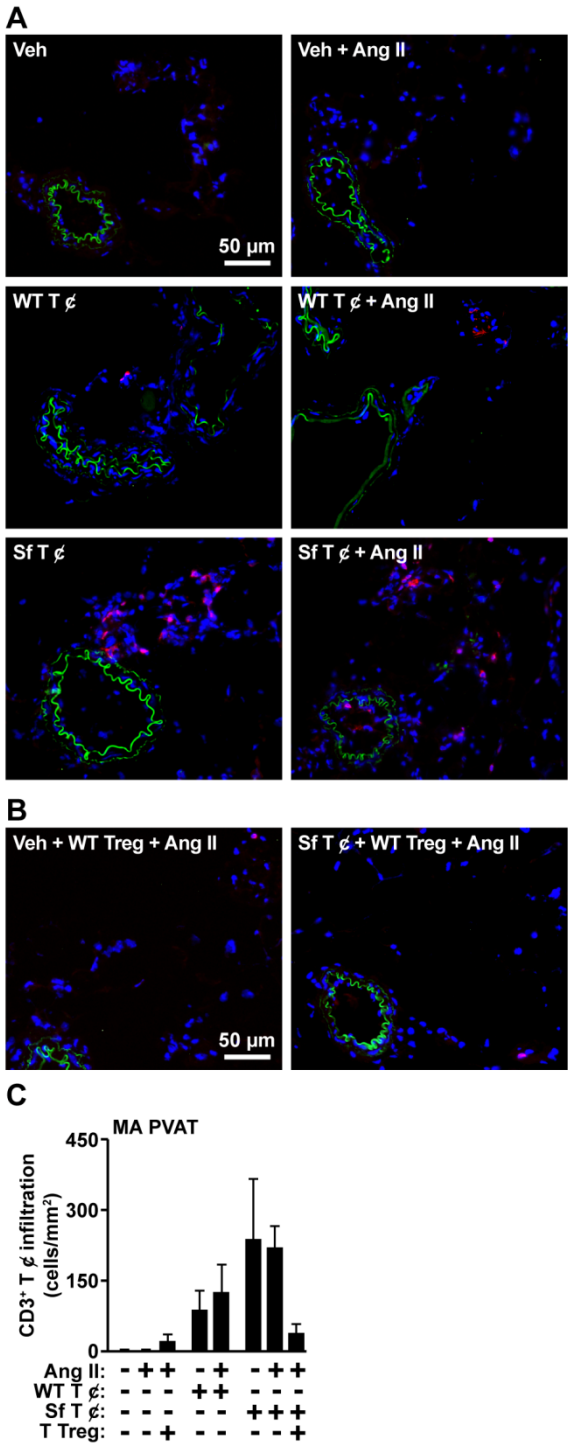

Figure IV-S6: $CD3^+$ cells (¢) infiltration status in mesenteric artery perivascular adipose tissue (PVAT). The number of $CD3^+$ ¢ was determined in the mesenteric artery PVAT of *Rag1*$^{-/-}$ mice injected with vehicle (Veh), 10^7 wild-type (WT) T

cells (♀) or Scurfy (Sf) T ♀, or 10^6 WT Treg alone or with Sf T ♀, and 2 weeks later were infused or not with Ang II for 14 days. Representative CD3 fluorescence (red) images (A and B) and quantification (C) are presented. Green and blue represent elastin autofluorescence and DAPI fluorescence, respectively. Data are means ± SEM, n = 4-5.

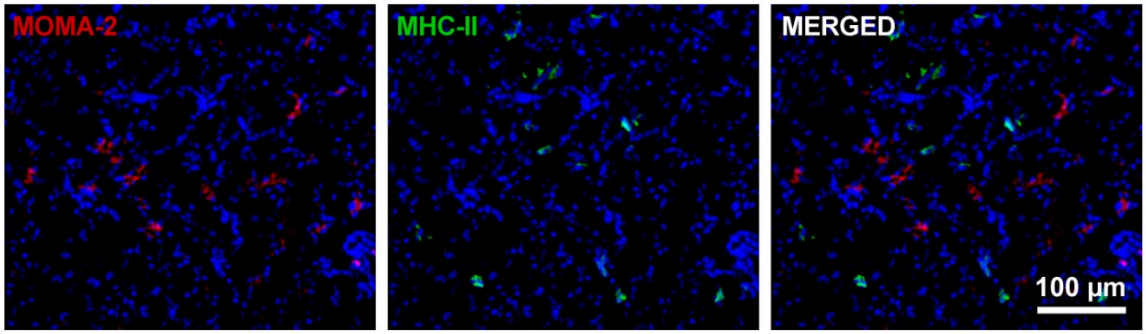

Figure IV-S7: Infiltrating monocyte/macrophages in the renal cortex had very low expression of major histocompatibility complex class II (MHC-II),a marker of classical activation. The proportion of MHC-II expressing monocytes/macrophages (MOMA-2) infiltrating the mesenteric artery PVAT was determined in *Rag1*$^{-/-}$ mice injected with vehicle (Veh), 10^7 wild-type (WT) T cells (♀) or Scurfy (Sf) T ♀, or 10^6 WT Treg alone or with Sf T ♀, and 2 weeks later were infused or not with Ang II for 14 days. Representative immunofluorescence images of mesenteric arteries co-staining with MOMA-2 (in red) and MHC-II (in green) are presented as independent and merged images. Blue represents DAPI fluorescence. n = 4 – 5.

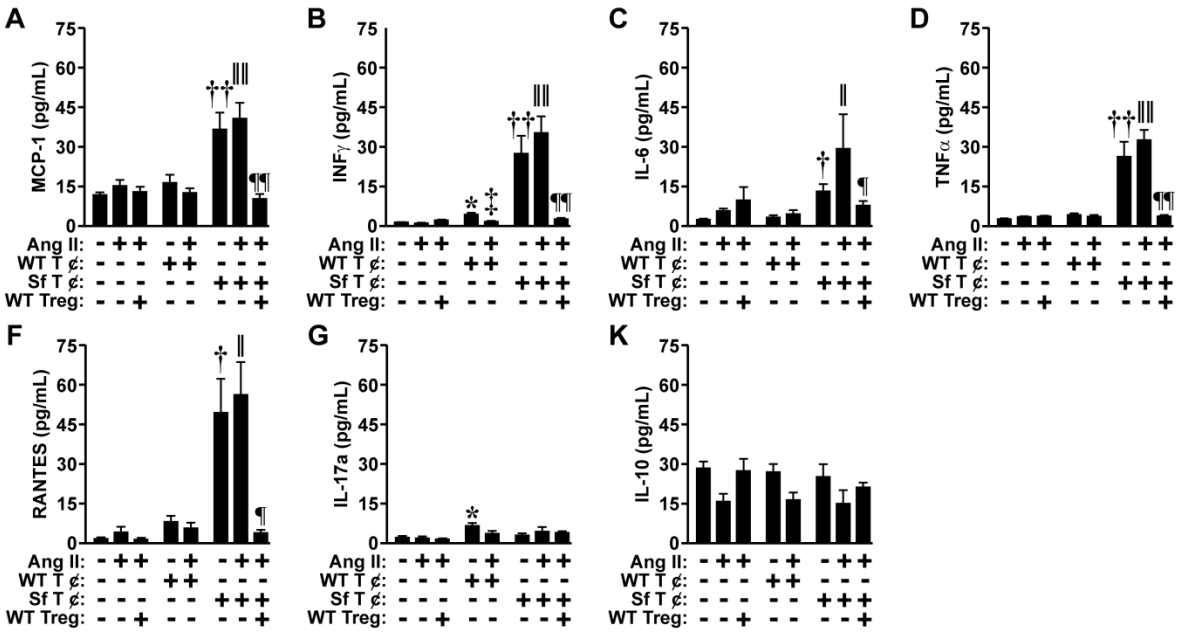

Figure IV-S8: Adoptive transfer of Treg-deficient Scurfy (Sf) T cells increased plasma levels of pro-inflammatory cytokines, which were not affected by Ang II treatment but prevented by co-transfer of wild-type (WT) Treg. Plasma levels of pro-inflammatory cytokines MCP-1 (A), interferon γ (INFγ, B), interleukin (IL)-6 (C), tumor necrosis factor α (TNFα, D), regulated on activation, normal T cell expressed and secreted (RANTES, E), and IL-17a (F), and anti-inflammatory cytokine IL-10 were measured using micro-bead multiplex immunoassays in *Rag1*$^{-/-}$ mice injected with vehicle (Veh), 10^7 WT T cells (¢) or Sf T ¢, or 10^6 WT Treg alone or with Sf T ¢, and 2 weeks later were infused or not with Ang II for 14 days. Data are means ± SEM, n = 5 – 10. ∗*P*<0.05 vs. Veh, †*P*<0.05 and ††*P*<0.001 vs. WT T ¢, ‡*P*<0.05 vs. respective control, ‖*P*<0.01 and ‖‖*P*<0.001 vs. WT T ¢ + Ang II, and ¶*P*<0.05 and ¶¶*P*<0.001 vs. Sf T ¢ + Ang II.

CHAPTER V: Discussion and conclusion

10. Discussion

In this thesis, we have investigated dysregulation of immune-inflammatory responses during ET-1 exaggerated atherosclerosis and Ang II-induced HTN in relation to vascular damage. First, using a model of endothelium-restricted ET-1 overexpression in HFD-fed *Apoe*$^{-/-}$ mice, we demonstrate that pro-oxidant and inflammatory mechanisms mediated by ET-1 worsen the progression of atherosclerosis and contributes to the pathogenesis of AAAs. ET-1 overexpression exaggerated aortic immune cell infiltration and oxidative stress, spleen pro-inflammatory monocytes, and expression of MMP-2 in the plaques. Second, using the same mouse model, we show that ET-1 overexpression results in remodeling of endothelial signaling pathways and potassium channels mediating endothelium-dependent relaxation. Although this remodeling preserved endothelial function, we propose that it may in fact represent loss of normal regulation of endothelium-dependent relaxation in resistance arteries in an atherosclerosis-prone state. Last, using T-and-B-cell deficient *Rag1*$^{-/-}$ mice adoptively transferred with wild-type or FOXP3-deficient T cells, we show that Ang II-induced microvascular inflammation and damage is enhanced in the absence of Treg, thereby unambiguously demonstrating the vascular protective role of Treg during HTN.

Vasoactive peptides such as Ang II and ET-1 can contribute to vascular inflammatory responses and damage, and have been implicated in the progression of both atherosclerosis and HTN. Vascular inflammation is a common element implicated in the vascular pathophysiology of atherosclerosis and HTN. The vascular inflammatory responses occurring during atherosclerosis and HTN are similar in many ways. However, certain distinctions are unique to each condition. This section will attempt to discuss the vascular immune-inflammatory responses that occur during atherosclerosis and HTN, in context of the findings of the studies presented and the literature review, and to comment on the similarities and differences between the two pathologies.

10.1 Vascular inflammation in atherosclerosis

Classically, the endothelial denuding injury model was used to describe atherosclerosis as a bland collection of cholesterol in the arterial wall complicated by VSMC proliferation and extracellular matrix deposition [446]. This cellular model extended Virchow's simplistic model of atherosclerosis as a passive arterial deposition of lipid debris in response to injury. Subsequent studies identified immune cells within atherosclerotic plaques to implicate immune-inflammatory mechanisms in the process of atherogenesis [447]. More recently, gene-targeting has allowed scientists to identify roles for particular immune cell subsets and inflammatory mediators in the pathogenesis and progress of atherosclerosis.

Several triggers of inflammation have been identified in atherogenesis that are also risk factors for atherosclerosis. The oxidation hypothesis is described most in the literature, according to which modified LDL are retained within the intima and become antigenic to induce adhesion molecule and chemokine expression, monocyte infiltration and activation of T cells, thereby promoting vascular inflammation [448]. Indeed, plasma LDL was increased in all atherosclerosis-prone *Apoe*$^{-/-}$ mice fed an HFD in our first and second studies, which could have been deposited and modified *in vivo*, and there was higher vascular inflammation and plaque formation in these mice compared to mice that did not have deletion of Apoe. Although the oxidation hypothesis is supported very well by experimental evidence, its relevance to human atherosclerosis is unclear, since the types of modified lipids and proteins isolated from human atheroma do not parallel those that have been formed in an *in vitro* setting and linked to inflammation, or have been implicated in animal models [448]. It is plausible that the different microenvironment in human atherosclerosis results in different modifications from what is observed in *in vitro* or *in vivo* animal studies. Therefore, in this regard, care must be taken when extrapolating experimental findings to humans. Other lipoproteins, such as VLDL and IDL, have also been shown to possess the potential to elicit inflammatory responses in the vascular

wall [449, 450]. These lipoproteins are increased in certain dyslipidemic conditions and in obesity.

Diabetes is another potent trigger of inflammation since the diabetic state promotes oxidative stress [451], and the hyperglycemia associated with diabetes leads to modification of macromolecules, for example via the formation of advanced glycation end products (AGE) [452]. Proteins modified by AGE can augment inflammatory pathways in ECs. Factors classically associated with HTN, such as Ang II and ET-1, can also stimulate vascular inflammation and thereby promote atherogenesis. Inflammation is therefore the link between atherosclerosis and these other diseases.

10.1.1 Endothelin-1, inflammation and atherosclerosis

Clinical and experimental data have implicated ET-1 in the progression of atherosclerosis and AAA formation. In the first study, we found that overexpression of ET-1 in HFD-fed *Apoe*$^{-/-}$ mice exaggerated development of atherosclerotic plaques in the aortic sinus and ascending aorta, and induced the formation of AAAs. This was associated with increased vascular and perivascular infiltration of monocyte/macrophages and $CD4^+$ T cells. Although the percentage of plaque monocyte/macrophage infiltration by area was equally high in the HFD-fed eET-1/*Apoe*$^{-/-}$ and *Apoe*$^{-/-}$ mice, the larger atherosclerotic plaques in eET-1/*Apoe*$^{-/-}$ mice means that these mice had more plaque monocyte/macrophages. Macrophages uptake modified LDL in the vascular wall to become foam cells, which leads to plaque development.

ET-1 can promote vascular inflammatory responses and contribute to plaque progression via several mechanisms. ET-1 enhances vascular permeability in part via the activation of ET_AR, a process that could facilitate the accumulation of LDL and immune cells in the vascular wall [453]. ET-1 antagonizes the apoptosis of VSMCs [454] and acts as a mitogen to stimulate proliferation of VSMCs [455], which further contributes to plaque progression. ET-1 can directly cause P-selectin-dependent leukocyte rolling and adhesion

[456]. In vessels from mice with endothelium-restricted overexpression of ET-1 (eET-1), the expression of MCP-1 and VCAM-1, infiltration of monocyte/macrophages, and activity of pro-inflammatory transcription factors NFκB and AP-1 was increased in a blood pressure-independent manner [97]. It has also been shown that ET-1 increases neutrophil attachment and production of platelet-activating factor to ET-1 stimulated human ECs [101]. In the first study, ET-1 overexpression in HFD-fed *Apoe*$^{-/-}$ mice exaggerated the increase in spleen pro-inflammatory Ly6C^{hi} monocytes, which could have contributed to increases in circulating Ly6C^{hi} monocytes, monocyte/macrophage infiltration, and atherosclerotic plaque progression and AAA formation. In hypercholesterolemic hamsters, ET_AR was shown to decrease the number and size of lipid-laden macrophages in atherosclerotic lesions, supporting a role for ET-1 signaling in promoting infiltration and lipid uptake by macrophages during atherosclerosis [457]. A role for CD4$^+$ T cell in atherosclerosis was previously demonstrated using T-andB-cell-deficient *Apoe*$^{-/-}$/*scid* mice, which had blunted plaque formation [239]. Adoptive transfer of CD4$^+$ T cells from *Apoe* $^{-/-}$ mice into immunodeficient *Apoe*$^{-/-}$/*scid* mice restored plaque development. Mechanisms of ET-1-induced T cell infiltration into the vasculature during atherosclerosis remain to be elucidated, although it is likely that those discussed above are involved.

In the first study, we observed that HFD-fed eET-1/*Apoe*$^{-/-}$ mice had elevated expression of MMP2 in the plaques. ET-1 is known to increase MMP2 expression in human osteosarcoma tissue [458] and in human optic nerve head astrocytes [459]. MMP2 is involved in extracellular matrix degradation and remodeling. Exaggerated plaque development and rupture, and AAA formation in HFD-fed eET-1/*Apoe*$^{-/-}$ mice could have been mediated in part by MMP2, perhaps produced by infiltrating macrophages. *Apoe*$^{-/-}$ mice deficient in MMP2 exhibit reduced severity of atherosclerosis [460]. It has also been shown that the processed active form of MMP2 is increased in AAA wall (PMID: 8691515). Mice knockout for MMP2 are resistant to aneurysm formation caused by abluminal application of calcium chloride [461]. Macrophage-derived MMP2 has been implicated in the progression of cerebral aneurysms [462].

Thus, the findings from the first study, supported by evidence from the literature, demonstrate that ET-1-induced vascular immune-inflammatory responses play a role in the progression of atherosclerosis and AAA formation.

10.2 Vascular inflammation in hypertension

The etiology of HTN is complex and multifactorial. Classically, the kidneys, the vasculature, and the central nervous system have all been implicated in the development of elevated blood pressure. The contribution of vascular inflammation has been underscored as a pivotal process in the development and progression of HTN. Increased expression of vascular adhesion molecules, infiltration of immune cells, and increased cytokine release and ROS production have been associated with activation of RAAS and ET-1 signaling systems in animal models of HTN. More recently, studies employing genetic or pharmacological targeting of various immune cells have supported a role for innate monocyte/macrophages and antigen-presenting dendritic cells and adaptive T cells in HTN and associated vascular damage.

Activation of the adaptive immune system during HTN suggests that antigen presentation by innate APCs occurs. However, the identity of antigens and how and when they are formed during HTN are issues that remain unresolved. It has been suggested that factors that cause HTN can induce neoantigen formation early on to lead to T cell activation [235, 463]. Neoantigens, or autoantigens, are endogenous molecules that undergo modifications such as oxidation, and are consequently no longer recognized as self by the host's immune system [463]. In this regard, Kirabo *et al.* [464] recently demonstrated that proteins oxidatively modified by the highly reactive isoketals accumulate during HTN and activate dendritic cells. Activated dendritic cells stimulate T cell proliferation and cytokine production to promote HTN.

The involvement of vascular inflammatory responses in the natural history of human HTN is unclear, although a model has been proposed based on experimental evidence [236, 465]. Hypertensive stimuli, which may include Ang

II, ET-1, aldosterone, salt and genes, may act directly on the vasculature or via enhanced sympathetic outflow through the activation of the central nervous system to cause minimal elevation of blood pressure. This can cause mild vascular injury, resulting in the formation of danger-associated neoantigens, which are recognized by innate cells. Subsequent immune-inflammatory responses mediated by activated innate and adaptive immunity results in enhanced ROS production and cytokine release, leading to vascular damage, end-organ damage and development of full-blown HTN. The process feeds positively to yield a low-grade chronic inflammatory response that progresses the disease. Activation of the innate immunity by pathogen-associated signals may also contribute to disease progression, as is observed in the case for periodontitis.

10.2.1 Angiotensin II, inflammation and hypertension

Ang II is a potent inducer of HTN and vascular inflammatory responses. The pro-inflammatory and mitogenic effects of Ang II in the vasculature are mediated mainly via the AT_1R. Ang II receptors are expressed on VSMCs, ECs, fibroblasts and on immune cells. Signaling mediated by Ang II stimulates expression of cytokines and adhesion molecules, ROS production and activates transcription factors NFκB and AP-1. Ang II receptor blockade was shown to eliminate VEGF-mediated enhancement of vascular permeability in mice [466], demonstrating a role for Ang II in mediating endothelial leakage. Both innate and adaptive immunity have been implicated in the progression of Ang II-induced hypertension. Previously it was shown that Ang II-induced HTN and vascular damage was blunted in MCSF-deficient mice, which have a generalized deficiency of macrophage subpopulations [222].

The role of adaptive T cells in the genesis of Ang II-induced HTN was first demonstrated by Guzik et al. [240], who showed that T-and-B-cell deficient *Rag1*$^{-/-}$ mice treated with Ang II have blunted rise in systolic and diastolic blood pressure; a phenotype corrected by the adoptive transfer of wild-type T cells. In

our third study, we partially corroborated these findings, since vehicle-injected *Rag1*$^{-/-}$ mice treated with Ang II had only blunted diastolic blood pressure rise. Alterations in gut microbiota have been shown to influence HTN in Dahl salt-sensitive rats [467]. Differences in environmental conditions that influence the intestinal microbiota may account in part for the discrepancy in our results and those of Guzik *et al*. Recently, it was shown that *Rag1*$^{-/-}$ mice treated with higher doses of Ang II had similar blood pressure rise compared to wild-type mice [468]. Thus, the pressor response of Ang II at higher doses is T cell-independent.

Ang II stimulates ROS production because it is a potent inducer of NADPH oxidase activity. Impaired vascular relaxation to acetylcholine is a manifestation of endothelial dysfunction caused by reduced NO bioavailability as a result of enhanced oxidative stress. In the third study, we showed that adoptive transfer of wild-type T cells into *Rag1*$^{-/-}$ mice increased Ang II-induced perivascular ROS production and tended to increase vascular ROS production, which could have contributed to the impaired microvascular relaxation observed in this group.

The role of T cell responses in Ang II-mediated vascular stiffness is unclear. In our study, Ang II treatment caused vascular stiffness in mesenteric arteries of *Rag1*$^{-/-}$ mice, which was blunted by adoptive transfer of wild-type T cells. Wu *et al.* [293] demonstrated that Ang II-induced aortic stiffness is T cell-dependent, since *Rag1*$^{-/-}$ mice treated with Ang II exhibited blunted aortic stiffness compared to wild-type mice. Differences in blood pressure elevation observed in *Rag1*$^{-/-}$ mice treated with Ang II and the type of vessel studied could account for the different results in both studies. Moreover, Treg contained within the T cell population could have counteracted the vascular stiffness, as was previously demonstrated [281]. *Rag1*$^{-/-}$ mice adoptively transferred with FOXP3-deficient T cells, which lack Treg, exhibited exaggerated Ang II-induced microvascular stiffness compared to mice injected with wild-type T cells. It is likely that inflammation and mechanical forces interplay to influence the stiffness of the vasculature during Ang II-induced HTN [293].

Pro-inflammatory cytokines play an important role in Ang II-induced HTN. Ang II stimulates vascular and immune cells to produce cytokines by activating

the transcription factor NFκB. Mice deficient in IL-6 [469] or TNF-α [470] do not develop HTN in response to Ang II. We did not observe an increase in plasma levels of pro-inflammatory cytokines IL6, IFN-γ and TNF-α in wild-type T cell-injected *Rag1*$^{-/-}$ mice treated with Ang II. However, their local levels in the vasculature could have been elevated.

Taken together, these data suggest that Ang II can directly mediate effects that initiate vascular inflammation, but propagation of vascular inflammatory responses by immune cells perhaps plays an important role in the development and progression of Ang II-induced HTN and end-organ damage.

10.3 Immune dysregulation in cardiovascular disease

The immune system consists of a repertoire of cells and subsets that perform specific functions. Inflammation is part of the normal healing process and is tightly regulated under physiological conditions. Activation and inflammatory phases are followed by a resolution phase. In atherosclerosis and HTN, chronic low-grade inflammation is observed, perhaps as a consequence of persistent stimuli, such as oxidized LDL, Ang II, and ET-1, and defective or diminished immunosuppressive capacity. Activation and pro-inflammatory polarization of monocyte/macrophages and of T cells is associated with the vascular pathologies of atherosclerosis and HTN.

10.3.1 Monocyte/macrophage infiltration and polarization in atherosclerosis and HTN

Monocyte/macrophages are implicated in the pathogenesis and progression of atherosclerosis and HTN. Vascular infiltration of monocyte/macrophage is observed in both pathologies. Whereas the phenotype of infiltrating monocyte has been somewhat characterized for atherosclerosis, our understanding of the role of various subsets of macrophages in atherosclerosis and HTN is rather limited.

In our model of ET-1-exaggerated atherosclerosis, we observed infiltration of monocyte/macrophages into plaques, and vascular and perivascular tissues and elevated levels of spleen pro-inflammatory Ly6C^{hi} monocytes in atherosclerosis-prone *Apoe*$^{-/-}$ mice, compared to wild-type and eET-1 mice that did not develop lesions. Exaggeration of atherosclerotic lesions and induction of AAA in eET-1/*Apoe*$^{-/-}$ mice, compared to *Apoe*$^{-/-}$ mice, was associated with greater number of infiltrating monocyte/macrophages detected in the vasculature and exaggerated increase in spleen Ly6C^{hi} monocytes. Ly6C^{hi}, or classically activated, monocytes are known to preferentially infiltrate the vascular wall during atherosclerosis, and differentiate into macrophages that possess an M1-like phenotype [220]. Increase in spleen Ly6C^{hi} monocytes in our study could have been reflective of increased circulating Ly6C^{hi} monocytes, which contribute to atherosclerosis development in *Apoe*$^{-/-}$ mice, and further exaggeration and AAA formation in eET-1/*Apoe*$^{-/-}$ mice. Evidence suggests that Ly6C^{+} monocytes are precursors to M1-type macrophages in tissues [213, 216, 217]. Thus, in our study, exaggeration of atherosclerosis and AAA formation in eET-1/*Apoe*$^{-/-}$ mice could have been due to elevated M1-like polarization of vascular macrophages derived from circulating Ly6C^{hi} monocytes. Macrophage polarization during atherosclerosis is not well understood. Atherosclerotic lesion macrophages in experimental studies express markers for all polarization states [220], but M1 polarization has been previously shown to predominate over M2 polarization [471, 472]. M1 and M2 macrophages coexist in human atheroma [473], and it is possible that progression of atherosclerosis occurs due to imbalance in the opposing roles of these states. Ang II-induced AAA formation in Apoe-/- mice was shown to be associated with increased expression of M1 marker and decreased expression of M2 marker in infiltrated macrophages [474]. Pharmacological inhibition of Notch signaling prevented AAA progression and macrophage pro-inflammatory polarization.

In the third study, Ang II treatment did not alter infiltration or polarization of vascular monocyte/macrophage in vehicle- or wild-type T-cell-injected *Rag1*$^{-/-}$ mice. However, in mice injected with FOXP3-deficient T cells, which lack Treg,

Ang II increased monocyte/macrophage infiltration in the vasculature and the kidney. Furthermore, infiltrating monocyte/macrophages exhibited elevated expression of M1 marker iNOS, and in the case for kidney monocyte/macrophages decreased expression of M2 marker Arg1. Thus, in the absence of Treg, Ang II not only increased monocyte/macrophage infiltration but also pro-inflammatory polarization. Ang II-induced M1 polarization in infiltrating monocytes/macrophages might be mediated via AT_1R expressed on monocytes/macrophages. Transplantation of bone marrow from Agtr1a/Apoe double knockout mice to *Apoe*$^{-/-}$ mice prevented renal injury-induced atherosclerosis by polarizing the macrophage phenotype to less M1 and more M2 [475].

This data show that monocyte/macrophages not only home to the vasculature during atherosclerosis and HTN, but exhibit altered phenotypes that are more pro-inflammatory. The switch in monocyte/macrophage phenotype is likely related to progression of vascular damage in both diseases.

10.3.2 T effector cells in atherosclerosis and HTN

$CD4^+$ T effector cells include Th1, Th2, and Th17 subsets. Atherosclerosis and HTN has been associated with imbalance in T effector subsets towards a more Th1 polarized response. Th1 cells produce pro-inflammatory cytokines IFN-γ, IL-2, TNF-α and TNF-β, and participate in cell-mediated defense against intracellular microorganisms, macrophage activation, and suppression of Th2 response [236].

In our atherosclerosis study, $CD4^+$ T cell infiltration was detected in the ascending aorta plaque of only one *Apoe*$^{-/-}$ mouse. The frequency of $CD4^+$ T cell infiltration was increased in eET-1/*Apoe*$^{-/-}$ group, and was detected in the perivascular tissue and plaque of both ascending and abdominal aorta. We did not characterize the relative proportions of T effector subsets in this study. However, we detected an increase in the percentage of activated $CD3^+CD4^+CD69^+$ in the spleen of *Apoe*$^{-/-}$ and *eET-1/Apoe*$^{-/-}$ mice, compared to

wild-type mice. CD69 is a generalized marker of activation, and does not differentiate T effector subsets. However, studies have shown that Th cells in atherosclerotic lesions polarize towards Th1 phenotype with increased IFN- γ and IL-2 production [244]. Atheroprotection in *Apoe*$^{-/-}$ mice mediated by B-cell depletion correlated with a decrease in percentage of spleen CD4^{+}CD69^{+} and IFN- γ producing CD4^{+} cells, and an increase in IL-17-producing CD4^{+} cells [476]. Thus, it could be postulated that activated spleen CD4^{+}CD69^{+} cells in *Apoe*$^{-/-}$ and eET-1/*Apoe*$^{-/-}$ mice polarize predominantly towards Th1 phenotype in our study.

Circulating levels of plasma pro-inflammatory cytokines have been previously used to characterize polarization of T cell responses [477-479]. In our model of Ang II-induced HTN, plasma pro-inflammatory cytokine levels were unaffected in vehicle-, Treg-, and wild-type T cell-injected *Rag1*$^{-/-}$ mice following Ang II treatment, compared to respective controls. *Rag1*$^{-/-}$ mice injected with FOXP3-deficient T cells, which lack Treg, exhibited significantly elevated levels of pro-inflammatory cytokines IFN- γ and TNF-α, reflective of a Th1-type response, indicating a role for Treg in suppressing T effector cells. Ang II tended to further increase the plasma levels of these cytokines. Cultured T cells isolated from Ang II-infused rats versus normotensive control rats have been shown to produce more IFN-γ and less IL-4, suggestive of polarization towards Th1 phenotype [247]. In the same study, the number of IFN-γ-secreting T cells was increased in Ang II-infused rats, an effect that was reversed by co-treatment with an angiotensin receptor blocker. Thus, Ang II is able to polarize T effectors towards a Th1 phenotype perhaps via its receptor on T cells. The lack of cytokine changes in wild-type T cell-injected *Rag1*$^{-/-}$ mice treated with Ang II could have been due to the fact that the number of CD3^{+} T cells adoptively transferred was insufficient to elicit a response in an immunodeficient model. Interestingly, we observed very low levels of circulating IL-17. This could be because mice on a C57Bl6/J background are a prototypical Th1-dominant strain [480].

10.3.3 T regulatory cells in atherosclerosis and HTN

Treg are anti-inflammatory cells that counteract the actions of other T cell subsets as well as cells of the innate immunity. The mechanisms of Treg action were described in chapter I section 7. Several studies support a role for FOXP3 as the master regulator of Treg development and function [254]. Evidence from our studies and the literature support the possibility the number and/or function of Treg are affected during atherosclerosis and HTN, and diminished Treg activity is associated with severity of vascular pathology.

In the first study, atherosclerosis development, enhanced vascular immune cell infiltration, and increased spleen activated T cells and $Ly6C^{hi}$ monocytes in *Apoe*$^{-/-}$ and eET-1/*Apoe*$^{-/-}$ groups occurred in parallel with increase in percentage of spleen $CD4^+CD25^+FOXP3^+$ Treg cells, compared to wild-type mice. The proportion of $CD3^+CD4^+FOXP3^+$ cells was increased in lymph nodes concomitantly with atherosclerosis development after 8 weeks of atherogenic diet in *Ldlr*$^{-/-}$ mice transplanted with DEREG bone marrow (but not injected with diphtheria toxin) [278]. In another study, Treg numbers were elevated with increasing age in *Apoe*$^{-/-}$ mice, but the suppressive ability of Treg was diminished [481]. Mor et al. showed that both the spleen number and functional suppressive properties of Treg were decreased in *Apoe*$^{-/-}$ mice fed a normal chow diet [276]. Together, these data suggest that Treg play a protective role in atherosclerosis. Decrease in Treg activity, either due to reduced numbers or functional suppressive capacity or both, occurs during atherosclerosis, which allows pro-inflammatory responses to persist and contribute to plaque progression and AAA development. Thus, in our atherosclerosis study, increased percentage of spleen Treg occurring in spite of plaque development and increased vascular and spleen inflammation was suggestive of impaired Treg function. It is also plausible that activated innate cells and effector T cells may have become resistant to the suppressive effects of Treg. Thus, in this situation, even a compensatory increase in Treg numbers would have been unable to control immune responses.

This evidence and previous studies from our lab prompted us to further explore the vascular protective role of Treg in a model of Ang II-induced HTN. We investigated the role of Treg by comparing Ang II-induced vascular inflammation and damage in T-and-B-cell-deficient *Rag1*$^{-/-}$ mice adoptively transferred with wild-type or FOXP3 (Scurfy, Sf)-deficient T cells, which lack Treg. Sf-injected *Rag1*$^{-/-}$ mice exhibited exaggerated Ang II responses compared to mice injected with wild-type T cells, including increased microvascular endothelial dysfunction, stiffness, and monocyte/macrophage infiltration. In addition to this, infiltrating monocyte/macrophage had elevated expression of M1 marker iNOS. Co-transfer of Sf T cells with $CD4^+CD25^+$ Treg, which contain a high proportion of $FOXP3^+$ cells, abrogated or prevented Ang II effects, demonstrating the protective role of Treg in suppressing innate and adaptive immune responses and regulating vascular damage during HTN. It should be noted that Ang II-induced blood pressure rise was delayed in *Rag1*$^{-/-}$ mice receiving co-transfer of Sf T cells and Treg, in contrast to mice injected with wild-type T cells where blood pressure rise was seen from onset of Ang II infusion. The additional protection observed in the mice receiving a co-transfer could be explained by reconstitution with higher proportion of Treg than normal. Indeed, although Sf T cells and Treg were adoptively transferred in a ratio observed normally, at the time of sacrifice the percentage of $CD3^+CD4^+FOXP3^+$ in co-transfer mice was almost twice as high than in wild-type T cell-injected *Rag1*$^{-/-}$ mice. Interestingly, adoptive transfer of Treg alone also reversed Ang II-induced blood pressure elevation and vascular stiffness that was observed in *Rag1*$^{-/-}$ mice injected with vehicle. This could have been due to suppressive actions of Treg on innate immune cells, which are present in *Rag1*$^{-/-}$ mice, or perhaps direct actions on the vasculature. Ang II treatment tended to decrease plasma level of anti-inflammatory cytokine IL-10 in all treatment groups, which was reversed when exogenous Treg were adoptively transferred. Systolic blood pressure, NADPH oxidase activity and endothelium-dependent relaxation was improved in AngII-infused *Il10*$^{-/-}$ mice receiving cultured Treg from control mice [285]. Thus, our

results and data from others support a protective role for Treg in Ang II-induced HTN via IL-10 production.

Altogether, our data and evidence from other studies suggest that the functional capacity of Treg is diminished during atherosclerosis and HTN, and this leads to dysregulated activation of pro-inflammatory responses that contributes to vascular damage and progression of the disease. Previously, adoptive transfer experiments suggested a protective role for Treg in atherosclerosis and HTN. However, these data did not rule out the possibility of a pharmacological effect of increasing Treg number, rather than the physiological role of Treg in the natural history of these diseases. Exacerbation of vascular pathology associated with atherosclerosis and HTN in the absence of Treg unambiguously demonstrate their vascular protective role. Further studies are required to understand how Treg become dysfunctional or effector cells become resistant to Treg suppression during the progression of atherosclerosis and HTN. A decrease in production of anti-inflammatory cytokines, such as IL-10, or expression of suppression molecules such as CTLA-4 by Treg might explain their reduced capacity to suppress effector immune cells.

10.4 Localization of vascular inflammation in atherosclerosis and HTN

A key difference in the vascular immune-inflammatory response observed in atherosclerosis and HTN is the localization of inflammation within the different regions of the arterial structure. The vascular inflammation during atherosclerosis development is canonically described using the popular “inside-out” theory, whereby infiltration of immune cells begins at the intima and progressively moves outwards [482]. Immune cell infiltration during atherosclerosis is observed in the vascular wall, plaque, and in the perivascular adipose tissue (PVAT). In contrast, vascular immune cell infiltration during experimental HTN has been predominantly reported in the adventitial and PVAT regions of the vasculature [240, 281]. The “outside-in” theory has been proposed to explain these

observations, which states that inflammation begins at the periphery of the vasculature and moves towards the vascular intima [482]. Possible sources of immune cell infiltration according to the “outside-in” theory could include the vasa vasorum in large arteries or the venous system in the case of resistance vasculature. Alternatively, immune cells residing in the periphery of vasculature could respond to stimuli and become activated and proliferate to participate in inflammatory responses. Localization of vascular immune cell infiltration in our models of ET-1 exaggerated atherosclerosis and Ang II-induced HTN was observed to be similar to the above-mentioned trends.

Recent studies have shown that vasa vasorum neovascularization and macrophage presence are increased in early atherosclerotic lesions [483-485], supporting a role for outside-in mechanisms in initiation of atherosclerotic disease. Descending aortae from *Apoe*$^{-/-}$ mice treated with granulocyte colony-stimulating factor or granulocyte macrophage colony-stimulating factor for 8 weeks exhibited increased adventitial vascularity and atherosclerotic lesion extent [486]. Thus, outside-in mechanisms are applicable also during atherosclerosis, and work in tandem with inflammatory responses arising from the intimal end. It has been proposed that adventitial inflammation during atherosclerosis may arise as a consequence of paracrine signaling from the dysfunctional endothelium activated by lipoproteins, nutrient starved SMCs, and chronic inflammation [482]. The different localization of vascular inflammation during atherosclerosis as a consequence of the contrasting mechanisms leading to it, compared to that in HTN, could explain how seemingly similar immune-inflammatory mechanisms can give rise to completely different vascular pathologies.

The role of PVAT in vascular pathologies has increasingly gained attention over the past decade or so. Previously, the knowledge of PVAT in vascular disease was limited since changes in the vascular wall were usually studied, and the PVAT was either removed or ignored during post-sacrifice experiments. In our atherosclerosis and HTN studies mentioned in this thesis, PVAT inflammation correlated with severity of vascular pathology. In a rodent model of

metabolic syndrome, perivascular adipose inflammation and oxidative stress was linked to resistance artery endothelial dysfunction (impaired EDR) and hypertrophic remodeling [487]. It could be speculated that pro-inflammatory adipocytokines, such as leptin and resistin, released by PVAT could participate in vacular inflammatory responses. Resistin can stimulate ECs to express VCAM-1, ICAM-1, MCP-1 and ET-1, and also induce production of pro-inflamatory cytokines IL-1, IL-6, IL-12, and TNF-α in several cell types [488]. Leptin can stimulate pro-inflammatory signaling pathways including ERK1/2 and Akt/PKB, and induce ROS generation by the mitochondria [488, 489]. However, under physiological conditions, PVAT is known to mediate important protective functions. Indeed, it was recently demonstrated that the thermogenic capacity of PVAT plays an important protective role in the pathogenesis of atherosclerosis [490]. Loss of PVAT due to VSMC PPARγ deletion in mice impaired thermogenic activity, temperature regulation, and endothelial function. *Apoe*$^{-/-}$ mice with VSMC PPARγ deletion exhibited atherosclerosis when exposed to cold temperatures as a consequence of impaired lipid handling. PVAT is a source of prostacyclin, which protects against endothelial dysfunction, and the adipocytokine adiponectin, which has potent anti-inflammatory and anti-atherogenic properties [491].

10.5 ROS in atherosclerosis and HTN

The vascular pathology of atherosclerosis and HTN is associated with enhanced vascular ROS production. Under physiological conditions, ROS production is countered by enzymes and agents that scavenge ROS, which include SODs, catalase, glutathione and thioredoxin. Increased ROS could occur as a result of increased production or decreased anti-oxidant capacity as a consequence of impaired scavenging system. ROS can regulate tone, promote vascular remodeling, and enhance inflammation via several mechanisms [340]. In our models of ET-1-exaggerated atherosclerosis and Ang II-induced HTN, the

severity of vascular pathology correlated with ROS production in vascular and perivascular tissues.

Both vascular and immune cells can contribute to ROS production. However, in our model of Ang II-induced HTN, immune cell infiltration was detected only in PVAT regions, whereas ROS production was observed in both the vascular wall and the PVAT. Thus, in this model, it is possible that ROS production in the vascular wall was predominantly derived from VSMCs. There are several sources of ROS which have been implicated in the pathophysiology of atherosclerosis and HTN, including NADPH oxidase, xanthine oxidase and the mitochondria. We did not investigate the sources of vascular and perivascular ROS in our studies. Previously, NADPH oxidase has been repeatedly been demonstrated to be the main source of ROS in Ang II-induced HTN [207]. The source of ET-1-induced ROS production during atherosclerosis remains to be investigated. In eET-1 mice, vascular oxidative stress and NADPH oxidase activity was shown to be increased [224]. However, in hypertensive rats associated with an activated ET-1 system, it was demonstrated that $\bullet O_2^-$ is derived from XO and mitochondrial oxidative enzymes in an ET_AR-dependent manner [362].

10.6 Endothelial dysfunction: a common denominator in atherosclerosis and hypertension

HTN is an independent risk factor for atherosclerosis. Indeed, vascular inflammation is a commonality in both pathologies. However, as discussed previously, immune cell infiltration in HTN is observed mostly in the perivascular tissues, whereas in atherosclerosis, immune cells are detectible in the PVAT, vascular wall and in the plaque. Endothelial dysfunction is implicated in both atherosclerosis and HTN, and may represent the common link between these vascular pathologies. Dysfunctional endothelium is characterized by a shift towards a vasoconstrictive, pro-inflammatory, and pro-thrombotic state. Enhanced oxidative stress and consequently reduced NO bioavailability are the

main mechanisms underlying endothelial dysfunction. In our studies, we investigated endothelial dysfunction as impairment of vasodilatory response to acetylcholine.

Consistent with the literature, in our second study, mesenteric arteries from atherosclerosis-prone, HFD-fed *Apoe*$^{-/-}$ mice exhibited impaired EDR compared to wild-type mice. This was consistent with the findings from the first study in which we observed higher ROS production in the vasculature of HFD-fed *Apoe*$^{-/-}$ mice versus in wild-type mice, although these observations were made in aortic tissue. *Apoe*$^{-/-}$ mice fed a normal diet also exhibited a certain degree of impaired EDR, albeit less than those fed an HFD, suggesting that these mice already had decreased production of or sensitivity to NO, or increased oxidative stress at baseline.

Given that endothelial ET-1 overexpression in HFD-fed *Apoe*$^{-/-}$ mice exaggerated atherosclerosis development and vascular ROS production, we expected a worsening of microvascular dysfunction in eET1/*Apoe*$^{-/-}$ compared to *Apoe*$^{-/-}$ mice. Interestingly, ET-1 overexpression in *Apoe*$^{-/-}$ mice resulted in remodeling of endothelial signaling pathways and potassium channels, which unexpectedly presented itself as preserved EDR. Mesenteric arteries from *Apoe*$^{-/-}$ have been previously shown to be more sensitive to endothelium-dependent vasodilators compared to wild-type mice [443]. Thus, it is possible that under certain experimental conditions, vessel from mice predisposed to hyperlipidemia may develop enhanced endothelium-dependent reactivity perhaps as a consequence of uncovering or establishment of signaling pathways that are not normally required to mediate EDR. For example, in our studies, excess superoxide production in eET-1/*Apoe*$^{-/-}$ mice could have resulted in formation of H_2O_2 that is known to be involved in EDR [492]. It should be noted that the preservation of EDR observed in eET-1/*Apoe*$^{-/-}$ mice does not necessarily mean that endothelial dysfunction in these animals is reversed or normalized. In our first study, we observed exaggerated vascular inflammation in HFD-fed eET-1/*Apoe*$^{-/-}$ compared to *Apoe*$^{-/-}$ mice, suggestive of enhanced endothelial cell activation and dysfunction. Thus, this situation may represent a “pseudo-normal”

condition whereby there is in fact loss of normal regulation of endothelium-dependent relaxation and vascular resistance in an atherosclerotic setting. The importance of this paradoxical finding within the pathology of atherosclerosis remains to be further investigated.

Endothelial dysfunction has been implicated in Ang II-induced HTN. In the third study, we observed that Ang II impaired EDR in wild-type T cell-injected *Rag1*$^{-/-}$ mice, with a concomitant increase in perivascular ROS production and tendency of increase in vascular ROS production. Mice injected with FOXP3-deficient T cells exhibited exaggerated impairment of EDR and increase in vascular and perivascular ROS production. Thus, in our model of Ang II-induced HTN, impaired EDR paralleled increase in vascular oxidative stress. It has been previously shown that Ang II, but not NE, infusion in rats impairs EDR to acetylcholine by enhancing vascular NADPH oxidase activity and superoxide production, despite producing a similar degrees of HTN [493]. Therefore, in context of HTN, impairment of EDR is blood pressure-independent and vascular inflammation-dependent.

Infusion of Ang II has been shown to promote lesion and AAA formation in *Apoe*$^{-/-}$ mice independently of alterations in blood pressure levels or serum cholesterol concentrations [494]. In the first study, ET-1 overexpression in the endothelium of HFD-fed *Apoe*$^{-/-}$ mice exaggerated atherosclerosis progression and induced AAA formation compared to HFD-fed *Apoe*$^{-/-}$ mice, despite having similar LDL levels and blood pressure. In the second study, eET-1 mice fed an HFD presented with impaired EDR compared to HFD-fed wild-type mice, indicating a role for ET-1 signaling in promoting endothelial dysfunction in HFD-fed conditions. Thus, factors normally associated with HTN may promote vascular inflammation and facilitate the development of atherosclerosis and AAA in susceptible regions of the vasculature by contributing to endothelial dysfunction.

11. Conclusion

Vascular inflammatory responses are important players in the vascular pathology of both atherosclerosis and HTN. Based on the literature review and the studies presented in this thesis, it appears that immune-inflammatory responses are not only activated by enhanced vasoactive peptide signaling during both vascular pathologies but also dysregulated, as indicated by impaired regulatory functions of Treg and anti-inflammatory mediators. This perhaps allows the low-grade inflammation to become chronic, thereby consistently contributing to vascular damage and progression of both diseases. Similar vascular immune-inflammatory responses are observed during atherosclerosis and HTN. Endothelial dysfunction, immune cell infiltration, activation and polarization, and enhanced oxidative stress are common mechanisms occurring during both vascular pathologies. However, the composition and localization of immune-inflammatory responses in different regions of the vascular wall is very different in atherosclerosis and HTN, which perhaps results in the contrasting vascular pathologies attributable to each disease but that still contributes to risk for the development of CVD. In this regard, understanding the establishment of vascular immune-inflammatory responses during atherosclerosis and HTN may provide insight into how these contrasting vascular pathologies arise from similar mechanisms.

12. Limitations

A limitation to the use of the transgenic mice constitutively overexpressing endothelial ET-1 in the first and second studies is that these mice presented a greater increase in plasma levels of ET-1 than what has been observed in humans with atherosclerosis or aneurysms. Although we believe that achieving greater increase in ET-1 expression allowed us to reveal the underlying pathophysiological mechanisms by which ET-1 contributes to the development of atherosclerosis and aneurysms, it is possible that such levels could have had

some non-physiological effects. In the third study, *Rag1*$^{-/-}$ mice were injected with similar numbers of wild-type or FOXP3-deficeint T cells, which lack Treg. However, at the time of sacrifice, mice injected with FOXP3-deficient T cells tended to have greater reconstitution of $CD3^+$ T cells in the spleen. This was not unexpected since in the absence of the immunosuppressive actions of $FOXP3^+$ Treg there is an increase in the proliferation of T effector subsets. The tendency of greater reconstitution could have contributed in part to the exaggerated Ang II responses observed in *Rag1*$^{-/-}$ mice injected with FOXP3-deficient T cells. Nevertheless, to confirm the protective role of Treg, we studied Ang II responses in *Rag1*$^{-/-}$ mice co-transferred with FOXP3-deficient T cells and Treg. In the third study only, we demonstrated using immunofluorescence that M1 marker iNOS was increased in infiltrating monocyte/macrophages in FOXP3-deficient T cell-injected *Rag1*$^{-/-}$ mice treated with Ang II. However, technical and expertise limitations prevented us from fully exploring the polarization of monocyte/macrophages and T effector subsets in the vasculature in our studies using flow cytometry, which is the gold standard for characterizing cell phenotypes. Characterization of immune cell subsets in the vasculature, and not only in the spleen, would allow us to better understand the role of each subset in relation to the vascular pathology in atherosclerosis and HTN. Moreover, it would be interesting to separately study in *in vitro* experiments the effects of specific stimuli, such as Ang II or ET-1, on the polarization and function of monocyte/macrophages and T cells. Finally, while we observed increased ROS to be related to the vascular pathology of atherosclerosis and HTN, we did not further explore the sources of ROS production in our studies.

13. Perspectives

Animal models are used to better understand the pathogenesis of human atherosclerosis and HTN. We found that elevated levels of circulating ET-1 is associated with enhanced progression of atherosclerosis and induction of AAA formation in hyperlipidemic conditions, finding that is relevant to human

atherosclerosis. In addition, we identified pro-oxidant and pro-inflammatory mechanisms as the basis for ET-1-mediated exaggeration of atherosclerosis that could be extrapolated to human atherosclerosis. Our results provide a mechanistic insight as to why specific ET_AR or mixed $ET_{A/B}R$ inhibitors blunt progression of experimental atherosclerosis [131-134], and advocate for the use of these drugs in the treatment of human atherosclerosis and AAA. Enhanced vascular immune-inflammatory responses are a consistent feature in experimental and human atherosclerosis and HTN, and suggestive of impaired regulation of inflammation. Diminished Treg functional capacity has been reported in experimental atherosclerosis, and the protective role of Treg in experimental atherosclerosis and HTN was demonstrated using an adoptive transfer protocol. We demonstrated mechanistically a protective role for Treg contained within the T cell population in limiting HTN and vascular damage by studying Ang II responses in the absence of $FOXP3^+$ Treg. The number of circulating Treg was decreased [495] and the induction of peripheral Treg was shown to be impaired [496] in patients suffering from preeclampsia, which involves Ang II-mediated mechanisms [497]; evidence that provides clinical relevance for a protective role of Treg in human HTN.

HTN is a risk factor for atherosclerosis, and vice versa. Evidence presented in this thesis and from the literature support a common role of dysregulated vascular immune-inflammatory responses in the progression of both diseases. Classical strategies employed for the treatment of atherosclerosis (statins) and HTN (ACE inhibitors and ARBs) have been shown to exert their effect in part via their anti-inflammatory actions [498]. The identification and use of anti-inflammatory or immune-modulation approaches are attractive possibilities for the treatment of atherosclerosis and HTN, especially in patients where these diseases co-exist. An example that highlights this is that patients with inflammatory disorders, such psoriaris, develop elevated blood pressure that can be lowered by immunosuppressive treatment. Clinical trials using anti-oxidant agents such as vitamins C and E have to date failed to report positive effect on the control of atherosclerosis [499] or HTN [500], although this may be due to the

fact that these trials did not last long enough. Further trials of non-steroidal anti-inflammatory drugs or macrolides (antibiotics) are underway. Moreover, elevated inflammatory mediators can be used to determine the risk for the development of cardiovascular pathologies, and perhaps identify patients who may benefit from early intervention strategies. Indeed, levels of C-reactive protein, a marker of acute inflammation, have been shown to associate with prevalent and incident hypertension, and predict risk for atherosclerotic cardiovascular disease [501, 502].

References

1. Mortality GBD, Causes of Death C. Global, regional, and national age-sex specific all-cause and cause-specific mortality for 240 causes of death, 1990-2013: a systematic analysis for the Global Burden of Disease Study 2013. Lancet. 2014.

2. Alexander RW. Theodore Cooper Memorial Lecture. Hypertension and the pathogenesis of atherosclerosis. Oxidative stress and the mediation of arterial inflammatory response: a new perspective. Hypertension. 1995; 25 (2):155-61.

3. Barton M, Traupe T, Haudenschild CC. Endothelin, hypercholesterolemia and atherosclerosis. Coronary artery disease. 2003; 14 (7):477-90.

4. Schiffrin EL. Vascular endothelin in hypertension. Vascular pharmacology. 2005; 43 (1):19-29.

5. Wagenseil JE, Mecham RP. Vascular extracellular matrix and arterial mechanics. Physiological reviews. 2009; 89 (3):957-89.

6. Aird WC. Phenotypic heterogeneity of the endothelium: II. Representative vascular beds. Circulation research. 2007; 100 (2):174-90.

7. Aird WC. Phenotypic heterogeneity of the endothelium: I. Structure, function, and mechanisms. Circulation research. 2007; 100 (2):158-73.

8. Thurston G, Baldwin AL, Wilson LM. Changes in endothelial actin cytoskeleton at leakage sites in the rat mesenteric microvasculature. The American journal of physiology. 1995; 268 (1 Pt 2):H316-29.

9. Martinez-Lemus LA. The dynamic structure of arterioles. Basic & clinical pharmacology & toxicology. 2012; 110 (1):5-11.

10. Jackson WF. Ion channels and vascular tone. Hypertension. 2000; 35 (1 Pt 2):173-8.

11. O'Connell MK, Murthy S, Phan S, Xu C, Buchanan J, Spilker R, et al. The three-dimensional micro- and nanostructure of the aortic medial lamellar unit measured using 3D confocal and electron microscopy imaging. Matrix biology : journal of the International Society for Matrix Biology. 2008; 27 (3):171-81.

12. Stenmark KR, Davie N, Frid M, Gerasimovskaya E, Das M. Role of the adventitia in pulmonary vascular remodeling. Physiology. 2006; 21:134-45.

13. Burton AC. Relation of structure to function of the tissues of the wall of blood vessels. Physiological reviews. 1954; 34 (4):619-42.

14. Haurani MJ, Pagano PJ. Adventitial fibroblast reactive oxygen species as autacrine and paracrine mediators of remodeling: bellwether for vascular disease? Cardiovascular research. 2007; 75 (4):679-89.

15. Di Wang H, Ratsep MT, Chapman A, Boyd R. Adventitial fibroblasts in vascular structure and function: the role of oxidative stress and beyond. Canadian journal of physiology and pharmacology. 2010; 88 (3):177-86.

16. Eble JA, Niland S. The extracellular matrix of blood vessels. Current pharmaceutical design. 2009; 15 (12):1385-400.

17. Wang M, Kim SH, Monticone RE, Lakatta EG. Matrix Metalloproteinases Promote Arterial Remodeling in Aging, Hypertension, and Atherosclerosis. Hypertension. 2015.

18. van den Akker J, Schoorl MJ, Bakker EN, Vanbavel E. Small artery remodeling: current concepts and questions. Journal of vascular research. 2010; 47 (3):183-202.

19. Intengan HD, Schiffrin EL. Structure and mechanical properties of resistance arteries in hypertension: role of adhesion molecules and extracellular matrix determinants. Hypertension. 2000; 36 (3):312-8.

20. Jacob MP. Extracellular matrix remodeling and matrix metalloproteinases in the vascular wall during aging and in pathological conditions. Biomedicine & pharmacotherapy = Biomedecine & pharmacotherapie. 2003; 57 (5-6):195-202.

21. Debelle L, Tamburro AM. Elastin: molecular description and function. The international journal of biochemistry & cell biology. 1999; 31 (2):261-72.

22. Rosenbloom J, Abrams WR, Mecham R. Extracellular matrix 4: the elastic fiber. FASEB journal : official publication of the Federation of American Societies for Experimental Biology. 1993; 7 (13):1208-18.

23. Wolinsky H, Glagov S. Structural Basis for the Static Mechanical Properties of the Aortic Media. Circulation research. 1964; 14:400-13.

24. Roach MR, Burton AC. The reason for the shape of the distensibility curves of arteries. Canadian journal of biochemistry and physiology. 1957; 35 (8):681-90.

25. Mayne R. Collagenous proteins of blood vessels. Arteriosclerosis. 1986; 6 (6):585-93.

26. Chothia C, Jones EY. The molecular structure of cell adhesion molecules. Annual review of biochemistry. 1997; 66:823-62.

27. Labat-Robert J. Cell-matrix interactions, alterations with aging, involvement in angiogenesis. Pathologie-biologie. 1998; 46 (7):527-33.

28. Chistiakov DA, Sobenin IA, Orekhov AN. Vascular extracellular matrix in atherosclerosis. Cardiology in review. 2013; 21 (6):270-88.

29. Lakatta EG. The reality of aging viewed from the arterial wall. Artery research. 2013; 7 (2):73-80.

30. Johnson JL. Matrix metalloproteinases: influence on smooth muscle cells and atherosclerotic plaque stability. Expert review of cardiovascular therapy. 2007; 5 (2):265-82.

31. Wang M, Jiang L, Monticone RE, Lakatta EG. Proinflammation: the key to arterial aging. Trends in endocrinology and metabolism: TEM. 2014; 25 (2):72-9.

32. Fleenor BS, Marshall KD, Durrant JR, Lesniewski LA, Seals DR. Arterial stiffening with ageing is associated with transforming growth factor-beta1-related changes in adventitial collagen: reversal by aerobic exercise. The Journal of physiology. 2010; 588 (Pt 20):3971-82.

33. Jiang L, Zhang J, Monticone RE, Telljohann R, Wu J, Wang M, et al. Calpain-1 regulation of matrix metalloproteinase 2 activity in vascular smooth muscle cells facilitates age-associated aortic wall calcification and fibrosis. Hypertension. 2012; 60 (5):1192-9.

34. Lemarie CA, Paradis P, Schiffrin EL. New insights on signaling cascades induced by cross-talk between angiotensin II and aldosterone. Journal of molecular medicine. 2008; 86 (6):673-8.

35. Munzel T, Sinning C, Post F, Warnholtz A, Schulz E. Pathophysiology, diagnosis and prognostic implications of endothelial dysfunction. Annals of medicine. 2008; 40 (3):180-96.

36. Stamler JS, Singel DJ, Loscalzo J. Biochemistry of nitric oxide and its redox-activated forms. Science. 1992; 258 (5090):1898-902.

37. Duran WN, Breslin JW, Sanchez FA. The NO cascade, eNOS location, and microvascular permeability. Cardiovascular research. 2010; 87 (2):254-61.

38. Boo YC, Hwang J, Sykes M, Michell BJ, Kemp BE, Lum H, et al. Shear stress stimulates phosphorylation of eNOS at Ser(635) by a protein kinase A-dependent mechanism. American journal of physiology Heart and circulatory physiology. 2002; 283 (5):H1819-28.

39. Yoshizumi M, Perrella MA, Burnett JC, Jr., Lee ME. Tumor necrosis factor downregulates an endothelial nitric oxide synthase mRNA by shortening its half-life. Circulation research. 1993; 73 (1):205-9.

40. Arnold WP, Mittal CK, Katsuki S, Murad F. Nitric oxide activates guanylate cyclase and increases guanosine 3':5'-cyclic monophosphate levels in various tissue preparations. Proceedings of the National Academy of Sciences of the United States of America. 1977; 74 (8):3203-7.

41. Loscalzo J, Welch G. Nitric oxide and its role in the cardiovascular system. Progress in cardiovascular diseases. 1995; 38 (2):87-104.

42. Maclouf J, Folco G, Patrono C. Eicosanoids and iso-eicosanoids: constitutive, inducible and transcellular biosynthesis in vascular disease. Thrombosis and haemostasis. 1998; 79 (4):691-705.

43. Moncada S, Vane JR. Prostacyclin and its clinical applications. Annals of clinical research. 1984; 16 (5-6):241-52.

44. Triggle CR, Dong H, Waldron GJ, Cole WC. Endothelium-derived hyperpolarizing factor(s): species and tissue heterogeneity. Clinical and experimental pharmacology & physiology. 1999; 26 (2):176-9.

45. Triggle CR, Ding H. Endothelium-derived hyperpolarizing factor: is there a novel chemical mediator? Clinical and experimental pharmacology & physiology. 2002; 29 (3):153-60.

46. Campbell WB, Gebremedhin D, Pratt PF, Harder DR. Identification of epoxyeicosatrienoic acids as endothelium-derived hyperpolarizing factors. Circulation research. 1996; 78 (3):415-23.

47. Randall MD, Alexander SP, Bennett T, Boyd EA, Fry JR, Gardiner SM, et al. An endogenous cannabinoid as an endothelium-derived vasorelaxant. Biochemical and biophysical research communications. 1996; 229 (1):114-20.

48. Chaytor AT, Evans WH, Griffith TM. Central role of heterocellular gap junctional communication in endothelium-dependent relaxations of rabbit arteries. The Journal of physiology. 1998; 508 (Pt 2):561-73.

49. Lee RT, Kamm RD. Vascular mechanics for the cardiologist. Journal of the American College of Cardiology. 1994; 23 (6):1289-95.

50. Kawasaki T, Sasayama S, Yagi S, Asakawa T, Hirai T. Non-invasive assessment of the age related changes in stiffness of major branches of the human arteries. Cardiovascular research. 1987; 21 (9):678-87.

51. Arnett DK, Evans GW, Riley WA. Arterial stiffness: a new cardiovascular risk factor? American journal of epidemiology. 1994; 140 (8):669-82.

52. George AJ, Thomas WG, Hannan RD. The renin-angiotensin system and cancer: old dog, new tricks. Nature reviews Cancer. 2010; 10 (11):745-59.

53. Rosendorff C. The renin-angiotensin system and vascular hypertrophy. Journal of the American College of Cardiology. 1996; 28 (4):803-12.

54. Bader M, Peters J, Baltatu O, Muller DN, Luft FC, Ganten D. Tissue renin-angiotensin systems: new insights from experimental animal models in hypertension research. Journal of molecular medicine. 2001; 79 (2-3):76-102.

55. Engeli S, Negrel R, Sharma AM. Physiology and pathophysiology of the adipose tissue renin-angiotensin system. Hypertension. 2000; 35 (6):1270-7.

56. Geara AS, Azzi J, Jurewicz M, Abdi R. The renin-angiotensin system: an old, newly discovered player in immunoregulation. Transplantation reviews. 2009; 23 (3):151-8.

57. Timmermans PB, Wong PC, Chiu AT, Herblin WF, Benfield P, Carini DJ, et al. Angiotensin II receptors and angiotensin II receptor antagonists. Pharmacological reviews. 1993; 45 (2):205-51.

58. Burson JM, Aguilera G, Gross KW, Sigmund CD. Differential expression of angiotensin receptor 1A and 1B in mouse. The American journal of physiology. 1994; 267 (2 Pt 1):E260-7.

59. Llorens-Cortes C, Greenberg B, Huang H, Corvol P. Tissular expression and regulation of type 1 angiotensin II receptor subtypes by quantitative reverse transcriptase-polymerase chain reaction analysis. Hypertension. 1994; 24 (5):538-48.

60. Oliverio MI, Kim HS, Ito M, Le T, Audoly L, Best CF, et al. Reduced growth, abnormal kidney structure, and type 2 (AT2) angiotensin receptor-mediated blood pressure regulation in mice lacking both AT1A and AT1B receptors for angiotensin II. Proceedings of the National Academy of Sciences of the United States of America. 1998; 95 (26):15496-501.

61. Ohtsu H, Suzuki H, Nakashima H, Dhobale S, Frank GD, Motley ED, et al. Angiotensin II signal transduction through small GTP-binding proteins: mechanism and significance in vascular smooth muscle cells. Hypertension. 2006; 48 (4):534-40.

62. Sugaya T, Nishimatsu S, Tanimoto K, Takimoto E, Yamagishi T, Imamura K, et al. Angiotensin II type 1a receptor-deficient mice with hypotension and hyperreninemia. The Journal of biological chemistry. 1995; 270 (32):18719-22.

63. Ruan X, Oliverio MI, Coffman TM, Arendshorst WJ. Renal vascular reactivity in mice: AngII-induced vasoconstriction in AT1A receptor null mice. Journal of the American Society of Nephrology : JASN. 1999; 10 (12):2620-30.

64. Shah BH, Catt KJ. Matrix metalloproteinase-dependent EGF receptor activation in hypertension and left ventricular hypertrophy. Trends in endocrinology and metabolism: TEM. 2004; 15 (6):241-3.

65. Griendling KK, Ushio-Fukai M, Lassegue B, Alexander RW. Angiotensin II signaling in vascular smooth muscle. New concepts. Hypertension. 1997; 29 (1 Pt 2):366-73.

66. Chen J, Chen JK, Neilson EG, Harris RC. Role of EGF receptor activation in angiotensin II-induced renal epithelial cell hypertrophy. Journal of the American Society of Nephrology : JASN. 2006; 17 (6):1615-23.

67. Manrique C, Lastra G, Gardner M, Sowers JR. The renin angiotensin aldosterone system in hypertension: roles of insulin resistance and oxidative stress. The Medical clinics of North America. 2009; 93 (3):569-82.

68. Carey RM, Wang ZQ, Siragy HM. Role of the angiotensin type 2 receptor in the regulation of blood pressure and renal function. Hypertension. 2000; 35 (1 Pt 2):155-63.

69. Iwai M, Chen R, Li Z, Shiuchi T, Suzuki J, Ide A, et al. Deletion of angiotensin II type 2 receptor exaggerated atherosclerosis in apolipoprotein E-null mice. Circulation. 2005; 112 (11):1636-43.

70. Touyz RM, Schiffrin EL. Role of endothelin in human hypertension. Canadian journal of physiology and pharmacology. 2003; 81 (6):533-41.

71. Hong HJ, Chan P, Liu JC, Juan SH, Huang MT, Lin JG, et al. Angiotensin II induces endothelin-1 gene expression via extracellular signal-regulated kinase pathway in rat aortic smooth muscle cells. Cardiovascular research. 2004; 61 (1):159-68.

72. Inoue A, Yanagisawa M, Takuwa Y, Mitsui Y, Kobayashi M, Masaki T. The human preproendothelin-1 gene. Complete nucleotide sequence and regulation of expression. The Journal of biological chemistry. 1989; 264 (25):14954-9.

73. Inoue A, Yanagisawa M, Kimura S, Kasuya Y, Miyauchi T, Goto K, et al. The human endothelin family: three structurally and pharmacologically distinct isopeptides predicted by three separate genes. Proceedings of the National Academy of Sciences of the United States of America. 1989; 86 (8):2863-7.

74. Matsuura A, Yamochi W, Hirata K, Kawashima S, Yokoyama M. Stimulatory interaction between vascular endothelial growth factor and endothelin-1 on each gene expression. Hypertension. 1998; 32 (1):89-95.

75. Sharefkin JB, Diamond SL, Eskin SG, McIntire LV, Dieffenbach CW. Fluid flow decreases preproendothelin mRNA levels and suppresses endothelin-1 peptide release in cultured human endothelial cells. Journal of vascular surgery. 1991; 14 (1):1-9.

76. Martin-Nizard F, Sahpaz S, Kandoussi A, Carpentier M, Fruchart JC, Duriez P, et al. Natural phenylpropanoids inhibit lipoprotein-induced endothelin-1

secretion by endothelial cells. The Journal of pharmacy and pharmacology. 2004; 56 (12):1607-11.

77. Hu RM, Chuang MY, Prins B, Kashyap ML, Frank HJ, Pedram A, et al. High density lipoproteins stimulate the production and secretion of endothelin-1 from cultured bovine aortic endothelial cells. The Journal of clinical investigation. 1994; 93 (3):1056-62.

78. Sugiura M, Inagami T, Kon V. Endotoxin stimulates endothelin-release in vivo and in vitro as determined by radioimmunoassay. Biochemical and biophysical research communications. 1989; 161 (3):1220-7.

79. Bourque SL, Davidge ST, Adams MA. The interaction between endothelin-1 and nitric oxide in the vasculature: new perspectives. American journal of physiology Regulatory, integrative and comparative physiology. 2011; 300 (6):R1288-95.

80. Emori T, Hirata Y, Imai T, Eguchi S, Kanno K, Marumo F. Cellular mechanism of natriuretic peptides-induced inhibition of endothelin-1 biosynthesis in rat endothelial cells. Endocrinology. 1993; 133 (6):2474-80.

81. Agapitov AV, Haynes WG. Role of endothelin in cardiovascular disease. Journal of the renin-angiotensin-aldosterone system : JRAAS. 2002; 3 (1):1-15.

82. Schiffrin EL, Touyz RM. Vascular biology of endothelin. Journal of cardiovascular pharmacology. 1998; 32 Suppl 3:S2-13.

83. Battistini B, Woods M, O'Donnell LJ, Warner TD, Corder R, Fournier A, et al. Contractile activity of endothelin precursors in the isolated gallbladder of the guinea-pig: presence of an endothelin-converting enzyme. British journal of pharmacology. 1995; 114 (7):1383-90.

84. Nagata N, Niwa Y, Nakaya Y. A novel 31-amino-acid-length endothelin, ET-1(1-31), can act as a biologically active peptide for vascular smooth muscle cells. Biochemical and biophysical research communications. 2000; 275 (2):595-600.

85. Sharmin S, Shiota M, Murata E, Cui P, Kitamura H, Yano M, et al. A novel bioactive 31-amino acid ET-1 peptide stimulates eosinophil recruitment and

increases the levels of eotaxin and IL-5. Inflammation research : official journal of the European Histamine Research Society [et al]. 2002; 51 (4):195-200.

86. Fernandez-Patron C, Radomski MW, Davidge ST. Vascular matrix metalloproteinase-2 cleaves big endothelin-1 yielding a novel vasoconstrictor. Circulation research. 1999; 85 (10):906-11.

87. Yoshimoto S, Ishizaki Y, Sasaki T, Murota S. Effect of carbon dioxide and oxygen on endothelin production by cultured porcine cerebral endothelial cells. Stroke; a journal of cerebral circulation. 1991; 22 (3):378-83.

88. Hosoda K, Nakao K, Hiroshi A, Suga S, Ogawa Y, Mukoyama M, et al. Cloning and expression of human endothelin-1 receptor cDNA. FEBS letters. 1991; 287 (1-2):23-6.

89. Ogawa Y, Nakao K, Arai H, Nakagawa O, Hosoda K, Suga S, et al. Molecular cloning of a non-isopeptide-selective human endothelin receptor. Biochemical and biophysical research communications. 1991; 178 (1):248-55.

90. Luscher TF. Endothelium-derived vasoactive factors and regulation of vascular tone in human blood vessels. Lung. 1990; 168 Suppl:27-34.

91. Oemar BS, Tschudi MR, Godoy N, Brovkovich V, Malinski T, Luscher TF. Reduced endothelial nitric oxide synthase expression and production in human atherosclerosis. Circulation. 1998; 97 (25):2494-8.

92. Mencarelli M, Pecorelli A, Carbotti P, Valacchi G, Grasso G, Muscettola M. Endothelin receptor A expression in human inflammatory cells. Regulatory peptides. 2009; 158 (1-3):1-5.

93. Iglarz M, Clozel M. At the heart of tissue: endothelin system and end-organ damage. Clinical science. 2010; 119 (11):453-63.

94. Komuro I, Kurihara H, Sugiyama T, Yoshizumi M, Takaku F, Yazaki Y. Endothelin stimulates c-fos and c-myc expression and proliferation of vascular smooth muscle cells. FEBS letters. 1988; 238 (2):249-52.

95. Ito H, Hirata Y, Hiroe M, Tsujino M, Adachi S, Takamoto T, et al. Endothelin-1 induces hypertrophy with enhanced expression of muscle-specific genes in cultured neonatal rat cardiomyocytes. Circulation research. 1991; 69 (1):209-15.

96. Badr KF, Murray JJ, Breyer MD, Takahashi K, Inagami T, Harris RC. Mesangial cell, glomerular and renal vascular responses to endothelin in the rat kidney. Elucidation of signal transduction pathways. The Journal of clinical investigation. 1989; 83 (1):336-42.

97. Amiri F, Paradis P, Reudelhuber TL, Schiffrin EL. Vascular inflammation in absence of blood pressure elevation in transgenic murine model overexpressing endothelin-1 in endothelial cells. Journal of hypertension. 2008; 26 (6):1102-9.

98. Rossi GP, Sacchetto A, Cesari M, Pessina AC. Interactions between endothelin-1 and the renin-angiotensin-aldosterone system. Cardiovascular research. 1999; 43 (2):300-7.

99. Gunther J, Kill A, Becker MO, Heidecke H, Rademacher J, Siegert E, et al. Angiotensin receptor type 1 and endothelin receptor type A on immune cells mediate migration and the expression of IL-8 and CCL18 when stimulated by autoantibodies from systemic sclerosis patients. Arthritis research & therapy. 2014; 16 (2):R65.

100. Cunningham ME, Huribal M, Bala RJ, McMillen MA. Endothelin-1 and endothelin-4 stimulate monocyte production of cytokines. Critical care medicine. 1997; 25 (6):958-64.

101. Zouki C, Baron C, Fournier A, Filep JG. Endothelin-1 enhances neutrophil adhesion to human coronary artery endothelial cells: role of ET(A) receptors and platelet-activating factor. British journal of pharmacology. 1999; 127 (4):969-79.

102. Hansson GK, Hermansson A. The immune system in atherosclerosis. Nature immunology. 2011; 12 (3):204-12.

103. Strong JP, Malcom GT, McMahan CA, Tracy RE, Newman WP, 3rd, Herderick EE, et al. Prevalence and extent of atherosclerosis in adolescents and young adults: implications for prevention from the Pathobiological Determinants of Atherosclerosis in Youth Study. Jama. 1999; 281 (8):727-35.

104. Hegele RA. Plasma lipoproteins: genetic influences and clinical implications. Nature reviews Genetics. 2009; 10 (2):109-21.

105. Gould AL, Rossouw JE, Santanello NC, Heyse JF, Furberg CD. Cholesterol reduction yields clinical benefit. A new look at old data. Circulation. 1995; 91 (8):2274-82.

106. Vogel RA. Coronary risk factors, endothelial function, and atherosclerosis: a review. Clinical cardiology. 1997; 20 (5):426-32.

107. Natural history of aortic and coronary atherosclerotic lesions in youth. Findings from the PDAY Study. Pathobiological Determinants of Atherosclerosis in Youth (PDAY) Research Group. Arteriosclerosis and thrombosis : a journal of vascular biology / American Heart Association. 1993; 13 (9):1291-8.

108. Insull W, Jr. The pathology of atherosclerosis: plaque development and plaque responses to medical treatment. The American journal of medicine. 2009; 122 (1 Suppl):S3-S14.

109. Madamanchi NR, Vendrov A, Runge MS. Oxidative stress and vascular disease. Arteriosclerosis, thrombosis, and vascular biology. 2005; 25 (1):29-38.

110. Eggen DA, Solberg LA. Variation of atherosclerosis with age. Laboratory investigation; a journal of technical methods and pathology. 1968; 18 (5):571-9.

111. Virmani R, Kolodgie FD, Burke AP, Farb A, Schwartz SM. Lessons from sudden coronary death: a comprehensive morphological classification scheme for atherosclerotic lesions. Arteriosclerosis, thrombosis, and vascular biology. 2000; 20 (5):1262-75.

112. Moreno PR, Purushothaman KR, Zias E, Sanz J, Fuster V. Neovascularization in human atherosclerosis. Current molecular medicine. 2006; 6 (5):457-77.

113. Cheruvu PK, Finn AV, Gardner C, Caplan J, Goldstein J, Stone GW, et al. Frequency and distribution of thin-cap fibroatheroma and ruptured plaques in human coronary arteries: a pathologic study. Journal of the American College of Cardiology. 2007; 50 (10):940-9.

114. Burke AP, Kolodgie FD, Farb A, Weber DK, Malcom GT, Smialek J, et al. Healed plaque ruptures and sudden coronary death: evidence that subclinical rupture has a role in plaque progression. Circulation. 2001; 103 (7):934-40.

115. Allison MA, Criqui MH, Wright CM. Patterns and risk factors for systemic calcified atherosclerosis. Arteriosclerosis, thrombosis, and vascular biology. 2004; 24 (2):331-6.

116. Alcorn HG, Wolfson SK, Jr., Sutton-Tyrrell K, Kuller LH, O'Leary D. Risk factors for abdominal aortic aneurysms in older adults enrolled in The Cardiovascular Health Study. Arteriosclerosis, thrombosis, and vascular biology. 1996; 16 (8):963-70.

117. Lederle FA, Johnson GR, Wilson SE, Chute EP, Littooy FN, Bandyk D, et al. Prevalence and associations of abdominal aortic aneurysm detected through screening. Aneurysm Detection and Management (ADAM) Veterans Affairs Cooperative Study Group. Annals of internal medicine. 1997; 126 (6):441-9.

118. Golledge J, Norman PE. Pathophysiology of abdominal aortic aneurysm relevant to improvements in patients' management. Current opinion in cardiology. 2009; 24 (6):532-8.

119. Golledge J, Muller J, Daugherty A, Norman P. Abdominal aortic aneurysm: pathogenesis and implications for management. Arteriosclerosis, thrombosis, and vascular biology. 2006; 26 (12):2605-13.

120. Ward MR, Pasterkamp G, Yeung AC, Borst C. Arterial remodeling. Mechanisms and clinical implications. Circulation. 2000; 102 (10):1186-91.

121. Lederle FA, Johnson GR, Wilson SE, Ballard DJ, Jordan WD, Jr., Blebea J, et al. Rupture rate of large abdominal aortic aneurysms in patients refusing or unfit for elective repair. Jama. 2002; 287 (22):2968-72.

122. Johnsen SH, Forsdahl SH, Singh K, Jacobsen BK. Atherosclerosis in abdominal aortic aneurysms: a causal event or a process running in parallel? The Tromso study. Arteriosclerosis, thrombosis, and vascular biology. 2010; 30 (6):1263-8.

123. Schlosser FJ, Tangelder MJ, Verhagen HJ, van der Heijden GJ, Muhs BE, van der Graaf Y, et al. Growth predictors and prognosis of small abdominal aortic aneurysms. Journal of vascular surgery. 2008; 47 (6):1127-33.

124. Ferguson CD, Clancy P, Bourke B, Walker PJ, Dear A, Buckenham T, et al. Association of statin prescription with small abdominal aortic aneurysm progression. American heart journal. 2010; 159 (2):307-13.

125. Golledge J, Norman PE. Atherosclerosis and abdominal aortic aneurysm: cause, response, or common risk factors? Arteriosclerosis, thrombosis, and vascular biology. 2010; 30 (6):1075-7.

126. Lerman A, Edwards BS, Hallett JW, Heublein DM, Sandberg SM, Burnett JC, Jr. Circulating and tissue endothelin immunoreactivity in advanced atherosclerosis. The New England journal of medicine. 1991; 325 (14):997-1001.

127. Lerman A, Holmes DR, Jr., Bell MR, Garratt KN, Nishimura RA, Burnett JC, Jr. Endothelin in coronary endothelial dysfunction and early atherosclerosis in humans. Circulation. 1995; 92 (9):2426-31.

128. Flondell-Site D, Lindblad B, Kolbel T, Gottsater A. Cytokines and systemic biomarkers are related to the size of abdominal aortic aneurysms. Cytokine. 2009; 46 (2):211-5.

129. Treska V, Wenham PW, Valenta J, Topolcan O, Pecen L. Plasma endothelin levels in patients with abdominal aortic aneurysms. European journal of vascular and endovascular surgery : the official journal of the European Society for Vascular Surgery. 1999; 17 (5):424-8.

130. Flondell-Site D, Lindblad B, Gottsater A. High levels of endothelin (ET)-1 and aneurysm diameter independently predict growth of stable abdominal aortic aneurysms. Angiology. 2010; 61 (4):324-8.

131. Babaei S, Picard P, Ravandi A, Monge JC, Lee TC, Cernacek P, et al. Blockade of endothelin receptors markedly reduces atherosclerosis in LDL receptor deficient mice: role of endothelin in macrophage foam cell formation. Cardiovascular research. 2000; 48 (1):158-67.

132. Barton M, Haudenschild CC, d'Uscio LV, Shaw S, Munter K, Luscher TF. Endothelin ETA receptor blockade restores NO-mediated endothelial function and inhibits atherosclerosis in apolipoprotein E-deficient mice. Proceedings of the National Academy of Sciences of the United States of America. 1998; 95 (24):14367-72.

133. Iwasa S, Fan J, Miyauchi T, Watanabe T. Blockade of endothelin receptors reduces diet-induced hypercholesterolemia and atherosclerosis in apolipoprotein E-deficient mice. Pathobiology : journal of immunopathology, molecular and cellular biology. 2001; 69 (1):1-10.

134. Kowala MC, Rose PM, Stein PD, Goller N, Recce R, Beyer S, et al. Selective blockade of the endothelin subtype A receptor decreases early atherosclerosis in hamsters fed cholesterol. The American journal of pathology. 1995; 146 (4):819-26.

135. Simeone SM, Li MW, Paradis P, Schiffrin EL. Vascular gene expression in mice overexpressing human endothelin-1 targeted to the endothelium. Physiological genomics. 2011; 43 (3):148-60.

136. Beaumont JL, Carlson LA, Cooper GR, Fejfar Z, Fredrickson DS, Strasser T. Classification of hyperlipidaemias and hyperlipoproteinaemias. Bulletin of the World Health Organization. 1970; 43 (6):891-915.

137. Stone NJ. Secondary causes of hyperlipidemia. The Medical clinics of North America. 1994; 78 (1):117-41.

138. Keys A, Aravanis C, Blackburn HW, Van Buchem FS, Buzina R, Djordjevic BD, et al. Epidemiological studies related to coronary heart disease: characteristics of men aged 40-59 in seven countries. Acta medica Scandinavica Supplementum. 1966; 460:1-392.

139. Farnier M, Davignon J. Current and future treatment of hyperlipidemia: the role of statins. The American journal of cardiology. 1998; 82 (4B):3J-10J.

140. The Lipid Research Clinics Coronary Primary Prevention Trial results. I. Reduction in incidence of coronary heart disease. Jama. 1984; 251 (3):351-64.

141. The Lipid Research Clinics Coronary Primary Prevention Trial results. II. The relationship of reduction in incidence of coronary heart disease to cholesterol lowering. Jama. 1984; 251 (3):365-74.

142. Manninen V, Elo MO, Frick MH, Haapa K, Heinonen OP, Heinsalmi P, et al. Lipid alterations and decline in the incidence of coronary heart disease in the Helsinki Heart Study. Jama. 1988; 260 (5):641-51.

143. Assmann G, Schulte H, Cullen P. New and classical risk factors--the Munster heart study (PROCAM). European journal of medical research. 1997; 2 (6):237-42.

144. Austin MA. Plasma triglyceride and coronary heart disease. Arteriosclerosis and thrombosis : a journal of vascular biology / American Heart Association. 1991; 11 (1):2-14.

145. Gordon DJ, Probstfield JL, Garrison RJ, Neaton JD, Castelli WP, Knoke JD, et al. High-density lipoprotein cholesterol and cardiovascular disease. Four prospective American studies. Circulation. 1989; 79 (1):8-15.

146. Stamler J, Neaton JD, Wentworth DN. Blood pressure (systolic and diastolic) and risk of fatal coronary heart disease. Hypertension. 1989; 13 (5 Suppl):I2-12.

147. Kannel WB, Neaton JD, Wentworth D, Thomas HE, Stamler J, Hulley SB, et al. Overall and coronary heart disease mortality rates in relation to major risk factors in 325,348 men screened for the MRFIT. Multiple Risk Factor Intervention Trial. American heart journal. 1986; 112 (4):825-36.

148. Chobanian AV, Lichtenstein AH, Nilakhe V, Haudenschild CC, Drago R, Nickerson C. Influence of hypertension on aortic atherosclerosis in the Watanabe rabbit. Hypertension. 1989; 14 (2):203-9.

149. Schiffrin EL. Reactivity of small blood vessels in hypertension: relation with structural changes. State of the art lecture. Hypertension. 1992; 19 (2 Suppl):II1-9.

150. Mulvany MJ. Small artery remodeling and significance in the development of hypertension. News in physiological sciences : an international journal of physiology produced jointly by the International Union of Physiological Sciences and the American Physiological Society. 2002; 17:105-9.

151. Hall JE, Granger JP, do Carmo JM, da Silva AA, Dubinion J, George E, et al. Hypertension: physiology and pathophysiology. Comprehensive Physiology. 2012; 2 (4):2393-442.

152. Schiffrin EL, Canadian Institutes of Health Research Multidisciplinary Research Group on H. Beyond blood pressure: the endothelium and

atherosclerosis progression. American journal of hypertension. 2002; 15 (10 Pt 2):115S-22S.

153. Landry DW, Levin HR, Gallant EM, Ashton RC, Jr., Seo S, D'Alessandro D, et al. Vasopressin deficiency contributes to the vasodilation of septic shock. Circulation. 1997; 95 (5):1122-5.

154. Haddy FJ, Overbeck HW, Daugherty RM, Jr. Peripheral vascular resistance. Annual review of medicine. 1968; 19:167-94.

155. Schiffrin EL. Remodeling of resistance arteries in essential hypertension and effects of antihypertensive treatment. American journal of hypertension. 2004; 17 (12 Pt 1):1192-200.

156. O'Rourke MF, Nichols WW. Aortic diameter, aortic stiffness, and wave reflection increase with age and isolated systolic hypertension. Hypertension. 2005; 45 (4):652-8.

157. Laurent S. Arterial wall hypertrophy and stiffness in essential hypertensive patients. Hypertension. 1995; 26 (2):355-62.

158. Lee RM, Garfield RE, Forrest JB, Daniel EE. Morphometric study of structural changes in the mesenteric blood vessels of spontaneously hypertensive rats. Blood vessels. 1983; 20 (2):57-71.

159. Mulvany MJ, Baandrup U, Gundersen HJ. Evidence for hyperplasia in mesenteric resistance vessels of spontaneously hypertensive rats using a three-dimensional disector. Circulation research. 1985; 57 (5):794-800.

160. Diep QN, Li JS, Schiffrin EL. In vivo study of AT(1) and AT(2) angiotensin receptors in apoptosis in rat blood vessels. Hypertension. 1999; 34 (4 Pt 1):617-24.

161. Sharifi AM, Schiffrin EL. Apoptosis in vasculature of spontaneously hypertensive rats: effect of an angiotensin converting enzyme inhibitor and a calcium channel antagonist. American journal of hypertension. 1998; 11 (9):1108-16.

162. Boumaza S, Arribas SM, Osborne-Pellegrin M, McGrath JC, Laurent S, Lacolley P, et al. Fenestrations of the carotid internal elastic lamina and structural

adaptation in stroke-prone spontaneously hypertensive rats. Hypertension. 2001; 37 (4):1101-7.

163. Schiffrin EL. Vascular remodeling in hypertension: mechanisms and treatment. Hypertension. 2012; 59 (2):367-74.

164. Chobanian AV. 1989 Corcoran lecture: adaptive and maladaptive responses of the arterial wall to hypertension. Hypertension. 1990; 15 (6 Pt 2):666-74.

165. Deanfield J, Donald A, Ferri C, Giannattasio C, Halcox J, Halligan S, et al. Endothelial function and dysfunction. Part I: Methodological issues for assessment in the different vascular beds: a statement by the Working Group on Endothelin and Endothelial Factors of the European Society of Hypertension. Journal of hypertension. 2005; 23 (1):7-17.

166. Laurent S, Boutouyrie P, Lacolley P. Structural and genetic bases of arterial stiffness. Hypertension. 2005; 45 (6):1050-5.

167. Mitchell GF, Vita JA, Larson MG, Parise H, Keyes MJ, Warner E, et al. Cross-sectional relations of peripheral microvascular function, cardiovascular disease risk factors, and aortic stiffness: the Framingham Heart Study. Circulation. 2005; 112 (24):3722-8.

168. Heagerty AM, Aalkjaer C, Bund SJ, Korsgaard N, Mulvany MJ. Small artery structure in hypertension. Dual processes of remodeling and growth. Hypertension. 1993; 21 (4):391-7.

169. Mulvany MJ, Baumbach GL, Aalkjaer C, Heagerty AM, Korsgaard N, Schiffrin EL, et al. Vascular remodeling. Hypertension. 1996; 28 (3):505-6.

170. Brassard P, Amiri F, Schiffrin EL. Combined angiotensin II type 1 and type 2 receptor blockade on vascular remodeling and matrix metalloproteinases in resistance arteries. Hypertension. 2005; 46 (3):598-606.

171. Schiffrin EL. The vascular phenotypes in hypertension: Relation with the natural history of hypertension. Journal of the American Society of Hypertension : JASH. 2007; 1 (1):56-67.

172. Rizzoni D, Porteri E, Castellano M, Bettoni G, Muiesan ML, Muiesan P, et al. Vascular hypertrophy and remodeling in secondary hypertension. Hypertension. 1996; 28 (5):785-90.

173. d'Uscio LV, Barton M, Shaw S, Moreau P, Luscher TF. Structure and function of small arteries in salt-induced hypertension: effects of chronic endothelin-subtype-A-receptor blockade. Hypertension. 1997; 30 (4):905-11.

174. Deng LY, Schiffrin EL. Effects of endothelin on resistance arteries of DOCA-salt hypertensive rats. The American journal of physiology. 1992; 262 (6 Pt 2):H1782-7.

175. Intengan HD, Deng LY, Li JS, Schiffrin EL. Mechanics and composition of human subcutaneous resistance arteries in essential hypertension. Hypertension. 1999; 33 (1 Pt 2):569-74.

176. Sharifi AM, Li JS, Endemann D, Schiffrin EL. Effects of enalapril and amlodipine on small-artery structure and composition, and on endothelial dysfunction in spontaneously hypertensive rats. Journal of hypertension. 1998; 16 (4):457-66.

177. Intengan HD, Thibault G, Li JS, Schiffrin EL. Resistance artery mechanics, structure, and extracellular components in spontaneously hypertensive rats : effects of angiotensin receptor antagonism and converting enzyme inhibition. Circulation. 1999; 100 (22):2267-75.

178. Himeno H, Crawford DC, Hosoi M, Chobanian AV, Brecher P. Angiotensin II alters aortic fibronectin independently of hypertension. Hypertension. 1994; 23 (6 Pt 2):823-6.

179. Saouaf R, Takasaki I, Eastman E, Chobanian AV, Brecher P. Fibronectin biosynthesis in the rat aorta in vitro. Changes due to experimental hypertension. The Journal of clinical investigation. 1991; 88 (4):1182-9.

180. Takasaki I, Takizawa T, Sugimoto K, Gotoh E, Shionoiri H, Ishii M. Effects of hypertension and aging on fibronectin expression in aorta of Dahl salt-sensitive rats. The American journal of physiology. 1994; 267 (4 Pt 2):H1523-9.

181. Intengan HD, Schiffrin EL. Vascular remodeling in hypertension: roles of apoptosis, inflammation, and fibrosis. Hypertension. 2001; 38 (3 Pt 2):581-7.

182. Savoia C, Schiffrin EL. Vascular inflammation in hypertension and diabetes: molecular mechanisms and therapeutic interventions. Clinical science. 2007; 112 (7):375-84.

183. Tea BS, Der Sarkissian S, Touyz RM, Hamet P, deBlois D. Proapoptotic and growth-inhibitory role of angiotensin II type 2 receptor in vascular smooth muscle cells of spontaneously hypertensive rats in vivo. Hypertension. 2000; 35 (5):1069-73.

184. Li Q, Muragaki Y, Hatamura I, Ueno H, Ooshima A. Stretch-induced collagen synthesis in cultured smooth muscle cells from rabbit aortic media and a possible involvement of angiotensin II and transforming growth factor-beta. Journal of vascular research. 1998; 35 (2):93-103.

185. Schlumberger W, Thie M, Rauterberg J, Robenek H. Collagen synthesis in cultured aortic smooth muscle cells. Modulation by collagen lattice culture, transforming growth factor-beta 1, and epidermal growth factor. Arteriosclerosis and thrombosis : a journal of vascular biology / American Heart Association. 1991; 11 (6):1660-6.

186. Tsoporis J, Keeley FW, Lee RM, Leenen FH. Arterial vasodilation and vascular connective tissue changes in spontaneously hypertensive rats. Journal of cardiovascular pharmacology. 1998; 31 (6):960-2.

187. Nishikawa K. Angiotensin AT1 receptor antagonism and protection against cardiovascular end-organ damage. Journal of human hypertension. 1998; 12 (5):301-9.

188. Kim S, Ohta K, Hamaguchi A, Omura T, Yukimura T, Miura K, et al. Angiotensin II type I receptor antagonist inhibits the gene expression of transforming growth factor-beta 1 and extracellular matrix in cardiac and vascular tissues of hypertensive rats. The Journal of pharmacology and experimental therapeutics. 1995; 273 (1):509-15.

189. Griendling KK, Ushio-Fukai M. Reactive oxygen species as mediators of angiotensin II signaling. Regulatory peptides. 2000; 91 (1-3):21-7.

190. Endemann DH, Schiffrin EL. Endothelial dysfunction. Journal of the American Society of Nephrology : JASN. 2004; 15 (8):1983-92.

191. Davignon J, Ganz P. Role of endothelial dysfunction in atherosclerosis. Circulation. 2004; 109 (23 Suppl 1):III27-32.

192. Kuzkaya N, Weissmann N, Harrison DG, Dikalov S. Interactions of peroxynitrite, tetrahydrobiopterin, ascorbic acid, and thiols: implications for uncoupling endothelial nitric-oxide synthase. The Journal of biological chemistry. 2003; 278 (25):22546-54.

193. Virdis A, Colucci R, Fornai M, Duranti E, Giannarelli C, Bernardini N, et al. Cyclooxygenase-1 is involved in endothelial dysfunction of mesenteric small arteries from angiotensin II-infused mice. Hypertension. 2007; 49 (3):679-86.

194. Cooke JP. Does ADMA cause endothelial dysfunction? Arteriosclerosis, thrombosis, and vascular biology. 2000; 20 (9):2032-7.

195. Li H, Witte K, August M, Brausch I, Godtel-Armbrust U, Habermeier A, et al. Reversal of endothelial nitric oxide synthase uncoupling and up-regulation of endothelial nitric oxide synthase expression lowers blood pressure in hypertensive rats. Journal of the American College of Cardiology. 2006; 47 (12):2536-44.

196. Spiecker M, Darius H, Kaboth K, Hubner F, Liao JK. Differential regulation of endothelial cell adhesion molecule expression by nitric oxide donors and antioxidants. Journal of leukocyte biology. 1998; 63 (6):732-9.

197. Garg UC, Hassid A. Nitric oxide-generating vasodilators and 8-bromo-cyclic guanosine monophosphate inhibit mitogenesis and proliferation of cultured rat vascular smooth muscle cells. The Journal of clinical investigation. 1989; 83 (5):1774-7.

198. Griendling KK, FitzGerald GA. Oxidative stress and cardiovascular injury: Part I: basic mechanisms and in vivo monitoring of ROS. Circulation. 2003; 108 (16):1912-6.

199. Skultetyova D, Filipova S, Riecansky I, Skultety J. The role of angiotensin type 1 receptor in inflammation and endothelial dysfunction. Recent patents on cardiovascular drug discovery. 2007; 2 (1):23-7.

200. Iglarz M, Clozel M. Mechanisms of ET-1-induced endothelial dysfunction. Journal of cardiovascular pharmacology. 2007; 50 (6):621-8.

201. Hart J. Inflammation. 1: Its role in the healing of acute wounds. Journal of wound care. 2002; 11 (6):205-9.

202. Hansson GK, Robertson AK, Soderberg-Naucler C. Inflammation and atherosclerosis. Annual review of pathology. 2006; 1:297-329.

203. Leibowitz A, Schiffrin EL. Immune mechanisms in hypertension. Current hypertension reports. 2011; 13 (6):465-72.

204. Ferrero-Miliani L, Nielsen OH, Andersen PS, Girardin SE. Chronic inflammation: importance of NOD2 and NALP3 in interleukin-1beta generation. Clinical and experimental immunology. 2007; 147 (2):227-35.

205. Benigni A, Cassis P, Remuzzi G. Angiotensin II revisited: new roles in inflammation, immunology and aging. EMBO molecular medicine. 2010; 2 (7):247-57.

206. Yeager ME, Belchenko DD, Nguyen CM, Colvin KL, Ivy DD, Stenmark KR. Endothelin-1, the unfolded protein response, and persistent inflammation: role of pulmonary artery smooth muscle cells. American journal of respiratory cell and molecular biology. 2012; 46 (1):14-22.

207. Touyz RM, Tabet F, Schiffrin EL. Redox-dependent signalling by angiotensin II and vascular remodelling in hypertension. Clinical and experimental pharmacology & physiology. 2003; 30 (11):860-6.

208. Virdis A, Schiffrin EL. Vascular inflammation: a role in vascular disease in hypertension? Current opinion in nephrology and hypertension. 2003; 12 (2):181-7.

209. von Rossum A, Laher I, Choy JC. Immune-mediated vascular injury and dysfunction in transplant arteriosclerosis. Frontiers in immunology. 2014; 5:684.

210. Linde A, Mosier D, Blecha F, Melgarejo T. Innate immunity and inflammation--New frontiers in comparative cardiovascular pathology. Cardiovascular research. 2007; 73 (1):26-36.

211. Epelman S, Liu PP, Mann DL. Role of innate and adaptive immune mechanisms in cardiac injury and repair. Nature reviews Immunology. 2015; 15 (2):117-29.

212. Imhof BA, Aurrand-Lions M. Adhesion mechanisms regulating the migration of monocytes. Nature reviews Immunology. 2004; 4 (6):432-44.

213. Italiani P, Boraschi D. From Monocytes to M1/M2 Macrophages: Phenotypical vs. Functional Differentiation. Frontiers in immunology. 2014; 5:514.

214. Khazen W, M'Bika J P, Tomkiewicz C, Benelli C, Chany C, Achour A, et al. Expression of macrophage-selective markers in human and rodent adipocytes. FEBS letters. 2005; 579 (25):5631-4.

215. Hao NB, Lu MH, Fan YH, Cao YL, Zhang ZR, Yang SM. Macrophages in tumor microenvironments and the progression of tumors. Clinical & developmental immunology. 2012; 2012:948098.

216. Auffray C, Fogg D, Garfa M, Elain G, Join-Lambert O, Kayal S, et al. Monitoring of blood vessels and tissues by a population of monocytes with patrolling behavior. Science. 2007; 317 (5838):666-70.

217. Nahrendorf M, Swirski FK, Aikawa E, Stangenberg L, Wurdinger T, Figueiredo JL, et al. The healing myocardium sequentially mobilizes two monocyte subsets with divergent and complementary functions. The Journal of experimental medicine. 2007; 204 (12):3037-47.

218. Crane MJ, Daley JM, van Houtte O, Brancato SK, Henry WL, Jr., Albina JE. The monocyte to macrophage transition in the murine sterile wound. PloS one. 2014; 9 (1):e86660.

219. Arnold L, Henry A, Poron F, Baba-Amer Y, van Rooijen N, Plonquet A, et al. Inflammatory monocytes recruited after skeletal muscle injury switch into antiinflammatory macrophages to support myogenesis. The Journal of experimental medicine. 2007; 204 (5):1057-69.

220. Ley K, Miller YI, Hedrick CC. Monocyte and macrophage dynamics during atherogenesis. Arteriosclerosis, thrombosis, and vascular biology. 2011; 31 (7):1506-16.

221. Woollard KJ, Geissmann F. Monocytes in atherosclerosis: subsets and functions. Nature reviews Cardiology. 2010; 7 (2):77-86.

222. De Ciuceis C, Amiri F, Brassard P, Endemann DH, Touyz RM, Schiffrin EL. Reduced vascular remodeling, endothelial dysfunction, and oxidative stress

in resistance arteries of angiotensin II-infused macrophage colony-stimulating factor-deficient mice: evidence for a role in inflammation in angiotensin-induced vascular injury. Arteriosclerosis, thrombosis, and vascular biology. 2005; 25 (10):2106-13.

223. Ko EA, Amiri F, Pandey NR, Javeshghani D, Leibovitz E, Touyz RM, et al. Resistance artery remodeling in deoxycorticosterone acetate-salt hypertension is dependent on vascular inflammation: evidence from m-CSF-deficient mice. American journal of physiology Heart and circulatory physiology. 2007; 292 (4):H1789-95.

224. Javeshghani D, Barhoumi T, Idris-Khodja N, Paradis P, Schiffrin EL. Reduced macrophage-dependent inflammation improves endothelin-1-induced vascular injury. Hypertension. 2013; 62 (1):112-7.

225. Machnik A, Neuhofer W, Jantsch J, Dahlmann A, Tammela T, Machura K, et al. Macrophages regulate salt-dependent volume and blood pressure by a vascular endothelial growth factor-C-dependent buffering mechanism. Nature medicine. 2009; 15 (5):545-52.

226. Machnik A, Dahlmann A, Kopp C, Goss J, Wagner H, van Rooijen N, et al. Mononuclear phagocyte system depletion blocks interstitial tonicity-responsive enhancer binding protein/vascular endothelial growth factor C expression and induces salt-sensitive hypertension in rats. Hypertension. 2010; 55 (3):755-61.

227. Hashimoto D, Miller J, Merad M. Dendritic cell and macrophage heterogeneity in vivo. Immunity. 2011; 35 (3):323-35.

228. Lanzavecchia A, Sallusto F. Regulation of T cell immunity by dendritic cells. Cell. 2001; 106 (3):263-6.

229. Buono C, Pang H, Uchida Y, Libby P, Sharpe AH, Lichtman AH. B7-1/B7-2 costimulation regulates plaque antigen-specific T-cell responses and atherogenesis in low-density lipoprotein receptor-deficient mice. Circulation. 2004; 109 (16):2009-15.

230. Faure-Andre G, Vargas P, Yuseff MI, Heuze M, Diaz J, Lankar D, et al. Regulation of dendritic cell migration by CD74, the MHC class II-associated invariant chain. Science. 2008; 322 (5908):1705-10.

231. Weber C, Meiler S, Doring Y, Koch M, Drechsler M, Megens RT, et al. CCL17-expressing dendritic cells drive atherosclerosis by restraining regulatory T cell homeostasis in mice. The Journal of clinical investigation. 2011; 121 (7):2898-910.

232. Erbel C, Sato K, Meyer FB, Kopecky SL, Frye RL, Goronzy JJ, et al. Functional profile of activated dendritic cells in unstable atherosclerotic plaque. Basic research in cardiology. 2007; 102 (2):123-32.

233. Maffia P, Zinselmeyer BH, Ialenti A, Kennedy S, Baker AH, McInnes IB, et al. Images in cardiovascular medicine. Multiphoton microscopy for 3-dimensional imaging of lymphocyte recruitment into apolipoprotein-E-deficient mouse carotid artery. Circulation. 2007; 115 (11):e326-8.

234. Koltsova EK, Garcia Z, Chodaczek G, Landau M, McArdle S, Scott SR, et al. Dynamic T cell-APC interactions sustain chronic inflammation in atherosclerosis. The Journal of clinical investigation. 2012; 122 (9):3114-26.

235. Vinh A, Chen W, Blinder Y, Weiss D, Taylor WR, Goronzy JJ, et al. Inhibition and genetic ablation of the B7/CD28 T-cell costimulation axis prevents experimental hypertension. Circulation. 2010; 122 (24):2529-37.

236. Idris-Khodja N, Mian MO, Paradis P, Schiffrin EL. Dual opposing roles of adaptive immunity in hypertension. European heart journal. 2014; 35 (19):1238-44.

237. Weber C, Zernecke A, Libby P. The multifaceted contributions of leukocyte subsets to atherosclerosis: lessons from mouse models. Nature reviews Immunology. 2008; 8 (10):802-15.

238. Tedgui A, Mallat Z. Cytokines in atherosclerosis: pathogenic and regulatory pathways. Physiological reviews. 2006; 86 (2):515-81.

239. Zhou X, Robertson AK, Hjerpe C, Hansson GK. Adoptive transfer of CD4+ T cells reactive to modified low-density lipoprotein aggravates atherosclerosis. Arteriosclerosis, thrombosis, and vascular biology. 2006; 26 (4):864-70.

240. Guzik TJ, Hoch NE, Brown KA, McCann LA, Rahman A, Dikalov S, et al. Role of the T cell in the genesis of angiotensin II induced hypertension and

vascular dysfunction. The Journal of experimental medicine. 2007; 204 (10):2449-60.

241. O'Shea JJ, Paul WE. Mechanisms underlying lineage commitment and plasticity of helper CD4+ T cells. Science. 2010; 327 (5969):1098-102.

242. Kidd P. Th1/Th2 balance: the hypothesis, its limitations, and implications for health and disease. Alternative medicine review : a journal of clinical therapeutic. 2003; 8 (3):223-46.

243. Uyemura K, Demer LL, Castle SC, Jullien D, Berliner JA, Gately MK, et al. Cross-regulatory roles of interleukin (IL)-12 and IL-10 in atherosclerosis. The Journal of clinical investigation. 1996; 97 (9):2130-8.

244. Frostegard J, Ulfgren AK, Nyberg P, Hedin U, Swedenborg J, Andersson U, et al. Cytokine expression in advanced human atherosclerotic plaques: dominance of pro-inflammatory (Th1) and macrophage-stimulating cytokines. Atherosclerosis. 1999; 145 (1):33-43.

245. Whitman SC, Ravisankar P, Elam H, Daugherty A. Exogenous interferon-gamma enhances atherosclerosis in apolipoprotein E-/- mice. The American journal of pathology. 2000; 157 (6):1819-24.

246. Gupta S, Pablo AM, Jiang X, Wang N, Tall AR, Schindler C. IFN-gamma potentiates atherosclerosis in ApoE knock-out mice. The Journal of clinical investigation. 1997; 99 (11):2752-61.

247. Shao J, Nangaku M, Miyata T, Inagi R, Yamada K, Kurokawa K, et al. Imbalance of T-cell subsets in angiotensin II-infused hypertensive rats with kidney injury. Hypertension. 2003; 42 (1):31-8.

248. Mazzolai L, Duchosal MA, Korber M, Bouzourene K, Aubert JF, Hao H, et al. Endogenous angiotensin II induces atherosclerotic plaque vulnerability and elicits a Th1 response in ApoE-/- mice. Hypertension. 2004; 44 (3):277-82.

249. Kossmann S, Schwenk M, Hausding M, Karbach SH, Schmidgen MI, Brandt M, et al. Angiotensin II-induced vascular dysfunction depends on interferon-gamma-driven immune cell recruitment and mutual activation of monocytes and NK-cells. Arteriosclerosis, thrombosis, and vascular biology. 2013; 33 (6):1313-9.

250. Xia Y, Entman ML, Wang Y. Critical role of CXCL16 in hypertensive kidney injury and fibrosis. Hypertension. 2013; 62 (6):1129-37.

251. Ishimitsu T, Uehara Y, Numabe A, Tsukada H, Ogawa Y, Iwai J, et al. Interferon gamma attenuates hypertensive renal injury in salt-sensitive Dahl rats. Hypertension. 1992; 19 (6 Pt 2):804-8.

252. van Heuven-Nolsen D, De Kimpe SJ, Muis T, van Ark I, Savelkoul H, Beems RB, et al. Opposite role of interferon-gamma and interleukin-4 on the regulation of blood pressure in mice. Biochemical and biophysical research communications. 1999; 254 (3):816-20.

253. Dejaco C, Duftner C, Grubeck-Loebenstein B, Schirmer M. Imbalance of regulatory T cells in human autoimmune diseases. Immunology. 2006; 117 (3):289-300.

254. Sakaguchi S. Naturally arising Foxp3-expressing CD25+CD4+ regulatory T cells in immunological tolerance to self and non-self. Nature immunology. 2005; 6 (4):345-52.

255. Vignali DA, Collison LW, Workman CJ. How regulatory T cells work. Nature reviews Immunology. 2008; 8 (7):523-32.

256. Zou Q, Wu B, Xue J, Fan X, Feng C, Geng S, et al. CD8+ Treg cells suppress CD8+ T cell-responses by IL-10-dependent mechanism during H5N1 influenza virus infection. European journal of immunology. 2014; 44 (1):103-14.

257. Gol-Ara M, Jadidi-Niaragh F, Sadria R, Azizi G, Mirshafiey A. The role of different subsets of regulatory T cells in immunopathogenesis of rheumatoid arthritis. Arthritis. 2012; 2012:805875.

258. Mocellin S, Marincola F, Rossi CR, Nitti D, Lise M. The multifaceted relationship between IL-10 and adaptive immunity: putting together the pieces of a puzzle. Cytokine & growth factor reviews. 2004; 15 (1):61-76.

259. Robertson AK, Hansson GK. T cells in atherogenesis: for better or for worse? Arteriosclerosis, thrombosis, and vascular biology. 2006; 26 (11):2421-32.

260. Taleb S, Tedgui A, Mallat Z. Regulatory T-cell immunity and its relevance to atherosclerosis. Journal of internal medicine. 2008; 263 (5):489-99.

261. Carrier Y, Yuan J, Kuchroo VK, Weiner HL. Th3 cells in peripheral tolerance. I. Induction of Foxp3-positive regulatory T cells by Th3 cells derived from TGF-beta T cell-transgenic mice. Journal of immunology. 2007; 178 (1):179-85.

262. Takahashi T, Kuniyasu Y, Toda M, Sakaguchi N, Itoh M, Iwata M, et al. Immunologic self-tolerance maintained by CD25+CD4+ naturally anergic and suppressive T cells: induction of autoimmune disease by breaking their anergic/suppressive state. International immunology. 1998; 10 (12):1969-80.

263. Gordon KJ, Blobe GC. Role of transforming growth factor-beta superfamily signaling pathways in human disease. Biochimica et biophysica acta. 2008; 1782 (4):197-228.

264. Niedbala W, Wei XQ, Cai B, Hueber AJ, Leung BP, McInnes IB, et al. IL-35 is a novel cytokine with therapeutic effects against collagen-induced arthritis through the expansion of regulatory T cells and suppression of Th17 cells. European journal of immunology. 2007; 37 (11):3021-9.

265. Garin MI, Chu CC, Golshayan D, Cernuda-Morollon E, Wait R, Lechler RI. Galectin-1: a key effector of regulation mediated by CD4+CD25+ T cells. Blood. 2007; 109 (5):2058-65.

266. Gondek DC, Lu LF, Quezada SA, Sakaguchi S, Noelle RJ. Cutting edge: contact-mediated suppression by CD4+CD25+ regulatory cells involves a granzyme B-dependent, perforin-independent mechanism. Journal of immunology. 2005; 174 (4):1783-6.

267. Grossman WJ, Verbsky JW, Barchet W, Colonna M, Atkinson JP, Ley TJ. Human T regulatory cells can use the perforin pathway to cause autologous target cell death. Immunity. 2004; 21 (4):589-601.

268. Kobie JJ, Shah PR, Yang L, Rebhahn JA, Fowell DJ, Mosmann TR. T regulatory and primed uncommitted CD4 T cells express CD73, which suppresses effector CD4 T cells by converting 5'-adenosine monophosphate to adenosine. Journal of immunology. 2006; 177 (10):6780-6.

269. Deaglio S, Dwyer KM, Gao W, Friedman D, Usheva A, Erat A, et al. Adenosine generation catalyzed by CD39 and CD73 expressed on regulatory T

cells mediates immune suppression. The Journal of experimental medicine. 2007; 204 (6):1257-65.

270. Misra N, Bayry J, Lacroix-Desmazes S, Kazatchkine MD, Kaveri SV. Cutting edge: human CD4+CD25+ T cells restrain the maturation and antigen-presenting function of dendritic cells. Journal of immunology. 2004; 172 (8):4676-80.

271. Watanabe K, Rao VP, Poutahidis T, Rickman BH, Ohtani M, Xu S, et al. Cytotoxic-T-lymphocyte-associated antigen 4 blockade abrogates protection by regulatory T cells in a mouse model of microbially induced innate immune-driven colitis. Infection and immunity. 2008; 76 (12):5834-42.

272. Sarris M, Andersen KG, Randow F, Mayr L, Betz AG. Neuropilin-1 expression on regulatory T cells enhances their interactions with dendritic cells during antigen recognition. Immunity. 2008; 28 (3):402-13.

273. Shalev I, Liu H, Koscik C, Bartczak A, Javadi M, Wong KM, et al. Targeted deletion of fgl2 leads to impaired regulatory T cell activity and development of autoimmune glomerulonephritis. Journal of immunology. 2008; 180 (1):249-60.

274. Schiffrin EL. Immune mechanisms in hypertension and vascular injury. Clinical science. 2014; 126 (4):267-74.

275. Ait-Oufella H, Salomon BL, Potteaux S, Robertson AK, Gourdy P, Zoll J, et al. Natural regulatory T cells control the development of atherosclerosis in mice. Nature medicine. 2006; 12 (2):178-80.

276. Mor A, Planer D, Luboshits G, Afek A, Metzger S, Chajek-Shaul T, et al. Role of naturally occurring CD4+ CD25+ regulatory T cells in experimental atherosclerosis. Arteriosclerosis, thrombosis, and vascular biology. 2007; 27 (4):893-900.

277. Mallat Z, Taleb S, Ait-Oufella H, Tedgui A. The role of adaptive T cell immunity in atherosclerosis. Journal of lipid research. 2009; 50 Suppl:S364-9.

278. Klingenberg R, Gerdes N, Badeau RM, Gistera A, Strodthoff D, Ketelhuth DF, et al. Depletion of FOXP3+ regulatory T cells promotes hypercholesterolemia and atherosclerosis. The Journal of clinical investigation. 2013; 123 (3):1323-34.

279. Viel EC, Lemarie CA, Benkirane K, Paradis P, Schiffrin EL. Immune regulation and vascular inflammation in genetic hypertension. American journal of physiology Heart and circulatory physiology. 2010; 298 (3):H938-44.

280. Kent WJ, Sugnet CW, Furey TS, Roskin KM, Pringle TH, Zahler AM, et al. The human genome browser at UCSC. Genome research. 2002; 12 (6):996-1006.

281. Barhoumi T, Kasal DA, Li MW, Shbat L, Laurant P, Neves MF, et al. T regulatory lymphocytes prevent angiotensin II-induced hypertension and vascular injury. Hypertension. 2011; 57 (3):469-76.

282. Kvakan H, Kleinewietfeld M, Qadri F, Park JK, Fischer R, Schwarz I, et al. Regulatory T cells ameliorate angiotensin II-induced cardiac damage. Circulation. 2009; 119 (22):2904-12.

283. Kasal DA, Barhoumi T, Li MW, Yamamoto N, Zdanovich E, Rehman A, et al. T regulatory lymphocytes prevent aldosterone-induced vascular injury. Hypertension. 2012; 59 (2):324-30.

284. Didion SP, Kinzenbaw DA, Schrader LI, Chu Y, Faraci FM. Endogenous interleukin-10 inhibits angiotensin II-induced vascular dysfunction. Hypertension. 2009; 54 (3):619-24.

285. Kassan M, Galan M, Partyka M, Trebak M, Matrougui K. Interleukin-10 released by CD4(+)CD25(+) natural regulatory T cells improves microvascular endothelial function through inhibition of NADPH oxidase activity in hypertensive mice. Arteriosclerosis, thrombosis, and vascular biology. 2011; 31 (11):2534-42.

286. Korn T, Bettelli E, Oukka M, Kuchroo VK. IL-17 and Th17 Cells. Annual review of immunology. 2009; 27:485-517.

287. Komiyama Y, Nakae S, Matsuki T, Nambu A, Ishigame H, Kakuta S, et al. IL-17 plays an important role in the development of experimental autoimmune encephalomyelitis. Journal of immunology. 2006; 177 (1):566-73.

288. Schnyder B, Schnyder-Candrian S, Pansky A, Schmitz ML, Heim M, Ryffel B, et al. IL-17 reduces TNF-induced Rantes and VCAM-1 expression. Cytokine. 2005; 31 (3):191-202.

289. Hashmi S, Zeng QT. Role of interleukin-17 and interleukin-17-induced cytokines interleukin-6 and interleukin-8 in unstable coronary artery disease. Coronary artery disease. 2006; 17 (8):699-706.

290. Taleb S, Tedgui A, Mallat Z. IL-17 and Th17 cells in atherosclerosis: subtle and contextual roles. Arteriosclerosis, thrombosis, and vascular biology. 2015; 35 (2):258-64.

291. Madhur MS, Lob HE, McCann LA, Iwakura Y, Blinder Y, Guzik TJ, et al. Interleukin 17 promotes angiotensin II-induced hypertension and vascular dysfunction. Hypertension. 2010; 55 (2):500-7.

292. Amador CA, Barrientos V, Pena J, Herrada AA, Gonzalez M, Valdes S, et al. Spironolactone decreases DOCA-salt-induced organ damage by blocking the activation of T helper 17 and the downregulation of regulatory T lymphocytes. Hypertension. 2014; 63 (4):797-803.

293. Wu J, Thabet SR, Kirabo A, Trott DW, Saleh MA, Xiao L, et al. Inflammation and mechanical stretch promote aortic stiffening in hypertension through activation of p38 mitogen-activated protein kinase. Circulation research. 2014; 114 (4):616-25.

294. Wallace K, Richards S, Dhillon P, Weimer A, Edholm ES, Bengten E, et al. CD4+ T-helper cells stimulated in response to placental ischemia mediate hypertension during pregnancy. Hypertension. 2011; 57 (5):949-55.

295. Cornelius DC, Hogg JP, Scott J, Wallace K, Herse F, Moseley J, et al. Administration of interleukin-17 soluble receptor C suppresses TH17 cells, oxidative stress, and hypertension in response to placental ischemia during pregnancy. Hypertension. 2013; 62 (6):1068-73.

296. Redmond WL, Wei CH, Kreuwel HT, Sherman LA. The apoptotic pathway contributing to the deletion of naive CD8 T cells during the induction of peripheral tolerance to a cross-presented self-antigen. Journal of immunology. 2008; 180 (8):5275-82.

297. Kolbus D, Ramos OH, Berg KE, Persson J, Wigren M, Bjorkbacka H, et al. CD8+ T cell activation predominate early immune responses to hypercholesterolemia in Apoe(-)(/)(-) mice. BMC immunology. 2010; 11:58.

298. Roselaar SE, Kakkanathu PX, Daugherty A. Lymphocyte populations in atherosclerotic lesions of apoE -/- and LDL receptor -/- mice. Decreasing density with disease progression. Arteriosclerosis, thrombosis, and vascular biology. 1996; 16 (8):1013-8.

299. Kyaw T, Winship A, Tay C, Kanellakis P, Hosseini H, Cao A, et al. Cytotoxic and proinflammatory CD8+ T lymphocytes promote development of vulnerable atherosclerotic plaques in apoE-deficient mice. Circulation. 2013; 127 (9):1028-39.

300. Gratze P, Dechend R, Stocker C, Park JK, Feldt S, Shagdarsuren E, et al. Novel role for inhibitor of differentiation 2 in the genesis of angiotensin II-induced hypertension. Circulation. 2008; 117 (20):2645-56.

301. Senchenkova EY, Russell J, Kurmaeva E, Ostanin D, Granger DN. Role of T lymphocytes in angiotensin II-mediated microvascular thrombosis. Hypertension. 2011; 58 (5):959-65.

302. Berliner JA, Navab M, Fogelman AM, Frank JS, Demer LL, Edwards PA, et al. Atherosclerosis: basic mechanisms. Oxidation, inflammation, and genetics. Circulation. 1995; 91 (9):2488-96.

303. McMaster WG, Kirabo A, Madhur MS, Harrison DG. Inflammation, immunity, and hypertensive end-organ damage. Circulation research. 2015; 116 (6):1022-33.

304. Notarangelo LD, Badolato R. Leukocyte trafficking in primary immunodeficiencies. Journal of leukocyte biology. 2009; 85 (3):335-43.

305. Olson TS, Ley K. Chemokines and chemokine receptors in leukocyte trafficking. American journal of physiology Regulatory, integrative and comparative physiology. 2002; 283 (1):R7-28.

306. Rollins BJ. Chemokines. Blood. 1997; 90 (3):909-28.

307. Yla-Herttuala S, Lipton BA, Rosenfeld ME, Sarkioja T, Yoshimura T, Leonard EJ, et al. Expression of monocyte chemoattractant protein 1 in macrophage-rich areas of human and rabbit atherosclerotic lesions. Proceedings of the National Academy of Sciences of the United States of America. 1991; 88 (12):5252-6.

308. Capers Qt, Alexander RW, Lou P, De Leon H, Wilcox JN, Ishizaka N, et al. Monocyte chemoattractant protein-1 expression in aortic tissues of hypertensive rats. Hypertension. 1997; 30 (6):1397-402.

309. Ley K, Laudanna C, Cybulsky MI, Nourshargh S. Getting to the site of inflammation: the leukocyte adhesion cascade updated. Nature reviews Immunology. 2007; 7 (9):678-89.

310. Rao RM, Yang L, Garcia-Cardena G, Luscinskas FW. Endothelial-dependent mechanisms of leukocyte recruitment to the vascular wall. Circulation research. 2007; 101 (3):234-47.

311. Galkina E, Ley K. Vascular adhesion molecules in atherosclerosis. Arteriosclerosis, thrombosis, and vascular biology. 2007; 27 (11):2292-301.

312. Sanada H, Midorikawa S, Yatabe J, Yatabe MS, Katoh T, Baba T, et al. Elevation of serum soluble E- and P-selectin in patients with hypertension is reversed by benidipine, a long-acting calcium channel blocker. Hypertension research : official journal of the Japanese Society of Hypertension. 2005; 28 (11):871-8.

313. Ramana KV, Bhatnagar A, Srivastava SK. Inhibition of aldose reductase attenuates TNF-alpha-induced expression of adhesion molecules in endothelial cells. FASEB journal : official publication of the Federation of American Societies for Experimental Biology. 2004; 18 (11):1209-18.

314. Davies MJ, Gordon JL, Gearing AJ, Pigott R, Woolf N, Katz D, et al. The expression of the adhesion molecules ICAM-1, VCAM-1, PECAM, and E-selectin in human atherosclerosis. The Journal of pathology. 1993; 171 (3):223-9.

315. Deem TL, Cook-Mills JM. Vascular cell adhesion molecule 1 (VCAM-1) activation of endothelial cell matrix metalloproteinases: role of reactive oxygen species. Blood. 2004; 104 (8):2385-93.

316. van Wetering S, van den Berk N, van Buul JD, Mul FP, Lommerse I, Mous R, et al. VCAM-1-mediated Rac signaling controls endothelial cell-cell contacts and leukocyte transmigration. American journal of physiology Cell physiology. 2003; 285 (2):C343-52.

317. Etienne S, Adamson P, Greenwood J, Strosberg AD, Cazaubon S, Couraud PO. ICAM-1 signaling pathways associated with Rho activation in microvascular brain endothelial cells. Journal of immunology. 1998; 161 (10):5755-61.

318. Petri B, Bixel MG. Molecular events during leukocyte diapedesis. The FEBS journal. 2006; 273 (19):4399-407.

319. Petri B, Phillipson M, Kubes P. The physiology of leukocyte recruitment: an in vivo perspective. Journal of immunology. 2008; 180 (10):6439-46.

320. Carman CV, Sage PT, Sciuto TE, de la Fuente MA, Geha RS, Ochs HD, et al. Transcellular diapedesis is initiated by invasive podosomes. Immunity. 2007; 26 (6):784-97.

321. Breviario F, Caveda L, Corada M, Martin-Padura I, Navarro P, Golay J, et al. Functional properties of human vascular endothelial cadherin (7B4/cadherin-5), an endothelium-specific cadherin. Arteriosclerosis, thrombosis, and vascular biology. 1995; 15 (8):1229-39.

322. Hermant B, Bibert S, Concord E, Dublet B, Weidenhaupt M, Vernet T, et al. Identification of proteases involved in the proteolysis of vascular endothelium cadherin during neutrophil transmigration. The Journal of biological chemistry. 2003; 278 (16):14002-12.

323. Allingham MJ, van Buul JD, Burridge K. ICAM-1-mediated, Src- and Pyk2-dependent vascular endothelial cadherin tyrosine phosphorylation is required for leukocyte transendothelial migration. Journal of immunology. 2007; 179 (6):4053-64.

324. Vestweber D. VE-cadherin: the major endothelial adhesion molecule controlling cellular junctions and blood vessel formation. Arteriosclerosis, thrombosis, and vascular biology. 2008; 28 (2):223-32.

325. Dangerfield J, Larbi KY, Huang MT, Dewar A, Nourshargh S. PECAM-1 (CD31) homophilic interaction up-regulates alpha6beta1 on transmigrated neutrophils in vivo and plays a functional role in the ability of alpha6 integrins to mediate leukocyte migration through the perivascular basement membrane. The Journal of experimental medicine. 2002; 196 (9):1201-11.

326. Schenkel AR, Mamdouh Z, Chen X, Liebman RM, Muller WA. CD99 plays a major role in the migration of monocytes through endothelial junctions. Nature immunology. 2002; 3 (2):143-50.

327. Muller WA. Leukocyte-endothelial-cell interactions in leukocyte transmigration and the inflammatory response. Trends in immunology. 2003; 24 (6):327-34.

328. Kvietys PR, Sandig M. Neutrophil diapedesis: paracellular or transcellular? News in physiological sciences : an international journal of physiology produced jointly by the International Union of Physiological Sciences and the American Physiological Society. 2001; 16:15-9.

329. Millan J, Hewlett L, Glyn M, Toomre D, Clark P, Ridley AJ. Lymphocyte transcellular migration occurs through recruitment of endothelial ICAM-1 to caveola- and F-actin-rich domains. Nature cell biology. 2006; 8 (2):113-23.

330. Oppenheimer-Marks N, Brezinschek RI, Mohamadzadeh M, Vita R, Lipsky PE. Interleukin 15 is produced by endothelial cells and increases the transendothelial migration of T cells In vitro and in the SCID mouse-human rheumatoid arthritis model In vivo. The Journal of clinical investigation. 1998; 101 (6):1261-72.

331. Kim HY, Kang YJ, Song IH, Choi HC, Kim HS. Upregulation of interleukin-8/CXCL8 in vascular smooth muscle cells from spontaneously hypertensive rats. Hypertension research : official journal of the Japanese Society of Hypertension. 2008; 31 (3):515-23.

332. Wojciak-Stothard B, Entwistle A, Garg R, Ridley AJ. Regulation of TNF-alpha-induced reorganization of the actin cytoskeleton and cell-cell junctions by Rho, Rac, and Cdc42 in human endothelial cells. Journal of cellular physiology. 1998; 176 (1):150-65.

333. Wakkach A, Fournier N, Brun V, Breittmayer JP, Cottrez F, Groux H. Characterization of dendritic cells that induce tolerance and T regulatory 1 cell differentiation in vivo. Immunity. 2003; 18 (5):605-17.

334. Ortega-Gomez A, Perretti M, Soehnlein O. Resolution of inflammation: an integrated view. EMBO molecular medicine. 2013; 5 (5):661-74.

335. Touyz RM, Schiffrin EL. Reactive oxygen species in vascular biology: implications in hypertension. Histochemistry and cell biology. 2004; 122 (4):339-52.

336. Stocker R, Keaney JF, Jr. Role of oxidative modifications in atherosclerosis. Physiological reviews. 2004; 84 (4):1381-478.

337. Harrison D, Griendling KK, Landmesser U, Hornig B, Drexler H. Role of oxidative stress in atherosclerosis. The American journal of cardiology. 2003; 91 (3A):7A-11A.

338. Cherubini A, Vigna GB, Zuliani G, Ruggiero C, Senin U, Fellin R. Role of antioxidants in atherosclerosis: epidemiological and clinical update. Current pharmaceutical design. 2005; 11 (16):2017-32.

339. Taddei S, Virdis A, Ghiadoni L, Magagna A, Salvetti A. Vitamin C improves endothelium-dependent vasodilation by restoring nitric oxide activity in essential hypertension. Circulation. 1998; 97 (22):2222-9.

340. Paravicini TM, Touyz RM. Redox signaling in hypertension. Cardiovascular research. 2006; 71 (2):247-58.

341. Schnabel R, Blankenberg S. Oxidative stress in cardiovascular disease: successful translation from bench to bedside? Circulation. 2007; 116 (12):1338-40.

342. Betteridge DJ. What is oxidative stress? Metabolism: clinical and experimental. 2000; 49 (2 Suppl 1):3-8.

343. Pacher P, Beckman JS, Liaudet L. Nitric oxide and peroxynitrite in health and disease. Physiological reviews. 2007; 87 (1):315-424.

344. Clempus RE, Griendling KK. Reactive oxygen species signaling in vascular smooth muscle cells. Cardiovascular research. 2006; 71 (2):216-25.

345. Jones SA, O'Donnell VB, Wood JD, Broughton JP, Hughes EJ, Jones OT. Expression of phagocyte NADPH oxidase components in human endothelial cells. The American journal of physiology. 1996; 271 (4 Pt 2):H1626-34.

346. Pagano PJ, Clark JK, Cifuentes-Pagano ME, Clark SM, Callis GM, Quinn MT. Localization of a constitutively active, phagocyte-like NADPH oxidase in rabbit aortic adventitia: enhancement by angiotensin II. Proceedings of the

National Academy of Sciences of the United States of America. 1997; 94 (26):14483-8.

347. Patterson C, Ruef J, Madamanchi NR, Barry-Lane P, Hu Z, Horaist C, et al. Stimulation of a vascular smooth muscle cell NAD(P)H oxidase by thrombin. Evidence that p47(phox) may participate in forming this oxidase in vitro and in vivo. The Journal of biological chemistry. 1999; 274 (28):19814-22.

348. Griendling KK, Sorescu D, Ushio-Fukai M. NAD(P)H oxidase: role in cardiovascular biology and disease. Circulation research. 2000; 86 (5):494-501.

349. Griendling KK, Minieri CA, Ollerenshaw JD, Alexander RW. Angiotensin II stimulates NADH and NADPH oxidase activity in cultured vascular smooth muscle cells. Circulation research. 1994; 74 (6):1141-8.

350. Li L, Fink GD, Watts SW, Northcott CA, Galligan JJ, Pagano PJ, et al. Endothelin-1 increases vascular superoxide via endothelin(A)-NADPH oxidase pathway in low-renin hypertension. Circulation. 2003; 107 (7):1053-8.

351. Chen DD, Dong YG, Yuan H, Chen AF. Endothelin 1 activation of endothelin A receptor/NADPH oxidase pathway and diminished antioxidants critically contribute to endothelial progenitor cell reduction and dysfunction in salt-sensitive hypertension. Hypertension. 2012; 59 (5):1037-43.

352. Barry-Lane PA, Patterson C, van der Merwe M, Hu Z, Holland SM, Yeh ET, et al. p47phox is required for atherosclerotic lesion progression in ApoE(-/-) mice. The Journal of clinical investigation. 2001; 108 (10):1513-22.

353. Warnholtz A, Nickenig G, Schulz E, Macharzina R, Brasen JH, Skatchkov M, et al. Increased NADH-oxidase-mediated superoxide production in the early stages of atherosclerosis: evidence for involvement of the renin-angiotensin system. Circulation. 1999; 99 (15):2027-33.

354. Matsuno K, Yamada H, Iwata K, Jin D, Katsuyama M, Matsuki M, et al. Nox1 is involved in angiotensin II-mediated hypertension: a study in Nox1-deficient mice. Circulation. 2005; 112 (17):2677-85.

355. Harrison R. Structure and function of xanthine oxidoreductase: where are we now? Free radical biology & medicine. 2002; 33 (6):774-97.

356. Landmesser U, Spiekermann S, Preuss C, Sorrentino S, Fischer D, Manes C, et al. Angiotensin II induces endothelial xanthine oxidase activation: role for endothelial dysfunction in patients with coronary disease. Arteriosclerosis, thrombosis, and vascular biology. 2007; 27 (4):943-8.

357. Spiekermann S, Landmesser U, Dikalov S, Bredt M, Gamez G, Tatge H, et al. Electron spin resonance characterization of vascular xanthine and NAD(P)H oxidase activity in patients with coronary artery disease: relation to endothelium-dependent vasodilation. Circulation. 2003; 107 (10):1383-9.

358. Ohara Y, Peterson TE, Harrison DG. Hypercholesterolemia increases endothelial superoxide anion production. The Journal of clinical investigation. 1993; 91 (6):2546-51.

359. Patetsios P, Song M, Shutze WP, Pappas C, Rodino W, Ramirez JA, et al. Identification of uric acid and xanthine oxidase in atherosclerotic plaque. The American journal of cardiology. 2001; 88 (2):188-91, A6.

360. Guzik TJ, Sadowski J, Guzik B, Jopek A, Kapelak B, Przybylowski P, et al. Coronary artery superoxide production and nox isoform expression in human coronary artery disease. Arteriosclerosis, thrombosis, and vascular biology. 2006; 26 (2):333-9.

361. Boueiz A, Damarla M, Hassoun PM. Xanthine oxidoreductase in respiratory and cardiovascular disorders. American journal of physiology Lung cellular and molecular physiology. 2008; 294 (5):L830-40.

362. Viel EC, Benkirane K, Javeshghani D, Touyz RM, Schiffrin EL. Xanthine oxidase and mitochondria contribute to vascular superoxide anion generation in DOCA-salt hypertensive rats. American journal of physiology Heart and circulatory physiology. 2008; 295 (1):H281-8.

363. Turrens JF, Boveris A. Generation of superoxide anion by the NADH dehydrogenase of bovine heart mitochondria. The Biochemical journal. 1980; 191 (2):421-7.

364. Boveris A, Cadenas E, Stoppani AO. Role of ubiquinone in the mitochondrial generation of hydrogen peroxide. The Biochemical journal. 1976; 156 (2):435-44.

365. Ballinger SW, Patterson C, Knight-Lozano CA, Burow DL, Conklin CA, Hu Z, et al. Mitochondrial integrity and function in atherogenesis. Circulation. 2002; 106 (5):544-9.

366. Clayton DA. Transcription of the mammalian mitochondrial genome. Annual review of biochemistry. 1984; 53:573-94.

367. Rodriguez-Iturbe B, Sepassi L, Quiroz Y, Ni Z, Wallace DC, Vaziri ND. Association of mitochondrial SOD deficiency with salt-sensitive hypertension and accelerated renal senescence. Journal of applied physiology. 2007; 102 (1):255-60.

368. Hulsmans M, Van Dooren E, Holvoet P. Mitochondrial reactive oxygen species and risk of atherosclerosis. Current atherosclerosis reports. 2012; 14 (3):264-76.

369. Burleigh ME, Babaev VR, Yancey PG, Major AS, McCaleb JL, Oates JA, et al. Cyclooxygenase-2 promotes early atherosclerotic lesion formation in ApoE-deficient and C57BL/6 mice. Journal of molecular and cellular cardiology. 2005; 39 (3):443-52.

370. Wu R, Duchemin S, Laplante MA, De Champlain J, Girouard H. Cyclo-oxygenase-2 knockout genotype in mice is associated with blunted angiotensin II-induced oxidative stress and hypertension. American journal of hypertension. 2011; 24 (11):1239-44.

371. Los M, Schenk H, Hexel K, Baeuerle PA, Droge W, Schulze-Osthoff K. IL-2 gene expression and NF-kappa B activation through CD28 requires reactive oxygen production by 5-lipoxygenase. The EMBO journal. 1995; 14 (15):3731-40.

372. Cyrus T, Witztum JL, Rader DJ, Tangirala R, Fazio S, Linton MF, et al. Disruption of the 12/15-lipoxygenase gene diminishes atherosclerosis in apo E-deficient mice. The Journal of clinical investigation. 1999; 103 (11):1597-604.

373. Nozawa K, Tuck ML, Golub M, Eggena P, Nadler JL, Stern N. Inhibition of lipoxygenase pathway reduces blood pressure in renovascular hypertensive rats. The American journal of physiology. 1990; 259 (6 Pt 2):H1774-80.

374. Fichtlscherer S, Dimmeler S, Breuer S, Busse R, Zeiher AM, Fleming I. Inhibition of cytochrome P450 2C9 improves endothelium-dependent, nitric oxide-mediated vasodilatation in patients with coronary artery disease. Circulation. 2004; 109 (2):178-83.

375. Jennings BL, Sahan-Firat S, Estes AM, Das K, Farjana N, Fang XR, et al. Cytochrome P450 1B1 contributes to angiotensin II-induced hypertension and associated pathophysiology. Hypertension. 2010; 56 (4):667-74.

376. Cheek S, Zhang H, Grishin NV. Sequence and structure classification of kinases. Journal of molecular biology. 2002; 320 (4):855-81.

377. Cargnello M, Roux PP. Activation and function of the MAPKs and their substrates, the MAPK-activated protein kinases. Microbiology and molecular biology reviews : MMBR. 2011; 75 (1):50-83.

378. Pearson G, Robinson F, Beers Gibson T, Xu BE, Karandikar M, Berman K, et al. Mitogen-activated protein (MAP) kinase pathways: regulation and physiological functions. Endocrine reviews. 2001; 22 (2):153-83.

379. Griendling KK, Sorescu D, Lassegue B, Ushio-Fukai M. Modulation of protein kinase activity and gene expression by reactive oxygen species and their role in vascular physiology and pathophysiology. Arteriosclerosis, thrombosis, and vascular biology. 2000; 20 (10):2175-83.

380. Touyz RM, Yao G, Viel E, Amiri F, Schiffrin EL. Angiotensin II and endothelin-1 regulate MAP kinases through different redox-dependent mechanisms in human vascular smooth muscle cells. Journal of hypertension. 2004; 22 (6):1141-9.

381. Thalhamer T, McGrath MA, Harnett MM. MAPKs and their relevance to arthritis and inflammation. Rheumatology. 2008; 47 (4):409-14.

382. Han Z, Boyle DL, Chang L, Bennett B, Karin M, Yang L, et al. c-Jun N-terminal kinase is required for metalloproteinase expression and joint destruction in inflammatory arthritis. The Journal of clinical investigation. 2001; 108 (1):73-81.

383. Fahmy RG, Waldman A, Zhang G, Mitchell A, Tedla N, Cai H, et al. Suppression of vascular permeability and inflammation by targeting of the transcription factor c-Jun. Nature biotechnology. 2006; 24 (7):856-63.

384. Rahaman SO, Lennon DJ, Febbraio M, Podrez EA, Hazen SL, Silverstein RL. A CD36-dependent signaling cascade is necessary for macrophage foam cell formation. Cell metabolism. 2006; 4 (3):211-21.

385. Zhao M, Liu Y, Wang X, New L, Han J, Brunk UT. Activation of the p38 MAP kinase pathway is required for foam cell formation from macrophages exposed to oxidized LDL. APMIS : acta pathologica, microbiologica, et immunologica Scandinavica. 2002; 110 (6):458-68.

386. Bao W, Behm DJ, Nerurkar SS, Ao Z, Bentley R, Mirabile RC, et al. Effects of p38 MAPK Inhibitor on angiotensin II-dependent hypertension, organ damage, and superoxide anion production. Journal of cardiovascular pharmacology. 2007; 49 (6):362-8.

387. Komers R, Schutzer W, Xue H, Oyama TT, Lindsley JN, Anderson S. Effects of p38 mitogen-activated protein kinase inhibition on blood pressure, renal hemodynamics, and renal vascular reactivity in normal and diabetic rats. Translational research : the journal of laboratory and clinical medicine. 2007; 150 (6):343-9.

388. Oudit GY, Sun H, Kerfant BG, Crackower MA, Penninger JM, Backx PH. The role of phosphoinositide-3 kinase and PTEN in cardiovascular physiology and disease. Journal of molecular and cellular cardiology. 2004; 37 (2):449-71.

389. Yousif MH, Benter IF, Hares N, Canatan H, Akhtar S. Phosphoinositide 3-kinase mediated signalling contributes to development of diabetes-induced abnormal vascular reactivity of rat carotid artery. Cell biochemistry and function. 2006; 24 (1):13-22.

390. Song J, Lei FT, Xiong X, Haque R. Intracellular signals of T cell costimulation. Cellular & molecular immunology. 2008; 5 (4):239-47.

391. Goncharova EA, Ammit AJ, Irani C, Carroll RG, Eszterhas AJ, Panettieri RA, et al. PI3K is required for proliferation and migration of human pulmonary

vascular smooth muscle cells. American journal of physiology Lung cellular and molecular physiology. 2002; 283 (2):L354-63.

392. Duan J, Yu Y, Yu Y, Li Y, Wang J, Geng W, et al. Silica nanoparticles induce autophagy and endothelial dysfunction via the PI3K/Akt/mTOR signaling pathway. International journal of nanomedicine. 2014; 9:5131-41.

393. Sasaki T, Irie-Sasaki J, Jones RG, Oliveira-dos-Santos AJ, Stanford WL, Bolon B, et al. Function of PI3Kgamma in thymocyte development, T cell activation, and neutrophil migration. Science. 2000; 287 (5455):1040-6.

394. Hirsch E, Katanaev VL, Garlanda C, Azzolino O, Pirola L, Silengo L, et al. Central role for G protein-coupled phosphoinositide 3-kinase gamma in inflammation. Science. 2000; 287 (5455):1049-53.

395. Pan ZK, Chen LY, Cochrane CG, Zuraw BL. fMet-Leu-Phe stimulates proinflammatory cytokine gene expression in human peripheral blood monocytes: the role of phosphatidylinositol 3-kinase. Journal of immunology. 2000; 164 (1):404-11.

396. Amin MA, Haas CS, Zhu K, Mansfield PJ, Kim MJ, Lackowski NP, et al. Migration inhibitory factor up-regulates vascular cell adhesion molecule-1 and intercellular adhesion molecule-1 via Src, PI3 kinase, and NFkappaB. Blood. 2006; 107 (6):2252-61.

397. Ghosh S, May MJ, Kopp EB. NF-kappa B and Rel proteins: evolutionarily conserved mediators of immune responses. Annual review of immunology. 1998; 16:225-60.

398. Sen R, Baltimore D. Multiple nuclear factors interact with the immunoglobulin enhancer sequences. Cell 1986. 46: 705-716. Journal of immunology. 2006; 177 (11):7485-96.

399. Van der Heiden K, Cuhlmann S, Luong le A, Zakkar M, Evans PC. Role of nuclear factor kappaB in cardiovascular health and disease. Clinical science. 2010; 118 (10):593-605.

400. Monaco C, Paleolog E. Nuclear factor kappaB: a potential therapeutic target in atherosclerosis and thrombosis. Cardiovascular research. 2004; 61 (4):671-82.

401. Luft FC, Mervaala E, Muller DN, Gross V, Schmidt F, Park JK, et al. Hypertension-induced end-organ damage : A new transgenic approach to an old problem. Hypertension. 1999; 33 (1 Pt 2):212-8.

402. Gareus R, Kotsaki E, Xanthoulea S, van der Made I, Gijbels MJ, Kardakaris R, et al. Endothelial cell-specific NF-kappaB inhibition protects mice from atherosclerosis. Cell metabolism. 2008; 8 (5):372-83.

403. Brand K, Page S, Rogler G, Bartsch A, Brandl R, Knuechel R, et al. Activated transcription factor nuclear factor-kappa B is present in the atherosclerotic lesion. The Journal of clinical investigation. 1996; 97 (7):1715-22.

404. Henke N, Schmidt-Ullrich R, Dechend R, Park JK, Qadri F, Wellner M, et al. Vascular endothelial cell-specific NF-kappaB suppression attenuates hypertension-induced renal damage. Circulation research. 2007; 101 (3):268-76.

405. Hartenstein B, Teurich S, Hess J, Schenkel J, Schorpp-Kistner M, Angel P. Th2 cell-specific cytokine expression and allergen-induced airway inflammation depend on JunB. The EMBO journal. 2002; 21 (23):6321-9.

406. Shaulian E, Karin M. AP-1 as a regulator of cell life and death. Nature cell biology. 2002; 4 (5):E131-6.

407. Horsley V, Pavlath GK. NFAT: ubiquitous regulator of cell differentiation and adaptation. The Journal of cell biology. 2002; 156 (5):771-4.

408. Rao A, Luo C, Hogan PG. Transcription factors of the NFAT family: regulation and function. Annual review of immunology. 1997; 15:707-47.

409. Germain P, Staels B, Dacquet C, Spedding M, Laudet V. Overview of nomenclature of nuclear receptors. Pharmacological reviews. 2006; 58 (4):685-704.

410. Young MJ. Mechanisms of mineralocorticoid receptor-mediated cardiac fibrosis and vascular inflammation. Current opinion in nephrology and hypertension. 2008; 17 (2):174-80.

411. Park JB, Schiffrin EL. Cardiac and vascular fibrosis and hypertrophy in aldosterone-infused rats: role of endothelin-1. American journal of hypertension. 2002; 15 (2 Pt 1):164-9.

412. Garwitz ET, Jones AW. Aldosterone infusion into the rat and dose-dependent changes in blood pressure and arterial ionic transport. Hypertension. 1982; 4 (3):374-81.

413. Savoia C, Touyz RM, Amiri F, Schiffrin EL. Selective mineralocorticoid receptor blocker eplerenone reduces resistance artery stiffness in hypertensive patients. Hypertension. 2008; 51 (2):432-9.

414. Bayorh MA, Rollins-Hairston A, Adiyiah J, Lyn D, Eatman D. Eplerenone suppresses aldosterone/ salt-induced expression of NOX-4. Journal of the renin-angiotensin-aldosterone system : JRAAS. 2011; 12 (3):195-201.

415. McGraw AP, Bagley J, Chen WS, Galayda C, Nickerson H, Armani A, et al. Aldosterone increases early atherosclerosis and promotes plaque inflammation through a placental growth factor-dependent mechanism. Journal of the American Heart Association. 2013; 2 (1):e000018.

416. Rajagopalan S, Duquaine D, King S, Pitt B, Patel P. Mineralocorticoid receptor antagonism in experimental atherosclerosis. Circulation. 2002; 105 (18):2212-6.

417. Berger J, Moller DE. The mechanisms of action of PPARs. Annual review of medicine. 2002; 53:409-35.

418. Delerive P, De Bosscher K, Besnard S, Vanden Berghe W, Peters JM, Gonzalez FJ, et al. Peroxisome proliferator-activated receptor alpha negatively regulates the vascular inflammatory gene response by negative cross-talk with transcription factors NF-kappaB and AP-1. The Journal of biological chemistry. 1999; 274 (45):32048-54.

419. Diep QN, Amiri F, Touyz RM, Cohn JS, Endemann D, Neves MF, et al. PPARalpha activator effects on Ang II-induced vascular oxidative stress and inflammation. Hypertension. 2002; 40 (6):866-71.

420. Piqueras L, Reynolds AR, Hodivala-Dilke KM, Alfranca A, Redondo JM, Hatae T, et al. Activation of PPARbeta/delta induces endothelial cell proliferation and angiogenesis. Arteriosclerosis, thrombosis, and vascular biology. 2007; 27 (1):63-9.

421. Lee CH, Chawla A, Urbiztondo N, Liao D, Boisvert WA, Evans RM, et al. Transcriptional repression of atherogenic inflammation: modulation by PPARdelta. Science. 2003; 302 (5644):453-7.

422. Fan Y, Wang Y, Tang Z, Zhang H, Qin X, Zhu Y, et al. Suppression of pro-inflammatory adhesion molecules by PPAR-delta in human vascular endothelial cells. Arteriosclerosis, thrombosis, and vascular biology. 2008; 28 (2):315-21.

423. Tontonoz P, Hu E, Spiegelman BM. Stimulation of adipogenesis in fibroblasts by PPAR gamma 2, a lipid-activated transcription factor. Cell. 1994; 79 (7):1147-56.

424. Olefsky JM, Saltiel AR. PPAR gamma and the treatment of insulin resistance. Trends in endocrinology and metabolism: TEM. 2000; 11 (9):362-8.

425. Duan SZ, Usher MG, Mortensen RM. Peroxisome proliferator-activated receptor-gamma-mediated effects in the vasculature. Circulation research. 2008; 102 (3):283-94.

426. Qu A, Shah YM, Manna SK, Gonzalez FJ. Disruption of endothelial peroxisome proliferator-activated receptor gamma accelerates diet-induced atherogenesis in LDL receptor-null mice. Arteriosclerosis, thrombosis, and vascular biology. 2012; 32 (1):65-73.

427. Li AC, Brown KK, Silvestre MJ, Willson TM, Palinski W, Glass CK. Peroxisome proliferator-activated receptor gamma ligands inhibit development of atherosclerosis in LDL receptor-deficient mice. The Journal of clinical investigation. 2000; 106 (4):523-31.

428. Calkin AC, Forbes JM, Smith CM, Lassila M, Cooper ME, Jandeleit-Dahm KA, et al. Rosiglitazone attenuates atherosclerosis in a model of insulin insufficiency independent of its metabolic effects. Arteriosclerosis, thrombosis, and vascular biology. 2005; 25 (9):1903-9.

429. Yee MS, Pavitt DV, Dhanjil S, Godsland IF, Richmond W, Johnston DG. The effects of rosiglitazone on atherosclerotic progression in patients with Type 2 diabetes at high cardiovascular risk. Diabetic medicine : a journal of the British Diabetic Association. 2010; 27 (12):1392-400.

430. Nissen SE, Nicholls SJ, Wolski K, Nesto R, Kupfer S, Perez A, et al. Comparison of pioglitazone vs glimepiride on progression of coronary atherosclerosis in patients with type 2 diabetes: the PERISCOPE randomized controlled trial. Jama. 2008; 299 (13):1561-73.

431. Marchesi C, Rehman A, Rautureau Y, Kasal DA, Briet M, Leibowitz A, et al. Protective role of vascular smooth muscle cell PPARgamma in angiotensin II-induced vascular disease. Cardiovascular research. 2013; 97 (3):562-70.

432. Benkirane K, Viel EC, Amiri F, Schiffrin EL. Peroxisome proliferator-activated receptor gamma regulates angiotensin II-stimulated phosphatidylinositol 3-kinase and mitogen-activated protein kinase in blood vessels in vivo. Hypertension. 2006; 47 (1):102-8.

433. Meir KS, Leitersdorf E. Atherosclerosis in the apolipoprotein-E-deficient mouse: a decade of progress. Arteriosclerosis, thrombosis, and vascular biology. 2004; 24 (6):1006-14.

434. Paigen B, Morrow A, Holmes PA, Mitchell D, Williams RA. Quantitative assessment of atherosclerotic lesions in mice. Atherosclerosis. 1987; 68 (3):231-40.

435. Zhang SH, Reddick RL, Piedrahita JA, Maeda N. Spontaneous hypercholesterolemia and arterial lesions in mice lacking apolipoprotein E. Science. 1992; 258 (5081):468-71.

436. Reddick RL, Zhang SH, Maeda N. Atherosclerosis in mice lacking apo E. Evaluation of lesional development and progression. Arteriosclerosis and thrombosis : a journal of vascular biology / American Heart Association. 1994; 14 (1):141-7.

437. Qin Y, Cao X, Guo J, Zhang Y, Pan L, Zhang H, et al. Deficiency of cathepsin S attenuates angiotensin II-induced abdominal aortic aneurysm formation in apolipoprotein E-deficient mice. Cardiovascular research. 2012; 96 (3):401-10.

438. Sarikonda KV, Watson RE, Opara OC, Dipette DJ. Experimental animal models of hypertension. Journal of the American Society of Hypertension : JASH. 2009; 3 (3):158-65.

439. Lohmeier TE. Angiotensin II infusion model of hypertension: is there an important sympathetic component? Hypertension. 2012; 59 (3):539-41.

440. Zhang W, Wang W, Yu H, Zhang Y, Dai Y, Ning C, et al. Interleukin 6 underlies angiotensin II-induced hypertension and chronic renal damage. Hypertension. 2012; 59 (1):136-44.

441. Crowley SD, Gurley SB, Herrera MJ, Ruiz P, Griffiths R, Kumar AP, et al. Angiotensin II causes hypertension and cardiac hypertrophy through its receptors in the kidney. Proceedings of the National Academy of Sciences of the United States of America. 2006; 103 (47):17985-90.

442. d'Uscio LV, Barton M, Shaw S, Luscher TF. Chronic ET(A) receptor blockade prevents endothelial dysfunction of small arteries in apolipoprotein E-deficient mice. Cardiovascular research. 2002; 53 (2):487-95.

443. Beleznai T, Takano H, Hamill C, Yarova P, Douglas G, Channon K, et al. Enhanced K(+)-channel-mediated endothelium-dependent local and conducted dilation of small mesenteric arteries from ApoE(-/-) mice. Cardiovascular research. 2011; 92 (2):199-208.

444. Leibowitz A, Rehman A, Paradis P, Schiffrin EL. Role of T regulatory lymphocytes in the pathogenesis of high-fructose diet-induced metabolic syndrome. Hypertension. 2013; 61 (6):1316-21.

445. Schadenberg AW, Vastert SJ, Evens FC, Kuis W, van Vught AJ, Jansen NJ, et al. FOXP3+ CD4+ Tregs lose suppressive potential but remain anergic during transient inflammation in human. European journal of immunology. 2011; 41 (4):1132-42.

446. Ross R, Glomset JA. The pathogenesis of atherosclerosis (first of two parts). The New England journal of medicine. 1976; 295 (7):369-77.

447. Libby P, Hansson GK. Involvement of the immune system in human atherogenesis: current knowledge and unanswered questions. Laboratory investigation; a journal of technical methods and pathology. 1991; 64 (1):5-15.

448. Libby P, Ridker PM, Maseri A. Inflammation and atherosclerosis. Circulation. 2002; 105 (9):1135-43.

449. Mackness MI, Mackness B, Durrington PN, Fogelman AM, Berliner J, Lusis AJ, et al. Paraoxonase and coronary heart disease. Current opinion in lipidology. 1998; 9 (4):319-24.

450. Dichtl W, Nilsson L, Goncalves I, Ares MP, Banfi C, Calara F, et al. Very low-density lipoprotein activates nuclear factor-kappaB in endothelial cells. Circulation research. 1999; 84 (9):1085-94.

451. Baynes JW, Thorpe SR. Role of oxidative stress in diabetic complications: a new perspective on an old paradigm. Diabetes. 1999; 48 (1):1-9.

452. Schmidt AM, Yan SD, Wautier JL, Stern D. Activation of receptor for advanced glycation end products: a mechanism for chronic vascular dysfunction in diabetic vasculopathy and atherosclerosis. Circulation research. 1999; 84 (5):489-97.

453. Filep JG, Sirois MG, Foldes-Filep E, Rousseau A, Plante GE, Fournier A, et al. Enhancement by endothelin-1 of microvascular permeability via the activation of ETA receptors. British journal of pharmacology. 1993; 109 (3):880-6.

454. Filippatos GS, Gangopadhyay N, Lalude O, Parameswaran N, Said SI, Spielman W, et al. Regulation of apoptosis by vasoactive peptides. American journal of physiology Lung cellular and molecular physiology. 2001; 281 (4):L749-61.

455. Bousette N, Giaid A. Endothelin-1 in atherosclerosis and other vasculopathies. Canadian journal of physiology and pharmacology. 2003; 81 (6):578-87.

456. Sanz MJ, Johnston B, Issekutz A, Kubes P. Endothelin-1 causes P-selectin-dependent leukocyte rolling and adhesion within rat mesenteric microvessels. The American journal of physiology. 1999; 277 (5 Pt 2):H1823-30.

457. Kafkewitz D. Improved growth media for Vibrio succinogenes. Applied microbiology. 1975; 29 (1):121-2.

458. Felx M, Guyot MC, Isler M, Turcotte RE, Doyon J, Khatib AM, et al. Endothelin-1 (ET-1) promotes MMP-2 and MMP-9 induction involving the transcription factor NF-kappaB in human osteosarcoma. Clinical science. 2006; 110 (6):645-54.

459. He S, Prasanna G, Yorio T. Endothelin-1-mediated signaling in the expression of matrix metalloproteinases and tissue inhibitors of metalloproteinases in astrocytes. Investigative ophthalmology & visual science. 2007; 48 (8):3737-45.

460. Kuzuya M, Nakamura K, Sasaki T, Cheng XW, Itohara S, Iguchi A. Effect of MMP-2 deficiency on atherosclerotic lesion formation in apoE-deficient mice. Arteriosclerosis, thrombosis, and vascular biology. 2006; 26 (5):1120-5.

461. Longo GM, Xiong W, Greiner TC, Zhao Y, Fiotti N, Baxter BT. Matrix metalloproteinases 2 and 9 work in concert to produce aortic aneurysms. The Journal of clinical investigation. 2002; 110 (5):625-32.

462. Aoki T, Kataoka H, Morimoto M, Nozaki K, Hashimoto N. Macrophage-derived matrix metalloproteinase-2 and -9 promote the progression of cerebral aneurysms in rats. Stroke; a journal of cerebral circulation. 2007; 38 (1):162-9.

463. Harrison DG, Guzik TJ, Lob HE, Madhur MS, Marvar PJ, Thabet SR, et al. Inflammation, immunity, and hypertension. Hypertension. 2011; 57 (2):132-40.

464. Kirabo A, Fontana V, de Faria AP, Loperena R, Galindo CL, Wu J, et al. DC isoketal-modified proteins activate T cells and promote hypertension. The Journal of clinical investigation. 2014; 124 (10):4642-56.

465. Mian MO, Paradis P, Schiffrin EL. Innate immunity in hypertension. Current hypertension reports. 2014; 16 (2):413.

466. Sano H, Hosokawa K, Kidoya H, Takakura N. Negative regulation of VEGF-induced vascular leakage by blockade of angiotensin II type 1 receptor. Arteriosclerosis, thrombosis, and vascular biology. 2006; 26 (12):2673-80.

467. Mell B, Jala VR, Mathew AV, Byun J, Waghulde H, Zhang Y, et al. Evidence for a link between Gut Microbiota and Hypertension in the Dahl rat model. Physiological genomics. 2015:physiolgenomics 00136 2014.

468. Ji H, Zheng W, Li X, Liu J, Wu X, Zhang MA, et al. Sex-specific T-cell regulation of angiotensin II-dependent hypertension. Hypertension. 2014; 64 (3):573-82.

469. Brands MW, Banes-Berceli AK, Inscho EW, Al-Azawi H, Allen AJ, Labazi H. Interleukin 6 knockout prevents angiotensin II hypertension: role of renal

vasoconstriction and janus kinase 2/signal transducer and activator of transcription 3 activation. Hypertension. 2010; 56 (5):879-84.

470. Sriramula S, Haque M, Majid DS, Francis J. Involvement of tumor necrosis factor-alpha in angiotensin II-mediated effects on salt appetite, hypertension, and cardiac hypertrophy. Hypertension. 2008; 51 (5):1345-51.

471. Martin-Fuentes P, Civeira F, Recalde D, Garcia-Otin AL, Jarauta E, Marzo I, et al. Individual variation of scavenger receptor expression in human macrophages with oxidized low-density lipoprotein is associated with a differential inflammatory response. Journal of immunology. 2007; 179 (5):3242-8.

472. Kadl A, Meher AK, Sharma PR, Lee MY, Doran AC, Johnstone SR, et al. Identification of a novel macrophage phenotype that develops in response to atherogenic phospholipids via Nrf2. Circulation research. 2010; 107 (6):737-46.

473. Bouhlel MA, Derudas B, Rigamonti E, Dievart R, Brozek J, Haulon S, et al. PPARgamma activation primes human monocytes into alternative M2 macrophages with anti-inflammatory properties. Cell metabolism. 2007; 6 (2):137-43.

474. Cheng J, Koenig SN, Kuivaniemi HS, Garg V, Hans CP. Pharmacological inhibitor of notch signaling stabilizes the progression of small abdominal aortic aneurysm in a mouse model. Journal of the American Heart Association. 2014; 3 (6):e001064.

475. Yamamoto S, Yancey PG, Zuo Y, Ma LJ, Kaseda R, Fogo AB, et al. Macrophage polarization by angiotensin II-type 1 receptor aggravates renal injury-acceleration of atherosclerosis. Arteriosclerosis, thrombosis, and vascular biology. 2011; 31 (12):2856-64.

476. Ait-Oufella H, Herbin O, Bouaziz JD, Binder CJ, Uyttenhove C, Laurans L, et al. B cell depletion reduces the development of atherosclerosis in mice. The Journal of experimental medicine. 2010; 207 (8):1579-87.

477. Liu ML, Xu G, Xue SR, Zhong XC, Chen GX, Chen ZJ. Plasma levels of Th1/Th2 type cytokine are associated with change of prolactin and GH/IGF-I in hemodialysis patients. The International journal of artificial organs. 2008; 31 (4):303-8.

478. Arriaga-Pizano L, Jimenez-Zamudio L, Vadillo-Ortega F, Martinez-Flores A, Herrerias-Canedo T, Hernandez-Guerrero C. The predominant Th1 cytokine profile in maternal plasma of preeclamptic women is not reflected in the choriodecidual and fetal compartments. Journal of the Society for Gynecologic Investigation. 2005; 12 (5):335-42.

479. Tetteh JK, Addae MM, Ishiwada N, Yempewu SM, Yamaguchi S, Ofori-Adjei D, et al. Plasma levels of Th1 and Th2 cytokines in Ghanaian children with vaccine-modified measles. European cytokine network. 2003; 14 (2):109-13.

480. Watanabe H, Numata K, Ito T, Takagi K, Matsukawa A. Innate immune response in Th1- and Th2-dominant mouse strains. Shock. 2004; 22 (5):460-6.

481. Seguchi T, Iwasaki A, Sugao H, Nakano E, Matsuda M, Sonoda T. [Clinical statistics of germinal testicular cancer]. Nihon Hinyokika Gakkai zasshi The japanese journal of urology. 1990; 81 (6):889-94.

482. Maiellaro K, Taylor WR. The role of the adventitia in vascular inflammation. Cardiovascular research. 2007; 75 (4):640-8.

483. Gossl M, Versari D, Mannheim D, Ritman EL, Lerman LO, Lerman A. Increased spatial vasa vasorum density in the proximal LAD in hypercholesterolemia--implications for vulnerable plaque-development. Atherosclerosis. 2007; 192 (2):246-52.

484. Herrmann J, Lerman LO, Rodriguez-Porcel M, Holmes DR, Jr., Richardson DM, Ritman EL, et al. Coronary vasa vasorum neovascularization precedes epicardial endothelial dysfunction in experimental hypercholesterolemia. Cardiovascular research. 2001; 51 (4):762-6.

485. Moulton KS, Vakili K, Zurakowski D, Soliman M, Butterfield C, Sylvin E, et al. Inhibition of plaque neovascularization reduces macrophage accumulation and progression of advanced atherosclerosis. Proceedings of the National Academy of Sciences of the United States of America. 2003; 100 (8):4736-41.

486. Haghighat A, Weiss D, Whalin MK, Cowan DP, Taylor WR. Granulocyte colony-stimulating factor and granulocyte macrophage colony-stimulating factor exacerbate atherosclerosis in apolipoprotein E-deficient mice. Circulation. 2007; 115 (15):2049-54.

487. Marchesi C, Ebrahimian T, Angulo O, Paradis P, Schiffrin EL. Endothelial nitric oxide synthase uncoupling and perivascular adipose oxidative stress and inflammation contribute to vascular dysfunction in a rodent model of metabolic syndrome. Hypertension. 2009; 54 (6):1384-92.

488. Tilg H, Moschen AR. Adipocytokines: mediators linking adipose tissue, inflammation and immunity. Nature reviews Immunology. 2006; 6 (10):772-83.

489. Yamagishi SI, Edelstein D, Du XL, Kaneda Y, Guzman M, Brownlee M. Leptin induces mitochondrial superoxide production and monocyte chemoattractant protein-1 expression in aortic endothelial cells by increasing fatty acid oxidation via protein kinase A. The Journal of biological chemistry. 2001; 276 (27):25096-100.

490. Chang L, Villacorta L, Li R, Hamblin M, Xu W, Dou C, et al. Loss of perivascular adipose tissue on peroxisome proliferator-activated receptor-gamma deletion in smooth muscle cells impairs intravascular thermoregulation and enhances atherosclerosis. Circulation. 2012; 126 (9):1067-78.

491. Lihn AS, Pedersen SB, Richelsen B. Adiponectin: action, regulation and association to insulin sensitivity. Obesity reviews : an official journal of the International Association for the Study of Obesity. 2005; 6 (1):13-21.

492. Takaki A, Morikawa K, Tsutsui M, Murayama Y, Tekes E, Yamagishi H, et al. Crucial role of nitric oxide synthases system in endothelium-dependent hyperpolarization in mice. The Journal of experimental medicine. 2008; 205 (9):2053-63.

493. Rajagopalan S, Kurz S, Munzel T, Tarpey M, Freeman BA, Griendling KK, et al. Angiotensin II-mediated hypertension in the rat increases vascular superoxide production via membrane NADH/NADPH oxidase activation. Contribution to alterations of vasomotor tone. The Journal of clinical investigation. 1996; 97 (8):1916-23.

494. Daugherty A, Manning MW, Cassis LA. Angiotensin II promotes atherosclerotic lesions and aneurysms in apolipoprotein E-deficient mice. The Journal of clinical investigation. 2000; 105 (11):1605-12.

495. Santner-Nanan B, Peek MJ, Khanam R, Richarts L, Zhu E, Fazekas de St Groth B, et al. Systemic increase in the ratio between Foxp3+ and IL-17-producing CD4+ T cells in healthy pregnancy but not in preeclampsia. Journal of immunology. 2009; 183 (11):7023-30.

496. Hsu P, Santner-Nanan B, Dahlstrom JE, Fadia M, Chandra A, Peek M, et al. Altered decidual DC-SIGN+ antigen-presenting cells and impaired regulatory T-cell induction in preeclampsia. The American journal of pathology. 2012; 181 (6):2149-60.

497. Shah DM. Role of the renin-angiotensin system in the pathogenesis of preeclampsia. American journal of physiology Renal physiology. 2005; 288 (4):F614-25.

498. Li JJ, Chen JL. Inflammation may be a bridge connecting hypertension and atherosclerosis. Medical hypotheses. 2005; 64 (5):925-9.

499. Ozkanlar S, Akcay F. Antioxidant vitamins in atherosclerosis--animal experiments and clinical studies. Advances in clinical and experimental medicine : official organ Wroclaw Medical University. 2012; 21 (1):115-23.

500. Czernichow S, Bertrais S, Blacher J, Galan P, Briancon S, Favier A, et al. Effect of supplementation with antioxidants upon long-term risk of hypertension in the SU.VI.MAX study: association with plasma antioxidant levels. Journal of hypertension. 2005; 23 (11):2013-8.

501. Davey Smith G, Lawlor DA, Harbord R, Timpson N, Rumley A, Lowe GD, et al. Association of C-reactive protein with blood pressure and hypertension: life course confounding and mendelian randomization tests of causality. Arteriosclerosis, thrombosis, and vascular biology. 2005; 25 (5):1051-6.

502. Tomiyama H, Okazaki R, Koji Y, Usui Y, Hayashi T, Hori S, et al. Elevated C-reactive protein: a common marker for atherosclerotic cardiovascular risk and subclinical stages of pulmonary dysfunction and osteopenia in a healthy population. Atherosclerosis. 2005; 178 (1):187-92.